Possible impacts of ice formation on physical characteristics of brown trout (*Salmo trutta*) spawning habitats - case study Große Mühl River / Upper Austria

"Winter's coming"

Author: Martin Guzelj, BSc

Master of Natural Resources Management and Ecological Engineering

Supervised by:

Univ. Prof. Dipl.-Ing. Dr.nat.techn. Helmut Habersack, BOKU Vienna

Priv. Doz. Dipl.Ing. Dr. nat. techn. Christoph Hauer, BOKU Vienna

Crile Doscher, BA MS PhD, Lincoln University

Acknowledgements

Here I want to thank all the people that supported me during the creative process of writing this thesis. To all the people who kept me writing: With out you I would have never made it!

Besides all the people who supported me I want thank in particular:

- My supervisors, Helmut Habersack and Crile Doscher who were very patient and answered any of my questions, how stupid they were from time to time.
- Christoph Hauer, who supported me with the data, all his experience and had an open ear for all my complaining when I didn't see, a way to solve my problems with the modelling. I am really grateful that you were my Co-Supervisor and for everything you taught me.
- All my friends and study colleagues all around the world. You guys did an amazing job with dealing with my changes in mood, picking up your phones even at 2 am and also for distracting me. Here the list of people would be at least as long as my thesis but my special thanks go to Schwani, Winnie, Alex, Liz, Philipp, Katja, Tonja, Kerstin, Michi, Daniela, Nina, Andrea, Mario, Shan, Sabine, Michaela and the "new Narmees". From time to time I am wondering that you are still talking to me after all.
- The "Park Haus Café" team. Thank you for letting me use your café as a "coffice" and for all the caffeine you supported me with.
- But on top of all the people I want to thank there are my parents and my sister. With out your support in any case possible and with any mood possible I would have never made it anywhere near to where I am now. I am so happy to have such a strong background!

Abstract

Brown Trout (*Salmo Trutta*) is one of the leading species in alpine rivers. It is a autumn and winter spawning fish. This means that the areas, where the fish spawn are prone to river ice formation in its various forms during incubation. This thesis deals with its impact on spawning areas.

The first part of this thesis describes the parameters that are responsible for the suitability of a spawning site. This includes temperature, flow velocities, grain sizes of the bed material and the conditions that are needed in the interstitial area.

The next part deals with the modelling approach to analyse and compare three different scenarios that can occur at the selected study site during the incubation time. Therefore HEC-RAS and River2D were used as tools. The modelling was done for a river section at Große Mühl River in Upper Austria where frequent spawning of Brown Trout had been observed. The base scenario is an open flow scenario. The water flows down the river without any additional things added to the river section. In the second scenario an ice cover was added to the sidearm, where the spawning areas are located. The third process modelled was the formation of an ice jam in the main channel. All three scenarios were run with different discharges that occurred during the incubation season in the last 6 years. A comparison between the scenarios and discharges was done afterwards. Further on an analysis of the water temperature monitored in the open flow was analyzed for the past 5 years. During the spawning season from 2012/2013 a second sensor was placed in the interstitial area to get comparable data. The difference between the open flow sensor and the interstitial sensor has been analyzed for its influence on hedging times to see if the difference is large enough to make a significant difference for the forecast of hedging times. Additionally to the flow velocities and the temperatures the grain size distribution at the spawning areas has been worked out. This was done to determine at which velocities and discharges the critical values are reached, which would lead to a renewal of the bed material.

The modelling results show that ice cover and ice jam have an impact on the water flow behaviour and the velocities in the sidearm compared to the free flowing scenario. The changes in velocities vary with the discharges. The analysis of the temperatures showed a difference in the daily changes. The summed up day-degrees did not show a significant difference. The analysis of the bed material showed that the spawning area is sedimented during summer season and the criteria for a fully renewal are hardly reached.

Keywords: Habitat modelling; spawning areas; ice formation; alpine rivers; Brown Trout

Kurzfassung

Die Bachforelle (*Salmo Trutta*) ist ein Leitfisch in alpinen Flüssen. Die Laichsaison dieser Art beginnt im Spätherbst. Dies hat zur Folge, dass die Laichgebiete im Winter Eisbildung in ihren unterschiedlichen Formen augesetzt sein können. Diese Masterarbeit behandelt die Frage, welche Auswirkungen auf die Laichplätze durch Eisbildung entstehen können.

Im einleitenden Teil werden die Grundvoraussetzungen beschrieben, die an einem Laichplatz gegeben sein müssen. Die bestimmenden Parameter hierbei sind Temperatur, Fließgeschwindigkeit, Korngrößen im Flussbettsubstrat und die Bedingungen im Interstitialbereich der Laichgrube.

Zur Analyse wurden mit HEC-RAS und River2D zwei unterschiedliche Simulationsprogramme verwendet. Im Zuge der Simulationen wurden drei verschiedene Szenarien verwendet. Im „Grundmodell“ wird die Situation während der Laichzeit beschrieben. Der Flussabschnitt ist eisfrei und ohne zusätzliche Einwirkungen. In weiterer Folge wurde in Bereich der Laichplätze eine durchgehende Eisdecke im Modell hinzugefügt. Im Anschluss wurde im Hauptgerinne ein Eisstau simuliert. Jedes dieser drei Szenarien wurde mit einer Reihe von verschieden Abflüssen simuliert, die während der letzten 6 Jahre in der Inkubationszeit aufgetreten sind. Im Anschluss wurden die Ergebnisse der beiden Programme miteinander verglichen. Weiters wurden im Vorfeld dieser Arbeit im Simulationsbereich zwei Temperatursensoren installiert. In der Auswertung der aufgezeichneten Daten wurden die Unterschiede zwischen dem Sensor im offenen Wasser und dem, im Interstitial positionierten, Sensor analysiert. In weitere Folge wurde analysiert, ob die Temperaturunterschiede eine Auswirkung auf die Dauer der Inkubationszeit haben, um die Zeit des Schlüpfens besser vorhersagen zu können. Des Weiteren wurde auch die Korngrößenverteilung ermittelt. Das Ergebnis wurde mit den Ergebnissen der Simulationen verglichen um festzustellen, ab welchem Abfluss die kritischen Schubspannungen und Geschwindigkeiten erreicht werden und ein Erneuerungsprozess im Bereich der Laichplätze stattfindet.

Die Ergebnisse zeigen einen signifikanten Unterschied bei den Fließgeschwindigkeiten und im Fließverhalten zwischen den drei Szenarien und den einzelnen Abflüssen. Bei den Temperaturen wurde ein Unterschied in der täglichen Schwankungsbreite festgestellt, jedoch die Auswirkungen auf die Inkubationszeit sind vernachlässigbar. Die Kriterien für eine Erneuerung des Flussbettes wurden in den Simulationen kaum erreicht.

Schlagwörter: Habitat Modellierung; Bachforelle; Eisbildung; Laichplatz; alpine Flüsse

Table of Content

1. Introduction and Research Questions

Brown Trout (*Salmo Trutta*) is one of the main fish species in alpine rivers and water bodies. These fish are common in two forms (Spindler, 1997):

- *Salmo trutta forma fario*
- *Salmo trutta forma lacustris*

Both forms have the common name Brown Trout, but the main difference is the habitat, where the adult fish live. While *Salmo trutta forma fario* stays its whole life in the river where they hedge or tributaries *Salmo trutta forma lacustris* migrates from the nursing area to lakes and spend their life there.

For spawning both forms need rivers, which fulfil specific criteria in flow velocity, size of the bed material and temperature. These characteristics will be described later on in this thesis. Brown Trout is a late autumn to winter spawning species. This means that redds (the excavated moulds, where the fish spawned) are potentially prone to the influence of ice in rivers with higher altitude and therefore it is important to figure out, what the differences in the physical attributes on the redd are after ice formed and what happens, when ice jams occur.

The spawning season of Brown Trout in Austria starts mainly in late October. This is the time when the temperature in the rivers decrease to a certain level. The fish migrate to their spawning sites at low flow conditions. Redds are excavated and after the fish spawned they do not look after the nest anymore.

In winter season when the air temperature drops below 0°C depending on the influence given by groundwater the river cools down as well. If the temperature remains below the freezing point for a longer period even during daytime ice formation in the river starts. River ice can occur in various forms which will be described in more detail later on in this thesis. This reaches from slush ice over boarder ice to a complete coverage of ice. This coverage can lead to changes in flow velocities and directions. This can go that far that adult fish have to change their winter habitats. When they have to move from one habitat to another this can use up their reserves to the point where they cannot recover anymore. (Brown, et al., 2011)

In early spring or in warm winter periods the ice cover loses strength in resistance to the forces applied to it. When the cover breaks up the ice shelves float downstream. If they get stuck for example in areas with lower flow depth they can clog the whole river section and build up to an ice jam. As long as the jam stays in place, it can redirect the flow, lead to chances in dividing ratios at river parts with sidearms, or fully block a river and dry up the

downstream section (which is more likely to happen in creeks than in rivers). If the pressure on the dam is getting too high due to e.g. increasing discharge from upstream, increase in temperature and melting snow etc. the jam will break up. This can cause flash floods in the downstream part of the river.
All the processes described above influence the flow conditions in the river section of occurrence. Therefore the following questions are worked out during this thesis.

1.1. Aims of this thesis

In this thesis the following research questions are worked out and discussed:

How can river ice and ice jams influence the physical properties of a spawning area?
Physical properties that are subject of this thesis are flow velocity and shear stress and critical shear stress applied to the bed material.

Is there a difference in temperature between the open water and the interstitial inter-gravel area?
The data measured is valid for the incubation period from the beginning of December 2012 to the end of April 2013.

Therefore the aim of this thesis is to figure out if the formation of a solid ice cover and ice jams has an influence on the spawning area.

1.2. Research site

The two research questions are investigated for a river section at the Große Mühl River in Upper Austria. The Große Mühl River is part of the Danube River basin and flows into the Danube River near Linz. The spring is set in the Bohemian Forest (Germany) on an altitude of 1260 meters above sea level. The Große Mühl River catchment has a size of 560 km² and a flow length of 71 km (Hauer, et al. , 2011).
The actual research site is situated in Aigen/Schlägel on an altitude of 540 meters above sea level. The characteristic rock forms in this area, and therefore responsible for the bed material in the research site, are gneiss and granite (Fink,et al., 2000) .

The geographic coordinates are 48.6451° North and 13.9589° East (Source: http://maps.google.com). Figure 1 shows the area investigated and the spawning site in the sidearm of Große Mühl River.

The river splits 25-30 m upstream to the spawning area. As shown in Figure 2 at the inlet of the side arm boulders build a natural barrier which limits water supply to the spawning area in low flow conditions.

Figure 1 Research Site and spawning area (Source: maps.google.com; editing: Martin Guzelj)

Figure 2 Dividing area at upstream of spawning site

Looking at Figure 2 above the river bed with its defined sharp edges looks like the river had been channelized. But this is not the case. The geographical and geological conditions in the area lead to this channelized looking riverbeds which occurs at Große Mühl river as well as at the rivers that flow through this region. (Fink, et al., 2000) In this area, the Große Mühl longitudinal zonation would be at the boarder between the grayling zone and the trout zone (after Huet's zonation for rivers (Huet, 1959)) but mainly in the trout zone. Therefore Brown Trout as endemic species was used as an indicator species for this area.

Most parts of the Große Mühl River are, according to Hauer et. al. (2013), plane bed sections which are specified by coarse bed substrate (mainly cobbles and gravel) and a lack of discrete

bars. Plane bed rivers are said to be fairly suitable for gravel spawning fish like Brown Trout. Never the less spawning areas occur locally and according to the observations done they are frequently used.

The fact that there are only very few suitable spawning sites leads to an “overspawning” effect, which means, that the areas are used more than once. Hereby fish might excavate existing redds again and destroy eggs which are already in the gravel. Even though the spawning habitats are limited in the Große Mühl River observations in summer 2013 had shown that there is a good age distribution of fish in the river. The results of the quantitative evaluation are shown in Figure 3. In this diagram it is exhibited that there is a healthy population of fish. The classification for the fish in this thesis is based on the criteria as follows (based on (Unfer, Hauer, & Lautsch, 2011) and edited according to Hauer for Große Mühl River):

- <120 mm = 0+ years
- 120mm < length <200 = 1+ years
- 200mm < length < 250mm = 2+ years
- 250mm < length <320mm = 3+ years
- Length >320mm =4+ years

The frequency-length diagram points out, that there is a relatively low number of 0+ fish – fish that are younger than one year old. This might be the case due to the high flood event that happened in June 2013 where a discharge of >60 [m³/s] was measured at the gauging station downstream of the research area. Whilst adult fish are strong enough to look for shelter the young fish might have been washed away by the erosion forces of the high flood event (Armstrong, Kemp, Kennedy, Ladle, & Milner, 2003).

The observation resulted in a fish density of 121.3 [kg brown trout/ha] and a fish amount of 1049 [brown trout / ha]. This shows that the population in the Große Mühl River is in a good condition. Furthermore the population is able to reproduce without anthropogenic interference.

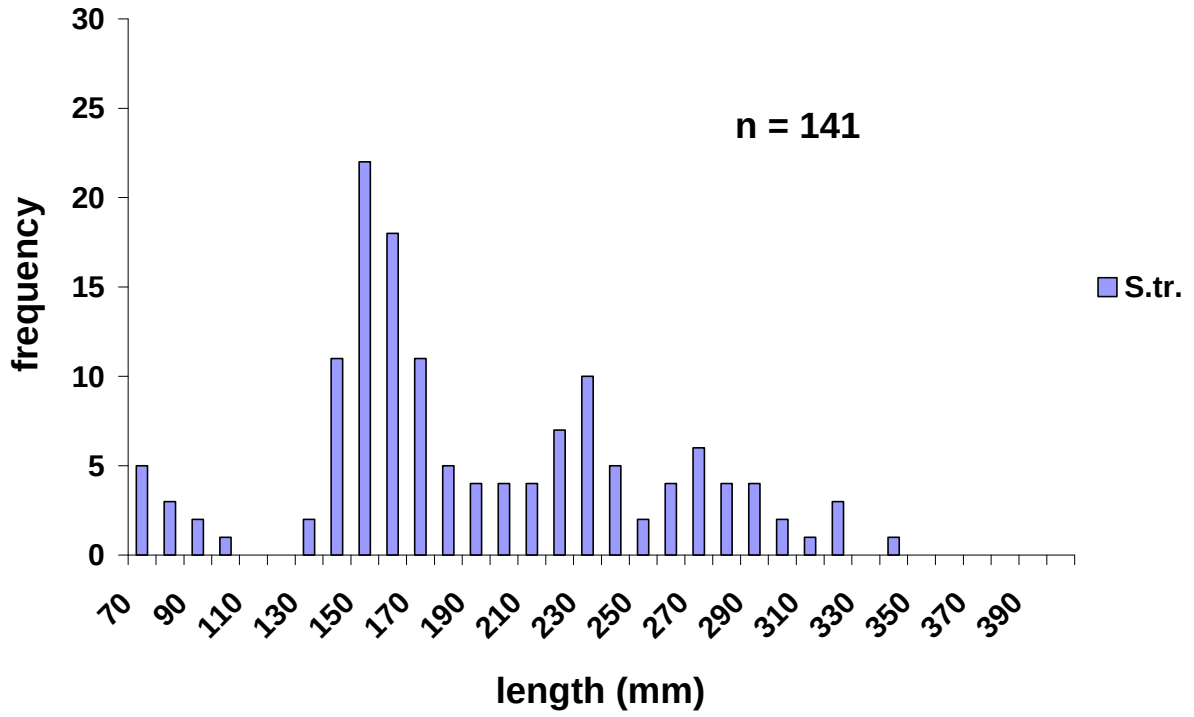

Figure 3 Results from electro fishing at Große Mühl river (Source: Christoph Hauer)

1.3. Why is research on the effects of ice on spawning habitats important?

Brow Trout is one of the most important economically used fish in Austria (Alp, 2010; Riedl & Peter, 2013). Other than the Danube Salmon (*Hucho Hucho*) and other salmonid species (e.g. *Salvelinus alpinus*), Brown Trout occurs through out the alpine areas in populations that used to be stable and it is not considered to be endangered. It is considered to be able to reproduce naturally in a quantity that keeps up the population (Spindler, 1997).

But Spindler (1997) also points out that those populations decrease due to anthropogenic influence on rivers and intensive economical use of the fish. Other influences to the decreasing numbers are:

- river regulations, which have an influence on the hydraulics of the habitats and might lead to a lack of substrate which fish need to spawn in
- power stations and dams, which hinder fish to migrate to their spawning areas
- problems in migration lead to a "local genetic degradation" as fish as there is no genetic "refreshment" by migrating fish

To avoid a bottleneck effect in natural reproduction of Brown Trout in rivers, the understanding of the processes within the spawning areas on a larger scale as well as within the redds themselves on a micro-scale basis is necessary. Reading through the literature various sources have shown, that there is research and modelling for fish habitats all around the world with various types of approaching the field (e.g. PHABSIM). Many of these modelling approaches are for juvenile or adult fish. As habitat requirements differ between adult and juvenile fish, they do between juvenile fish and the incubation period for the eggs and therefore for spawning areas (Louhi, et al., 2008). Whilst juvenile and adult fish can migrate to areas, where the conditions suit their needs, spawning habitats are set on local criteria. In Figure 4 the changes at the selected spawning site through out the year are shown. Some salmonidae species like the Atlantic Salmon (*Salmo salar*) and even Brown Trouts in their form as Sea Trout migrate long distances in their life. Brown trout has been found in the Baltic Sea or Black Sea. Even though some variations of trout have been observed to spawn in brackish water with a salt concentration up to 5%, most of the fish travel the way back to the area where they hatched and spawn there. (Klemetsen et al., 2003).

Brown Trout is an autumn and winter spawning fish. This means that the spawning cycle starts, depending on the altitude and location, when the water temperature decreases to a certain threshold temperature. For the Große Mühl river the spawning period lasts from mid October to early December. According to various sources (e.g. (Klemetsen, et al., 2003)) the migration of fish is induced by a certain combination of discharge level and water temperature. The migration of female fish to spawning grounds starts at a water temperature between 13°C and 4°C. Besides the temperature studies had shown that fish only migrate when there is low flow condition. In rivers with higher altitude the winter spawning habit of Brown Trout leads to the fact, that the redds can be covered with ice or in some cases, that rivers might be completely frozen over the whole cross section during the winter month. The covering of solid ice shelves as well as the formation of slush or anchor ice can have an influence on the physical condition within the spawning area.

Figure 4 Spawning area at three seasons (Source Winter season: Christoph Hauer)

1.4. Requirements for spawning habitats

The following chapter deals with the abiotic condition for a spawning area of Brown trout. Besides some other factors the main physical properties looked at in this thesis are:

- Temperature
- Flow velocity
- Substrate or grain size
- Shear stress
- Intergravel conditions
- Oxygen concentration in the water, which is due to lack of data for the observed spawning sites not part of this thesis

According to Louhi et al. (2008) the spawning conditions are narrower and more critical than the conditions for juvenile or adult fish. They may differ according to the size of the river as well as from the beginning of the incubation time to the end.

1.4.1. Temperature

Temperature is one of the main factors in salmonidae spawning behaviour. First of all changes in temperature lead to the migration of the fish to their spawning habitats and secondly it is important for the incubation and incubation duration of the eggs.

Spawning starts at the beginning of October when water temperature lower than 13 °C. So water temperature should be between 3°C and 13°C for spawning while studies have shown that depending on the area those values can differ (Alp, 2010; Armstrong, et al., 2003; Louhi, et al., 2008) The higher the altitude and the further north in latitude the areas are located the earlier the spawning season starts. This is because the temperature drops below the threshold levels earlier in the year. The high season for spawning of Brown Trout in mountainous rivers, which are comparable to Große Mühl River is according to Riedl & Peter (2013) in mid November. This fits with the observed behaviour of Brown Trout in the research area of this study. According to different sources Brown Trout redds need between 378 and 420 day-degrees for hedging, depending in which area they are (Alp, 2010; Riedl & Peter, 2013). This means that the average temperature per day summed up leads to the amount of days which are needed for the fish to incubate.

For the eggs themselves it is important that the water temperature within the gravel is above 0°C. In his paper "*Thermotolerance of brown trout, Salmo trutta, gametes and embryos to increased water temperatures*" from 2012, Lahnsteiner points out, that as soon as the

temperature decreases close to the freezing point the development of the eggs is arrested and the mortality rate increases. The best survival rates are found between 4°C and 10°C (Lahnsteiner, 2012).

In winter, when air temperature decreases below the freezing point, water starts to cool down. Depending on the local characteristics of the river (flow velocity, depth and exposure to the sky (Brown, et al., 2011)) there is a horizontal layering or stratification in temperature within the water body. As known water has its highest density at 4°C of about 1000 [kg/m³] and becomes lighter when the temperature decreases. According to that physical phenomenon, in parts of the river with flow conditions of very low turbulences and low or almost no flow velocity, water with higher density starts to sink and if the pool is deep enough it stays at a temperature of approximately 4°C. Those habitats are use by adult fish as winter habitats (Brown, et al., 2011).

In areas with high turbulence the layering is can be less observed as mixing within the water due to turbulent flow occurs. In those areas supercooled water is found. This means that under certain circumstances (depending on pressure and flow velocity etc.) water can be liquid at temperatures lower than 0°C. Within rivers the supercooling effects are small and have been observed to at a temperature level of 0.1°C in temperature difference.

Another influence to the water temperature are groundwater springs. This optional input of water in the river varies in amount and in spatial distribution during winter season. They can lead to a “stabilisation” of the temperature in a certain area within the interstitial zone. The reason for this is that groundwater is independent from changes in air temperature. Therefore the temperature of the water coming from a groundwater source varies in a smaller field than open flow water. In rivers with higher altitude those areas might be preferred by fish or spawning as well as in the use of these areas as winter habitats. (Brown, et al., 2011)

1.4.2. Flow velocity

According to Louhi et. al. (2008) the flow velocity and the water depth at the spawning site depend on the size of the river. Whilst in smaller rivers with a mean annual discharge of about 10m³/s shallower areas with a depth up to a maximum of 0.45m with higher flow velocities between 0.20[m/s] and 0.55[m/s] were chosen by the female fish, in large rivers with a discharge >10[m³/s] the depth increases up to 0.55m whilst the velocities decrease to a maximum of 0.40[m/s].

Studies all around the world have shown that the flow velocities in the spawning areas vary depending on the region those areas are in. While Brown Trouts in Ontario, Canada had been

found spawning in rivers at a flow range from about 0.11 – 0.81[m/s] in New Zealand the range was narrower and between 0.15 – 0.75[m/s] (Armstrong, et al., 2003). Armstrong et al. suggests that instead of the flow velocity the mean Froude number should be considered as indicator for suitability of a spawning ground as the velocities chosen by the fish varies with the water depth in the region. Also the density in population has an influence on the ranges chosen as an overpopulated area might lead to sub-optimal choice for spawning areas.

1.4.3. Substrate and Grain size

Salmonides are gravel spawning fish. This means that the adult female fish burry their eggs in the river bed substrate. Therefore the grain size distribution is an important factor for the suitability for the spawning area. A high percentage of coarse material might have the effect, that the fish can't excavate the redd or that the eggs might be washed out of the nest as the space between the cobbles is too large (Armstrong, et al., 2003). A too high percentage of fine sediments hinders the supply with fresh water and therefore is suboptimal for the aeration and the oxygen supply for the eggs. Therefore the fine sediment content (diameter < 0.125mm) within the bed material should not be higher 1.5% (Louhi, et al., 2008) whereas Armstrong et al. (2003) define the concentration of fine materials and sand smaller than 1.0 mm of 15% as critical.

Armstrong et al. (2003) describes that the mean diameter of the spawning area material is about 10% of the body length of the fish and a maximum size of the bed material of about 0.4 – 0.6 times the body length of the fish. This means that larger fish can excavate larger materials. Over all it can be said, that the optimal spawning area consists of gravel with a size of 8 – 64 mm (Louhi, et al., 2008). Talking about gravel and the size of the bed material leads to the next chapter, where the optimal requirements in the interstitial zone are described.

1.4.4. Intergravel conditions and Oxygen concentration

The main factors in the interstitial zone are determined by the bed material. The coarser the bed material the higher the amount of water which can infiltrate the interstitial zone. This also means that a high percentage of finer particles like clay, fine sand and silt can cover the space between the cobbles. This leads to a shortage in fresh water supply within the redd. The breeding success depends on the oxygen supply for the eggs. As mentioned before the conditions change from the beginning of the incubation time until the end. Louhi et al. (2008) point out that with a tolerance level of 0.8 [mg/l] for early eggs is lower than for hatching eggs (7 [mg/l]).

Sedimentation in river sections with low flow velocities can lead to the effect, that basically suitable areas are covered with fine sediments as mentioned before. Therefore a “renewing” process is very important. This can happen by artificial influence or by natural events like high floods, or flash floods caused by breaking ice dam. For the research area at Große Mühl River the renewing process is done by artificial influence. As the area is a river bath in summer people are walking in the river and the side channel and loosen up the riverbed. The fine sediments are lifted up and washed away. Investigations along the river had shown in areas where the riverbed is not moved on a regular time basis, that the sedimentation rate is quite high and after some years areas are completely covered with sand. This is the case for example downstream of the Schlägel power station. Therefore the human interference due to the river bath and children playing in the river is good for the ecological status of the river section as it loosens up the riverbed every summer and the spawning areas stay suitable for Brown Trout.

1.5. Formation of river ice

As the analysis of changes in flow behaviour and the physical conditions of the river is main topic of this thesis the next chapter describes the formation of river ice. This process is linked to the conditions within the river, especially flow velocity and discharge.
As shown in Figure 5 this process is complex and there are more than one possibilities of how ice can occur in rivers. The main steps observed in Große Mühl River are as follows:

- Slush or frazil ice
- Ground or anchor ice
- Ice formation at riverbanks (boarder ice formation)
- Complete ice cover
- Hanging dams
- Ice jam formation (especially in the main channel)

The process of ice formation is started when the air temperature drops below the freezing point for a longer period of time. The surface layer cools down first as it is exposed to the cold air.

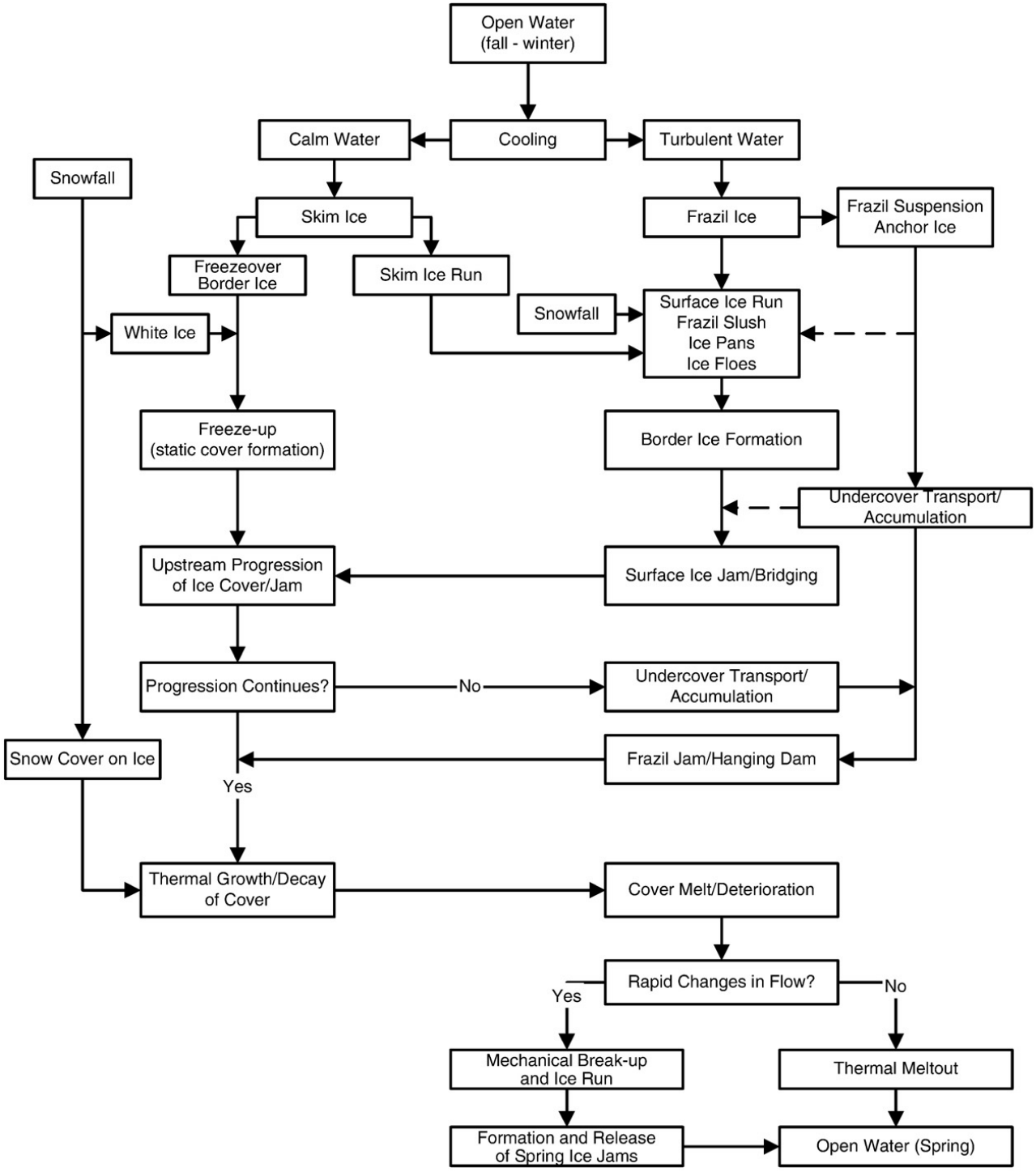

Figure 5 Processes in river ice formation (Shen, 2010)

In parts of the river where the flow velocity is very low a layering effect occurs. Water has its highest density at a temperature of 4°C (Schuh, 2011). Therefore this water will sink until the whole water body reaches this temperature and the cooling process progresses. A layering effect (stratification) can be observed. The colder and therefore lighter (lower in density) layers will remain exposed to air and due to outgoing radiation (in clear nights) and further decrease in temperature the top layers start to freeze (Brown, et al., 2011; Schuh, 2011).

If higher turbulence occurs the layering effect cannot be observed. Due to the mixing process the temperature level will be homogeneous throughout the water body. As mentioned before, if the turbulence is strong enough to overcome the layering effect, water can be supercooled. According to Brown et al. (2011) the definition of supercooling is when the temperature drops below 0°C. This means that as long as there is no ice cover the heat exchange between water and air is going on. In nature supercooling effects are small and of about 0.1 to 0.3 °C. (Brown, et al., 2011) In this supercooled environment initial crystals are formed. Those crystals are called seed crystals (Brown, et al., 2011) and are responsible for ice forming processes in turbulent water. As basis for the seed crystals fine sediments, floating material or especially snow crystals have been observed (Schuh, 2011; Turcotte, et al., 2011).

Once started more crystals are formed and accumulate in the supercooled water. Due to the turbulence in the water those crystals do not form a surface ice layer as they do not remain on top of the water body. Those conditions are responsible for the ice form called frazil ice or slush ice. Due to the suspension of ice and water the river gets a milky appearance. If frazil ice deposits and consolidates on the river bed, it forms anchor ice (Brown, et al., 2011).

When it lifts up again, which can happen due to changes in discharge or water temperature during daytime, it picks up and transports bed material, sediments as well as small invertebrates (Brown, et al., 2011).

As long as the slush ice is floating and suspended in the water it has no significant influence to the physical properties and the flow behaviour. When slush ice gets caught in obstacles like branches hanging into the water, rocks, woody debris or bridge pylons it accumulates to a thickness where it locally changes flow behaviour of the river for example like (Bisaillon & Bergeron, 2009):

- Diverting of the river
- Shifting the ratio of discharge between the parts of the channel
- Increase in water level
- Increase in shear stress
- Reducing intergravel flow and therefore oxygen supply for eggs
- Dewatering parts of the river by creating dams
- Locally higher erosion

When slush gets caught it consolidates (Figure 6). The solid ice layer strengthens. After some time it is able to resist higher forces of shear stress. This can form an initial layer as boarder ice or form ice floes. If the ice layer is strong enough to resist the applied forces it starts

growing. If the weather is below the freezing point for a long period the accumulated ice floes connect to a solid layer of ice and the growing proceeds upstream.

Figure 6 Boarder ice in an alpine river

In alpine rivers, parts with higher velocity are common. When parts with lower velocity are covered with a solid layer of ice, those parts are still open. In this highly turbulent areas however slush is still formed. It is transported downstream and accumulates under the ice cover. These accumulations can spread out across whole river sections. This phenomenon is called “hanging dam”. This is because the accumulations form dams under the ice shelf that are growing from top down. Hanging dams can reach an extension that covers complete cross sections (Brown, et al., 2011).

Hanging dams have large influence on the flow behaviour. But as they are underneath the ice cover, their occurrence is hard to estimate and research on them is difficult. Brown et al. (2011) describe, that the influence of hanging dams on the flow behaviour is similar to clogged woody debris and can reach from increasing flow velocity to a restriction in the water flow.

All changes in flow behaviour caused by iceformation put stress on the fish living in those areas. Their winter habitats might change to a point where the fish have to migrate to another area in the river. This might use up their energy reserves to a point from which the fish cannot recover.

1.6. Formation of ice jams

The ice cover lasts until it melts away (thermal meltout) or increased discharge applies too much pressure on the ice so it breaks up and is washed away in spring. Mostly it is a combination of both processes. The thermal meltout starts as soon as the temperature increases above the freezing point even during night. It is thinning the ice cover. The thinner the ice cover the lower the resistance to the stress applied to the ice even if the discharge remains the same.

Warmer temperatures in early spring lead to an increase of discharge in alpine areas as the snow starts to melt as well. In combination with the thinning ice cover the stress to the ice rises again. This leads to formation of cracks and/or if the stress applied is too high to a mechanical break up of the ice cover.

If the ice cover is finally broken, the resulting ice floes float downstream. When the floes get caught they form dams. Those dams can cause flooding in upstream parts of the river or lead to redirecting of the water. If the dam is not covering the whole cross section the flow is concentrated and the velocity in the open part increases (Brown, et al., 2011).

In the case of the research area ice jams in the main part of the river have been observed (Figure 1). In this case the water is forced to run through the side channel.

2. Methodology

For this thesis 2 different types of simulation tools were used to analyze the flow behaviour during the occurrence of ice cover and ice jams in the river. Both programs have a different background to ensure that the general change in behaviour resulting of one approach is accurate. The first program used is HEC-RAS which is a one dimensional tool developed for river simulation.

The second part is done with River2D which is as the name already says a two dimensional tool developed for research purpose on habitat modelling. Both programs will be basically described and also the various steps in deriving the results. Besides the two simulation tools, on site measures in the river were taken to calibrate the models produced and to see where the spawning sites are located in the research area.

As a last step the resulting velocities and the shear stress occurring according to the simulation results will be studied to their influence on the riverbed and the bed material. When is the renewing process starting, when is material transported?

Another point analyzed in this thesis is the change of the temperature over the year (with focus on the incubation time) in the open water and in the interstitial area. The differences in temperature in the interstitial and the open water flow will be investigated and brought into relation to each other and the hedging time of brown trout.

2.1. Basic Data

The following chapter describes the methodological approach of this thesis to address the problems. It will deal with the questions:

- What kind of data is needed?
- Where is the data derived from?
- How will this data be processed?
- What are the differences in the modelling programmes?
- How was the temperature measured?
- How is the temperature analysed?

This thesis is based on on-site collected data as well as on running and evaluating numerical modells. Before this thesis started, temperature sensors with implemented data loggers were put in place at Große Mühl River. With those sensors the open flow water temperature and the

intergravel water temperature have been measured and recorded. The set of data used in this thesis for the open channel flow areas starts at the beginning of December 2008 (07.12.2008). The sensor used for the intergravel temperature was installed in December 2012 (10.12.2012). Therefore a dataset for a whole incubation season (2012/13) was available for this thesis.

Further on sediment samples from the riverbed were taken and sieved. The samples were derived from the surface layer and the subsurface layer along the river section of the side arm where most of the spawning happens. The resulting grain size distribution was used to see from which critical velocity and/or critical discharge a natural renewing process may occur based on comparing the critical shear stress with the data set derived from the modelling.

Further on a Digital Terrain Model (DTM) was created for this area. To do so, two data sets were collected in the research area. The first dataset, which was the basis for the DTM in River2D consists of 24251 points with x-, y- and z-coordinates to create an 3D model of the terrain. For further processing of the data an average roughness was estimated which was used as initial condition for calculating. The results delivered by the program are in tabelaric form and in a graphical form.

For the basic HEC-RAS modelling part the DTM is divided into cross sections along the riverbed. The procedure with the data was the same as with the River2D data and the final calibration was done with the data derived from the measures done in the field.

To be able to compare the modelling results, the same initial conditions for both models were chosen. As the discharge varies over the incubation season, different discharges were used do see the changes in water levels and velocities as well as the changes in shear stress. The discharges chosen reach from low flow, which occurs in winter up to a 1-year-flood event which might occur in spring when the snow melting process and precipitation in form of rain is increasing the run-off and/or up to a 3 years high flood event, which occurred in late spring 2013. All of the discharges used were applied to the three different modelling scenarios. In the end the following modelling variations were used:

- Without ice cover
- With ice cover on the sidearm of a thickness of 10cm
- With ice cover on the side arm and ice jam on the main channel parallel to the sidearm

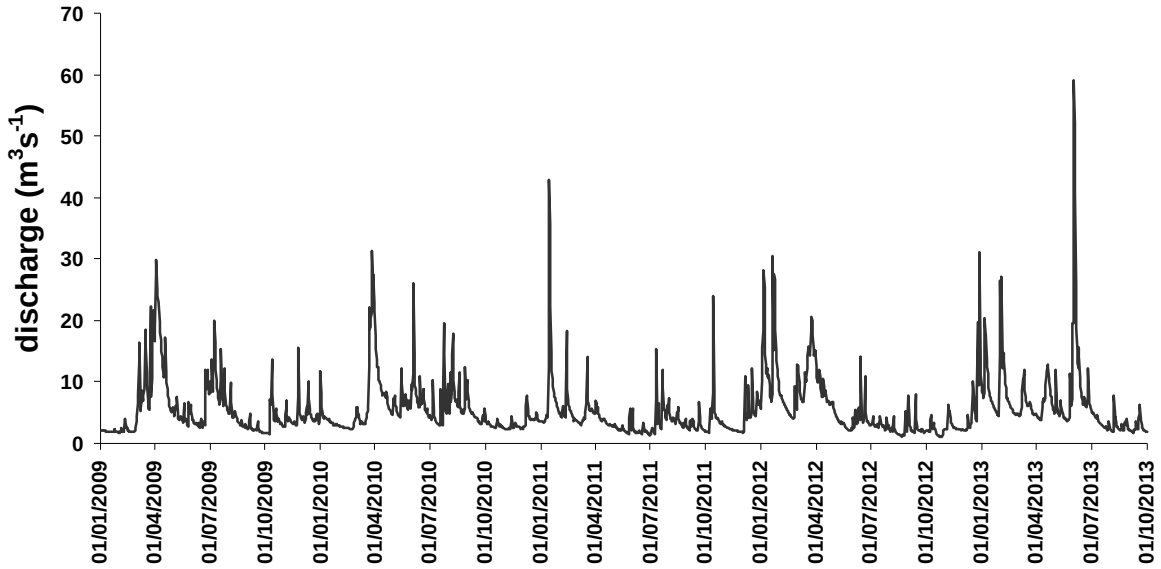

Figure 7 Hydrograph taken into account for the discharges chosen for the modelling of the research area

- Variations in Discharge chosen for the comparison after the hydrograph from Große Mühl River (Figure 7)
    - 1[m³/s]
    - 2[m³/s]
    - 3[m³/s]
    - 5[m³/s]
    - 10[m³/s]
    - 15[m³/s]
    - 20[m³/s]
    - 40[m³/s]
    - 70[m³/s] (only for the scenario with free flowing water)

The calibration of both models was done with the dataset measures in October 2013. Velocity measures were carried out for 3 cross-sections in the sidearm close to the spawning sites as well as one in the main channel at the beginning of the modelling area. Based on the measures the depth average velocity and the discharge amount were calculated and used as initial conditions for to the models. After this the flow distributions as well as the roughness were changed to the point until the measured data and the results derived from the simulations fitted up to a certain point of tolerance.

2.2. HEC-RAS

For details and further information to the following chapter see sources Brunner, 2010a and Brunner, 2010b.

HEC-RAS is a river system simulation and analyzing program developed by the US Army Corps for Engineering. The first version of the program was released in July 1995 and has been updated and extended since. The program version used for the modelling for this thesis is the latest release which is V4.1.0.
HEC-RAS is a one dimensional simulation program which can model steady and unsteady flow operations as well as sediment transport and more. The most important feature for this thesis was the steady flow analysis. Further on the ice module of the program was used to simulate ice cover in the side arm and the ice jam in the main channel. Due to the fact that the program is from the US Army it has to be mentioned, that the default setting for the program is in US Customary Units and not in SI-Units. This has to be defined at the beginning of the modelling to overcome calculation mistakes due to different units in the basic data.

The data needed to get an appropriate result from the modelling is:

- Geometric data based on cross sections (Figure 8)
    - Form of the river bed
    - Data for the main channel boundaries to divide the cross section into Left over bank, main channel and right over bank
- Roughness coefficients in Strickler/Manning's values
- Observed water heights at a specific discharge for the calibration
- Data for the ice cover

The Steady Flow Analysis part of HEC-RAS is based on the one dimensional energy equation. It can be processed in:

- Subcritical flow conditions
- Supercritical flow conditions
- Mixed flow conditions

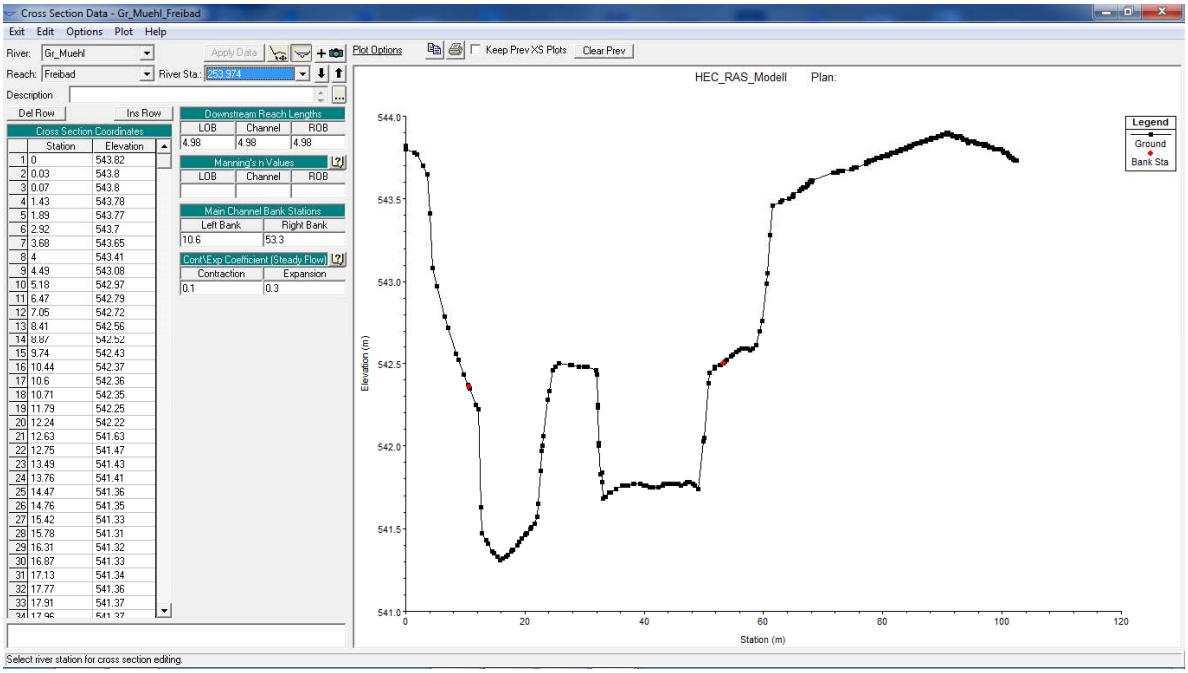

Figure 8 Basic cross section data in HEC-RAS

For this thesis the mixed flow condition calculation was used as described later. The basic principle for the HEC-RAS modelling is calculated from one cross section to the next with an iterative approach and based on Formula 1 (Brunner, 2010b).

$$Z_2 + Y_2 + \frac{a_2 v_2^{\,2}}{2g} = Z_1 + Y_1 + \frac{a_1 v_1^{\,2}}{2g} + h_e$$

Formula 1

The variables in the energy conservation formula are described as follows

$Z_1;Z_2$ ... elevation of the main channel inverts [m]

Y_1; Y_2 ... depth of water at cross sections [m]

v_1; v_2 … average velocities (total discharge/ total flow area) [m/s]

a_1; a_2 … velocity weighting coefficients

g … gravitational acceleration [m/s²]

h_e … energy head loss, contraction-, expansion losses [m]

For conveyance calculations in HEC-RAS the Manning's or Strickler values have to be defined in the cross sections. They can vary from one station point to the next. Therefore HEC-RAS divides the whole cross section into subdivisions, where the Manning's value is

equal and sums up the whole discharge over the cross section in the end. The formula for the subdivision is shown in

$$Q = KS_f^{1/2}$$

Formula 2

$$K = \frac{a}{n} AR^{2/3}$$

Formula 3

Q … Discharge for subdivision [m³/s]

S_f … representative friction slope [-]

K … conveyance for subdivision [m³/s]

a … 1.49 for US customary units, 1.00 for SI units

n … Manning's roughness coefficient for subdivision [$m^{1/3}/s$]

A … flow area for subdivision [m²]

R … hydraulic radius for subdivision [m]

To perform a mixed flow analysis the critical depth between sub- and supercritical flow has to be determined. The critical surface elevation is found at the minimum of the energy head. In HEC-RAS a critical depth will be determined if any of the following conditions are fulfilled (Brunner, 2010c):

- *The supercritical flow regime has been specified*
- *The calculation of critical flow depth has been requested by the user*
- *This is an external boundary cross section and critical depth must be determined to ensure the user entered boundary condition is in the correct flow regime*
- *The Froude number check for a supercritical depth needs to be determined to verify the flow regime associated with the balance equation*
- *The program could not balance the energy equation […] before reaching the maximum number of iterations*

To calculate the total energy head Formula 4 is used.

$$H = WS + \frac{av^2}{2g}$$

Formula 4

Where as:

H … Total energy head [m]

WS … Water surface elevation [m]

$\frac{av^2}{2g}$ … Velocity head [m]

Limitations for HEC-RAS steady flow analyzes are given by the following conditions:

- Flow is steady
- Flow is gradually varied (exceptions are buildings in the river like weirs or bridges…)
- Flow is one dimensional (only velocity components in flow direction are taken into account)
- River channels have small slopes (less than 1:10; which limits the use in mountainous areas)

The research area fulfils all the criteria for an appropriate use of HEC-RAS and so the model application is valid for the analysis of the area.

After the calibration of the basic hydraulic conditions, ice cover on the side arm and an ice jam in the main channel (besides the side arm) are added to the model. The additional formulas that are used in HEC-RAS to process the ice cover and the jam are described below (Formula 5 to Formula 8).

As ice cover floats on top of the water surface the main value added to the energy equilibrium above is an additional Manning's value. To calculate the conveyance for subsections covered with ice Manning's equation is used.

$$K_i = \frac{a}{n_c} A_i R_i^{2/3}$$

Formula 5

Where:

K_i … conveyance of subsection [m³/s]

a … 1.486 for US coustomary units, 1 for SI units

n_c … the composite roughness [$m^{1/3}$/s]

A_i … the flow area beneath the ice cover [m²]

R_i … the hydraulic radius modified to account the for the presence of ice [m]

n_c is calculated as follows:

$$n_c = \left(\frac{n_b^{3/2} + n_i^{3/2}}{2} \right)^{2/3}$$

Formula 6

Where:

n_b … Bed Manning's roughness value

n_i … Ice manning's roughness value

For the hydraulic radius calculated to the presence of ice cover Formula 7 is used.

$$R_i = \frac{A_i}{P_b + B_i}$$

Formula 7

Variables are defined as:

P_b … wetted perimeter associated with the channel bottom and side slopes [m]

B_i … width of the underside of the ice cover [m]

To solve the ice jam the main formulas used are the stress equation and the force balance equation in variations from the basic formulas presented here. To see the whole process and all equations used see (Brunner, 2010b), chapter "*Modelling Ice-covered Rivers*". The basic stress formula is described there is:

$$\frac{d\left(\overline{\sigma_x} t\right)}{dx} + \frac{2\tau_b t}{B} = \rho' g S_w t + \tau_i$$

Formula 8

Where:

$\overline{\sigma}_x$ … Longitudinal stress (in stream direction) [N/m²]

t … Accumulation thickness [m]

τ_b … shear resistance of the banks [N/m²]

B … accumulation width [m]

ρ' … ice density [kg/m³]

g … acceleration of gravity [m/s²]

S_w … water surface slope [-]

τ_i … shear stress applied to the underside of the ice by the flowing water [N/m²]

To solve the problem the ice jam force balance is used in an iterative process. The ice thickness at the upstream section is known and the ice thickness at the downstream section is assumed and then computed from:

$$t_{ds} = t_{us} + \overline{F}L$$

Formula 9

$$\overline{F} = \frac{F_{us} + F_{ds}}{2}$$

Formula 10

Where:

t_{ds} … ice thickness downstream [m]

t_{us} … ice thickness upstream [m]

F_{us} … force balance equation for upstream section [N]

F_{ds} … force balance equation for downstream section [N]

$\overline{F}$ … mean value of upstream and downstream forces [N]

To solve the equations a maximum number of 50 iterations is used in HEC-RAS or a user defined number below that value. If this number is not enough to compute a result within the program's level of tolerance the starting conditions have to be though over again.

2.2.1. The Modelling process

In this chapter the modelling process is described in detail from the beginning of the data determing the river bathymetry, which was provided by the Institute of Water Management, Hydrology and Hydraulic Engineering at the University for Applied Life Sciences Vienna (BOKU), to the final processing of the results. The main steps are as follows:

- Loading Cross sections
- Editing distances between the cross sections with AutoCAD
- Editing roughness for channel and river banks
- Calibrating model with data measured
- First approach with entering roughness for main channel and different roughness for side arm
- Run simulations
- Checking if the water levels are different between the main channel and the side arm
- Changing to two reaches
- Changing roughness for sidearm
- Calibrating ratio between reaches
- Calibrating roughness with data measured
- Running model with an ice cover of 10cm
- Running model with ice cover on side arm
- Running model with ice cover in the sidearm and ice jam in the main channel
- Exporting results to Microsoft Excel
- Comparing results

The first two steps and the first two approaches which did not lead to valid results will just be described shortly. This includes the steps from step “editing roughness for channels and river banks” to step “checking if the water levels are different … “. The final steps that lead to the results compared later in this thesis will be described in more detail.

2.2.1.1. Loading Cross sections

As mentioned earlier in HEC-RAS the water flow between two cross sections is calculated. Therefore the coordinates for each point of the cross section have to be defined. The rough model of the riverbed and the cross sections for this thesis were provided by the University. Therefore the points were not specified each by each but the whole riverbed of the modelling area was loaded into the program. The most important thing with loading the data into HEC-RAS is to be aware of the default setting in the units. As mentioned earlier HEC-RAS is an American program with the default setting on the English measuring system. The unit system has to be set on metric system before hand and then the data can be imported to the cross section editor as shown in Figure 9.

After importing the station points the channel boarders to the left and right side of the channel have to be defined in the "Cross section editor". To receive an appropriate result this was done by using pictures taken at the on-site inspection in late spring 2013 as well as with aerial photographs. Figure 10 shows a selection of the imported cross sections after they have been imported to HEC-RAS where the red dots are symbolizing the default bank stations.

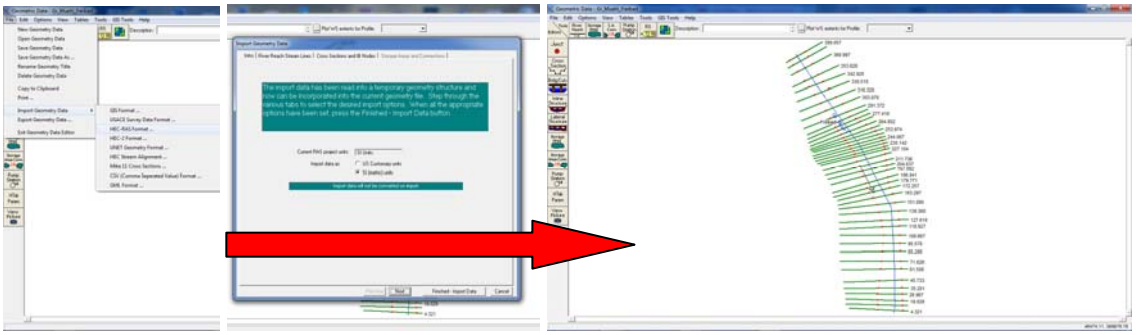

Figure 9 Importing geometric data to HEC-RAS

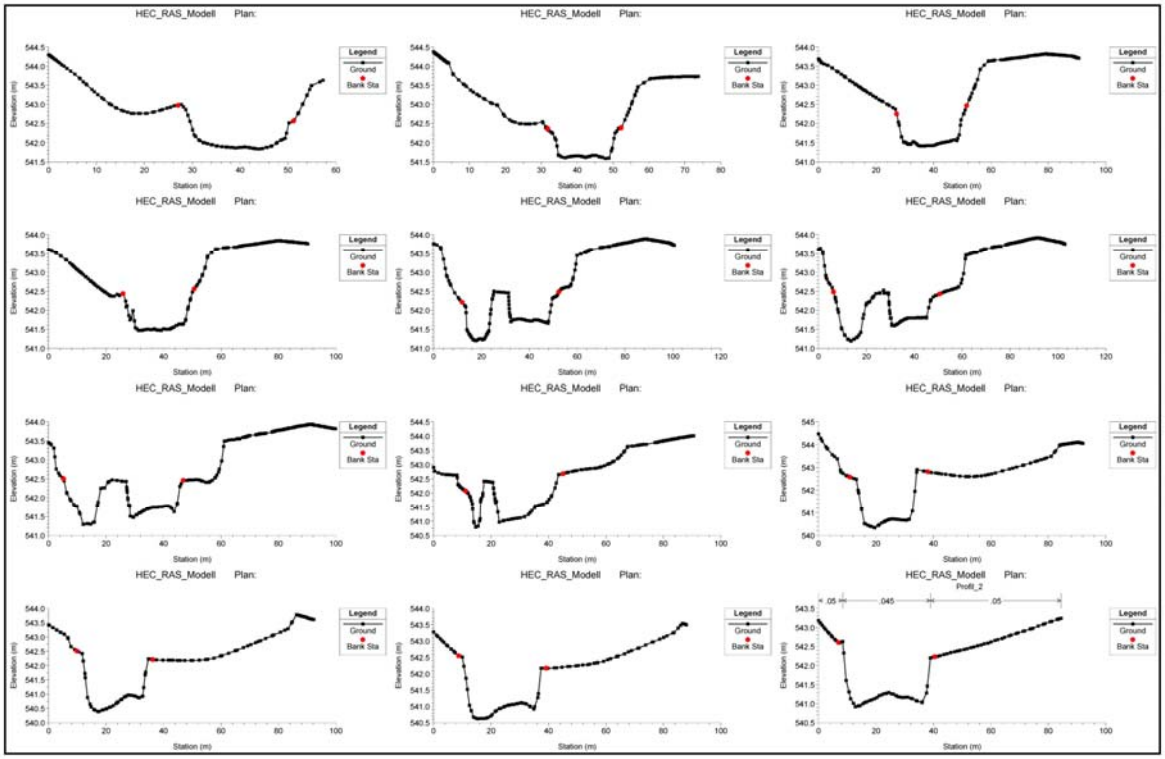

Figure 10 Cross sections after importing without editing

2.2.1.2. Editing of the distances between the cross sections with AutoCAD

When the importing of the data has been done, it is necessary to check if the cross sections are imported in the correct unit system and to see if the distances are according to the real data collected. To do so the X- and the Y- coordinates of the station points are copied to a text file and then formatted to a script file to import them to AutoCAD. In AutoCAD the script were loaded and the data points transferred. Afterwards the outermost points of each cross section are connected with lines and the vertical distances between the outermost points were measured. Those values are transferred back to HEC-RAS into the downstream reach length on the left and right overbank distances if they varied from the starting values in the “Cross section editor”. The riverbank stations or the boarder line for the river is shown in Figure 9 as red dots.

2.2.1.3. Editing roughness for channel and river banks

The Manning's values are entered in the "Cross section editor". As the riverbanks are not the main part in this thesis only one value for the left and the right site of the river bank was chosen as shown in Figure 11.

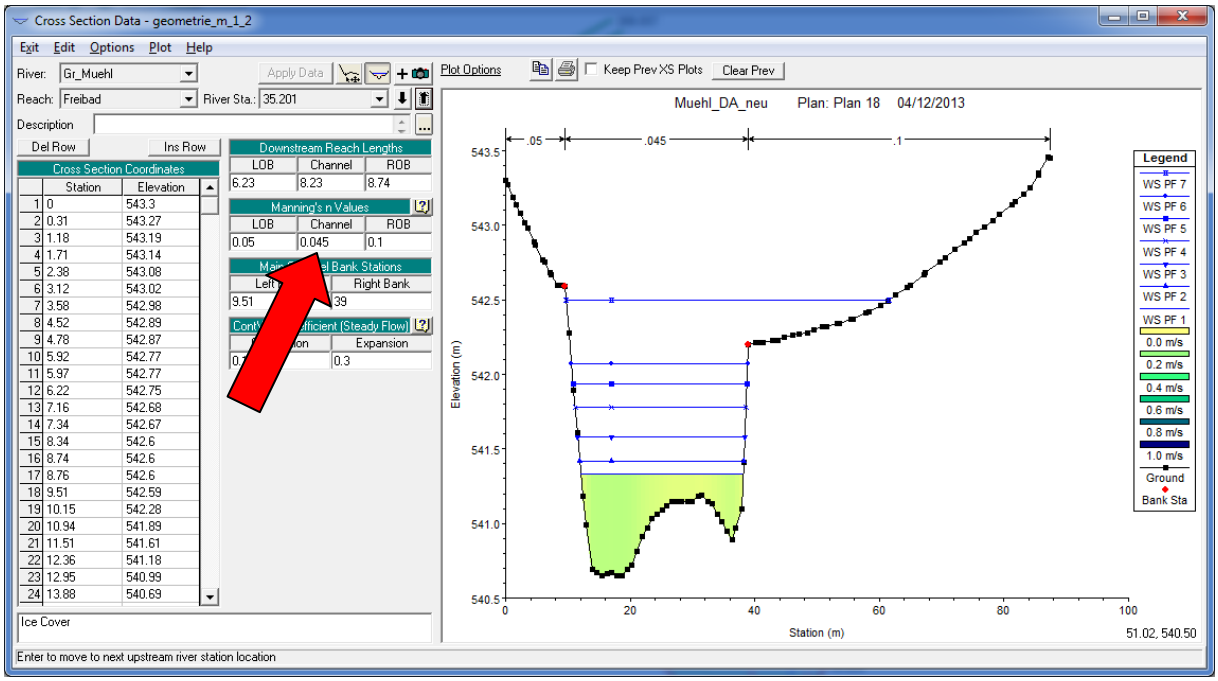

Figure 11 Editing of Manning's values for a whole cross section

The Manning's values for the roughness of the riverbed were taken from the table in (Brunner, 2010b) as well as from former simulations done on the investigated river section. To receive adequate values for the riverbanks pictures from the on-site observations were taken as well as aerial photographs. This is only important for the calibration part of the high flood events as well as for parts of the ice jam modelling as the water might flood the surrounding areas as well as the island that divides the river.

The Manning's values for the main channel and the sidearm were chosen after former simulation data that had been calibrated already. As the Manning's values vary along the river section investigated for this thesis the values had to be defined for every cross section.

The final Manning's values chosen are as shown in Table 1:

Table 1 Manning's values chosen

Description	Value
Light brush and trees, in winter	0.050
Heavy stand of timber, few down trees	0.100
Main channel bed (from former modelling)	0.045
High grass with bushes	0.0625
Ice cover rippled (thickness lower than 1ft)	0.01
Ice jam (thickness sheet ice lower than 1ft)	0.01

2.2.1.4. Calibrating model with data observed and existing models

After entering and editing all Manning's values in the model the first simulation was done. The simulation was run with the discharge measured (2[m³/s]) at the day of the on-site observation in spring 2013. After the computation was done the water levels were compared with the data measured. A selection of the results is shown in Figure 12.

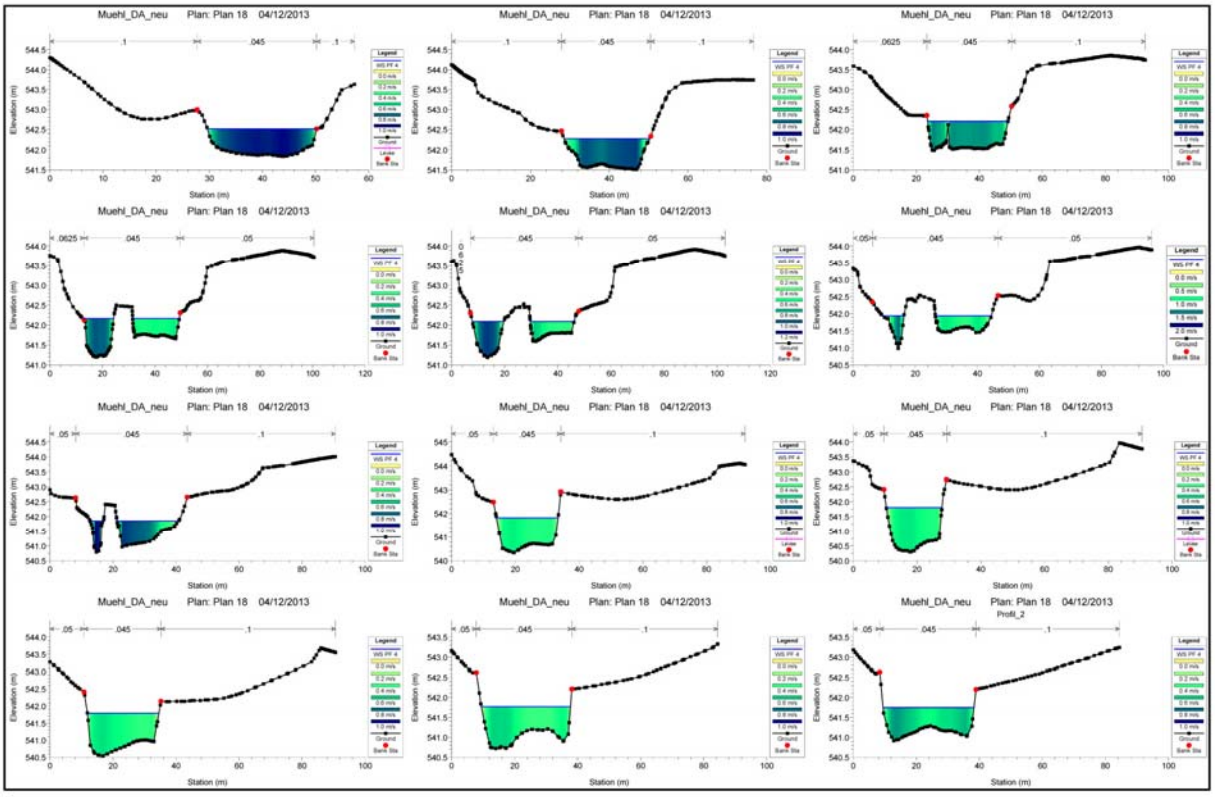

Figure 12 first run of the model for calibration and validation of the data

As Manning's values for the river bed had been taken from a model that has been already calibrated and validated for modelling the main channel, only the values for the riverbanks had to be slightly changed in their longitudinal distribution after calibrating the model to high flood events according the high flood in late spring 2013.

2.2.1.5. Optimization in model geometry

Looking at Figure 13 a difference in the elevation between the main channel and the sidearm is present. This was not the case in the first attempt of the modelling in HEC-RAS as shown Figure 12. The reason for this is that HEC-RAS calculates one water level across the whole cross section where the roughness is the same and therefore the effect of diversion at the inlet of the sidearm is not taken to account in a tolerable way. The water level in the side arm was too high to lead to a proper result in the velocity occurring at low flow conditions.

Figure 13 Picture from the on-site observations in spring 2013 among others used to calibrate the model

This lead to the approach of varying Manning's values between the main channel and the side arm to increase flow velocity in the side arm and therefore lowers the water level in the sidearm. The Manning's value for the river bed in the sidearm was set on a value of 0.03. Afterwards the simulation was done with the same discharge as for the calibration run. As the water level remained the same as in the main channel only the velocity increased, this approach was put aside and not taken into account for this thesis.

2.2.1.6. Model split up into main and side channel

As the approach with different Manning's numbers failed, the basic model was changed into two reaches, one for the main channel and one for the sidearm. This was done to make sure that the side arm and the main channel were calculated separately and therefore different water levels could be simulated.

The first junction point was set one cross section upstream of the actual junction point to be sure that the calculation of the separation is done right and to minimize the calculative error for the sidearm. After drawing the new junction and splitting the section into two reaches the channel had to be defined again. (Figure 14)

First of all, all cross sections that are along the sidearm had to be copied into the new reach. After doing so, the boarder line of the river had to be newly defined for the main channel as for the side arm. Moreover the Manning's values had to be reedited. The Manning's value for the channel bed of the side arm was chosen the same as the one for the main channel. The values for the riverbanks remained the same as in the first approach as the have been already calibrated.

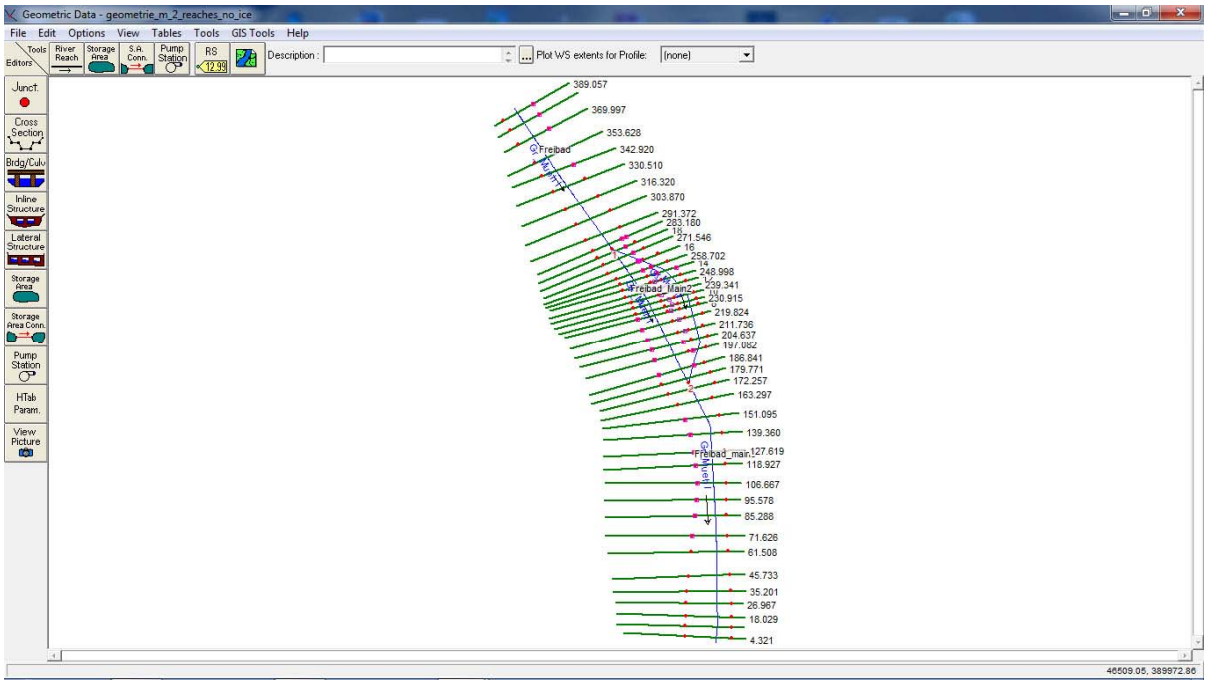

Figure 14 Splitting flow into two reaches

Secondly the island and some parts of the riverbank were defined as levees, to make sure that the water level of each reach only influences the other when the island is overtopped in a high flood event. These points can bee seen as pink spots in Figure 14.

The next step was to figure out what rate of diversion should be chosen. Field observations had shown that there is a ratio of approximately 70% / 30% between main channel and sidearm at low flow conditions.
Three different ratios had been calculated and taken into account for the modelling process.

- 90% of the discharge remains in the main channel
- 80% of the discharge remains in the main channel
- 70% of the discharge remains in the main channel

In Table 2 we see four lines for each discharge scenario

- The first line describes the discharge coming into the research area from upstream
- Second line is the ratio of water running into the side arm
- The third line is the amount of water that remains in the main channel
- Fourth line is the amount after the junction point

As shown in Table 2 different ratios in discharges had been tested to make sure that the amount of discharge is right for each channel. The discharges for testing and calibrating the new model were chosen again for different scenarios.

- From 1[m^3/s] for discharges in low flow conditions during winter time
- To 40[m^3/s] for the high flood event

The ratio with 70% of the amount of discharge remaining in the main channel was fitting best to the water levels observed on-site. To calibrate and to validate the model another on-site observation was done in October 2013. For a detailed description of the measures taken and the final calibration process see chapter 2.4 as this was done for both models.

Table 2 Variation in discharge for the model with two reaches prepared in Excel for the simulation of the new approach with two reaches.

Discharge [m³/s] 90% Main Channel											
Input	1	3	5	10	15	20	25	30	35	40	45
Side arm	0.1	0.3	0.5	1	1.5	2	2.5	3	3.5	4	4.5
Main Channel	0.9	2.7	4.5	9	13.5	18	22.5	27	31.5	36	40.5
Outflow	1	3	5	10	15	20	25	30	35	40	45
Discharge [m³/s] 80% Main Channel											
Input	1	3	5	10	15	20	25	30	35	40	45
Side arm	0.2	0.6	1	2	3	4	5	6	7	8	9
Main Channel	0.8	2.4	4	8	12	16	20	24	28	32	36
Outflow	1	3	5	10	15	20	25	30	35	40	45
Discharge [m³/s] 70% Main Channel											
Input	1	3	5	10	15	20	25	30	35	40	45
Side arm	0.3	0.9	1.5	3	4.5	6	7.5	9	10.5	12	13.5
Main Channel	0.7	2.1	3.5	7	10.5	14	17.5	21	24.5	28	31.5
Outflow	1	3	5	10	15	20	25	30	35	40	45

After calculating the discharge for the main channel and the sidearm from the depth averaged velocity measurements the resulting discharges were put in the model and computed. As the results of the computation were the same as the ones derived from the field observations the model was run again with the discharges shown in Table 2 at 70% of the discharge remaining in the main channel. Figure 15 and Figure 16 show the graphical results for the model after changing the base model to a two reaches approach. In Figure 15 we can clearly see that the water levels are of different height for the main channel and the sidearm.

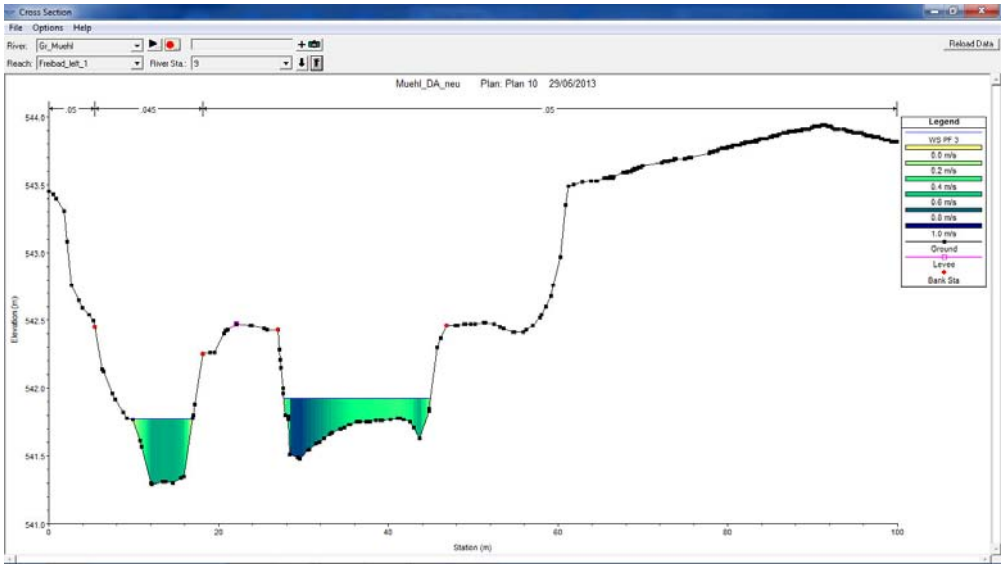

Figure 15 Example of a cross section with different water levels after changing to two reaches stitched together

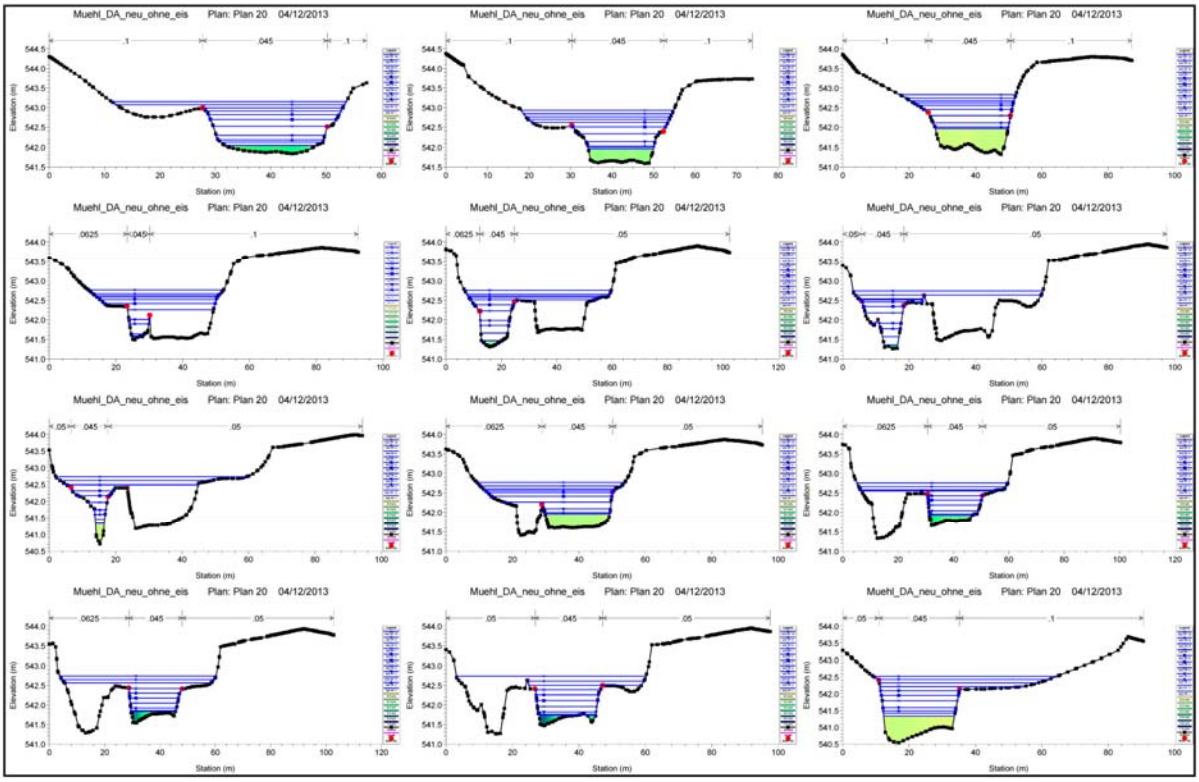

Figure 16 Examples of cross sections after changing to discharge divided into two reaches

2.2.1.7. Running simulations with ice cover

After creating a new project and loading the cross sections and the discharges, the next step was to place an ice cover of 10cm thickness in the sidearm. This was done with the ice module of HEC-RAS. There the ice cover thickness and the Manning's values for each of the cross sections have to be defined (Figure 17). As shown in Table 1 the Manning's value

chosen for the stable ice cover is 0.01 (Brunner, 2010b). When this step was finished simulations were run with the same discharges as done without the ice cover.

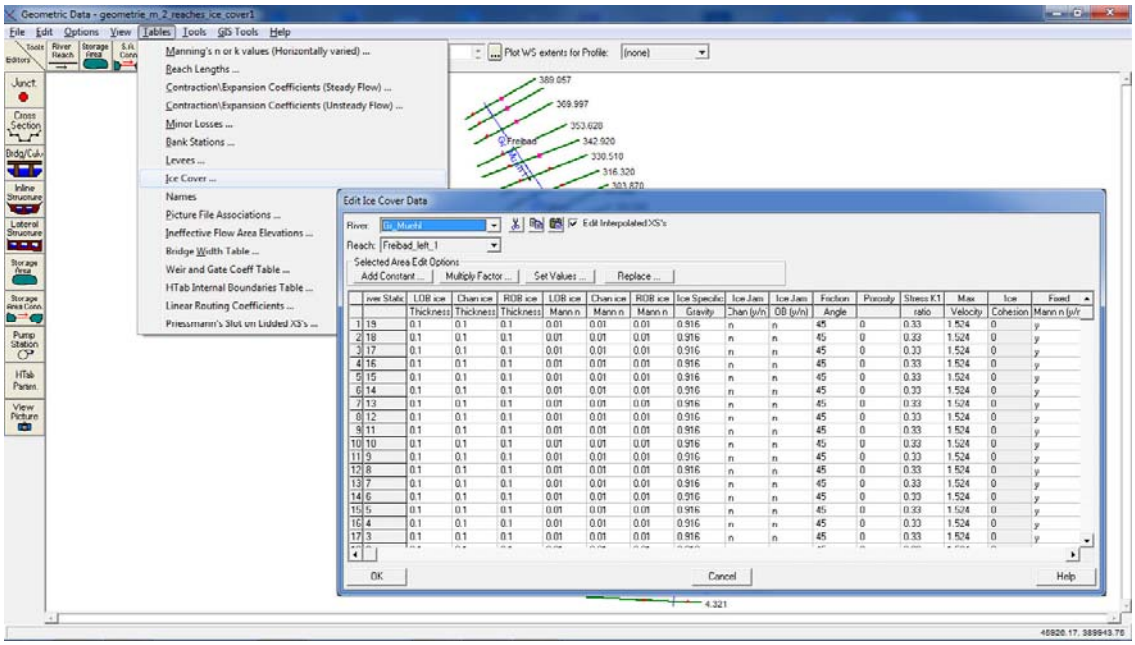

Figure 17 Input mask for ice cover in HEC-RAS

2.2.1.8. Running simulations with ice cover and ice jam in the main channel

Ice jams are set in HEC-RAS in a similar way as the ice cover. To determine in HEC-RAS that there is an ice jam between two or more cross sections the value for the ice jam in the ice module has to be set on “y” (yes) for at least two cross sections. For this thesis the ice jam was set across three cross sections at the shallowest part of the main channel downstream of the diversion. After this was done the same procedure as in the steps before was done (same discharges etc.). Figure 17 shows the input mask for ice and ice jams in HEC-RAS.

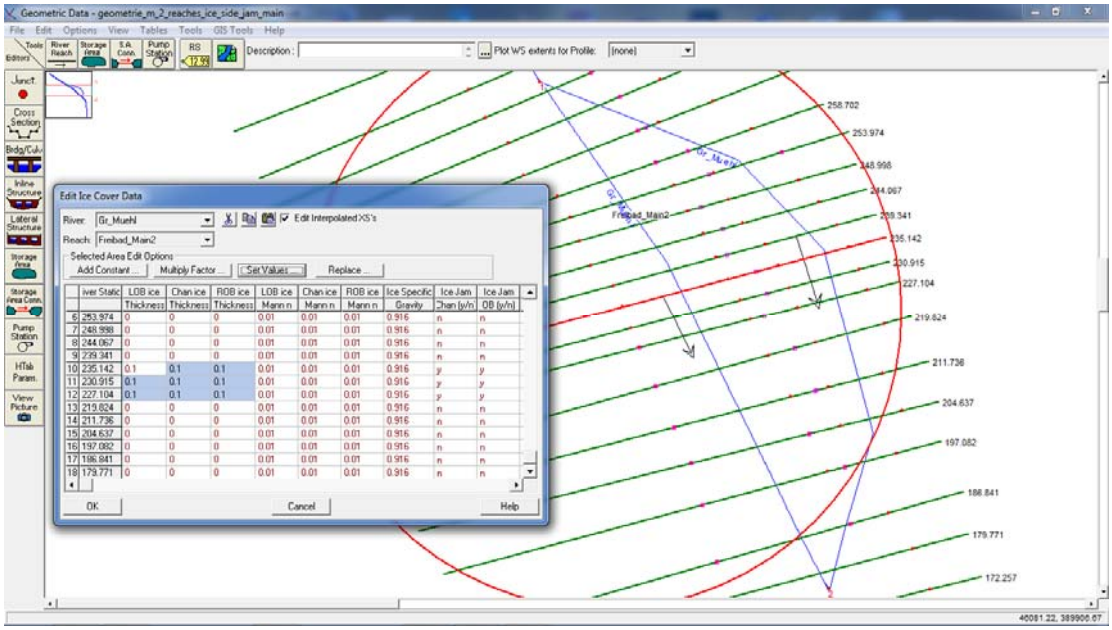

Figure 18 Input mask for ice jams in HEC-RAS

2.2.1.9. Exporting results to Microsoft Excel and comparing the results

After the simulation has been done the results are available in different forms. (Figure 19)

- As cross sectional view with velocity distribution
- As longitudinal plot for flow profiles
- As 3D plot
- As table

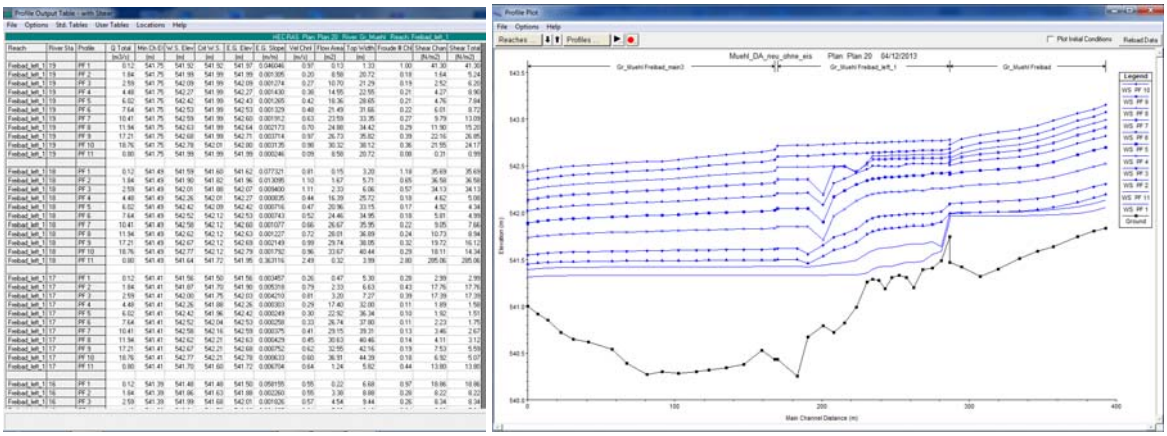

Figure 19 Examples of how results can be displayed in HEC-RAS
(table and longitudinal profile with flow depth)

To compare the results in a quantitative way the table for each simulation (without ice, with ice cover, with ice cover and ice jam) was copied to Microsoft Excel and then the differences

in e.g. velocity or bottom stress were calculated. The difference is important as the resulting numbers show how the ice cover changes the velocity as well as what happens if the main channel is blacked with the ice jam. The differences were calculated between:

- Ice free river and ice cover in the side arm
- Ice free river and ice jam in the main channel
- Ice cover and ice jam in the main channel

The main focus of this thesis is on changes in the physical properties. Therefore the results for the cross sections have been compared and the difference in flow velocity was calculated.
The Results of this step are shown and discussed in the “Results” section of this thesis.

2.3. River 2D

The following chapter describes the basics of handling River2D and the various steps of modelling process in this program. For further information and details see source (Steffler & Blackburn, 2002a)

River2D is a 2 dimensional program developed in a joined program by the University of Alberta, Fisheries and Oceans, Canada and the United State Geological Survey. It is split up in 4 different modules which are:

- R2D_Bed

This module is used to create the basic geometry file for the river section.

- R2D_Mesh

Here the grid for the simulation is created.

- R2D_Ice

In this module ice of certain sections as well as for the whole river part looked at is defined.

- River2D

This is the “head program”. Here all the parts designed and edited in the other 3 modules are combined and the simulation is run in this module. The version used for this thesis version 0.95a and was released in 2010.

The River2D model itself is a depth averaged finite element model that works on the basis of an irregular triangular grid network. It was developed to model natural rivers and streams with focus on fish habitats. This module is based on the PHABSIM approach. Different to HEC-RAS the data used and processed in River2D is in the SI-System. Another difference in River2D is that there is no explicit option to create ice jams so they have to be modelled in a different way.

To start a model in River2D more or less the same base data is needed as in HEC-RAS. First of all the DTM has to be defined which is the most important part of the whole modelling process in River2D. The data points needed therefore are derived from GPS points taken within the modelling area. An accurate DTM takes a lot of time to be produced but it saves a lot of time in processing the model later on. The better the DTM the better the outcome will be.

The next data needed for the model is the bed roughness. Here usually reasonable initial estimates are enough as most of the flow is abstracted to a resistance value and it only counts for the direct shear stress.

Boundary conditions in River2D are mainly inflow discharge and the height of the water level at the downstream boundary of the river section modelled. Here for the same discharges as in the HEC-RAS part had been chosen. The outflow height is needed for every amount of discharge. As a starting condition the values derived from the HEC-RAS modelling were taken after calibration and validation of the HEC-RAS model as actual heights data for the research area is missing for the section of the river modelled. The closer the starting conditions are to the actual result the less iterative steps are needed to solve the equations.

The next step to be taken is the design of an appropriate grid. Depending on the time available and the grade of details needed the solution of the grid should be chosen. The thumb rule for the choice of the grids should be based on “The finer the grid the longer the computation time”. In the manual it is mentioned that a number of about 100 000 nodes is a good value for “modern” PCs. As this was written in 2002 the number for an overnight calculation is higher now.

The basic physical formulations used in River2D are the conservation of mass and the conservation of the momentum as they are (for details of the formulas for the computation see (Steffler & Blackburn, 2002a) :

$$\frac{\delta H}{\delta t} + \frac{\delta q_x}{\delta x} + \frac{\delta q_y}{\delta y} = 0$$

Formula 11

Where as for the conservation of mass:

δH … Change of depth of water [m]

δq_x … Change in specific discharge in x – direction

δq_y … Change in specific discharge in y - direction

For the conservation of momentum (written down for the momentum in direction x):

$$\frac{\delta qx}{\delta t} + \frac{\delta}{\delta x}(Uq_x) + \frac{\delta}{\delta x}(Vq_x) + \frac{g}{2}\frac{\delta}{\delta x}H^2 = gH(S_{0x} - S_{fx}) + \frac{1}{\rho}\left(\frac{\delta}{\delta x}(H\tau_{xx})\right) + \frac{1}{\rho}\left(\frac{\delta}{\delta y}(H\tau_{xy})\right)$$

Formula 12

Where:

g … Acceleration due to gravity [m/s²]

U … input from side [m³/s]

V … input in flow direction [m³/s]

H … Flow depth [m]

τ_{xx} … Shear stress [N/m²]

S_{0x} … Bed slope in x – direction [-]

S_{fx} … Friction slope defined after Manning as

$$S_{fx} = \frac{n^2 U\sqrt{U^2 + V^2}}{H^{4/3}}$$

Formula 13

Where:

n … Manning’s value

After introducing the main equations the next step that should be mentioned here is the way to the solution of the numerical modelling that is used in River2D.

- The first step the discretization where the number of unknowns is brought down to a finite number so that they can be solved with algebraic operations.
- Secondly those algebraic operations are used to solve the nodal values.

To solve the problem with the River2D model following assumptions have to be taken into account (Steffler & Blackburn, 2002b):

- Bed slopes have to be lower than 10%
- The water pressure in vertical direction is hydrostatic
- The velocity in horizontal direction is roughly constant
- The velocity is assumed to be constant in vertical direction for internal calculations
- The velocities are depth averaged
- Wind forces and the rotational force (Coriolis force) does not have influence on the water body modelled

For solving the ice cover a mixed approach of bed resistance and an ice cover model is used. Therefore the friction slope equation is modified according to the additional shear stress applied to the ice cover.

$$S_{fx} = \frac{\tau_{bx} + \tau_{ix}}{\rho g D}$$

Formula 14

Where the variables are defined as:

S_{fx} … friction slope [-]

τ_{bx} … bed shear stress in x direction [N/m²]

τ_{ix} … ice shear stress in x direction [N/m²]

D … depth from underneath the ice cover to the river bed [m]

2.3.1. The modelling process

The description of the modelling process is split into the different parts done in each module of River2D. The basic data set for the DTM was provided by the Institute of Water Management, Hydrology and Hydraulic Engineering steps taken are as follows:

- River2D_Bed
  - Editing the base file
  - Entering the roughness values
  - Loading the data points
  - Checking the DTM
  - Setting break lines
  - Triangulation
  - Saving as .bed file for the simulation without ice and with ice cover
  - Changing bed elevation for the simulation of an ice jam
  - Saving again

- River2D_ice
  - Loading .bed file data
  - Creating ice shelf in the side arm
  - Saving as .ice file

- River2D_mesh
  - Loading bed file
  - Setting external boundaries
  - Setting internal boundaries
  - Setting inflow discharge
  - Setting outflow values derived from HEC-RAS
  - Generating boundary nodes
  - Generating data nodes for the mesh
  - Creating mesh
  - Saving mesh and data in .cdg format

- River2D
    - Opening River2D modelling module
    - Loading .cdg file
    - Loading .bed file
    - Triangulate the .bed file
    - Start steady flow
    - Run transient flow
    - Save physical attributes of the nodes
    - Save velocity distribution as .jpg

For time reasons the hydrological scenarios have been reduced for this thesis. The discharges modelled were:

- 1[m³/s]
- 2[m³/s]
- 3[m³/s]
- 5[m³/s]
- 10[m³/s]
- 15[m³/s]
- 20[m³/s]
- 40[m³/s]

2.3.1.1. Modelling the DTM in R2D_Bed

.

Before starting to feed the data to R2D_Bed the received GPS data from the Institute of Water Management, Hydrology and Hydraulic Engineering at the University for Applied Life Sciences Vienna in a .doc file has to be put into the right format. This was done by changing the .doc file into a .txt file. Afterwards the data was imported into Microsoft Excel to set the headings for each column. Further on each point gets its own node number. An example of how the table looked after the first editing process with Excel is shown in the table below (Table 3). Here we can see that every of the data points consists of a node number and the coordinates in x-, y- and z-directions.

For further details to the program and the .bed file structure see (Steffler, 2002)

Table 3 Example for basic RIVER2D data points after first editing

Node #	x	y	z
1	46078.297	389990.685	542.722
2	46076.5759	389991.679	542.474
3	46074.8391	389992.671	542.221
4	46078.2767	389992.664	542.87
5	46076.5752	389993.674	542.783
6	46073.1288	389993.667	542.056
7	46074.8516	389994.664	542.516
8	46071.4058	389994.663	541.962
9	46078.2767	389994.651	542.88
10	46080.0043	389989.683	542.811
11	46080	389991.669	542.848
12	46080.0143	389987.699	542.669
13	46078.2993	389988.698	542.441
14	46076.5596	389989.686	542.215
15	46074.8458	389990.679	542.022

The next step taken is to set a roughness value for each of the points. As the focus in this project is on the influence of ice on the river bed only one value for the relative roughness was used through out the whole modelling area. Therefore the value might not be valid for the surrounding areas with the high flood events. This value was chosen due to former projects done in this area according to low flow conditions and the bed material analysis. Therefore the roughness value chosen after the calibration of the model is:

- k = 0.55

After adding the column with the roughness value to the table the file was exported as .txt file that can be imported in R2D_Bed. All the actions taken in Excel could have been done in a text-editing program like WordPad as well. The roughness values can be changed in the Bed_2D interface node by node if necessary.

After opening R2D_Bed the .txt file was imported. Some points through out the modelling areas were checked for their accuracy by double clicking in the model on the node. If done so the input mask shown in Figure 20 shows up and the values can be edited.

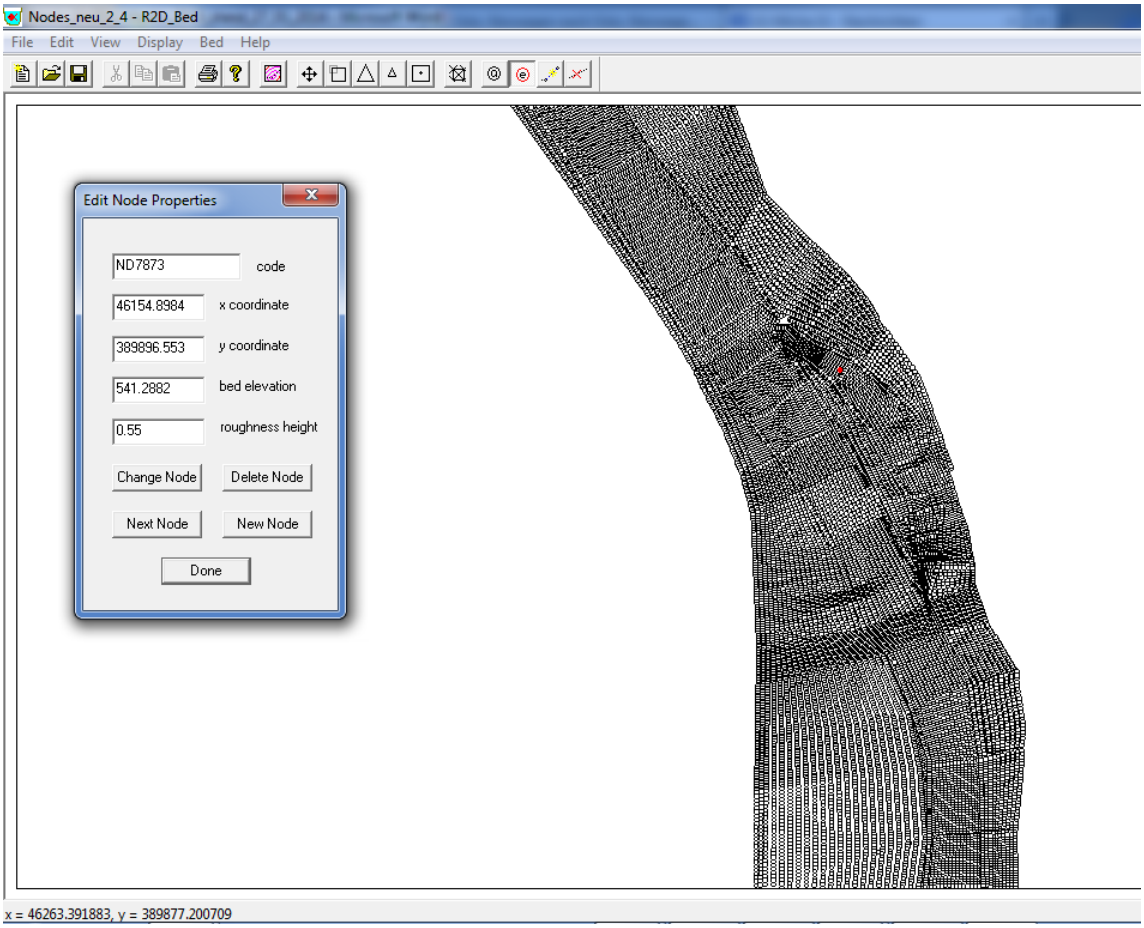

Figure 20 Example of node data in the interface of R2D_Bed

After checking the points the file is saved as a .bed file. Similar to HEC-RAS the break lines have to be defined additionally. This can be done by entering the main points in the in the .bed file in a text file editor or in the graphical interface in R2D_Bed under the point “define new break line”. Here the contour line of the riverbed is defined. If done so in R2D_Bed the nodes chosen for the contour are added in the .bed file under a new section break lines and can be edited there as well. The break lines define the boundaries of the river channel.

As next step the DTM has to be triangulated. If everything was done right the DTM can now be shown in a coloured contour line graphic (Figure 21). Afterwards the file is saved and ready to be read in R2D_ice and R2D_Mesh editors.

As there is no explicit option in River2D to set ice jams it has to be defined in the .bed file. For this thesis the bed elevation in the main channel was lifted to produce a “natural jam” in the main channel. The value taken for the new elevation was chosen after the highest point of the island in the river in this cross section. The cross section itself was chosen as it is the most prone area to produce ice jams in the late winter/early spring as there is a natural step in the riverbed with a shallower area and cobbles, where ice shelf might be caught.

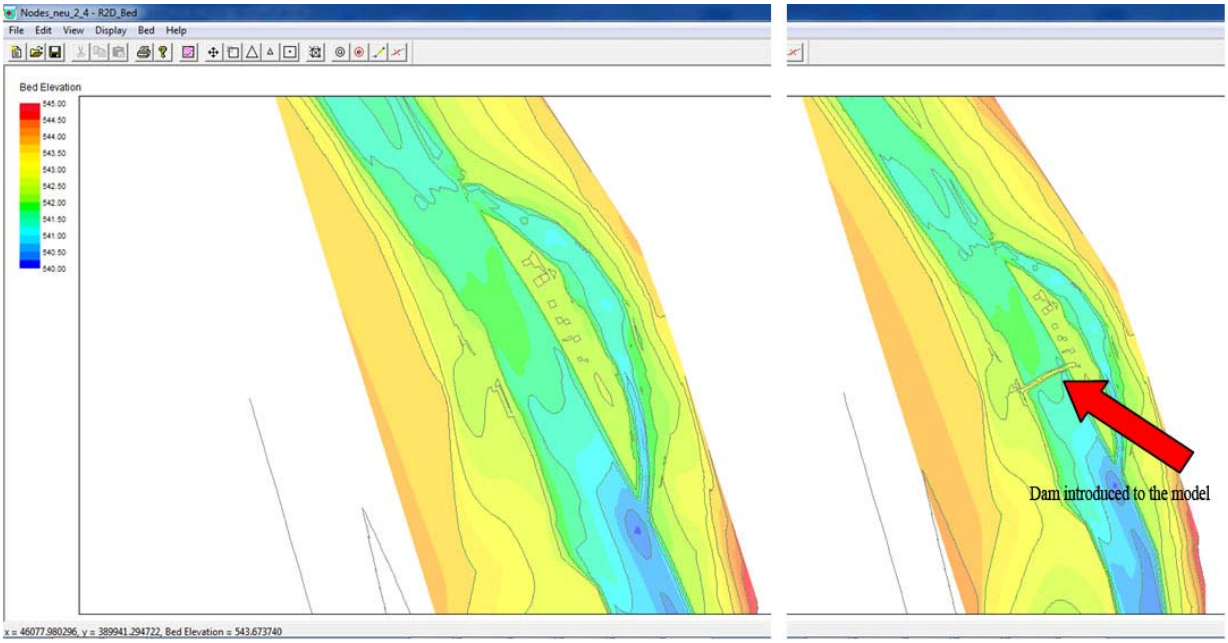

Figure 21 Colour shading graphics for the base file and the "natural jam" for the ice jam simulation

2.3.1.2. Creating the ice cover in R2D_Ice

The first step in creating the ice cover in R2D_Ice is to import the .bed file created in R2D_Bed. By doing so all nodes that are in the file and all properties entered as well as the boundary and break lines are loaded.

The second step is to enter the areas covered with ice. This can be done in two ways. Either the nodes for the boundaries are programmed in the text file like the break lines in R2D_Bed or drawn in the graphical interface of R2D_ice. The second option was chosen for this thesis. As the area covered with ice should be suitable for all discharges, the area covered with ice is larger than needed for the low flow conditions. This was done with "setting ice thickness by area". With this command the area covered with ice is defined counter-clockwise. The ice cover then is set for the enclosed area. Variations of ice thickness across a river section are possible but in this case not needed. The ice thickness for the side arm was set at 10cm over the whole section for the river.

The third step was to set the ice roughness. This can be also done for single areas or for the whole river. Here the option for setting the global ice roughness for the whole area was chosen as only areas that have an ice cover are taken into account. In River 2D a relative roughness is used for the calculation. Therefore a converter for the roughness values is integrated in the program. This converter was used to transfer the Manning's value into the right value for the model. The value chosen for the ice roughness is the same as in HEC-RAS:

- Manning's value $k_i = 0.01$
- Value set in the program: k= 0.1

The following graphic (Figure 22) shows the contour lines of the riverbed, the estimated edge of the water flow (blue lines) and the area covered in ice clipped to the edge of the water. To be able to compare the results with HEC-RAS the same are was chosen as well as the ice thickness of 10cm.

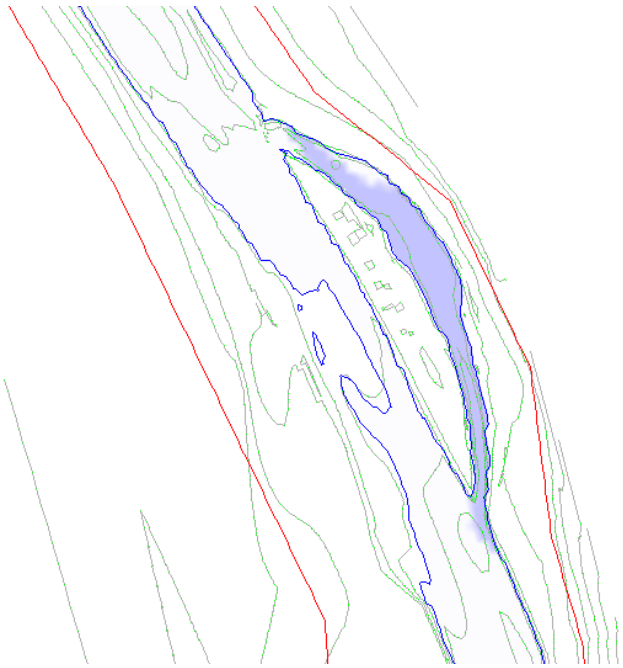

Figure 22 Ice cover added in R2D_Ice displayed in River 2D with contour lines and water's edge

2.3.1.3. Creating the grid with R2D_Mesh

After modelling river bed and ice cover the next step was to create the grid for the simulation of the water flow. In this chapter focus is set on the creation of the mesh for the simulation. The steps taken for creating the mesh are the same as mentioned for the "basic" model. "The basic model" means the simulation of the flow with the discharges listed in chapter "Basic Data" without ice cover and ice jam. This is done in the R2D_Mesh module of the River 2D system.

First of all, similar to the R2D_Ice module, the .bed file has to be opened in the mesh editor. As next step the imported data have to be checked for their validity. After doing so the external boundaries have to be defined. These boundaries are important as they limit the

simulated area as well as the outlines of the mesh. The boundaries should include all the area that might be covered with water through out the simulation.

The command to create the external boundaries is found under the menu point “Boundary”. After clicking on “Define external boundary” the points along the boundary line have to be clicked on. This has to be done clock wise. The area on the right hand side of the line will be defined as mesh area. After closing the boundary line by clicking on the starting point the field will be created. The next step would be to define the “internal boundary”. This command creates an area within the boundary defined before that is not part of the modelling area. This is important especially for large modelling areas when there are fields in there which are not of interest.

Due to the fact that the modelling area is not large, the island which separates the side arm from the main channel could have been defined as an internal boundary. This was not done as observation showed that it will be flooded in the high discharge scenarios and therefore the mesh would not have been accurate for all scenarios modelled.

The third step in defining boundaries is to set the inflow discharge. Different to HEC-RAS only one amount of discharge can be set for a grid. After choosing “Set Inflow” the area where the water enters the mesh has to be defined by clicking on the external boundary line. Afterwards the discharge has to be entered in [m^3/sec]. The model is based on the mass continuum. Therefore the inflow discharge equals the outflow.

As the model needs initial conditions the next step is to set the outflow boundaries. Here not the discharge is asked, as mentioned before, for but the height of the water level in the outflow area of the modelling reach. The value given to the model has not to be the correct height but should be close to reality. The closer the value entered is to reality the fewer steps are needed in the iteration process later on. This height can be measures at a gauging station for different discharges do get an accurate value for each discharge. As there is no gauging station within the outflow area for the model used for this thesis as starting values the outflow heights from the calibrated HEC-RAS model had been used as starting values as shown in Figure 23. On the left hand side the longitudinal plot of the modelling area from the HEC-RAS model is shown. On the right hand picture the outflow conditions are entered in R2D_Mesh.

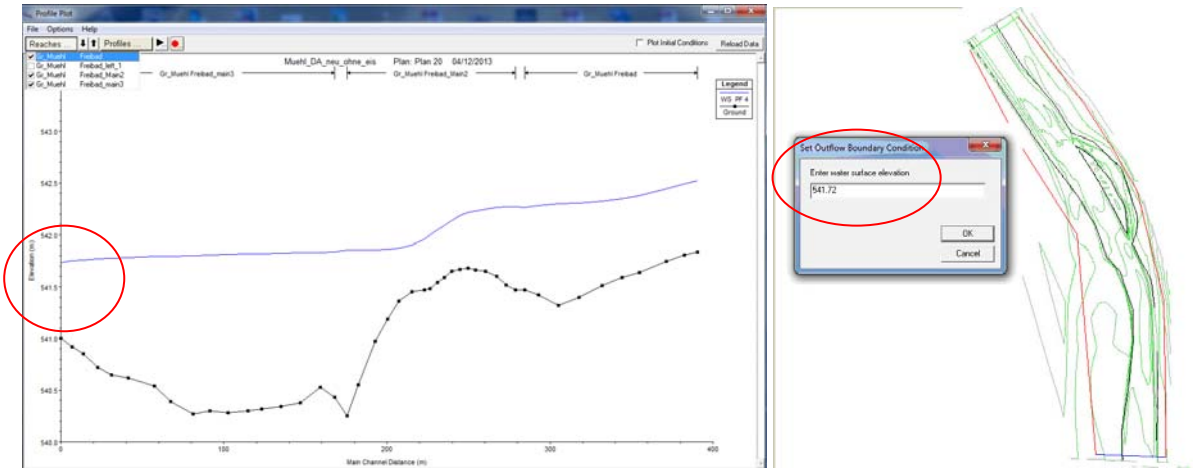

Figure 23 Entering outflow water level on the example of 5m³/sec discharge

If all boundary conditions are entered, there should be a green line for the inflow area, a blue line for the outflow section and red lines for the rest of the external boundaries as shown in Figure 23 on the right hand side.

To create a mesh the area within the boundaries has to be filled with nodes. The first nodes that are generated are the boundary notes. The nodes along the boundary for all meshes created for this thesis have the distance of 3m. After generating the boundary nodes there are a few options to fill the simulation area with nodes. Possibilities are:

- Uniform fill
- Area fill
- Region fill
- Radial fill

The option of "Uniform Fill" was chosen for this thesis. Hereby the whole area within the boundaries is filled with a regular grid of nodes where the distance between the nodes and the angle of the grid have to be defined. The spacing between the points was different to the boundaries reduced to two meters and after some try and error the angle chosen for the fill has been set to 45°.

The following picture (Figure 24) shows the inlet of the sidearm. On top of the DTM the mesh created in R2D_Mesh with the values mentioned before is displayed. We can see that it is equally distributed with an angle of 45°. The irregular triangles on the side derive from the difference in spacing between the mesh - and the boundary nodes as well as from the contour-given to the boundary lines.

After the mesh was triangulated the file can be saved as a .cdg format. This here all the information fed to the model is combined in a form that can be read from the head-program (River2D) and will be used later on to run the simulation.

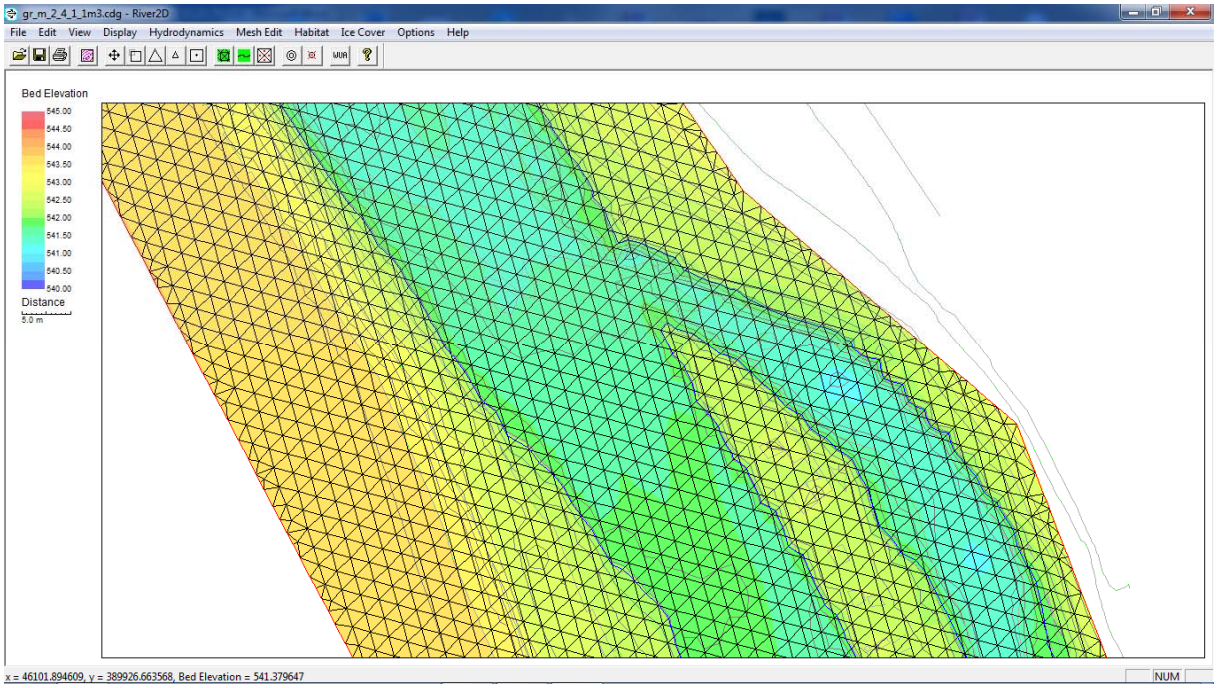

Figure 24 Mesh after triangulation displayed on the inlet of the sidearm (displayed in River 2D)

The steps mentioned in this chapter were repeated for every discharge and for every scenario of the simulation. The distances between the nodes as well as the angle were the same in every mesh to receive comparable results. In the end 25 .cdg files were created including the file for the calibration of the model.

- discharges from 1 to 40m³/second for every approach
  → 1 for the calibration
  → 8 models without ice cover and ice jam
  → 8 models with ice cover
  → 8 models with ice jam in the main channel

2.3.1.4. Running the models created in River 2D

After creating the two DTMs, the ice cover and all meshes in the base modules of the River 2D system the data generated is combined in a .cdg file. This format is used in the “head program” – River 2D. As the process to run the simulation was always the same it will be described for one approach only. The example shown is for the discharge with 1m³/sec.

First of all the .cdg file was opened in River 2D. As shown in the following picture where the steps are displayed on hand of the change in the displayed model, the graphic shown includes the boundary lines (green, blue, red) and an estimation of the water's edge (blue lines within the boundaries).

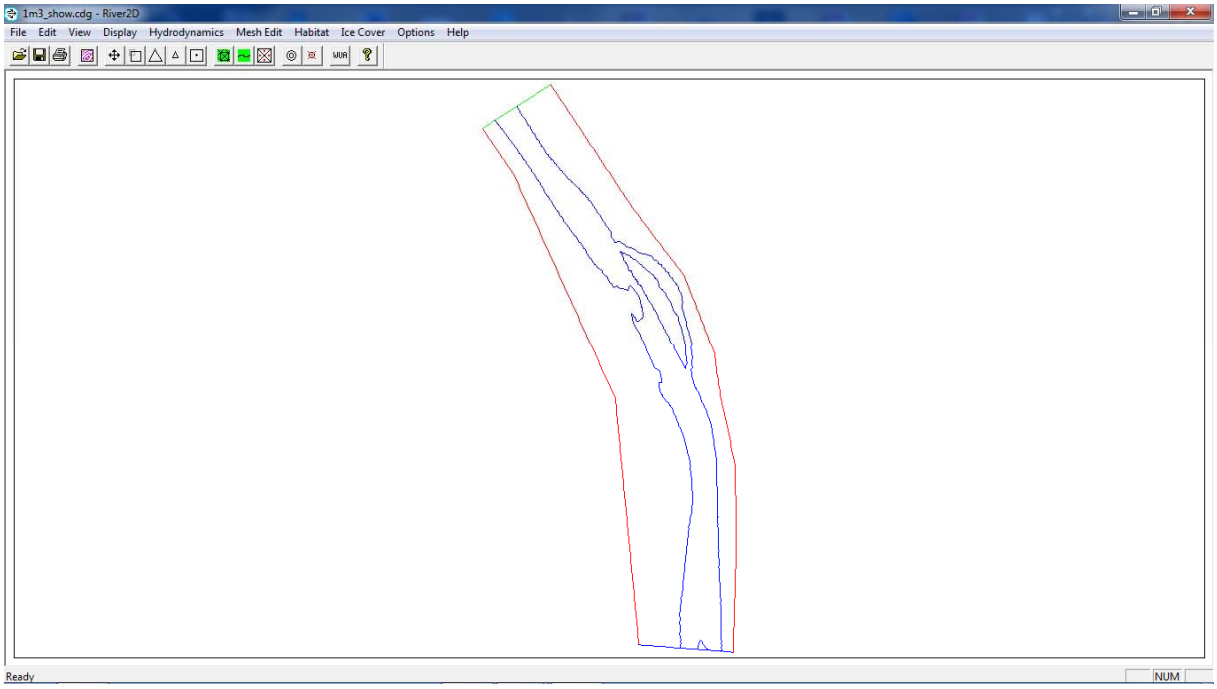

Figure 25 loading .cdg file into River 2D

The next step needed is to load the DTM needed into the model. As soon as the DTM is loaded the contour lines of the riverbed show up on the screen. For the ice cover modelling approach the ice cover has to be loaded into the model additionally but is not shown in Figure 26. Before you can run the simulation the model has to be triangulated again.

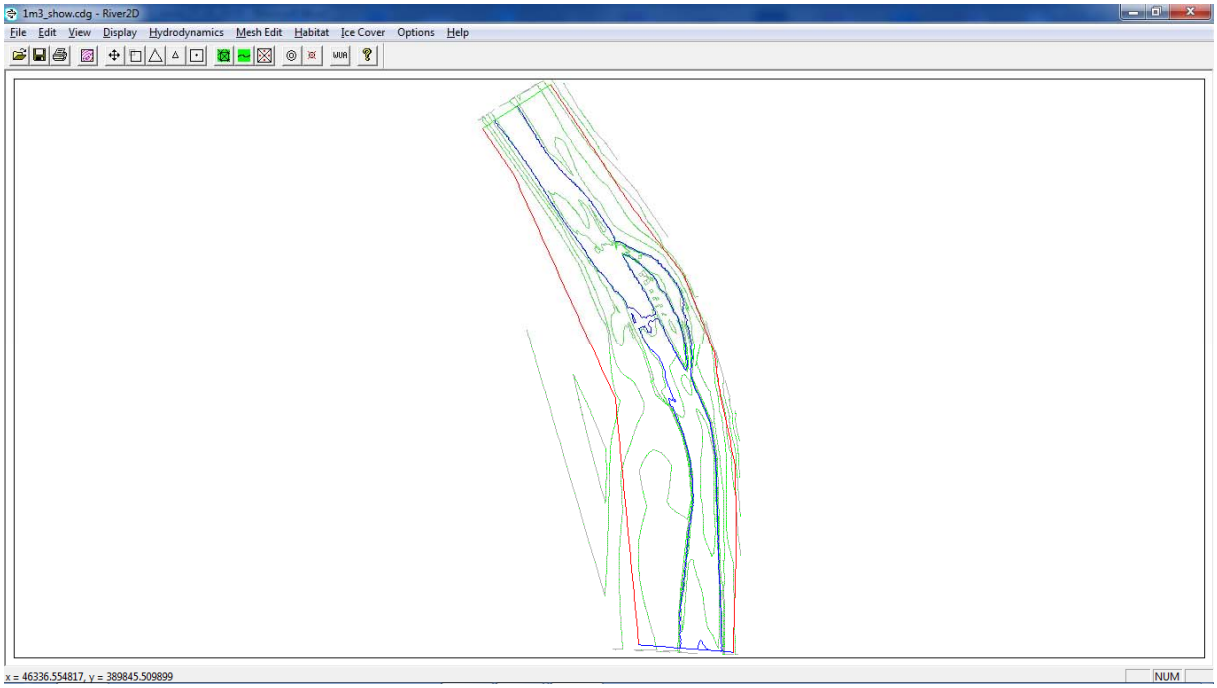

Figure 26 Loaded .cdg with .bed file (DTM) in the background

As the main focus in this thesis is on the velocities the display option of colour shading is used with the setting on velocity magnitude. The colour shading is clipped to the waters edge. Under the menu "Hydrodynamics" the option to run a steady flow is chosen first. The time increments for the starting conditions have to be chosen carefully. If the starting steps are too large the simulation might not come to a result and the iteration process will take a long time! The starting condition chosen for all simulations were as shown in the graphic below (Figure 27).

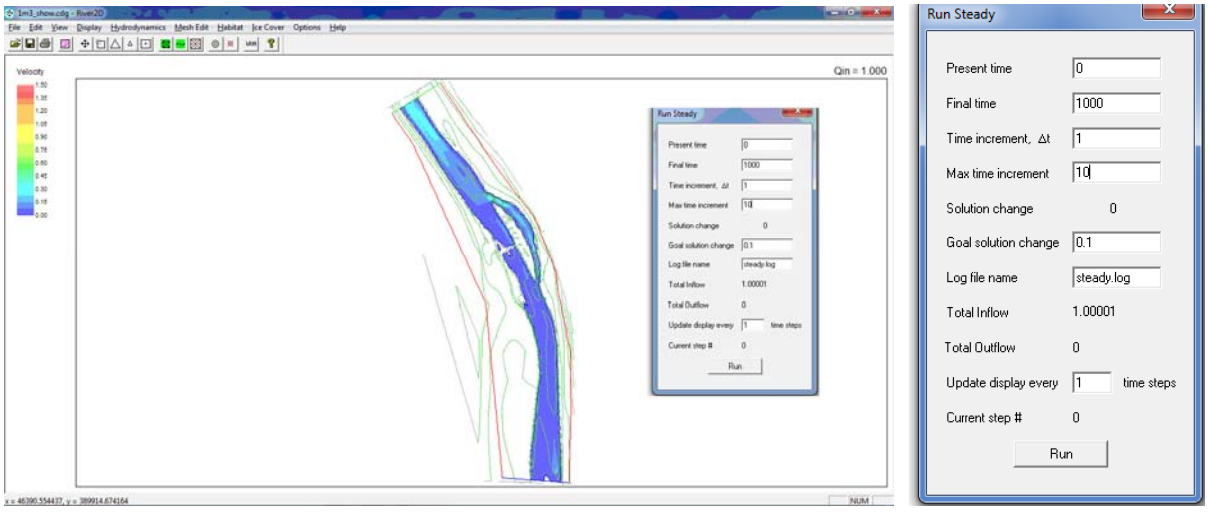

Figure 27 Model before running steady flow analysis and starting values

The value for the goal solution change is set to 0.1. This means that the iterative processing of the flow calculation is done until the difference in the results is lower than 10%. If the difference is higher the time increment will be lowered to point where the program is able to produce results with a change lower than that threshold. If the goal is reached the time steps will be increased again up to the maximum value set in the interface (see Figure 27 right hand side).

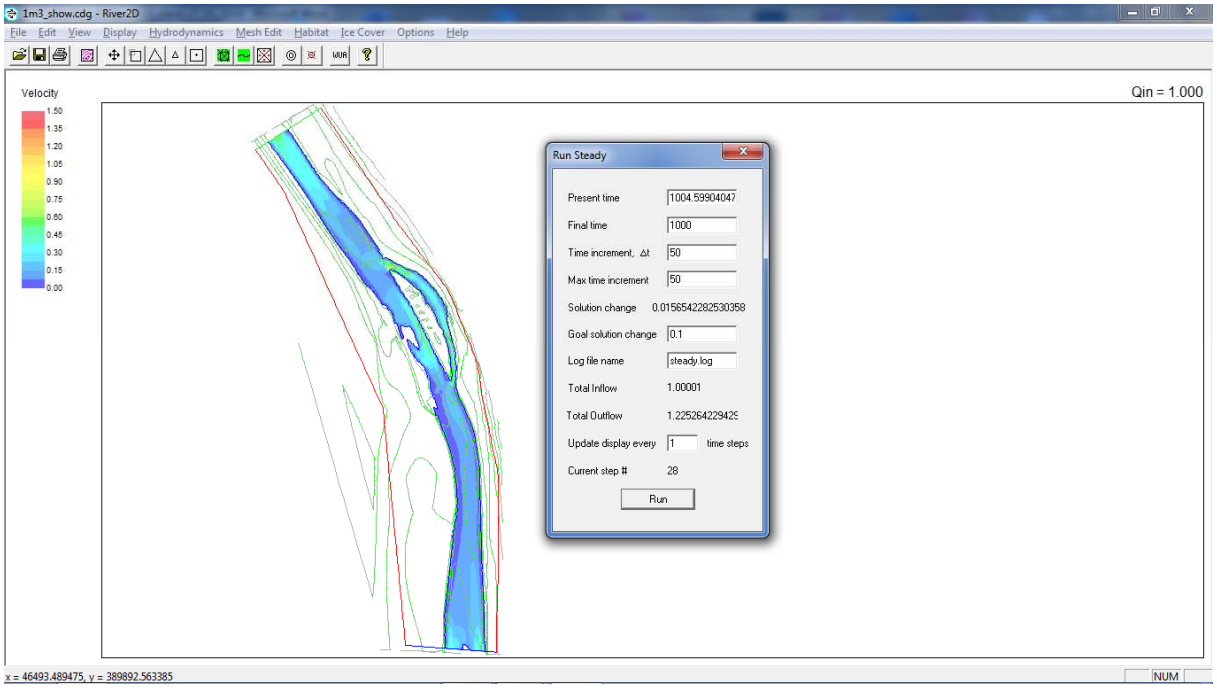

Figure 28 Screenshot taken during steady flow analysis

Figure 28 shows a screenshot taken during the simulation run. On behalf of the colouring in the flow part of the river we can see that the flow velocities are different to time step 0 (compare Figure 27 and Figure 28). The graphic is updated every time step taken in the simulation. The steady flow should be run until there is no change in the velocity distribution to be seen and Q_{in} equals Q_{out}. The results can be saved as a picture or in a tabular form as Excel file. This is done under "Habitat → Save Physical Attributes". As node numbers and the position of the nodes changed after simulation in this thesis the analysis of the results derived from River2D were analysed in a graphical way on behalf of reference areas and cross sections, which derive from the location of the spawning sites.

2.4. On site observations and collecting the dataset for the final calibration

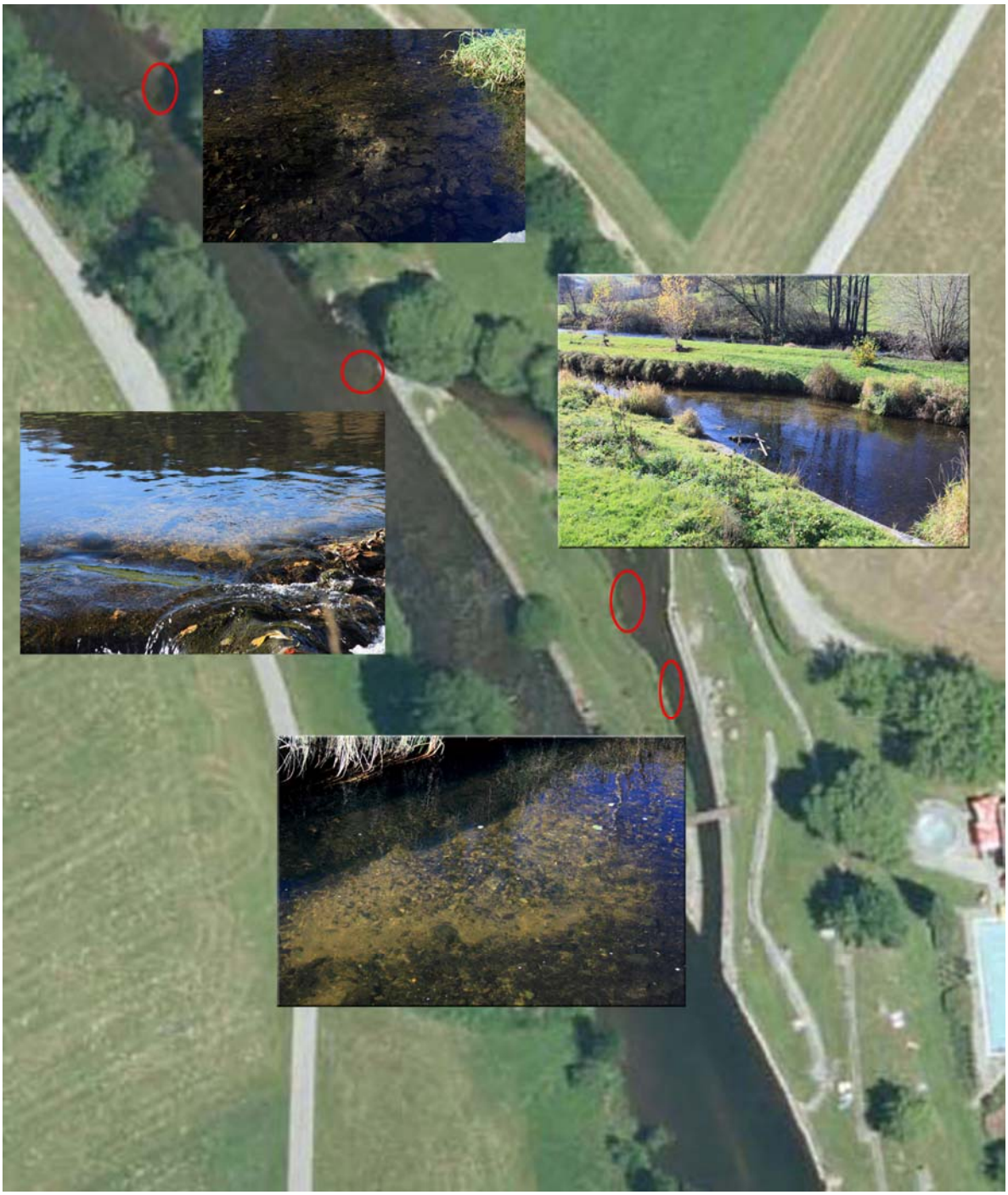

Figure 29 Spawning sites within the research area observed on October 31, 2013

The data collection for the final calibration of the models created in the year before was done at the end of October 2013. The data collection was combined with an on-site observation of

the spawning grounds on the research area as well as at selected spots at the power station in Schlägel downstream and the junction with the Hammerbach creek upstream of the research site. In Figure 30 two different spawning sites are shown which were fotographed at the on-site observation. In the left picture the “spawning hotspot” can bee seen. This is the lighter coloured area in the riverbed in the middle of the picture. During summer the area covers with algae and which gives the riverbed a dark brownish colour. With the excavation of the spawning site the algae is removed from the surface and the plane gravel can be seen afterwards. In the left picture two male brown trouts are waiting on the spawning site for a female.

Figure 30 Spawning sites at the research area (left) and Hammerbach creek (right)

The choice to set the sampling cross sections as close as possible to the spawning sites was taken because spawning season had already started. The redds should not be disturbed or even destroyed by stepping into so it was not possible to take measures directly on the cross sections where the spawning sites are situated.

The data received in this observation was further on used to calibrate the channel bed roughness as well as the ratio of discharge. Hereby the velocity in the sidearm was measured close to the redds on three different cross sections and one cross section was measured in the main channel upstream of the diversion point.

The velocity measures were taken with the OTT ADC which is a digital current meter. The data points were collected for depth averaged values. This means that the velocity was measured at a 40% height above the ground of the depth at the specific point. The distance between the points in the sidearm was either 0.5m or 1m across the section measured (XS1 to XS3). The 0.5m distance was chosen for higher resolution at spots where the flow depth changed more while 1m distance was chosen for parts with about the same depth. For the upstream measuring in the main channel a distances of 1m and 2m between each point was chosen (XS4 in Figure 31) for the same reason as the different distances used in the sidearm.

The velocities and positions were transferred to an Excel mask provided by the Institute to calculate the discharge and the average velocity at the cross section. The four cross sections chosen were later compared with the results from the modelling approaches. The differences between the measured data and the simulated data are resulting from some changes in the topography had been taken place during summer in the riverbed like:

- additional rocks placed upstream of the spawning hot spot
- changes in topography according to the high flood event in June

But it has to be mentioned that the over all topography remained the same and therefore and for time reasons the models were not changed in the topography. The comparison showed that the roughness values chosen are delivering a result that is in the threshold levels set for this thesis ($\pm 10\%$ of the results for the velocities).

Figure 31 Cross sections of the on-site observations and discharge measures in October 2013 for the final calibration in HEC-RAS

Another problem with the measures of the velocity was the low water levels at the day and the transported material (leaves, small branches etc.) To receive a result the velocity is measures

over 30 seconds and then averaged directly in the device. When a leave floats through the measure field it might change the velocity measured.

The low water level also might have had an influence to the measure. As it was done at a 40% height as along the cross sections larger cobbles etc. have influence on the local velocities (turbulence, local increase of the velocity) which cannot be simulated accurate with the degree of detail in the models. The calibration showed that the model was accurate and the results are accurate to use the data produced.

In Figure 32 the input mask for the Excel sheet is shown. On top the area is defined. Further on the date of the observation, the cross section name and the width of the profile (B) have to be typed in.

Teststrecke: Aigen/Flussbad

Aufnahmedatum: 31-Oct-13 Bemerkung: Messung 1

Meßprofil: XS 2

Profilbreite B = 7.00 m

Meßlotrechte	1	2	3	4	5	6	7	8	9	10	11	12
Abst.v.l.Ufer [m]	0.500	1.000	1.500	2.000	2.500	3.000	4.000	4.500	5.000	6.000	6.500	7.000
Wassertiefe [m]	0.120	0.210	0.320	0.350	0.350	0.380	0.400	0.420	0.420	0.400	0.350	0.250
Abstand von der Sohle [m] / v [m/s]	0.048	0.010	0.084	0.020	0.128	0.070	0.140	0.170	0.140	0.260	0.152	0.360	0.160	0.330	0.168	0.280	0.168	0.220	0.160	0.280	0.140	0.130	0.100	0.010
f_{vi} [m²/s]	0.001	0.003	0.018	0.048	0.073	0.109	0.106	0.094	0.074	0.090	0.036	0.002
v_{mi} [m/s]	0.008	0.016	0.056	0.136	0.208	0.288	0.264	0.224	0.176	0.224	0.104	0.008

A = 2.323 m²

v_m = 0.181 m/s

Q = 0.421 m³/s = 421 l/s

Figure 32 Input mask for depth averaged velocity and discharge calculations

Further on the distance to the riverbanks and the absolute water depth have to be defined. After defining the absolute distance to the 0m-point (left riverbank) and the depth at the spot the measured velocities are put into the mask. Here measures at 6 different heights can be defined with the corresponding velocities. As the measures were taken for the depth averaged models only one point was measured as mentioned before. Therefore only the value for 40% of the depth and the velocity value are entered here.

- Abstand von der Sohle = Distance from ground
- v [m/s] = velocity at the point

Everything further down will be calculated automatically. Where as:

f_{vi} … Velocity field over the vertical column

v_{mi} … Average velocity for the vertical column

A … Flow area of the cross section

v_m … Average velocity for the whole cross section

Q … Discharge calculated from velocity and flow area

After calculating the discharge from the measurement for the main channel upstream and the sidearm downstream the resulting discharges were fed to the models and the results were compared with the data gathered on site. As the models were already calibrated with projects done before no more changes were needed and the velocities were within the tolerance levels.

2.5. Temperature data

For the time series measured for this thesis two sensors were placed in the river on the positions shown in Figure 33. One collected the open water temperature since December 2008 as part of the monitoring program at Große Mühl River. This sensor was positioned on top of the modelling area. The other one was placed in the gravel bed to measure the temperature in the interstitial area. The time series started in December 2012 and was placed there as part of the thesis.

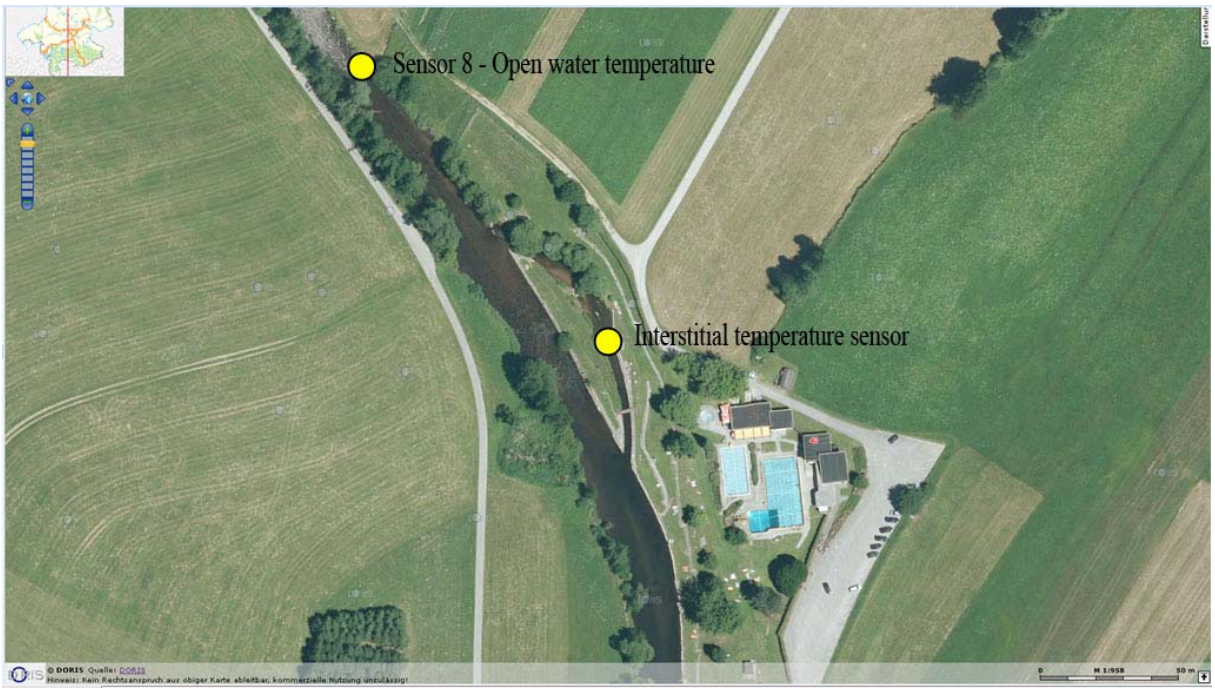

Figure 33 Positions of the temperature sensors at the research area

For the open water sensor the data was collected in a two hours interval from December 7 2008 until May 9 2013. The data is stored in the internal data logger of the sensor and was transferred every 4 month to a hard drive. The sensors used for this thesis are MAXIM iButton sensors for measuring temperature. To see a detailed description f the sensor and the

program added to it see the datasheet in the appendix. The sensor is placed in a waterproof case with a chain, so that the sensor can float in the water. The resulting temperature curve is shown in Figure 34.

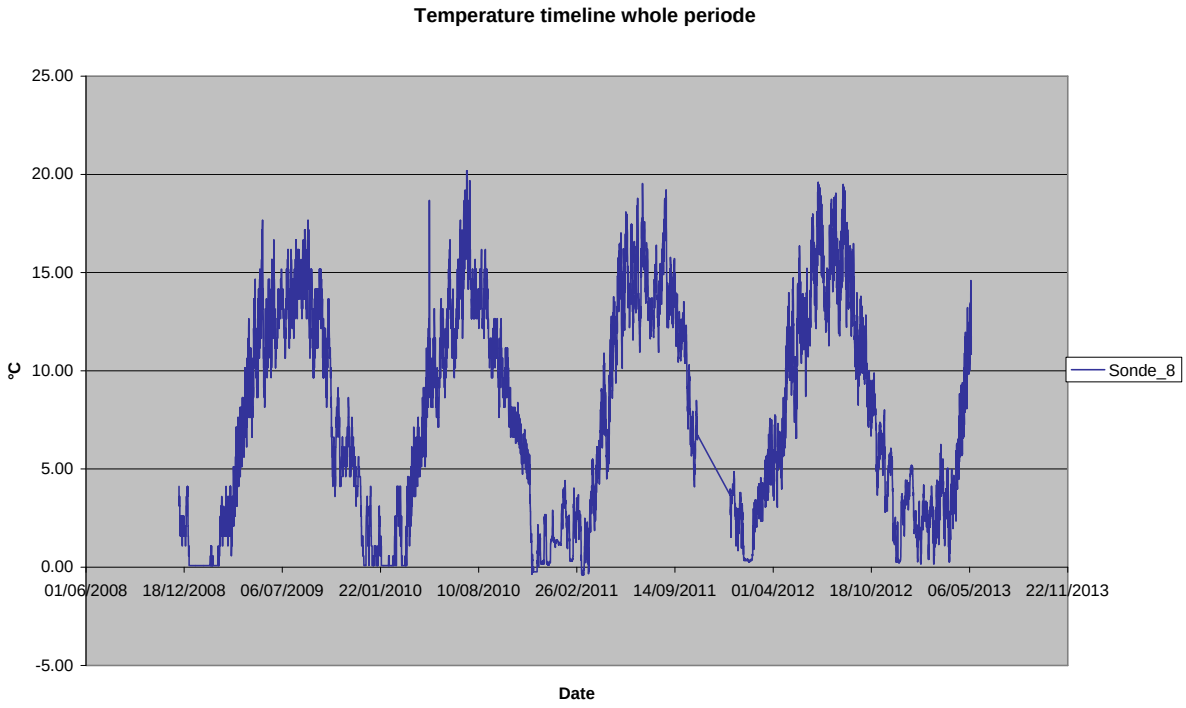

Figure 34 Temperature – Time – diagram derived for the open water flow (all data)

The sensor for the interstitial temperature was put into a water proof case as well. The case was buried in a depth of about 20cm and fixed in the riverbed from December 12th 2012 and taken out of the water May 1st 2013. The time interval set was one temperature log every hour (Figure 35).

The data is stored in the internal data logger in the specific data format from MAXIM. As mentioned before every 4 month the data is transferred to a hard drive and with the iButton software transformed to a .txt file. The data stored includes date, time of the measure taken and the temperature.

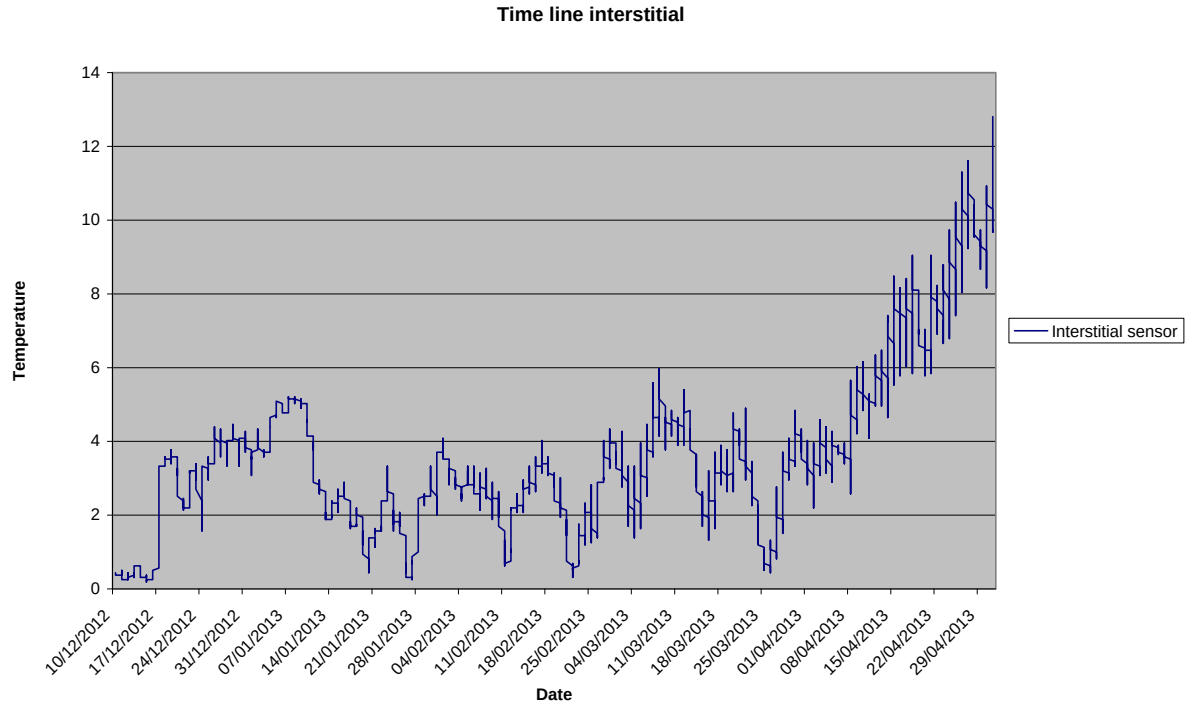

Figure 35 Time line interstitial sensor

The .txt file was imported into Microsoft Excel. The first step taken in the analysis of the temperature data was to create a temperature-time diagram to see if the data stored is complete and accurate. As we can see in the chart (Figure 34) there is a data gap between October 29, 2011 and January 4, 2012. In this time the data logger recorded an internal error and therefore no data has been stored for the open water sensor during this period. The tolerance error for both sensors is the same. Therefore it has not been taken into account in this thesis. The temperature difference between the two sensors is the main part of the analysis.

As the data logging intervals are different for both sensors the data with the same time and date was copied to an extra worksheet and the differences for the data at the same time were calculated afterwards. The difference in temperature between the open water flow and the interstitial area was calculated and will be analyzed later on in this thesis. The analysis was done for the whole time interval when data for both sensors are available. The focus here is set on the time intervals, where ice cover can be in place (temperatures around 0°C).

2.6. Sediment data

The data of the riverbed sediments were collected beforehand of this thesis. The results of the sieving samples were provided by the Institute of Water Management, Hydrology and

Hydraulic Engineering at BOKU. After analyzing the grain size distribution for the suitability for spawning (grain size and content of fine sediments) the possibilities according to the natural renewing process was analyzed. Therefore the sediment data was used to determine the critical velocity and the critical shear stress for initiation of motion derived from the samples. Afterwards the velocities and the shear stress derived from the modelling part were used to determine the discharge needed to renew the riverbed at the spawning sites.

The data provided by the Institute is shown in Table 4. Where as:

SL … Surface layer

SSL … Subsurface layer

D … Diameter

Table 4 Characteristic grain sizes derived from Große Mühl River bed analysis

	SL_1	SL_2	SL_3	SL_4	SL_5
	(mm)	(mm)	(mm)	(mm)	(mm)
D(10)	3.75	7.51	1.78	2.18	1.2
D(20)	56.26	40.4	3.2	3.83	2.11
D(30)	68.53	59.66	6.48	8.91	2.71
D(40)	92.16	74.26	12.07	15.1	3.48
D(50)	118.58	93.37	18.53	22.11	4.61
D(60)	152.59	120.49	27.6	35.56	6.35
D(70)	196.34	155.5	44.25	54.65	8.65
D(80)	252.64	200.67	73.37	77.45	11.54
D(90)	325.08	258.98	101.79	99.12	16.85
D(m)	30.94	35.89	35.47	38.56	7.27
	SSL_1	SSL_2	SSL_3	SSL_4	SSL_5
	(mm)	(mm)	(mm)	(mm)	(mm)
D(10)	3.08	3.11	0.61	1.21	0.63
D(20)	9.9	14.4	1.97	2.18	1.5
D(30)	17.72	28.48	3.05	3.02	2.28
D(40)	25.64	39.55	5.39	4.27	2.93
D(50	36.39	52.05	12.4	7.1	3.77
D(60)	51.05	62.86	23.85	11.34	5.34
D(70)	64.98	71.28	45.93	18.53	7.82
D(80)	91.92	80.78	73.14	35.27	11.89
D(90)	107.19	93.63	96.96	67.89	19.01
D(m)	47.48	51.29	32.8	19.52	7.57

For this thesis the values from the columns of SL_3, SL_4, SL_5 and SSL_3, SSL_4, SSL_5 were taken to account as they are situated at the spawning sites in the research area. After doing the analysis the critical shear stress for the D_{50} grain size was used to determine the threshold value for a renewing of the riverbed. The calculations were done after Meyer – Peter – Müller and by using the Hjulström – Curves (Figure 36). Different to the Shields diagram the Hjulström curves are calculated for flow velocity referring to the grain size instead of the shear stress.

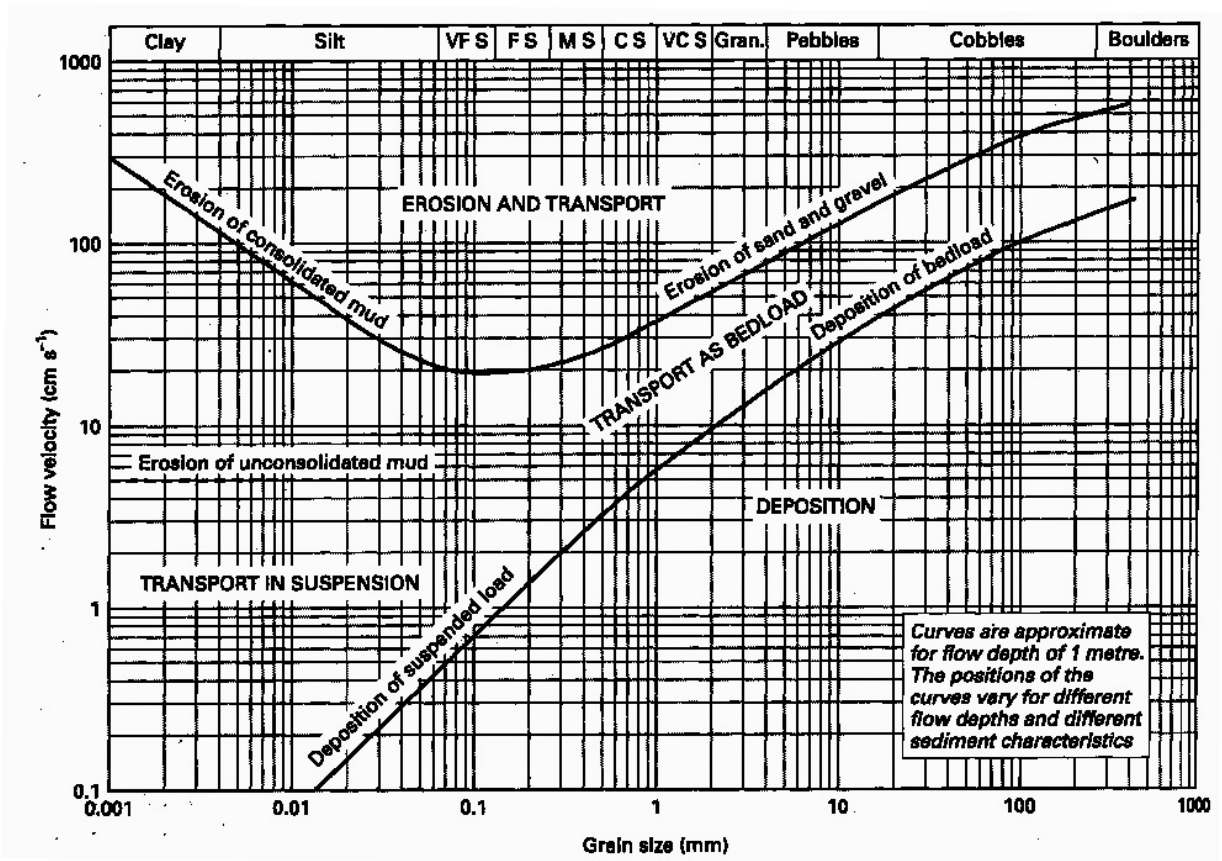

Figure 36 Hjulström Curve (source: http://www.coolgeography.co.uk/A-level/AQA/Year%2012/Rivers,%20Floods/Long%20profile/hjulstrom_curve.jpg, 17. 02. 2014)

In Figure 36 it is presented that the curves are valid for a flow depth of approximately 1m. The flow depth at the spawning sites is normally below this value during spawning season. But the value of one meter depth is valid for this thesis as the critical velocity and therefore the discharge on the spawning areas is analyzed. The renewing process takes place in events with high discharge when the armouring layer breaks up and the gravel and pebbles underneath are eroded and transported downstream. This means that gravel supply from

upstream is given. The area of interest is found within the range of optimal grain sizes for spawning areas. As mentioned in Chapter “Substrate and Grain size” the important grain sizes are:

- Minimum value 8mm
- Average D_{50} of the surface layer examples
- Average D_{50} of the sub surface layer examples
- Maximum value of 64mm

The formula used for this thesis is the basic Meyer-Peter&Müller formula which is defined as follows (Patt & Gonsowski, 2011) :

$$\tau_{Cvi} = 0.047 \cdot (\rho_s - \rho) \cdot g \cdot d_m$$

Formula 15

Where as:

τ_{Cvi} … critical shear stress $\left[N/m^2\right]$

ρ_s … bed material density (2650 $\left[kg/m^3\right]$)

ρ … water density (1000 $\left[kg/m^3\right]$)

g … acceleration due to gravity (9.81 $\left[m/s^2\right]$)

d_m … grain size diameter

The results of the critical shearstress are later on compared with the results from HEC-RAS as the shear stress occurring at the cross section is an output of the program. The results from River2D will be compared with the resulting critical velocities from the Hjulström curves. As the critical shear stress is defined as stress applied where erosion starts the critical velocities for the grain sizes were chosen as well from the curve where the transport as bed load starts.

3. Results

The following chapters show the results worked out during the time of this thesis. The first part shows the results of the modelling in relation to the on site observations. The spawning sites observed were taken into account during the analysis of the data derived from the simulations to see the changes over the cross sections through out the scenarios. The chapters are split into the same parts as in the methodology part of this thesis. First of all the results from HEC-RAS approaches are shown, moving on with the results of the River2D part of this thesis, followed by the analysis of the temperature data and the analysis of the bed material and the renewing process of this area. The modelling topics are structured in the various discharges and the tree scenarios (open water flow, with ice cover and with ice cover and jam in the main channel).

3.1. HEC-RAS modelling

The HEC-RAS modelling part is split into 4 sections. These sections are

- Open water flow
- Ice cover on sidearm
- Ice cover on side arm and ice in the main channel
- Comparison between the three sections above in the “Comparison” part

This structure derives from the way the models are built in HEC-RAS. This means that, as mentioned before in the methodology section, for each part a set with varying discharges was set up. In the following chapters the main structure is to see what happens along the whole modelling area and especially in the sidearm as it is a “spawning hotspot” in the region. Besides the graphical analysis with the plots from HEC-RAS the results were analyzed by using Excel and calculating the differences for each profile (PF, amount of discharge). At the beginning it has to be mentioned that the longitudinal scale (Main Channel distance) in HEC-RAS always starts with 0 (zero) at the lowest point of the reaches displayed in the graph. Therefore the plots derived directly out of HEC-RAS always start at the length 0. This is the case for the plots of the whole section as well as for the plots from the sidearm.

3.1.1. Open water flow

The scenario is open water flow which means that there is no ice cover and no ice jam in the model. The additional scenario was added to see if there is a significant change in the flow behaviour in the case of high flood events larger than HQ_3. As these floods normally occur in late spring or early summer the additional scenario was not taken to account for the winter modelling part. In Figure 38 and Figure 39 the resulting flow depths are shown. In Figure 38 it can be seen that at the divide (at length 283m of the simulated river section) the water level drops right after the inlet to the side arm. This is the case up to a discharge between profile 5 and 6. This correlates with a discharge between 5m³/sec and 10m³/sec.

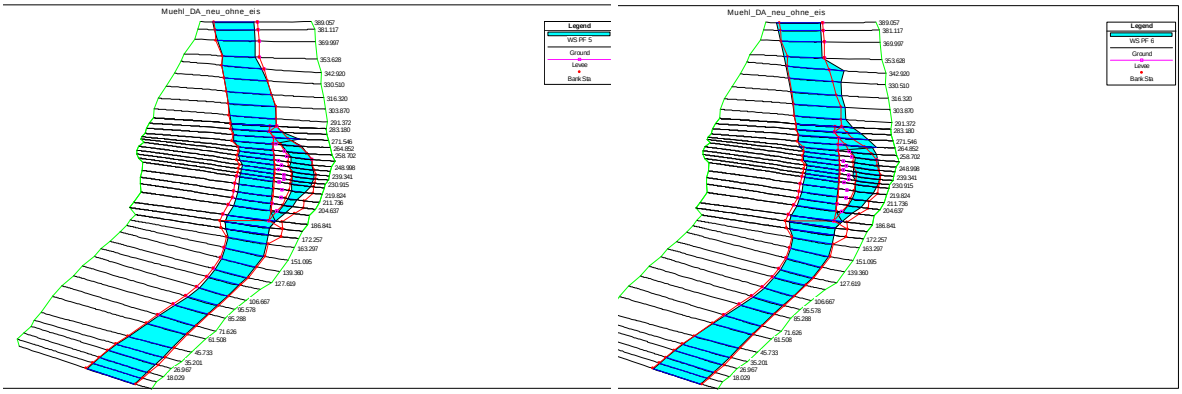

Figure 37 3D-display of the simulation area (Profiles 5 and 6)

After this point the river starts to overtop the bank stations which can be seen in Figure 37. From the discharge level of 30m³/sec (PF 10) on the island in the river is completely overtopped. From there on the water level in the side arm and the main channel are equal. The water levels in between vary as the island is partly overtopped and water is exchanged between the main channel and the side arm.

The next thing seen is that from 200m on downstream the water level is affected by the area after the joint of the two river parts and the water level doesn't show any significant changes (Figure 38).

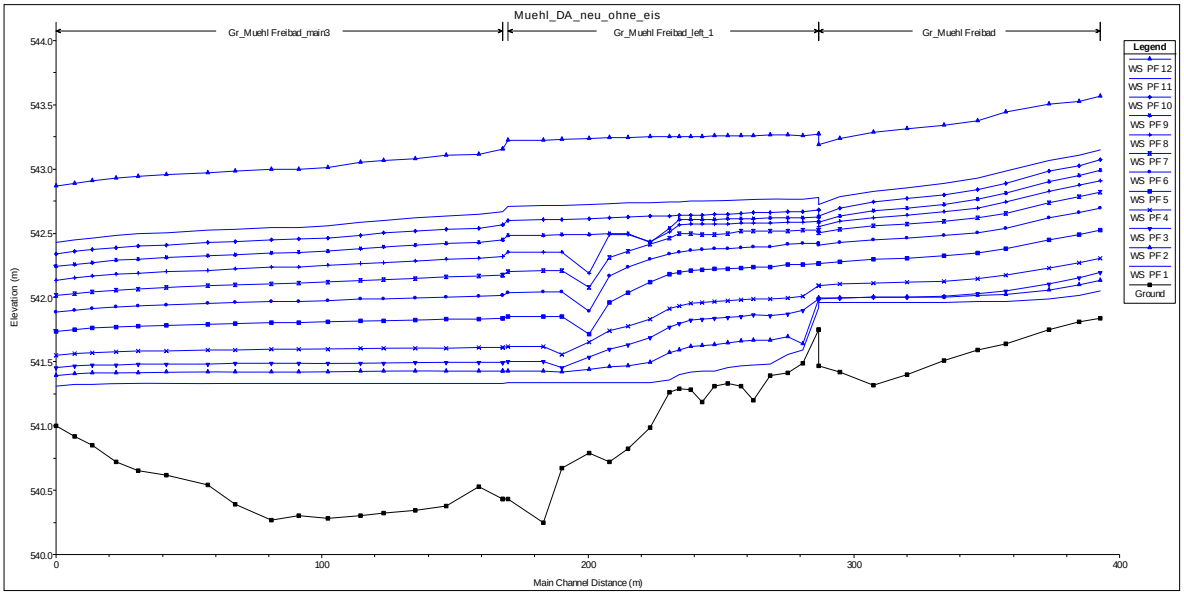

Figure 38 Flow depths at the open water flow scenario for the sidearm (main channel left out)

In Figure 39 the flow depth of the main channel is shown. For profile 1 (1m³/sec) the divide of the sections is clearly to see with the decrease of the water level at main channel distance 283m. Different to the side arm the water level in the main channel is constantly rising according to the increase in discharge. The curves remain almost the same up to the point when the island is overtopped. Further on the graphs show that after the overtopping of the island the changes in flow depth only vary in depth according to the increase in discharge. The so the threshold level here is profile 9. This correlates with a discharge of 30m³/sec at the input side of the modelling area. After the slight drop in the topography in between main channel distance 250m and 200m the water level again is influenced by the lower area and is more or less constant to the outlet of the modelling area. It also can be seen that at the joint the water level does not increase any further which correlates with the field observation done.

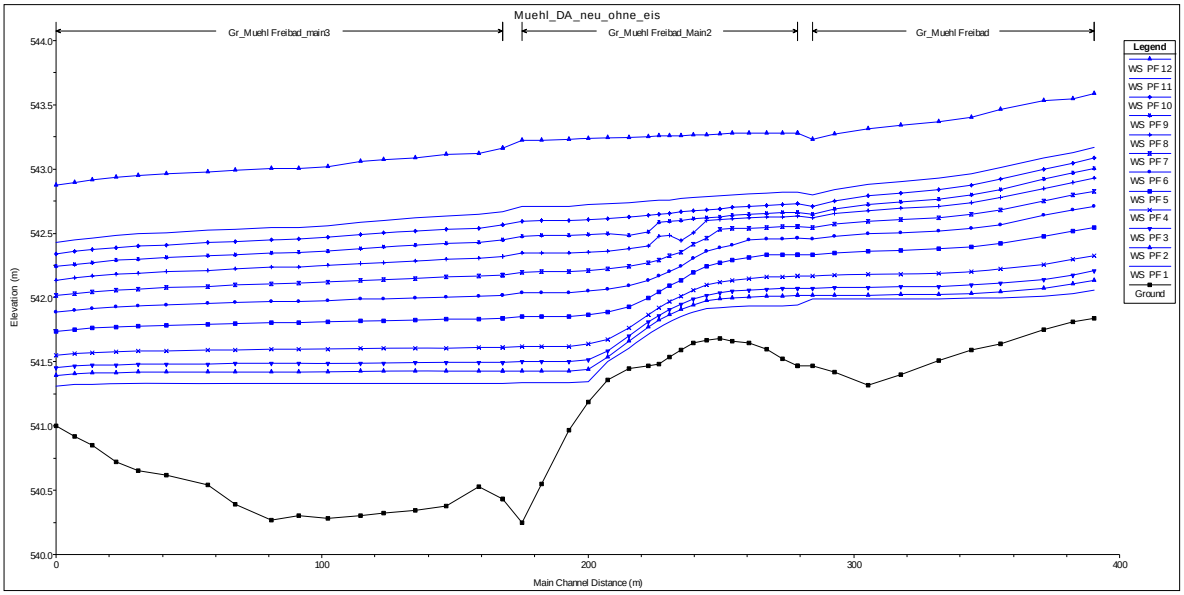

Figure 39 depths at the open water flow scenario for the main channel (sidearm left out)

Compared with Figure 38 it can be seen that a difference in the water level occurs for low flow conditions right after the divide at 283m until the area where the influence of the downstream part occurs (~200m to 220m, depending on the discharge). Looking at the section in between these areas the graphs show this. The following figure (Figure 41) shows the cross section at 249m (stitched together). It can be seen that the water level in the sidearm is at 541.5m (above sea level) while in the main channel is at an elevation of 541.9m. (Figure 40) This means that the first approach of having one reach along the river section with one resulting water level would have lead to inaccurate results.

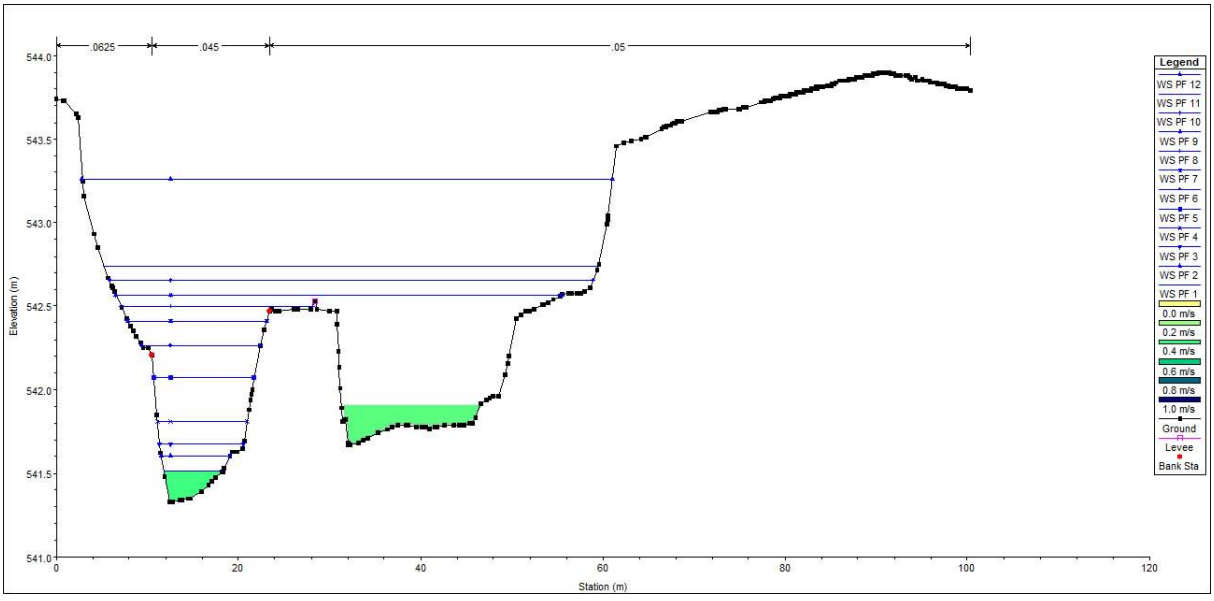

Figure 40 Difference in water levels between sidearm and main channel (Cross section 248.998)

The velocity distribution in Figure 40 is not representative as it is only one velocity shown across the section. A higher resolution for the distribution will be used in the comparison part of this thesis to see the difference between the modelling approaches.

Taking a look at the cross-sectional averaged velocities along the river section it can be clearly seen that in the first section of the river and the final part of the modelling section the velocity rises with the increase of discharge. Looking at the side channel a different flow behaviour can be observed.

During low flow conditions the influence of the step at the inlet can be observed. This is shown with the velocity peak at 283m where the velocity rises from 0.1 to 2.71[m/s] and remains almost constant between 0.4[m/s] and 0.5[m/s] until the junction. In general it can be said: The higher the discharge the lower the influence of the split up part (Figure 41 and Figure 44).

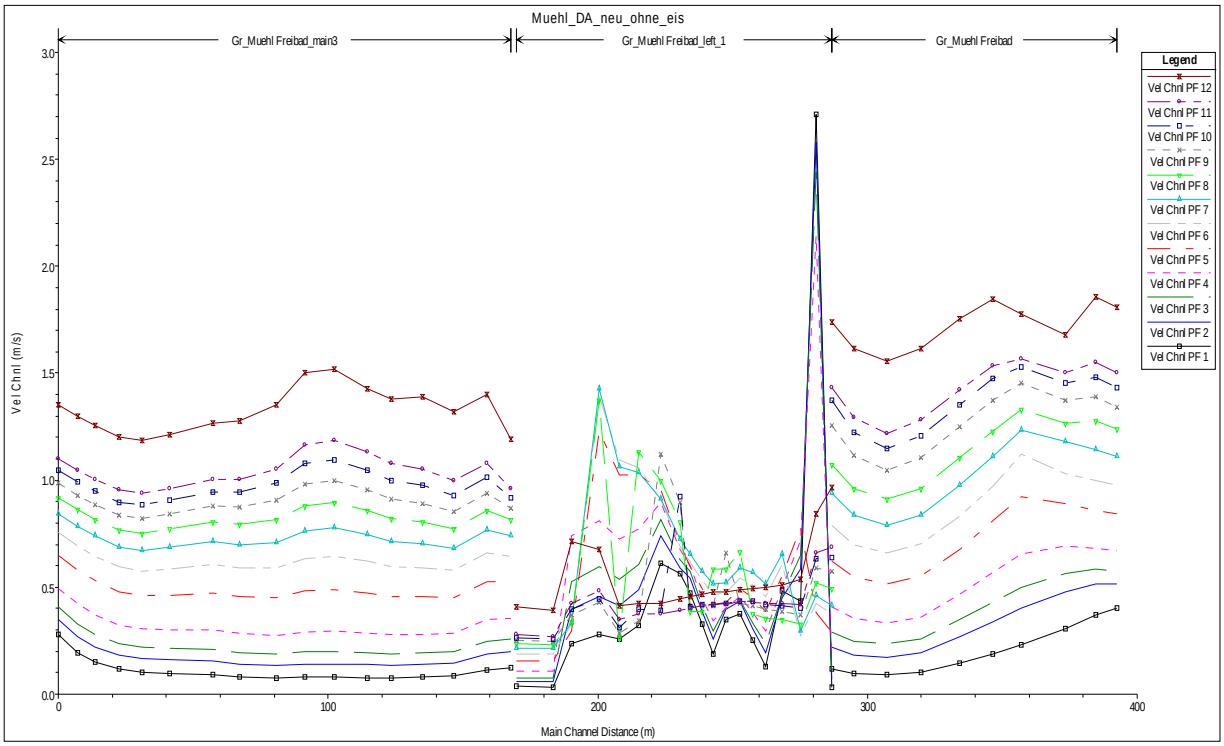

Figure 41 Flow velocities for the whole modelling area with sidearm (main channel left out at the widening, all profiles); open water flow

The graph in Figure 42 shows that the velocity in the main channel at the dividing section is mainly influenced by the discharge. The divide makes a difference in the velocity of 31% which means that the velocity drops by the amount of discharge entering the side channel. As soon as the island is overtopped similar development to the flow depth can be observed. The resulting increase in flow area leads to a flattening in the velocity curve. The average velocity remains almost constant through out the river sections.

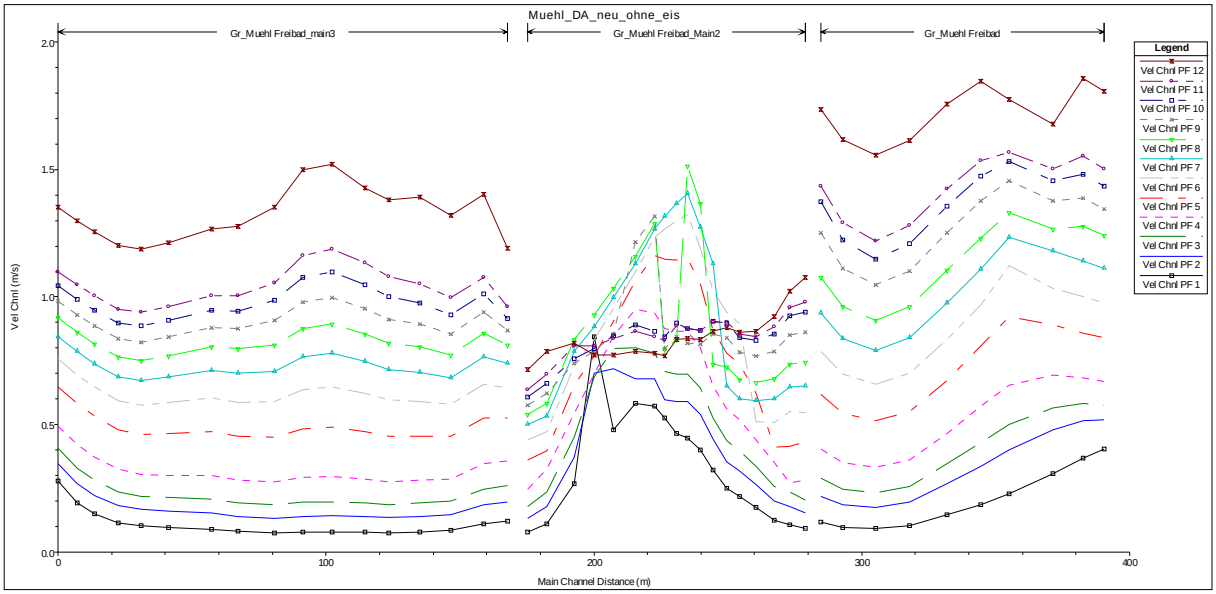

Figure 42 Flow velocities for the whole modelling area of the main channel (side channel left out at the widening, all profiles); open water flow

The following graphs show that the inlet into the side arm has an influence to the water levels up to an discharge of 5[m³/s]. Higher discharges overtop the small dam easier and the influence decreases. In the high flood scenarios almost no influence is given by the topography of the riverbed to the changes in flow depth along the river section. Figure 44 shows the detailed view of the change in velocity along the side arm. While the changes in velocity at the beginning of the section decrease with increasing discharge, it increases at the downstream part. This can be explained with the shape of the river. While the upstream part is a more or less natural part the downstream part is channelized. Therefore the increase in discharge leads to an increase in velocity. The part from 0m to 16m (channel distances from ~170m to ~285m) is already influenced by the outlet and the opening section into the main channel. The influence given by the island in case of a high flood event is a reduction in velocity as the whole section is functioning as a widening part in the river.

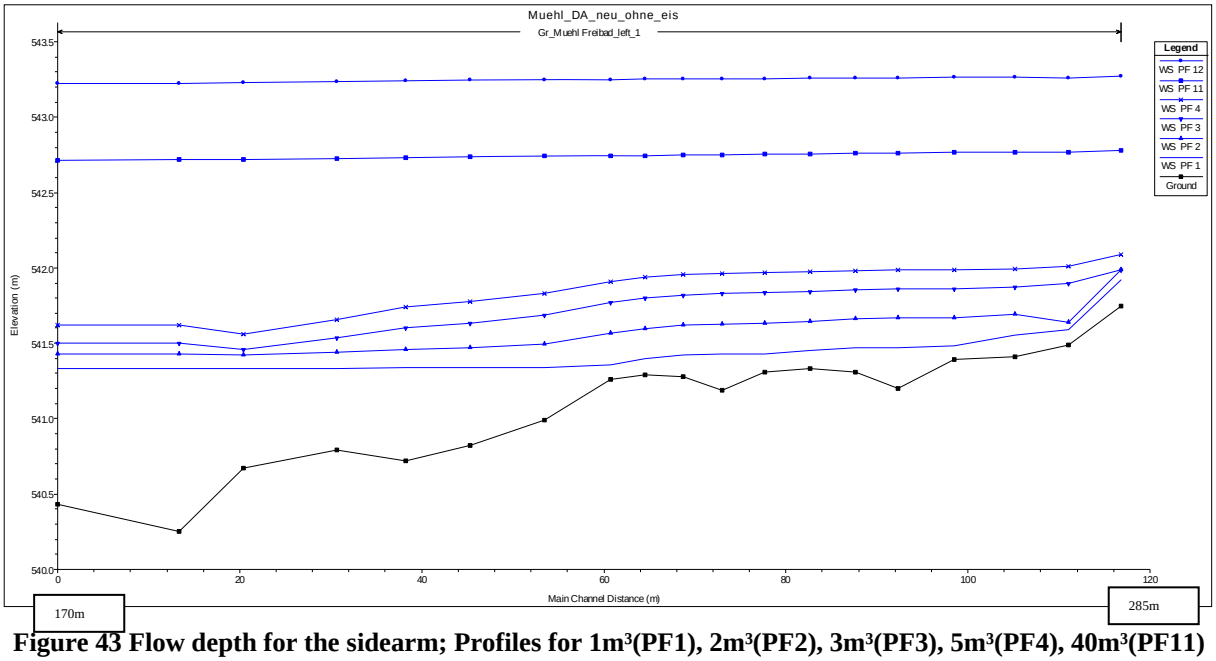

Figure 43 Flow depth for the sidearm; Profiles for 1m³(PF1), 2m³(PF2), 3m³(PF3), 5m³(PF4), 40m³(PF11) and 70m³ (PF12)

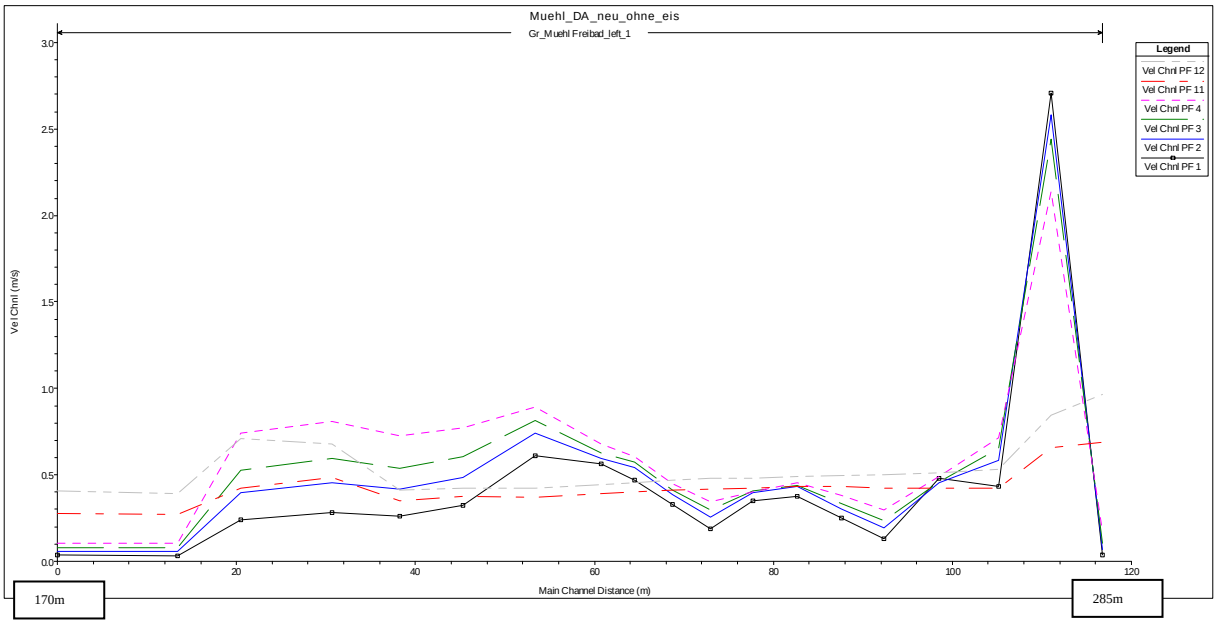

Figure 44 Flow velocity for the sidearm; Profiles for 1m³(PF1), 2m³(PF2), 3m³(PF3), 5m³(PF4), 40m³(PF11) and 70m³ (PF12)

3.1.2. Results with ice

The following chapter will show the results derived from the HEC-RAS simulations with ice cover on the side arm. Different to the results from the open flow part the scenario with 70 [m³/s] discharges was left out. This was done because the open flow part did not show a significant difference between the high flood event and the discharge of 40 [m³/s].

The results following are derived from the scenario that the side arm with the spawning areas is covered with a 10cm thick ice shelf while the main channel remains ice free. As mentioned before, this scenario may occur at the spawning site during winter months. Therefore it is important for the understanding of the processes in the area during the incubation time.

The main results from the HEC-RAS simulation for the ice cover scenario are shown in this chapter. The graph shows that the water level until the point of the divide is increasing proportional to the increase in of the discharge. At the point of the divide the water level drops until Profile 3 (discharge: 3 [m³/s]) (Figure 45). At Profile 4 the water level smoothens and the influence of the inlet reduces. A retaining effect upstream of the inlet can be observed for low flow conditions.

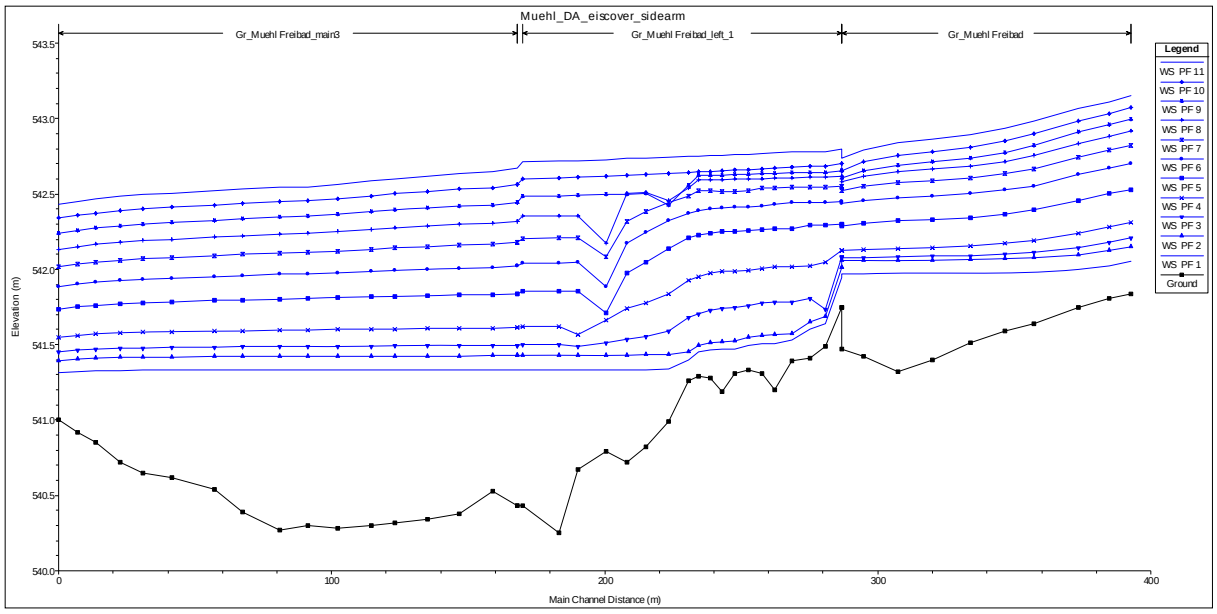

Figure 45 Water surface elevation for the ice cover scenario for the sidearm (main channel left out)

For discharges >5[m³/s] this effect cannot be observed anymore. From Profile 5 to Profile 9 a drop in flow depth can be observed at 200m. This is due to the shape of the riverbed and the surrounding areas as the water already overtops the channelized part of the sidearm as shown in Figure 46. The overtopping of the island starts with Profile 6 (Q=15[m³/s]). After Profile 9 (discharges larger than 30[m³/s]) the island is completely flooded. Downstream of the junction part the increase in water is again constant proportional to the increase in discharge. The lowest value of elevation at the outlet part of the section is at 541.3m above sea level. The highest point with the yearly high flood event discharge is found at 542.45m.

In comparison to the sidearm the changes in flow depth with increasing discharge are minimal. With increasing discharge the curve of the water level flattens out. The only

inconsistency in the curves occurs at Profile 8 when the water from the side channel and the main channel intermix and the profile of the island influences the interchange (Figure 47). At profiles for the longitudinal section it can be seen that the middle and the lower sections of the island are overtopped first.

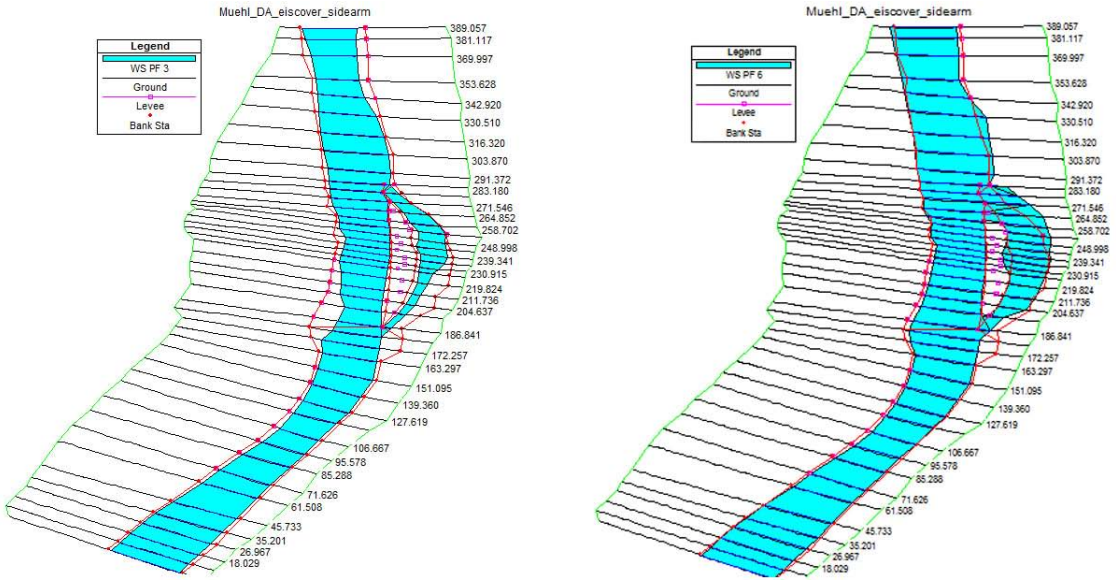

Figure 46 Water overtopping riverbed in sidearm; difference in extension between PF3 and PF6

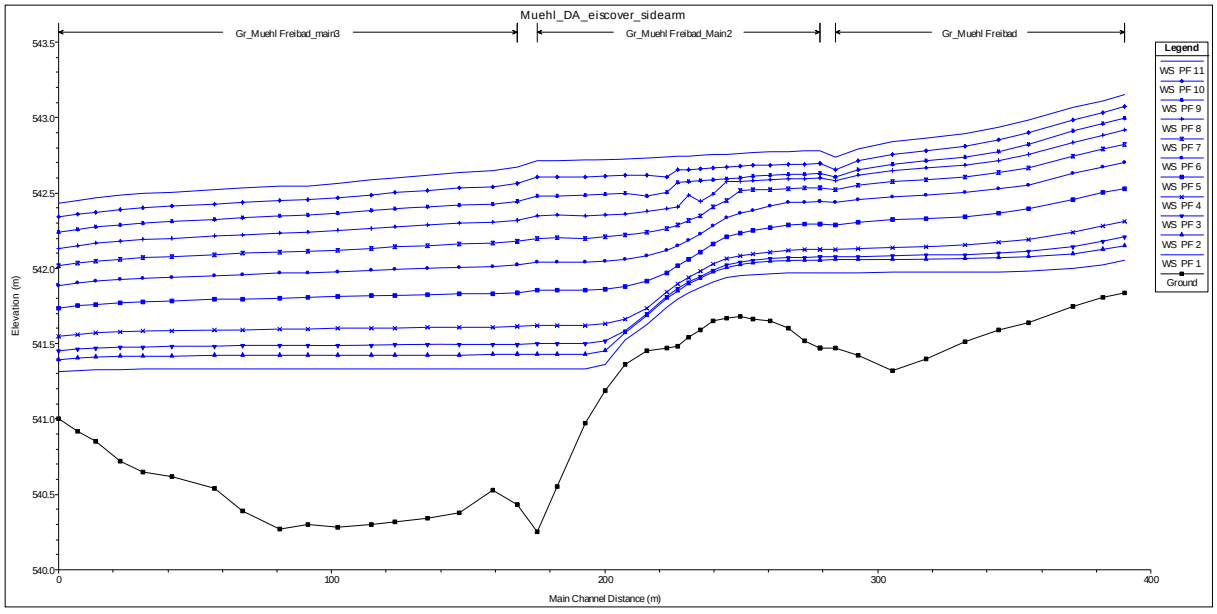

Figure 47 Water surface elevation at ice cover scenario for the main channel (sidearm left out)

Looking at the velocity distribution it can be said that the averaged velocities for the upstream and downstream section are homogeneous. Looking at the midsection of the area (Gr_Muehl Freibad_left_1) a different picture is shown. The main things to be seen in the overview are the peaks in Profile 4 with 2.46[m/s] at 280m and the increase in velocity from Profile 3 to

Profile 9 between 183m and 234m with the peak velocity of 2.43[m/s] in Profile 8. For Profiles 10 and 11 the velocity along the section is more or less constant. As there is no general trend found throughout the profiles, they will be analyzed later on in groups with similar flow conditions (Figure 48).

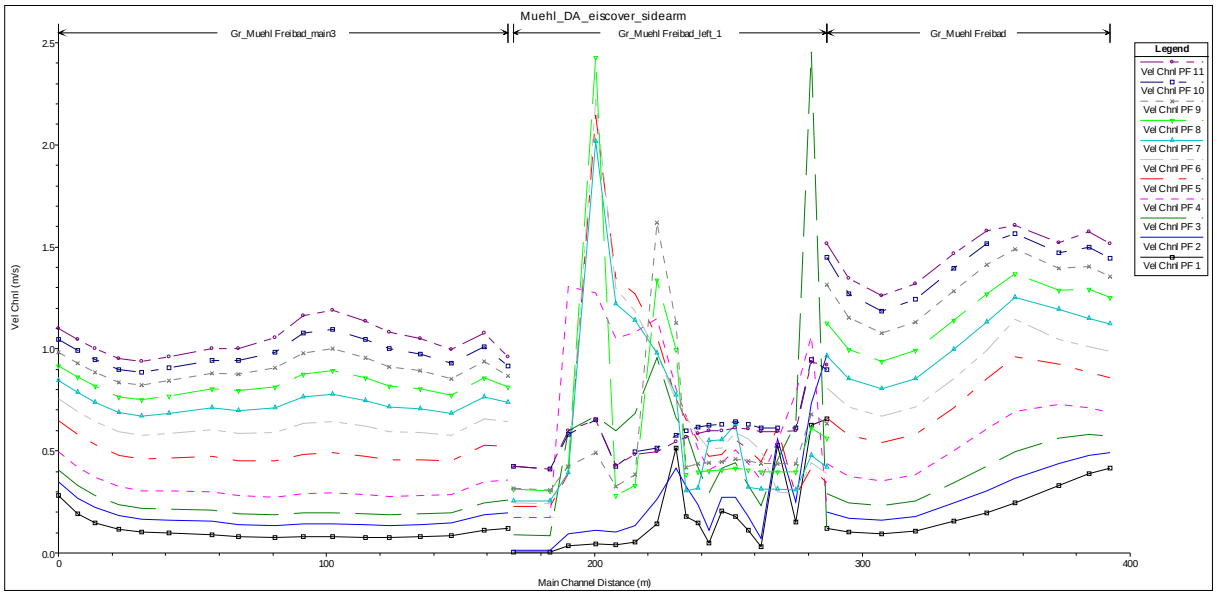

Figure 48 Flow velocities for the whole modelling area with sidearm (main channel left out at the widening, all profiles); Ice cover scenario

As mentioned before the distribution in flow depth for the ice cover scenario is rather homogeneous. This is not the case for the flow velocities. For Profile 1 and Profile 2 the highest velocity is found at the inlet of the sidearm. Afterwards the velocity decreases to almost 0[m/s] at the outlet part of the sidearm. Profile 3 has a peak of 2.46[m/s] at the upstream part of the section and decreases afterwards until the beginning of the channelized part. The velocity at the outlet is 0.09[m/s].

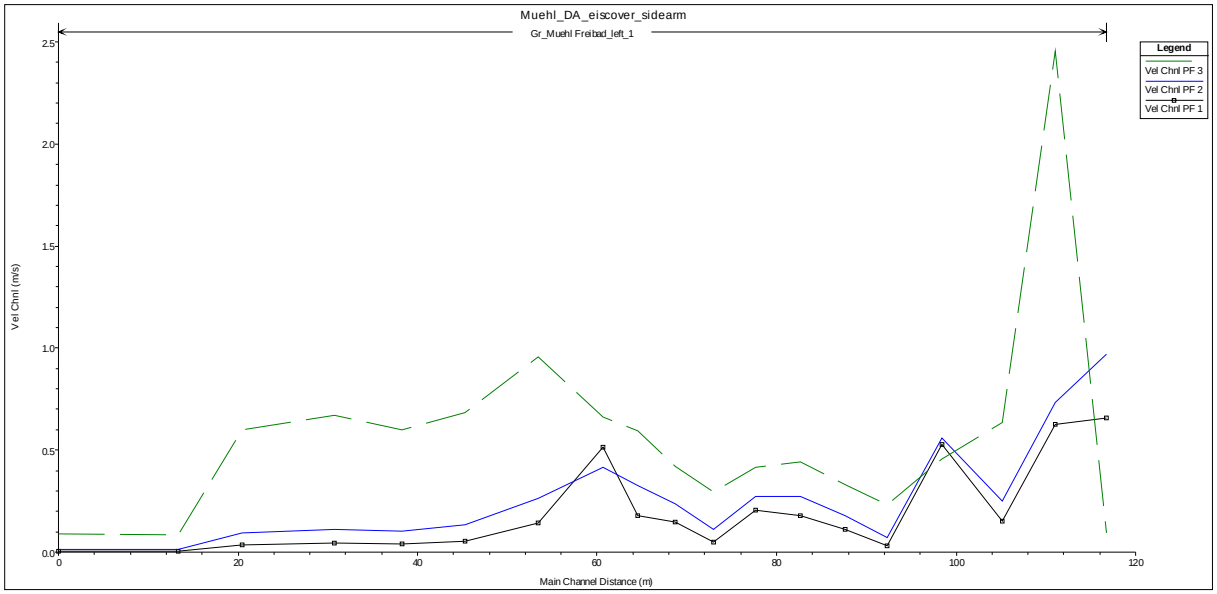

Figure 49 Flow velocities Profiles 1 – 3; sidearm; ice cover scenario

The following graph (Figure 50) shows the average velocity distribution for Profiles 4-8 (discharges from 5[m³/s] to 25[m³/s]). While in Profile 4 an influence of the inlet part can still be recognized this effect cannot be seen for the other profiles shown in the diagram. Further on the influence of the channelized part can be seen from station 64m (in Figure 50) downstream until the influence of the opening section to the main channel sets in. This effect leads to the increase in velocity which peaks as mentioned before at a velocity of 2.43[m/s]. The peaks of the velocity profiles correlate with the drops in water surface elevation (compare Figure 45). The peaks in velocity also show the areas where the island is not overtopped and therefore a reduction in the flow area occurs. After the island is completely flooded the flow velocity varies between 0.93[m/s] in the upstream part and 0.41[m/s] downstream without peaks along the section.

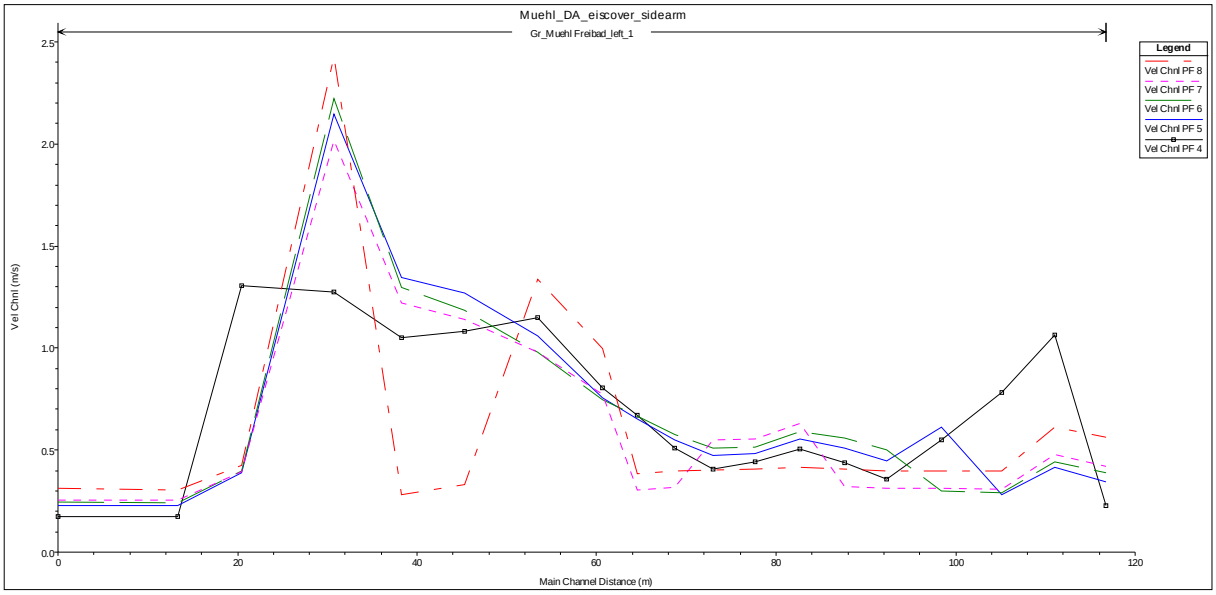

Figure 50 Flow velocities Profiles 4 – 8; sidearm; ice cover scenario

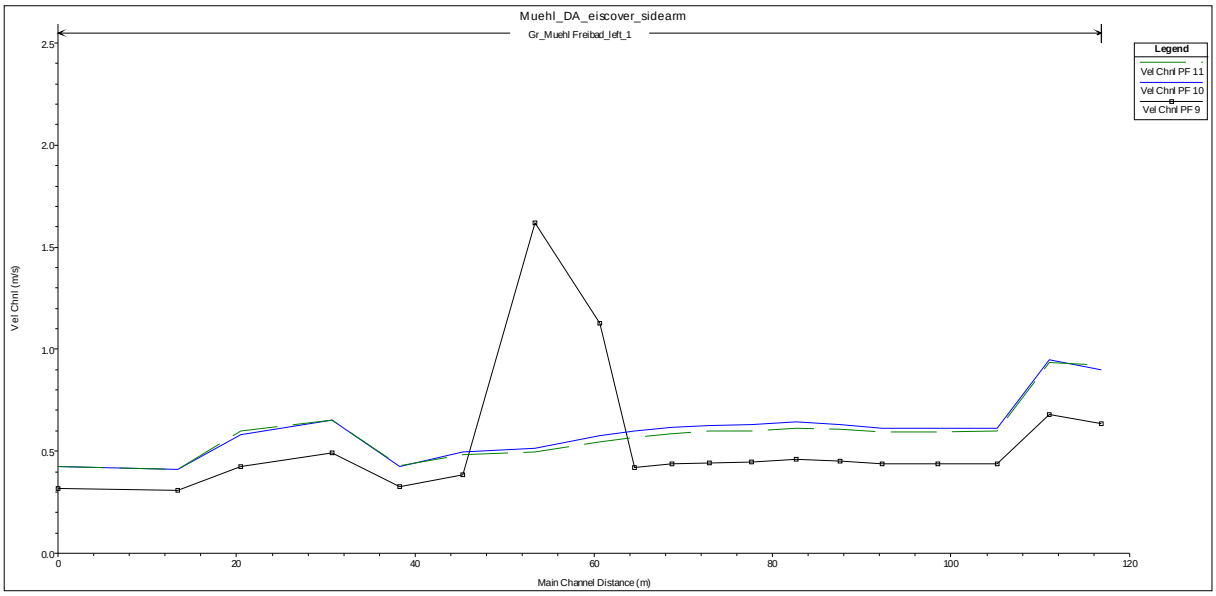

Figure 51 Flow velocities Profiles 9 - 11; sidearm; ice cover scenario

As there were no spawning areas found during the on field observation the results for the changes in flow velocity are only shortly mentioned here. For detailed results see the HER-RAS data attached to the thesis.

For the midsection – the section between the divide of the reaches upstream and the junction downstream – the graph shows that the peak of velocity is found at Profile 7. The peak in velocity moves upstream with increasing discharge until the island is overtopped and the flow area increases due to connection between the reaches. For Profiles 10 and 11 the curves are the same as for the side arm. All velocity curves are shown in Figure 53.

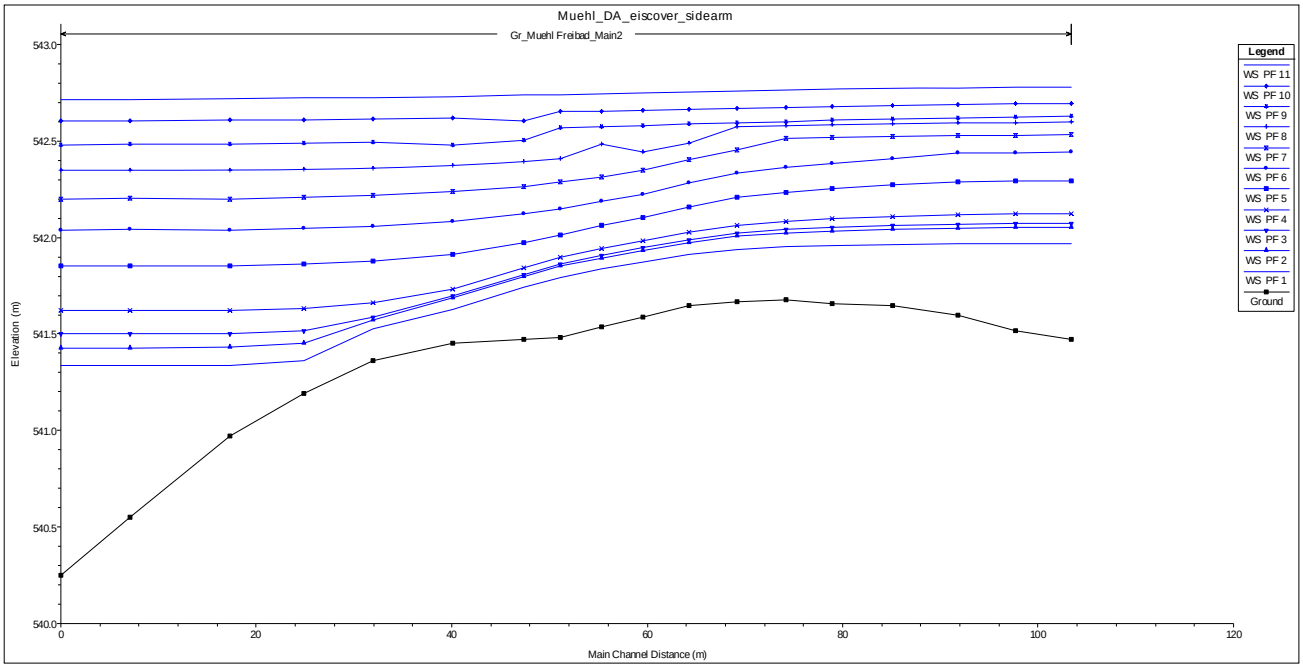

Figure 52 Flow depth midsection of the main channel

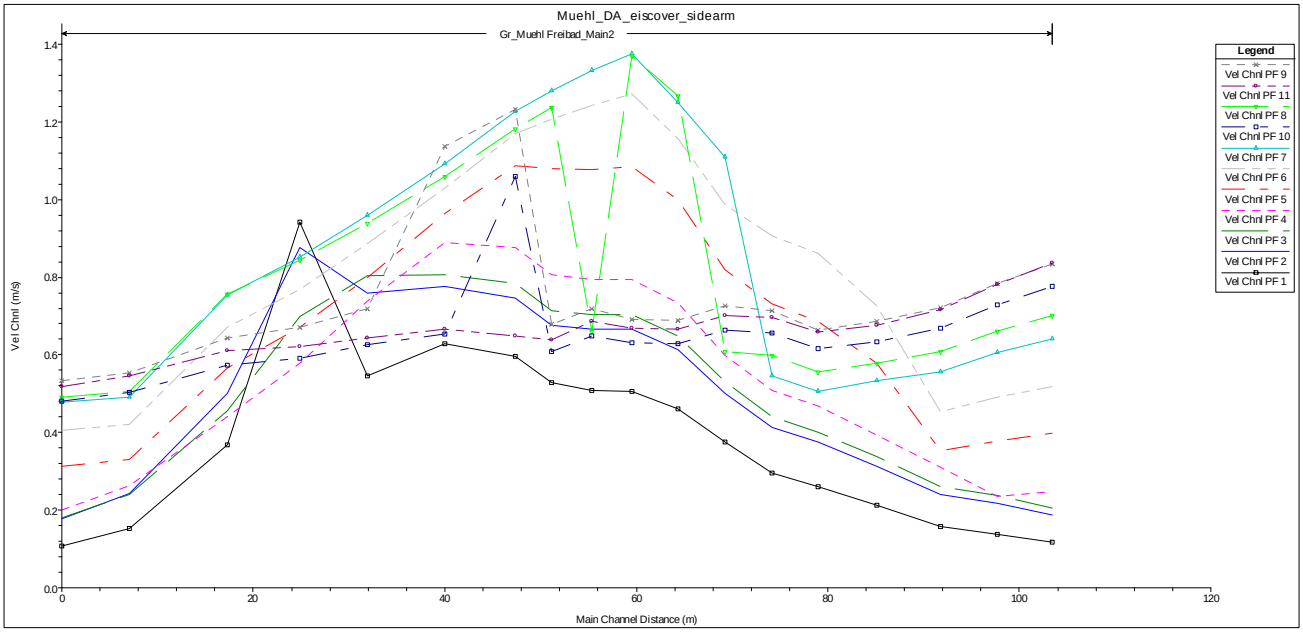

Figure 53 Flow velocities for all profiles at the midsection of the main channel

The next chapter will describe the results of the third scenario simulated in HEC-RAS. The difference to the scenario described in this chapter is the ice jam in the main channel caused by ice deposits in the main channel.

3.1.3. Results with ice cover and ice jam

In this chapter the results for the third scenario in HEC-RAS are shown. The scenario describes the case in spring when an ice jam is formed in the main channel and the flow is blocked. The water is forced through the side arm which is still covered in ice.

For the water depth a similar graph to the ice cover scenario (scenario 2) is resulting. For Profile 1 (Q=1[m³/s]) the discharge is constant until the dividing part. It can be seen that the water level for the upstream part is higher than for Profile 2 and Profile 3. At the divide the water level drops from 543.3m to 541.75m. Further downstream the water level lowers to 542.32m and remains at this level until the final cross section of the modelling area.

For Profile 2 to Profile 8 similar conditions can be observed. The water level slightly decreases until the length of 235m. It drops before stabilizing at the level of the outlet area. The island is partly overtopped at Profile 5 and completely flooded at Profile 7.

Looking at Profile 8 the water level slowly decreases at the upstream part. The water level drops at the length of 223.5m. Profiles 10 and 11 are not influenced by the island and the levels increase parallel to each other according to the discharge (Figure 54).

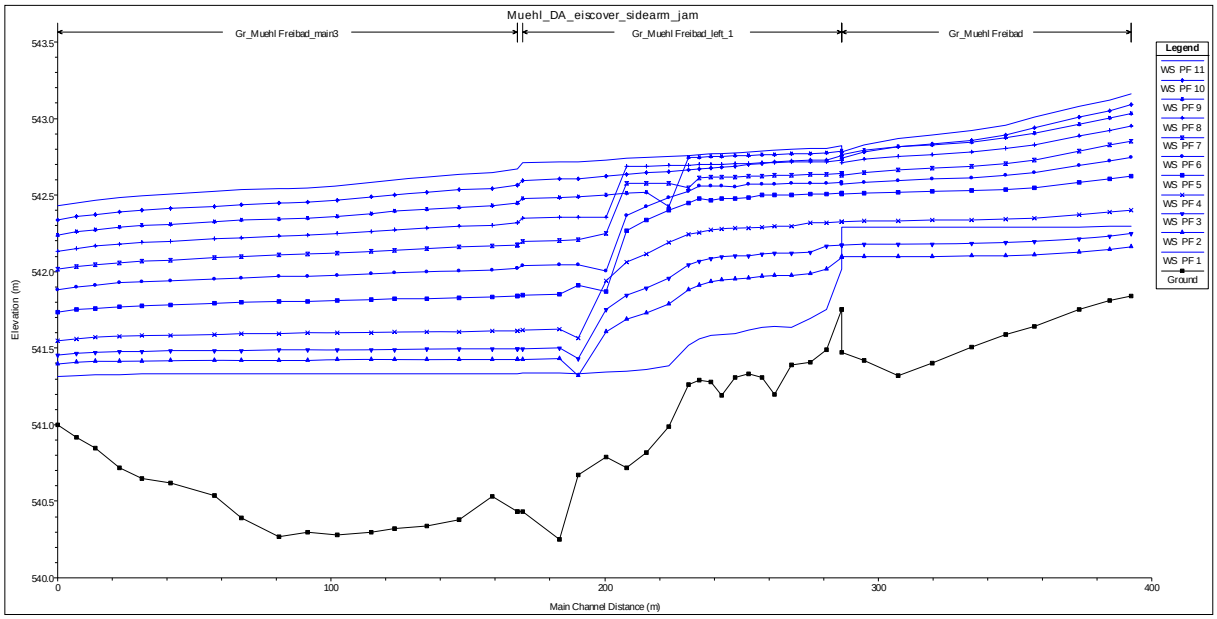

Figure 54 Water surface elevation for the ice jam scenario for the whole reach (main channel left out)

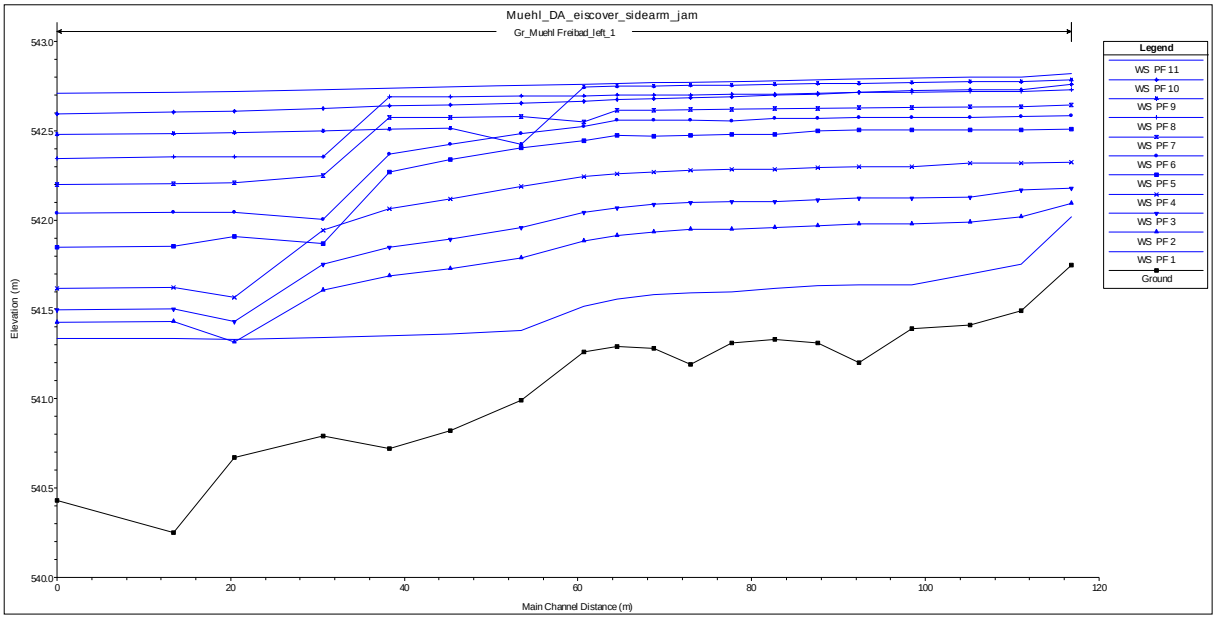

Figure 55 Water surface elevation for the ice jam scenario for the side arm

In the main channel the ice jam set with a thickness of 50cm leads to a retaining effect upstream. The water levels remain constant according to the discharge. The largest effect seen in Figure 56 can be observed for Profile 1, where the water level outreaches profiles 2 and 3. At the jam (situated between reach length 215m and 222m) the water level drops to the elevation of the downstream part. The differences between the water levels decrease with increasing discharge and therefore with the overtopping of the island. (Figure 56)

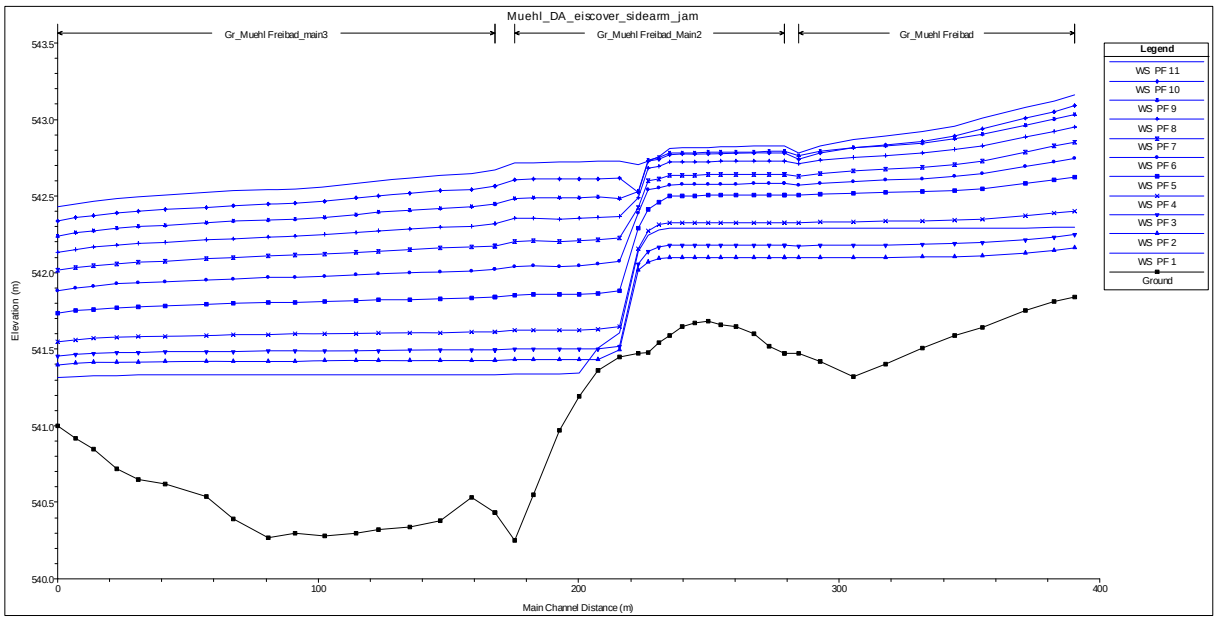

Figure 56 Water surface elevation for the ice jam scenario for the whole reach (side arm left out)

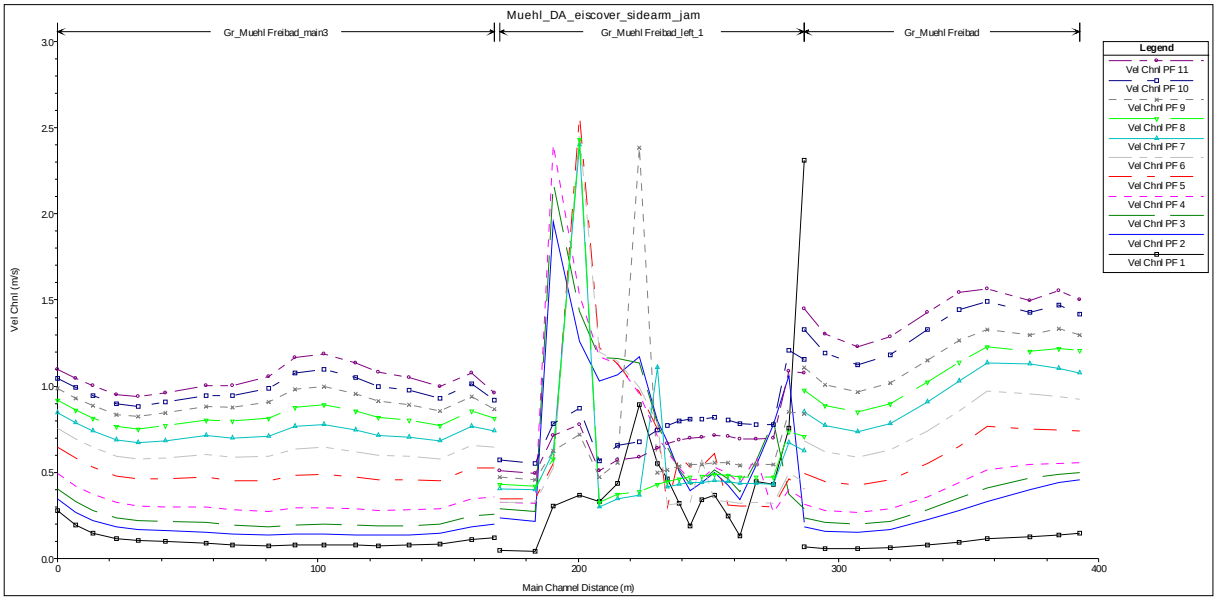

Figure 57 Flow velocities for the whole modelling area with sidearm (main channel left out at the widening, all profiles); Ice jam scenario

Looking at the velocity distribution along the river section it can be seen, that similar to the ice cover scenario, the increase for the upper and the lower section is proportional to the increase in discharge. The variation however is low. For the mid section (side arm) the variation in velocity can be defined as high. While Profile 1 has its highest peak right at the inlet to the sidearm with 2.31[m/s] profiles 2 to 8 peak at the channelized part of the sidearm. The largest peaks are found downstream of the spawning hotspot. The highest velocity found is 2.58[m/s] at Profile 5. Profiles 10 and 11 are almost constant throughout the section. The velocities vary between 0.5[m/s] and 0.75[m/s].

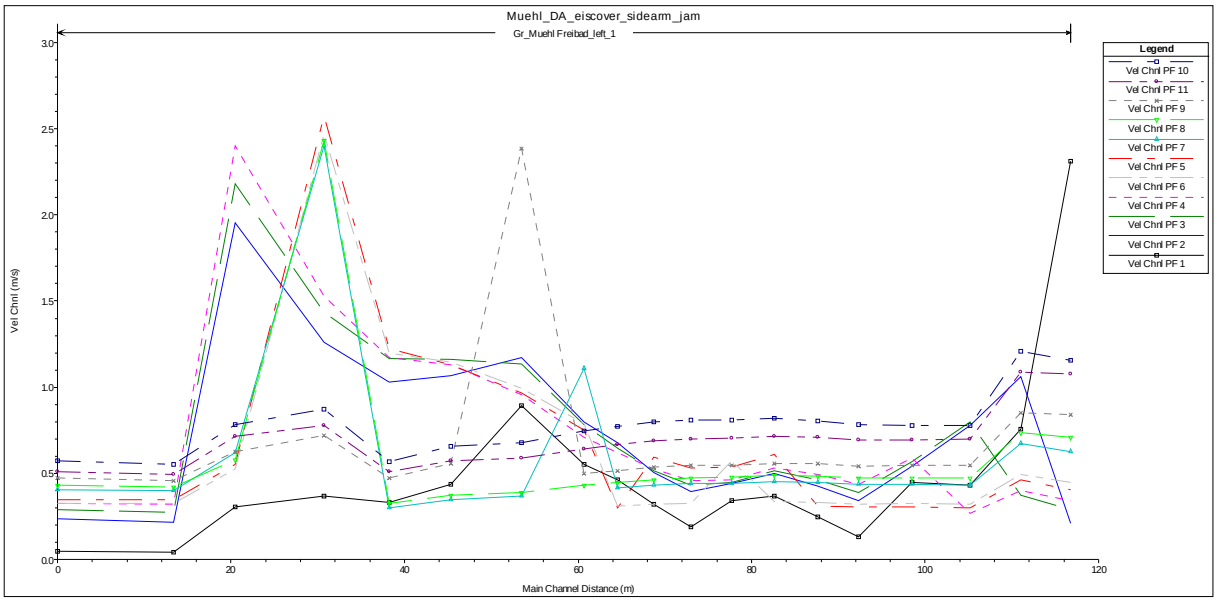

Figure 58 Mean velocities for all profiles; sidearm; jam scenario

The velocity distribution for the midsection of the main channel the velocity curves show that the velocity is stagnant until the jammed section. For all profiles the peak is found at the jam due to overtopping. The velocity rapidly increases and drops right after the jam. The highest peak found is at Profile 9 with a velocity of 1.98[m/s].

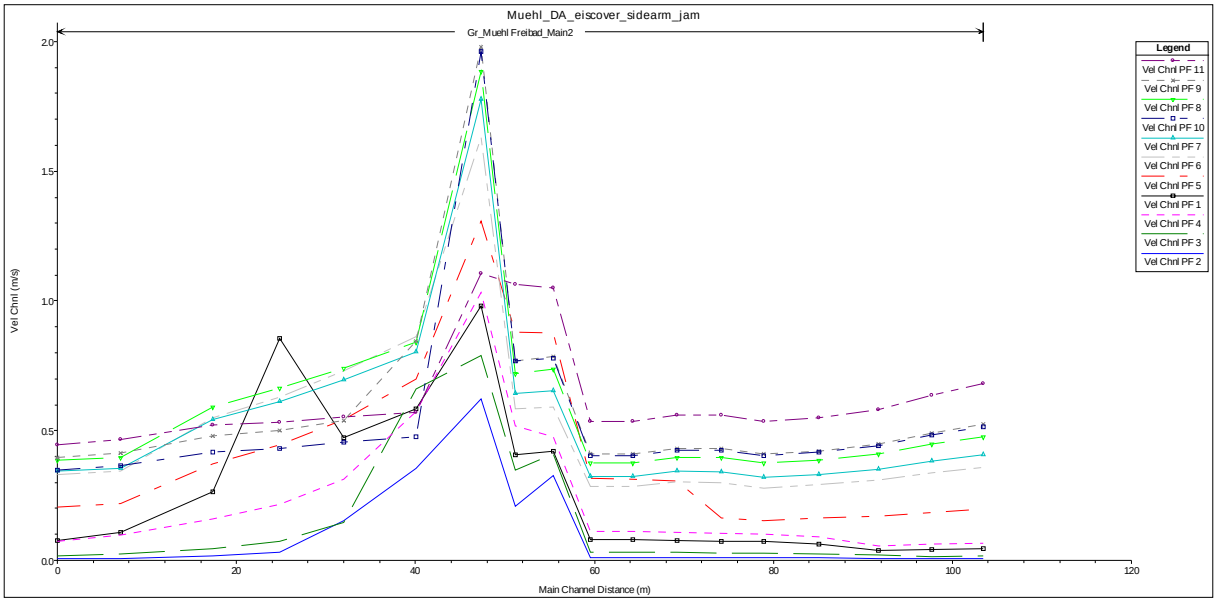

Figure 59 Mean velocities for all profiles; main channel midsection; jam scenario

The comparison of the results and the different scenarios are shown in chapter “Comparison”. The next chapter will describe the results of the River2D modelling. There every scenario had to be modelled separately.

3.2. River 2D modelling

The following chapter shows the results of the modelling part from the River2D modelling system. As mentioned before, each case had to be modelled separately. The results will be shown in a graphical form. The results chapter for River2D is divided into 4 sections. The results will be shown for the midsection of the modelling area. The first part presents the results for the ice free scenario followed by the results derived from the ice cover scenario. The third section will cover the results from the third scenario where the main channel is jammed with ice. The last part where the differences between the scenarios are shown will be described in “3.3 Comparison” where the focus will be set on the spawning areas and they will be analysed in more detail.

In the following chapter focus is set on the velocities occurring in the section with the main focus on the sidearm section. Each chapter will show step by step the increase of discharge from 1[m³/s] to 40[m³/s] in the steps described in Chapter 2.3.

3.2.1. Open water flow

In this chapter the resulting flow distributions for the ice free scenario will be shown. As mentioned before a direct comparison as in HEC-RAS could not be performed as the location nodes between the scenarios and within the scenarios changed and this could not be fixed until the end of the thesis. Further on the scale of the velocities are adjusted to each scenario so the distribution can be figured out more easily. So the colours change between each scenario. It is not possible to change the colours in River2D itself. Only the range in the velocities shown can be adjusted from the lowest to the highest point whereas the intervals are automatically generated.

The following picture shows the bed elevation for the area analysed (midsection of the river part). The riverbed and the channel area can be clearly seen as areas with the colour range from green to blue (540.2m up to ~542m) with the island area between the channels. It also can be seen that there is a step at the inlet area of the side channel and at the midsection of the main channel. The side channel is lower in elevation as the main channel for the beginning of the divided section which correlates with the on-site observations (Figure 60). For the side channel it can be seen that it is shallower at the side areas close to the river bank until the channelized part at the downstream end of the section. Figure 60 shows a pool section at the joint of the two channels. For the main channel a drop in elevation can be seen at the midsection of the dividing part.

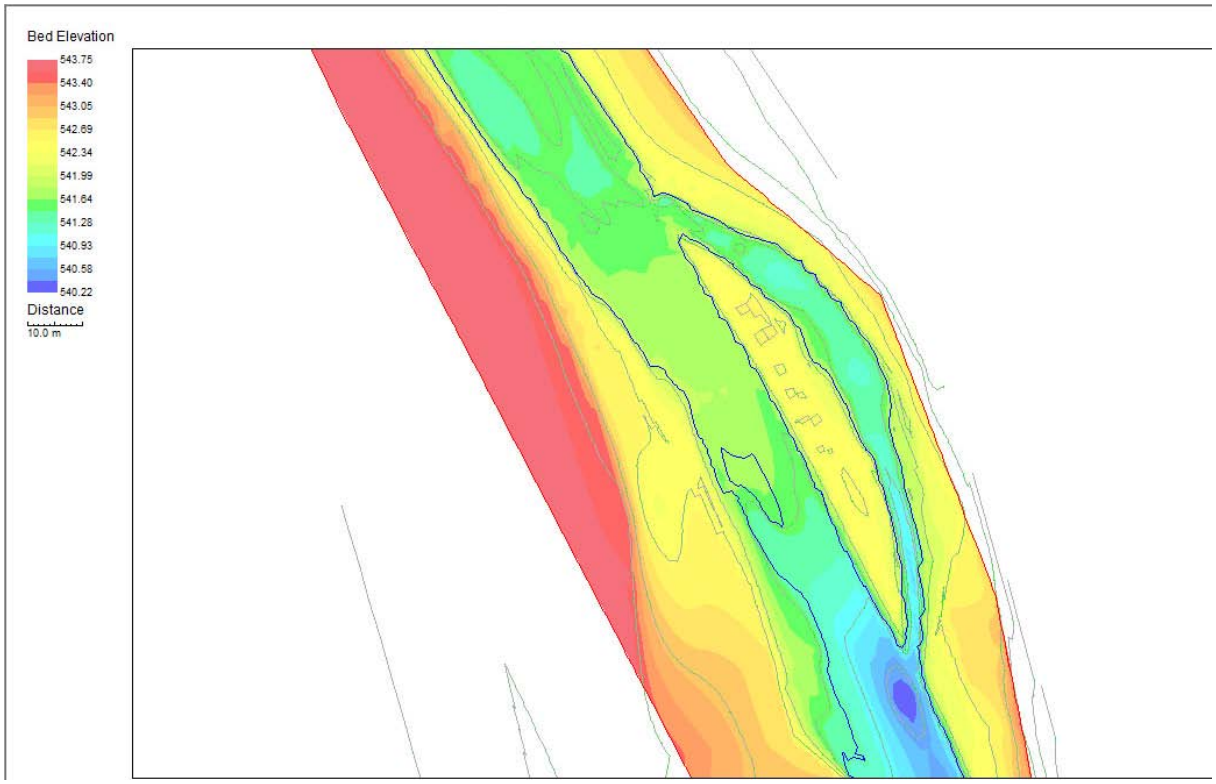

Figure 60 Colour shaped riverbed section used for analysis of the section

From Figure 61 to Figure 68 the results for the velocity distribution for the discharges from 1[m³/s] up to 40 [m³/s] are presented. For each picture the legend to the colours is shown at the lefthand side of the figures. As mentioned before the distribution on velocity varies too much to use one scale for all the displayed figures. It also can be seen that the display of the velocity is clipped to the wetted area so the changes in extension of the river can be seen as well.

In Figure 61 the highest velocities are found at the inlet section of the sidearm. These are the white spots right at the beginning of the section within the flow area. These spots are white because they exceed the scale chosen (0[m/s] to 0.75 [m/s]). Further on it clearly shown that the shallower boarder areas at the sidearm have low flow velocities (0 [m/s] to 0.1 [m/s]). Between the inlet part upstream and the channelized part at the downstream section the velocity distribution follows the shape of the riverbed with higher velocities in the middle of the flowing area. As the cross section narrows at the channelized section, the velocity increases to an almost constant velocity between 0.45 [m/s] and 0.48 [m/s].

Due to the slightly lifted area in the mid part of the dividing section the flow concentrates to the area close to the island. The velocity increases there and decreases after the step. For the scenario with 1[m³/s] not the whole riverbed is wetted in the main channel. This changes from a discharge of 2[m³/s] on. The whole section is covered with water from there on as shown in Figure 62.

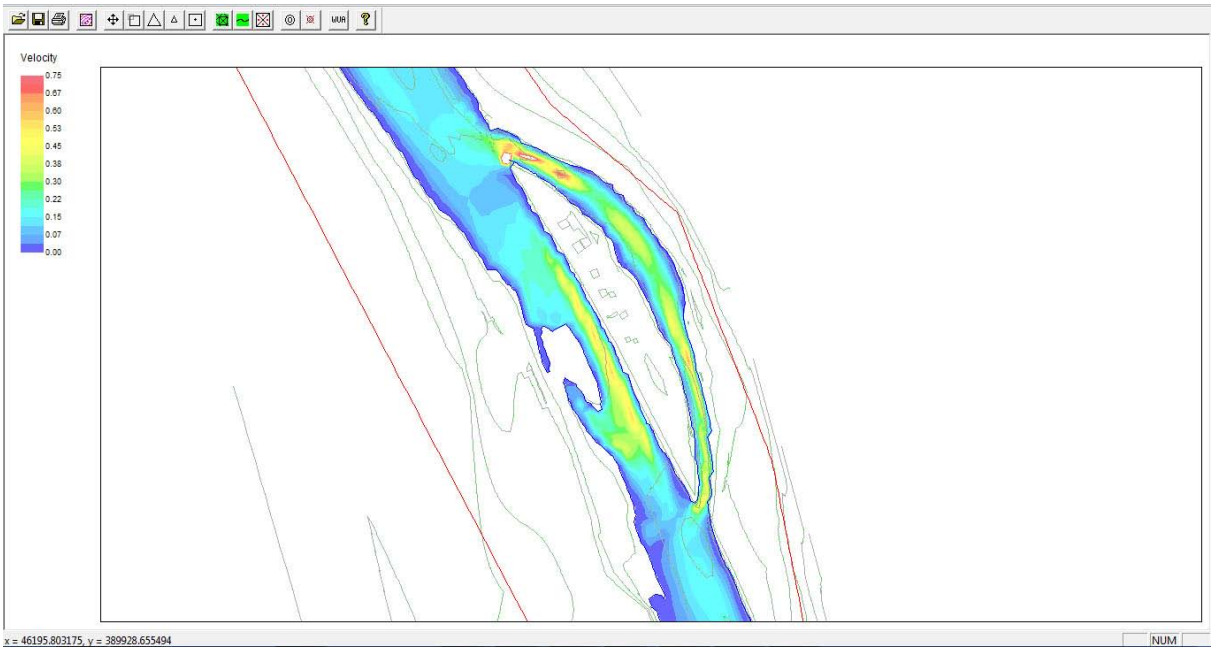

Figure 61 Open water flow, scenario 1m³/s, River2D

The flow conditions remain almost the same with increasing discharge. With the increasing discharge the whole river section in the main channel is covered with water as mentioned before. The flow velocity increases up to 1[m/s]. The highest flow velocity is found at the inlet section of the sidearm. At the inlet step the velocity increases to 1[m/s] and slows down to about 0.5[m/s] for the downstream part. It increases again at the narrower downstream section to 0.7[m/s]. At the main channel the velocity increases along the island. In the natural section of the sidearm the velocity increases by 0.1[m/s].

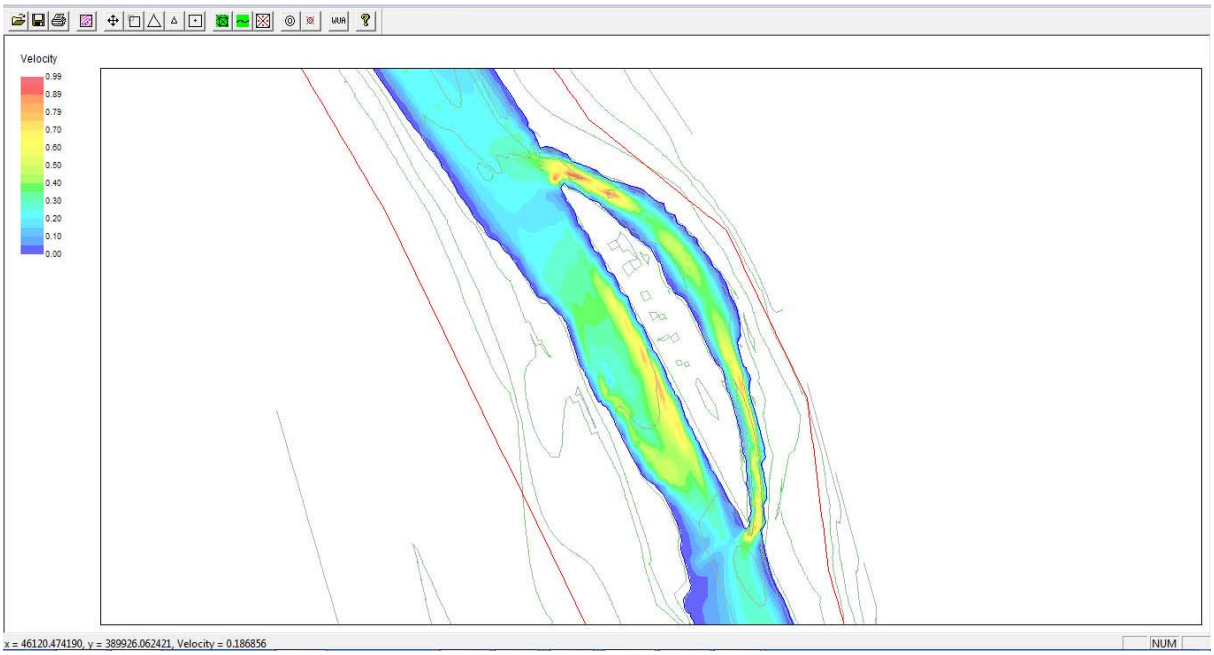

Figure 62 Open water flow, scenario 2m³/s, River2D

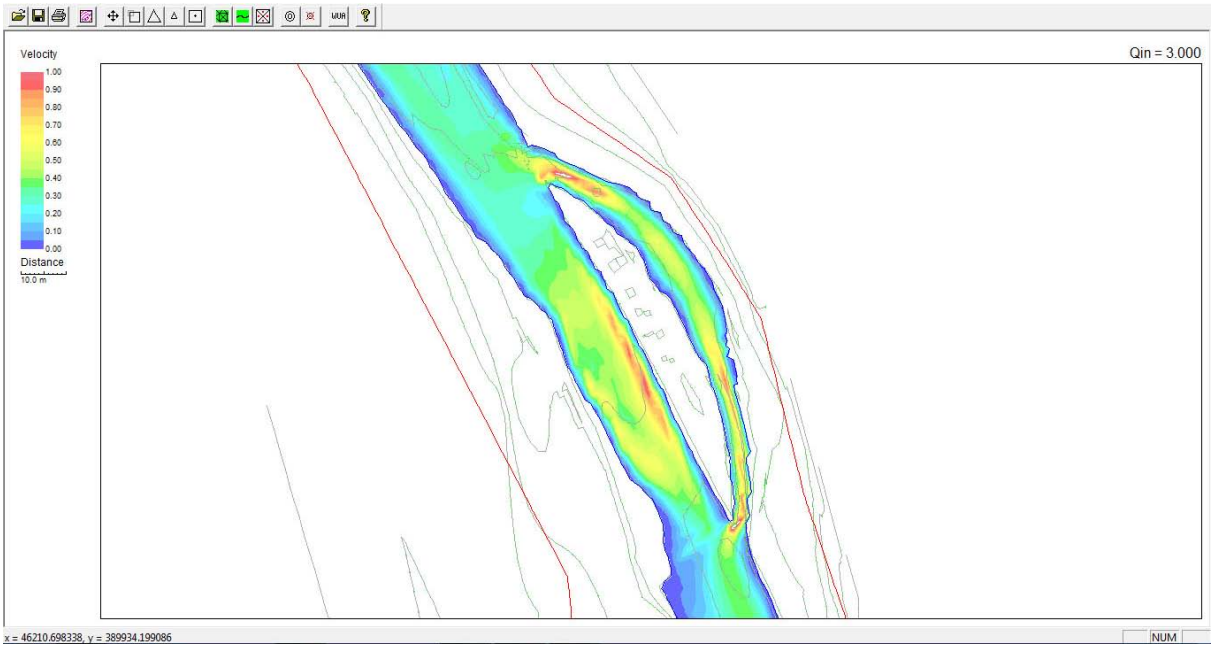

Figure 63 Open water flow, scenario 3m³/s, River2D

For discharges between 3[m³/s] and 40[m³/s] an increase in velocity at the outlet part of the sidearm can be observed. The "additional" water re-entering the main channel influences the water coming from the main channel and decreases the velocity from the water that flows in the main channel upstream of the joint. The acceleration in this section leads to the result that the velocity goes up to more than 1.9[m/s] as shown in Figure 68. This effect remains through out all scenarios for the open water flow.

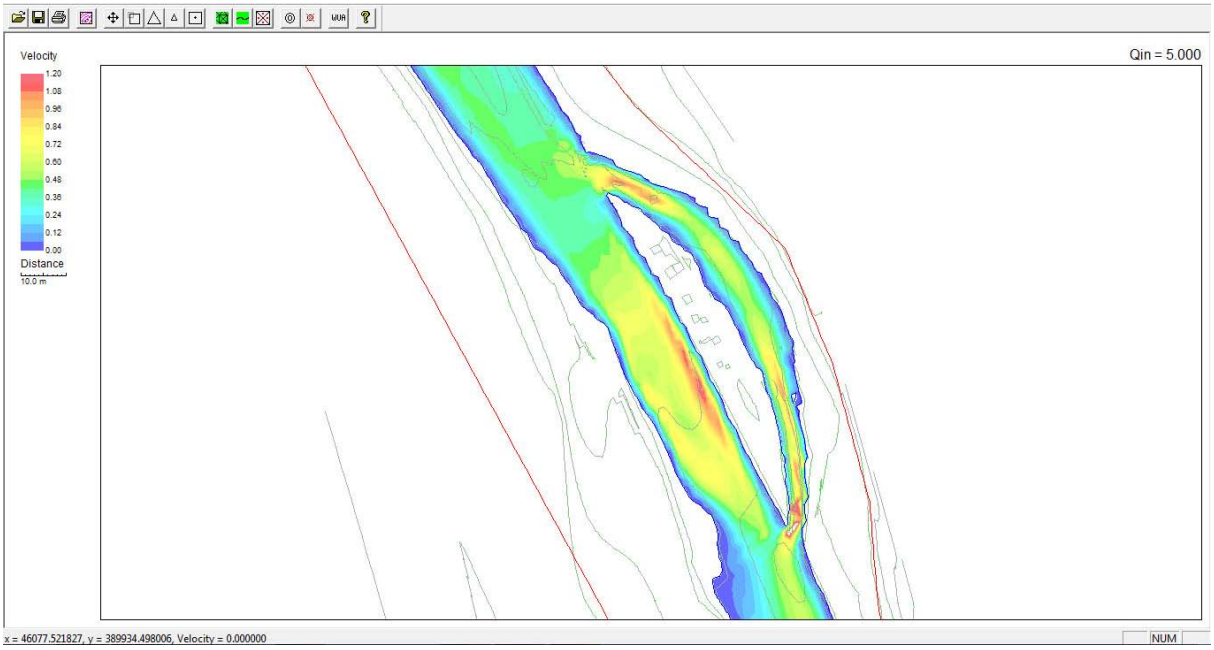

Figure 64 Open water flow, scenario 5m³/s, River2D

The flow behaviour with the increase of velocity over the inlet step to the sidearm, the channelized downstream part of the sidearm and along the island in the main channel remains the same until the river starts exceeding the riverbed. For the simulation series for the scenario without ice cover this is the case from 10[m³/s] which is shown in Figure 65.

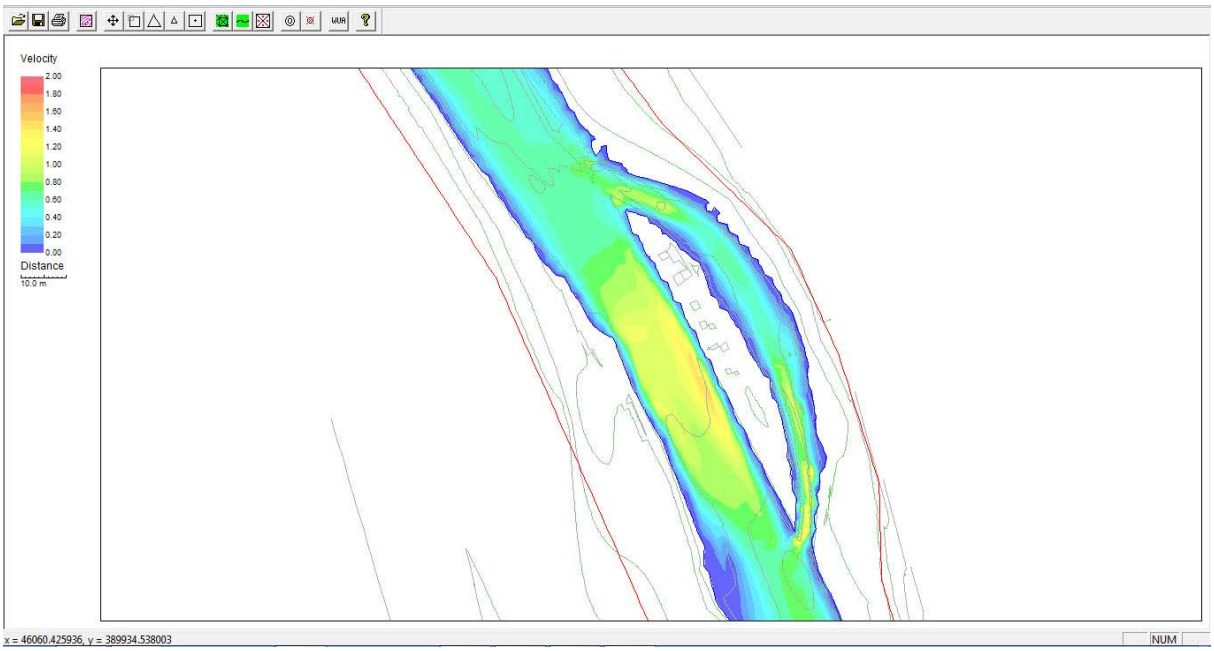

Figure 65 Open water flow, scenario 10m³/s, River2D

From 10[m³/s] on the velocity distribution starts to change. The areas surrounding the sidearm are starting to be flooded. The effect of the inlet step starts to flatten out where as the influence in of the step in the main channel starts to increase.

Looking at the section with the island in the middle it can be observed that the velocity along the island increases with the increasing discharge.

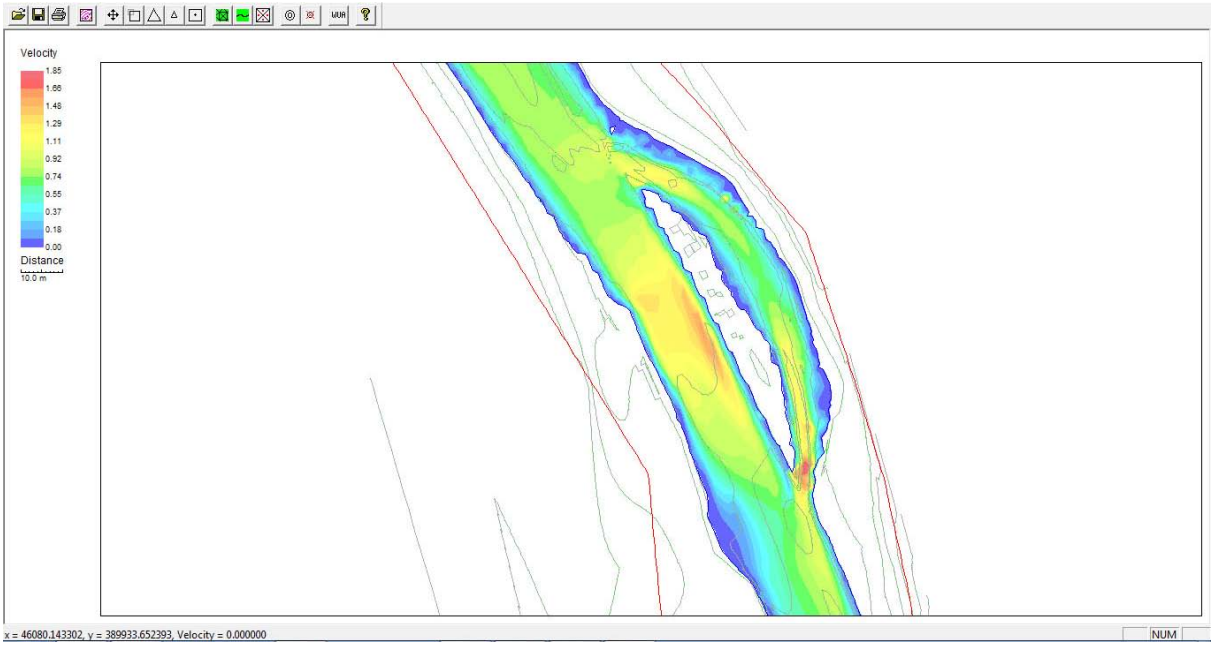

Figure 66 Open water flow, scenario 15m³/s, River2D

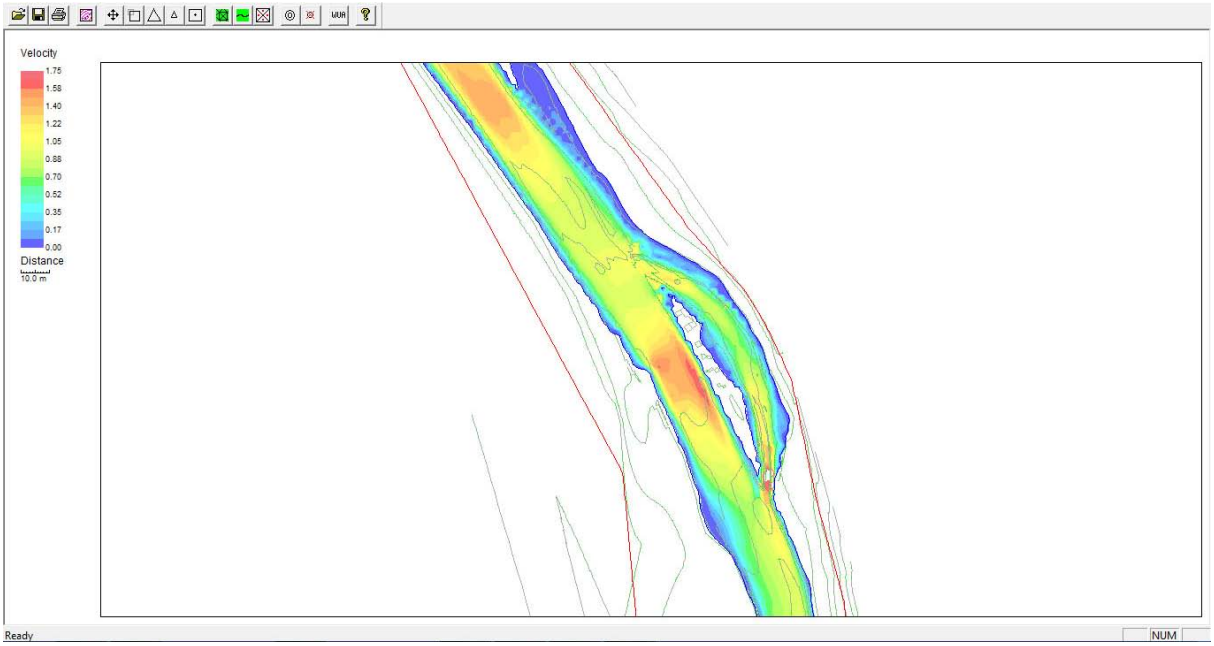

Figure 67 Open water flow, scenario 20m³/s, River2D

Between the discharges of 20[m³/s] and 40[m³/s] the island is completely overtopped. The acceleration effect along the island in the main channel cannot be observed anymore whereas the increased velocity over the step remains. The velocity in the sidearm section remains between 1[m/s] and 1.2[m/s] with a velocity peak at the final section of the channelized part of about 1.7[m/s].

It also could be observed (Figure 68) that there is a higher velocity in midsection of the island. At a discharge of 40[m³/s] the river fully exceeds the riverbed and the surrounding areas are flooded. For the part of the simulation area downstream an almost constant velocity throughout the section can be seen.

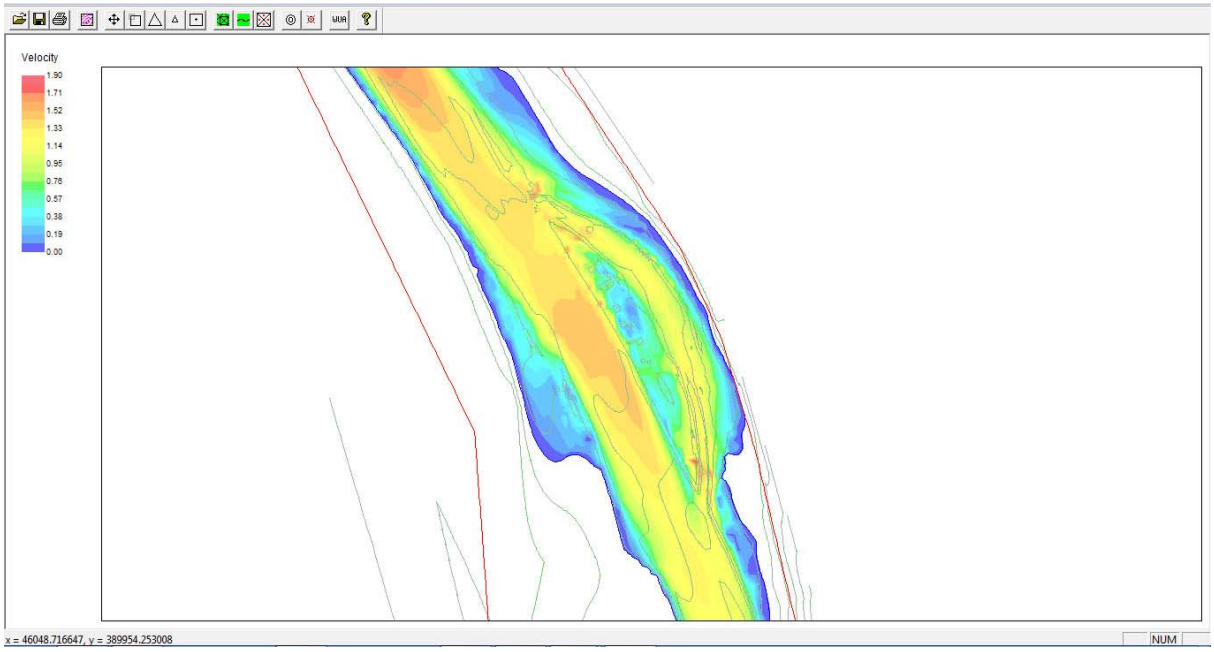

Figure 68 Open water flow, scenario 40m³/s, River2D

3.2.2. Results with ice

As mentioned before the second step in River2D was to add an ice cover onto the sidearm area. The purpose of this was to see how the water flow changes under the influence of ice occurring on the river. Therefore a 10cm thick ice layer was added to the open water flow models. The ice covered area was chosen as shown in Figure 69. The coloured area is the ice free part where as the area within the boarders is the ice covered area. As mentioned before the colour shading is automatically generated in River2D and cannot be changed. The ice covered area was chosen larger than the actual riverbed to ensure that the sidearm is covered even with higher discharges. To get velocities throughout the whole simulation area the not covered part had to be covered with an ice layer with a thickness of 0cm and a roughness value of 0.

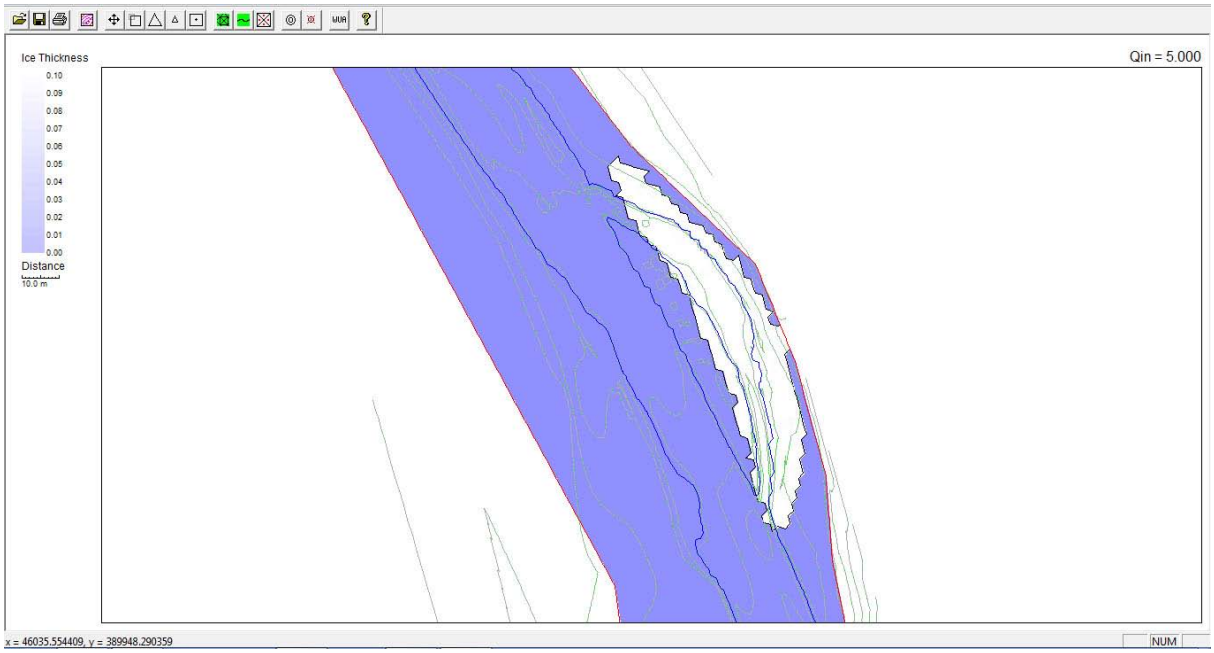

Figure 69 Ice cover on sidearm, thickness 10cm, River2D

To show the results of the simulations, the midsection of the whole simulation area was chosen to be analyzed as in chapter 3.2.1. The following pictures show the results of the simulation runs starting with the lowest discharge of 1[m³/s] and ending at 40 [m³/s].

In Figure 70 it could be figured out that the main channel is almost completely wetted. The highest velocities are found along the section of the island at the height of the natural step in the main channel. Here the peak velocity reaches a value of 0.71[m/s].

At the 1[m³/s] discharge scenario an increase of velocity at the inlet part of the sidearm can be observed. After the step section at the inlet the velocities in the sidearm vary between almost 0[m/s] and 0.2[m/s]. At the narrowing section where the more natural part enters the channelized section an increase in velocity up to 0.5[m/s] is shown in the graphic following.

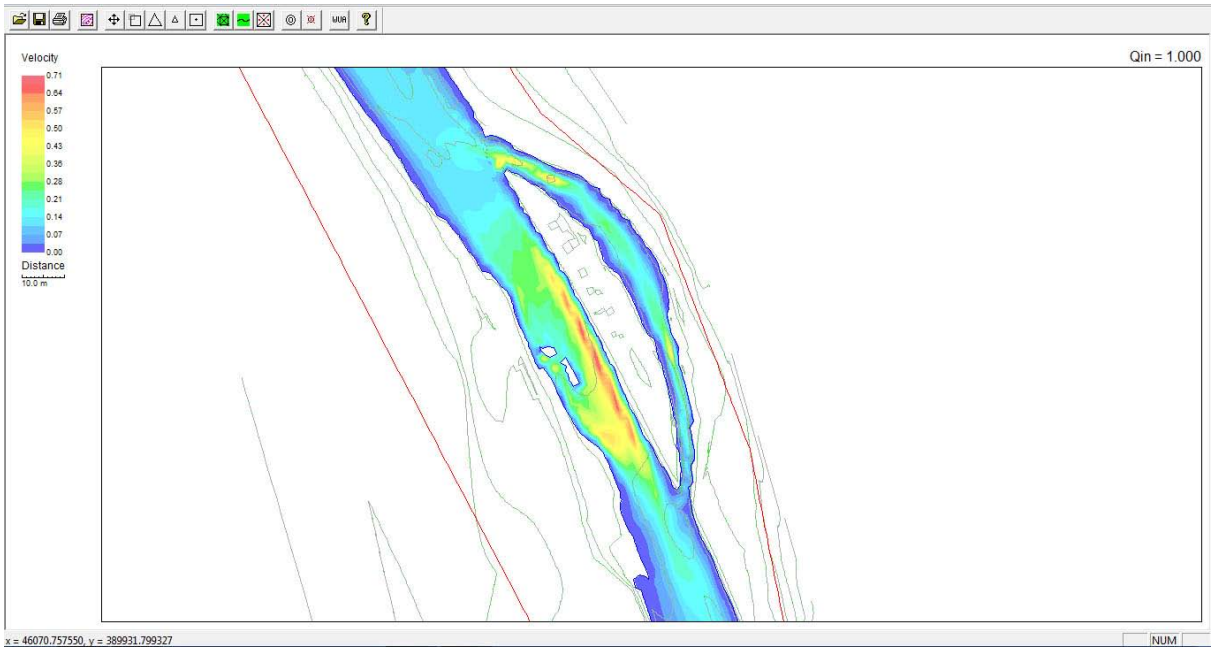

Figure 70 Ice cover on sidearm, scenario 1m³/s, River2D

The flow behaviour for the 2[m³/s] scenario is basically the same as in the first model. The highest velocities are found along the island section. The velocities increase to 1[m/s].

Looking at the sidearm the water velocities up from 0.3[m/s] to 0.6[m/s] as it enters the side arm over the inlet step to the ice covered area. At the observed spawning sites within this area the velocities between Figure 70 and Figure 71 remain between 0.05[m/s] and 0.2[m/s].

In Figure 71 it is shown that the acceleration effect at the narrowing section in the sidearm leads to an short increase in velocity up to 0.65[m/s]. The water however slows down to 0.2[m/s] at the joining part with the main channel.

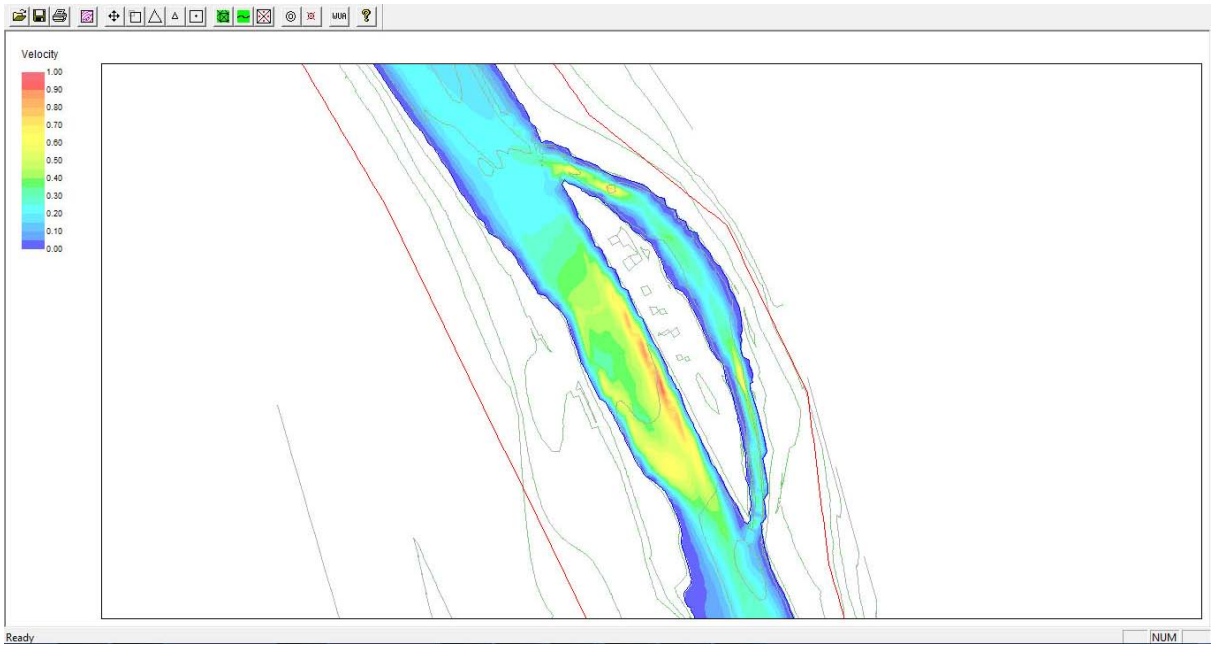

Figure 71 Ice cover on sidearm, scenario 2m³/s, River2D

As it can be seen in Figure 72 the river bed is fully wetted at a discharge of 3[m³/s]. With increasing discharges the velocities along the section increase too. Along the side of the island the velocities have a peak of 1.2[m/s] and the velocity in the main channel downstream of the divide increases by 0.1[m/s] to 0.2[m/s].

In the side channel the influence of the inlet section stretches out further downstream as well as the nozzle effect in the downstream part. The highest velocities found in the sidearm are in those two sections with a peak velocity of about 0.85[m/s]. The velocity at the midsection of the sidearm is found between 0.05[m/s] close to the riverbanks and 0.35[m/s] in the middle of the cross section.

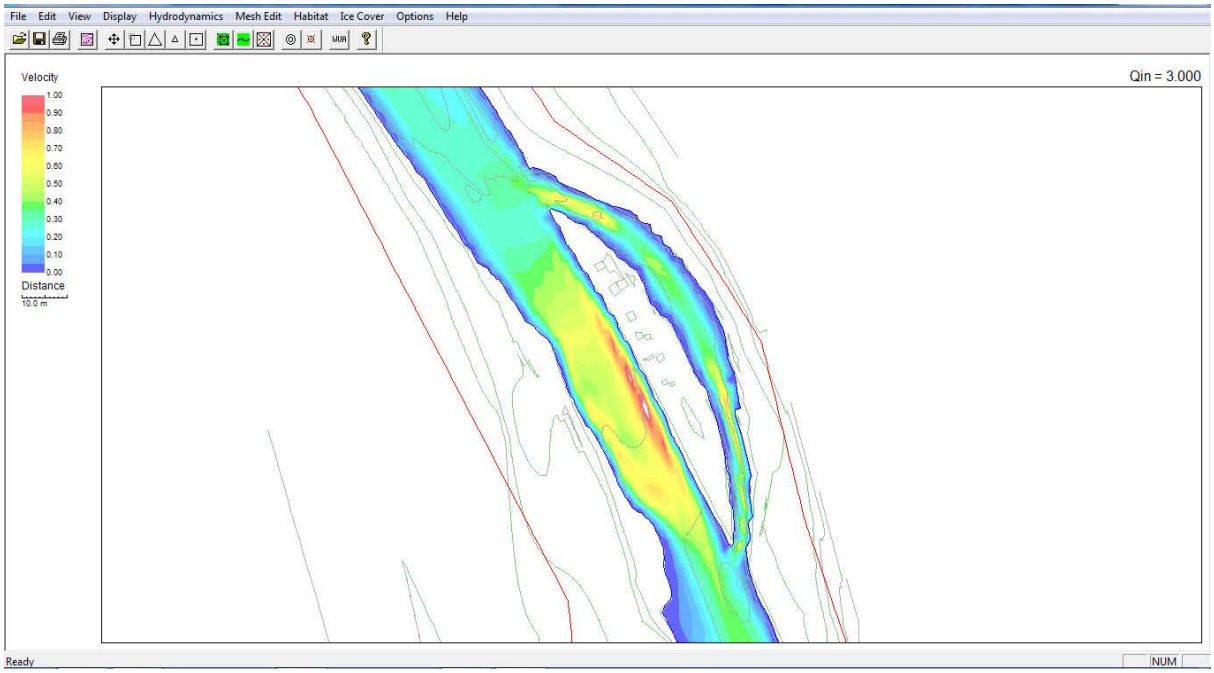

Figure 72 Ice cover on sidearm, scenario 3m³/s, River2D

From 5[m³/s] on the river starts to exceed the riverbed at the sidearm and upstream section of the divide. The highest velocity is found in the main channel as shown in Figure 64. It has a value of about 1.3[m/s].

The sidearm still can be divided into three sections depending on the velocity distribution. At the inlet section acceleration can be observed even though the effect is not as large as seen in the figures above. After that the water slows down until the channelized part of the sidearm. The highest value for the inlet section is about 0.75[m/s], in the midsection the values are between 0.2 [m/s] and 0.6[m/s] and in the outlet part the velocity increases up to 0.75[m/s] at the beginning and slows down to 0.4[m/s] to 0.5[m/s] at the joint with the main channel.

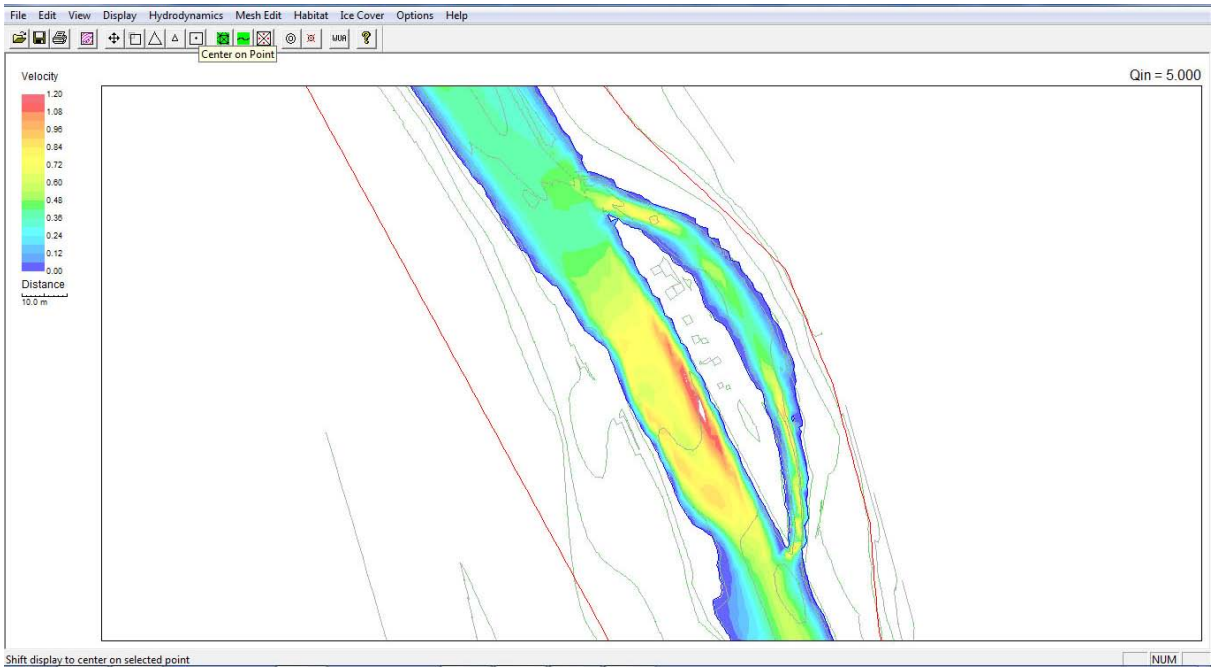

Figure 73 Ice cover on sidearm, scenario 5m³/s, River2D

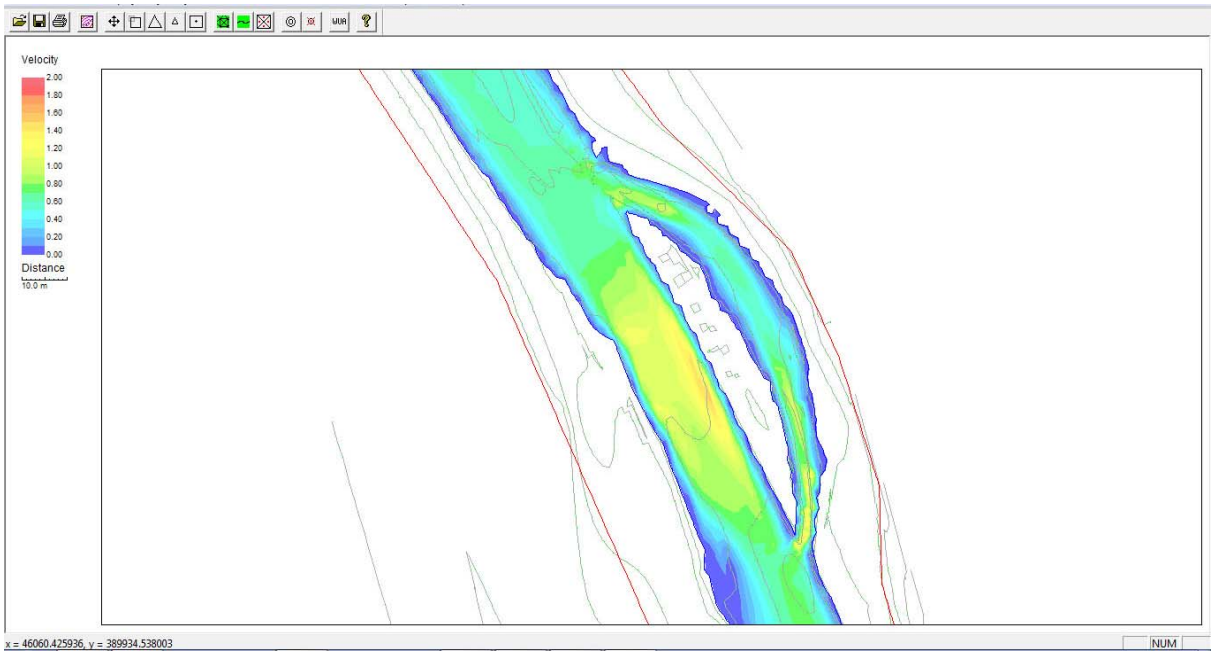

Figure 74 Ice cover on sidearm, scenario 10m³/s, River2D

For the higher discharges (10[m³/s] to 40[m³/s]) it can be said that the flow behaviour changes. While the highest velocities are still found at the section along the island in the main channel, the effects of the topography in the sidearm decrease. As it can be seen in Figure 74 the surrounding areas of the sidearm are flooded and therefore the flow area increases. This increase leads to the fact that the flow paths change and the narrowing sections widen due to the overtopping of the riverbanks in the sidearm.

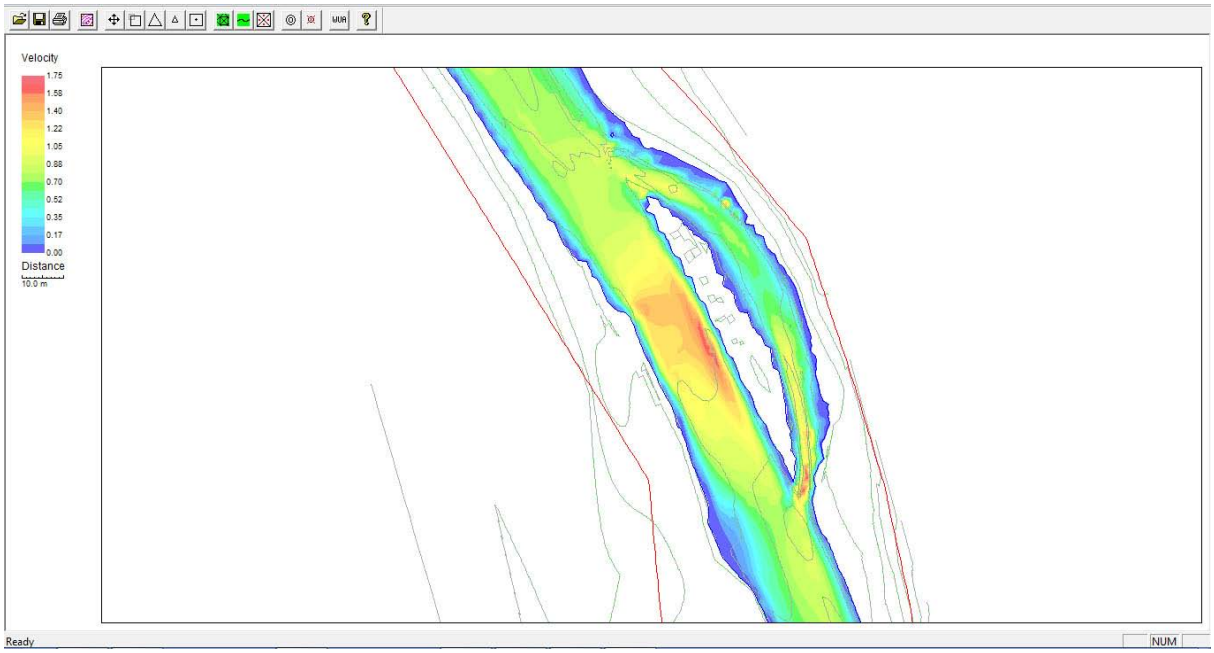

Figure 75 Ice cover on sidearm, scenario 15m³/s, River2D

The velocity in the midsection of the sidearm only slightly increases after the overtopping of the riverbanks as seen in Figure 75 and Figure 76. The downstream section in the sidearm is affected by the acceleration directing to the outlet. The highest velocity in the whole section is now found at the outlet of the sidearm wit 1.9[m/s]. Further on the island is mostly overtopped from the discharge of 20[m³/s]. In the main channel the largest effect seen is the overtopping of the riverbanks upstream of the divide and the increase in velocity due to the higher discharges.

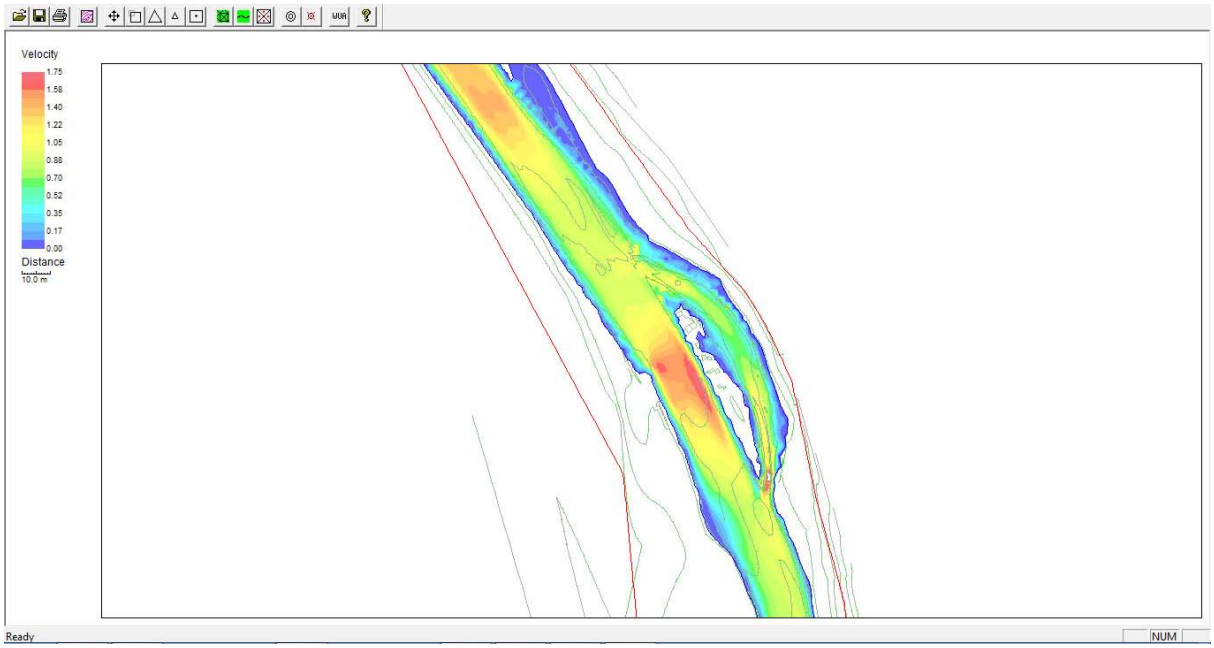

Figure 76 Ice cover on sidearm, scenario 20m³/s, River2D

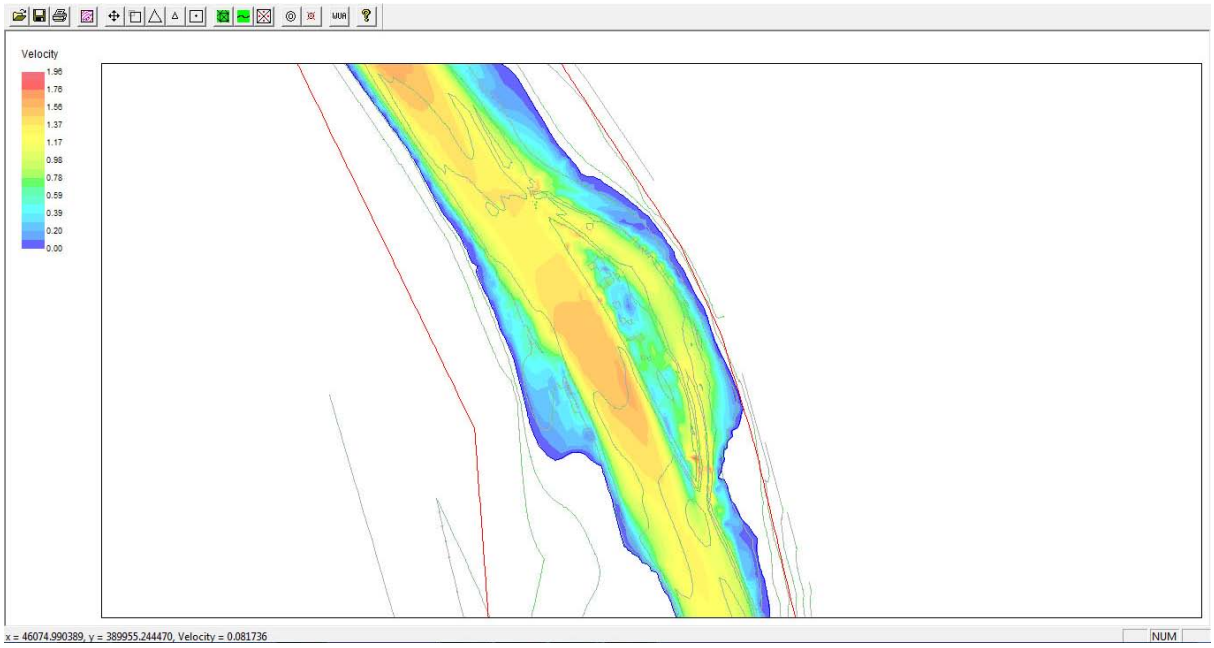

Figure 77 Ice cover on sidearm, scenario 40m³/s, River2D

For the HQ_1 scenario it can be said that the velocities in the channel bed are higher than in the flooded surrounding areas. The highest velocities are found upstream of the divide, at the step in the main channel and the outlet part of the sidearm. Compared to the 20[m³/s] scenario the velocities decrease.

Most of the high flood events occur in springtime. Some of them are created by breaking ice dams. The scenarios where blocking of the main channel due to an ice jam is simulated and the resulting graphs are shown in the following chapter.

3.2.3. Results with ice cover and ice jam

After the results of the free lowing water and the ice cover scenario in this chapter the results of the ice jam scenario are shown. As already mentioned ice jams occur in spring or winter with changing temperatures when the ice cover starts breaking up and the floating pieces get caught. This can lead to a total blockage of the river.

In the case of the research area it has been observed that ice jams may occur in the main channel at the step in the dividing section. This has been taken into account for the modelling process as already mentioned in the methodology part of this thesis. As there is no option in River2D to create an ice jam with the ice cover, the jam was created in lifting the riverbed elevation to the lowest point of the island at the cross section. Additionally to the ice jam in the main channel the sidearm is covered with ice. To receive comparable results the same ice cover as used in the second scenario was used (Figure 69). The changes done at the riverbed are shown in Figure 21.

As the jam created is up to the required height of the lowest point on the island, it is "overtopped" as soon as the island is flooded. As shown in the following graphs the jam is not completely blocking out the water from the section downstream of the jam to the area where the sidearm enters the main channel. In Figure 78 the flow directions are shown at the example of a discharge of 3[m³/s]. It can be seen that the main flow is redirected to the sidearm. The water seen downstream of the jam is leaking through and from the downstream section.

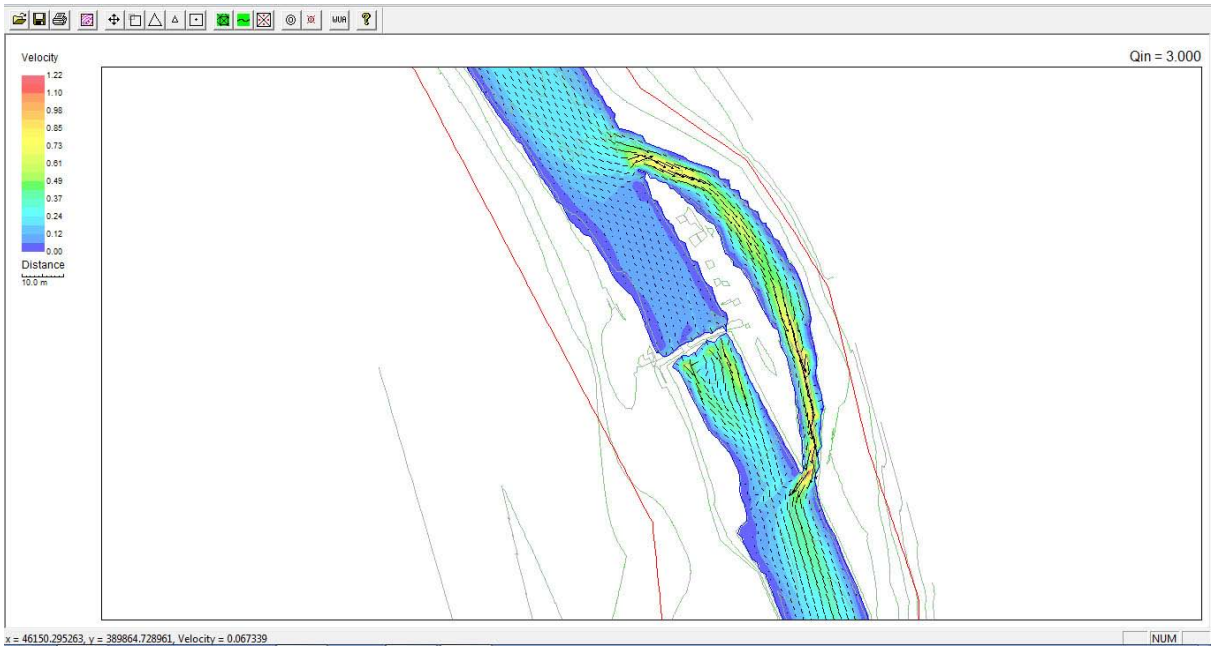

Figure 78 Ice cover on sidearm and jam in the main channel, scenario 3m³/s, flow directions, River2D

The ice jam causes a redirecting of flow to the sidearm. In Figure 79 it can be seen that this leads to an almost full riverbed even at low flow conditions. At the inlet step to the sidearm the velocity increases up to 0.55[m/s]. It slows down in the midsection of the sidearm to a maximum of 0.3[m/s] and increases up at the narrowing section before the outlet to 0.6[m/s].
The main channel is affected by the jam. The flow velocity almost decreases to zero towards the jam. The water leaking through the jam reaches a velocity of 0.6[m/s] downstream of the jam. The riffle in the main channel is only partly covered in water.

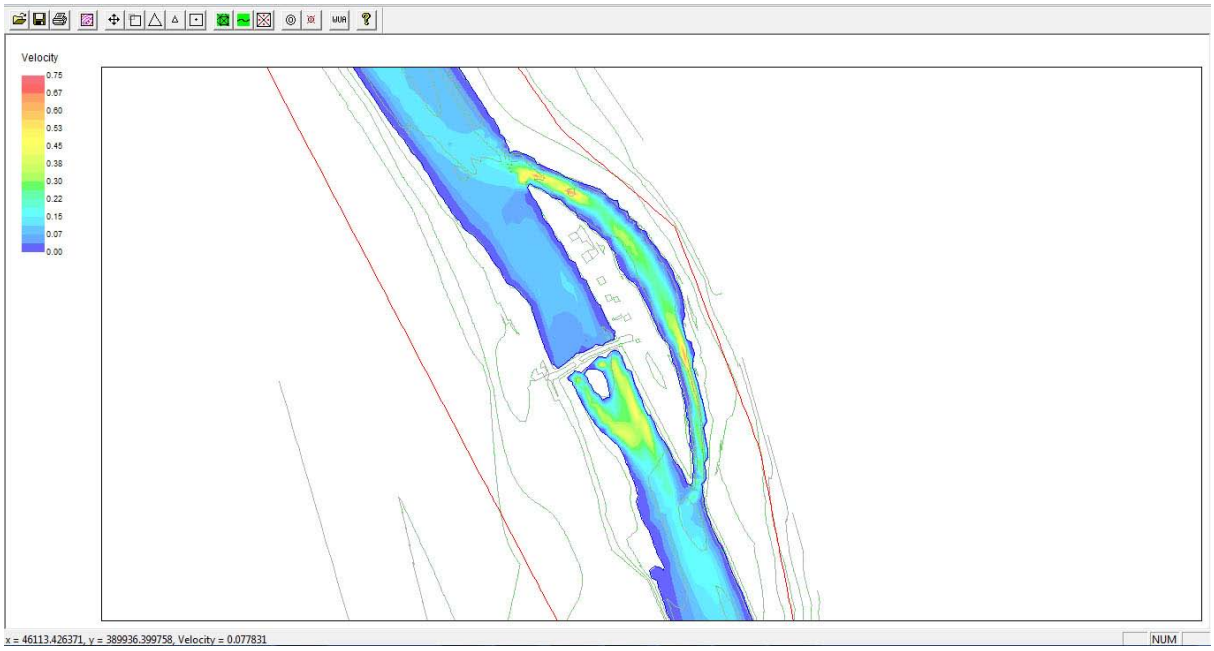

Figure 79 Ice cover on sidearm and jam in the main channel, scenario 1m³/s, River2D

With increasing discharges the velocity in the sidearm increases as well. With a doubling of the discharge to 2[m³/s] (compared to Figure 79), the velocity in the sidearm increases up to a value between 0.2[m/s] and 0.3[m/s]. This leads to a peak velocity at the inlet section of 0.8 [m/s] and in the channelized part of 0.75[m/s]. It can be seen that the redirecting in flow leads to the effect that the riverbed in the sidearm is already full. At the spawning sides in the midsection the velocity increases to a value between 0.4[m/s] and 0.5[m/s]. Downstream of the redds the velocity increases again up to 0.75[m/s] before entering the main channel (Figure 80).
While the velocity in the sidearm increases the water remains almost not flowing in the main channel. Hence the water surface elevation increases upstream of the jam. At a discharge of 3[m³/s] the outer areas of the island are already overtopped.
Even though the riverbed is already full the effect of acceleration in the side channel can be seen at 3[m³/s]. The flow velocity rises according to the higher discharge and the same effects

as described earlier can be seen. The peak velocity in the most downstream part of the sidearm increases to 1.2[m/s]. (Figure 81)

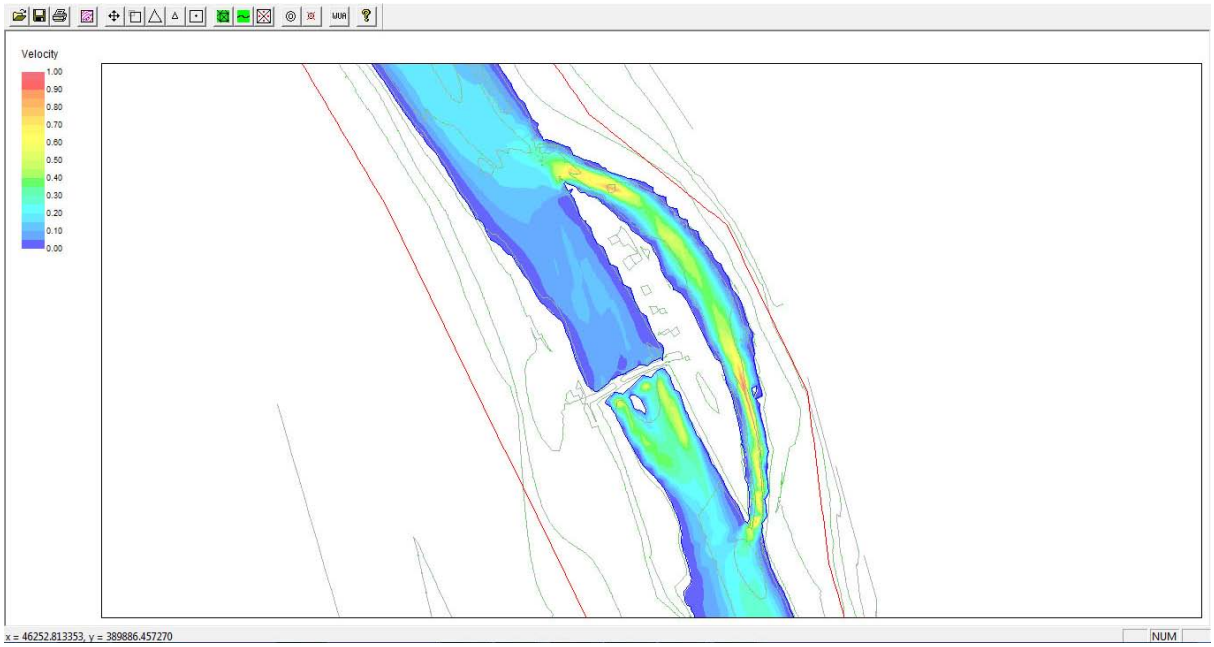

Figure 80 Ice cover on sidearm and jam in the main channel, scenario 2m³/s, River2D

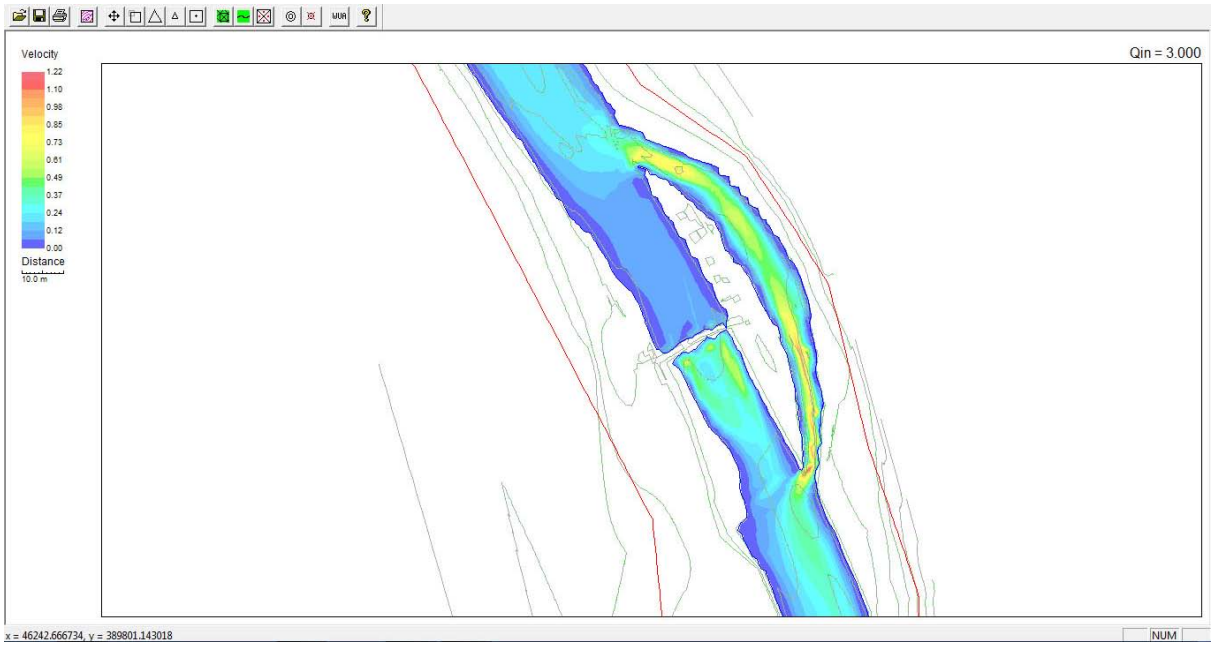

Figure 81 Ice cover on sidearm and jam in the main channel, scenario 3m³/s, River2D

At 5[m³/s] the run-off exceeds the channel capacity. This can be observed as well in the main channel upstream of the jam as well as in the sidearm. It can bee seen that the jam created is already overtopped but the backwater effect of the water in the upstream section can be

observed. The step effect of the inlet decreases from here on and cannot be observed from a discharge of 15[m³/s] onwards. (Figure 84)

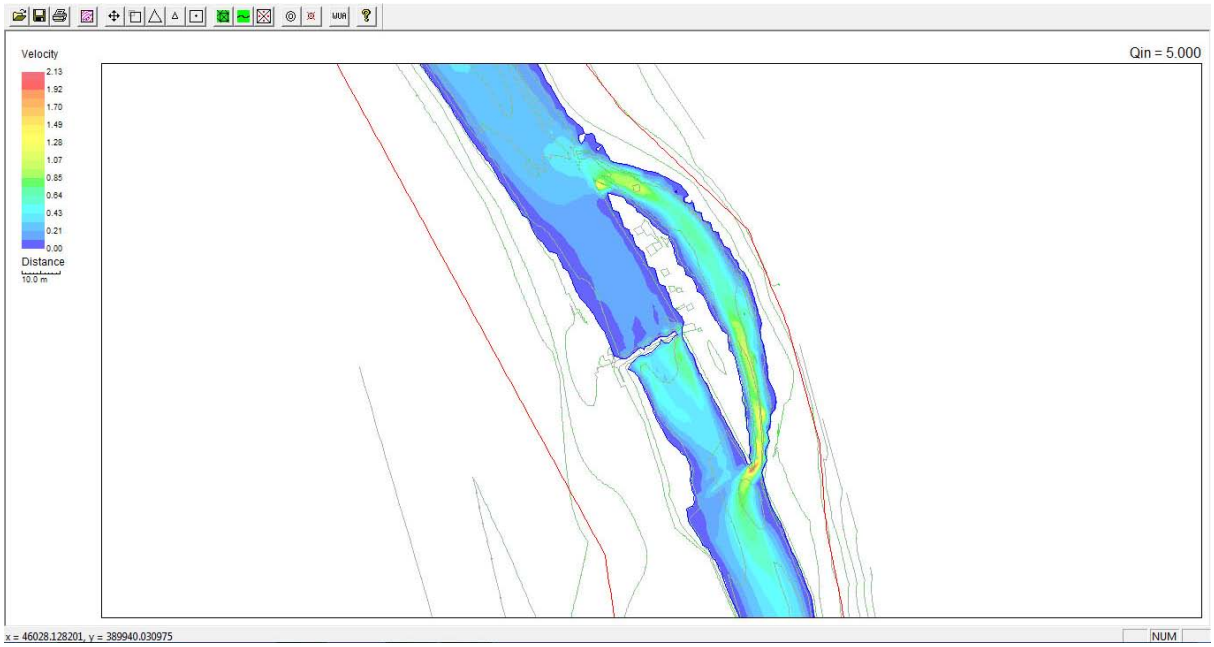

Figure 82 Ice cover on sidearm and jam in the main channel, scenario 5m³/s, River2D

Looking at Figure 83 the island is already flooded upstream of the jam and the lifted riverbed is overtopped. Even though the jam is overtopped the flow concentrates in the sidearm. The run-off upstream of the jam overtops the island and flows into the sidearm. Due to the higher areas surrounding the channelized section a nozzle effect towards the outlet of the sidearm can be observed the flow velocity increases from 0.6[m/s] at the midsection of the sidearm up to 2.45[m/s] before flowing back into the main channel.

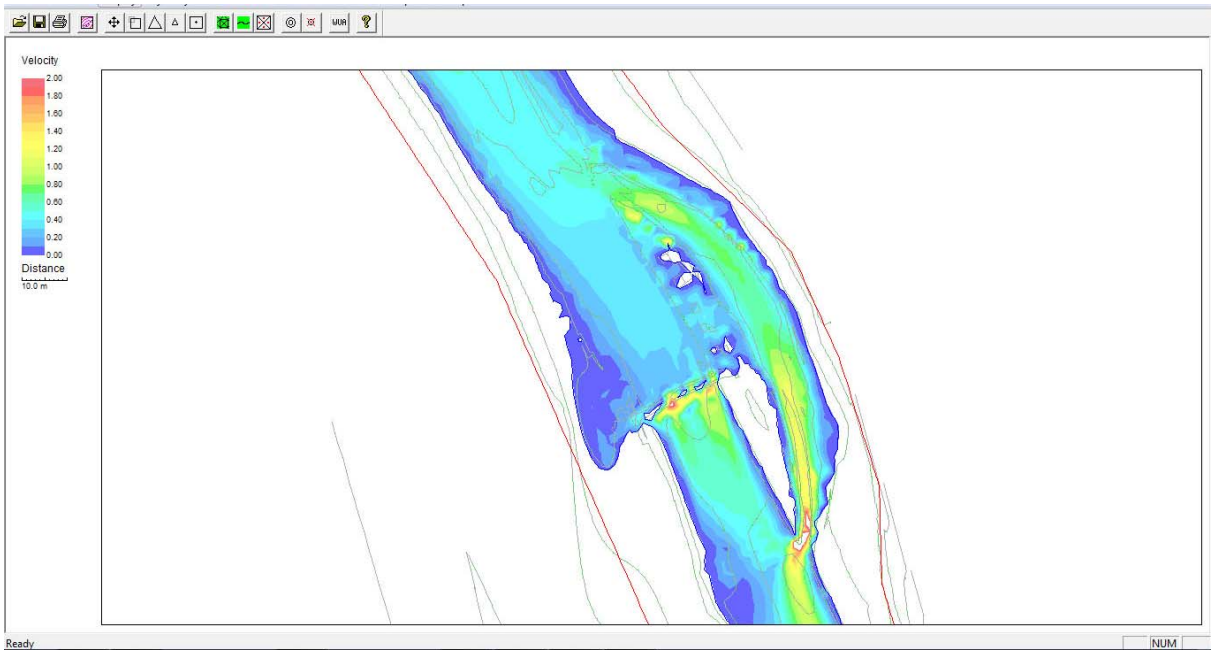

Figure 83 Ice cover on sidearm and jam in the main channel, scenario 10m³/s, River2D

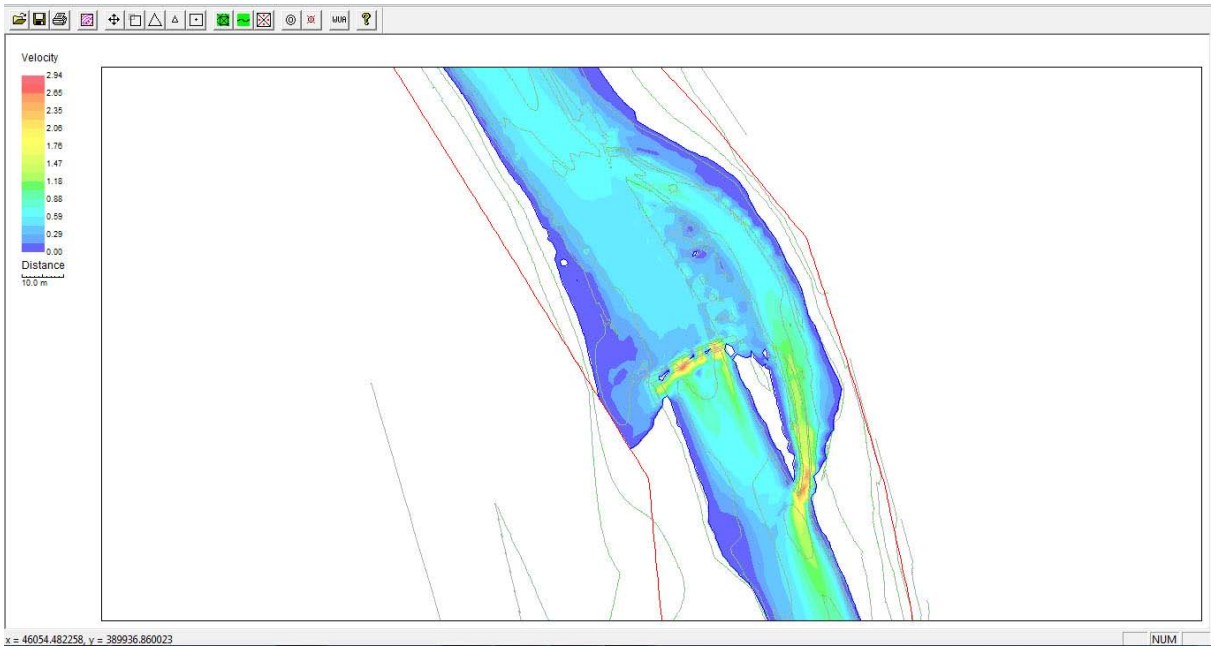

Figure 84 Ice cover on sidearm and jam in the main channel, scenario 15m³/s, River2D

In Figure 84 the flow area with a discharge of 15[m³/s] is shown. It can be seen that the whole upstream part of the island is flooded due to the ice jam in the main channel. The main part of the discharge runs off through the sidearm. The water wetted area on the left reaches the outer boundaries of the simulation area. The jam is almost completely overtopped but still has a backwater potential.

For the sidearm it can be said that due to the nozzle effect at the rejoining section the water overtops the riverbanks on the whole length of the sidearm as the flowing area is narrowed. The acceleration effect at the outlet as described before is still given and the water accelerates to a maximum velocity of 2.65[m/s].

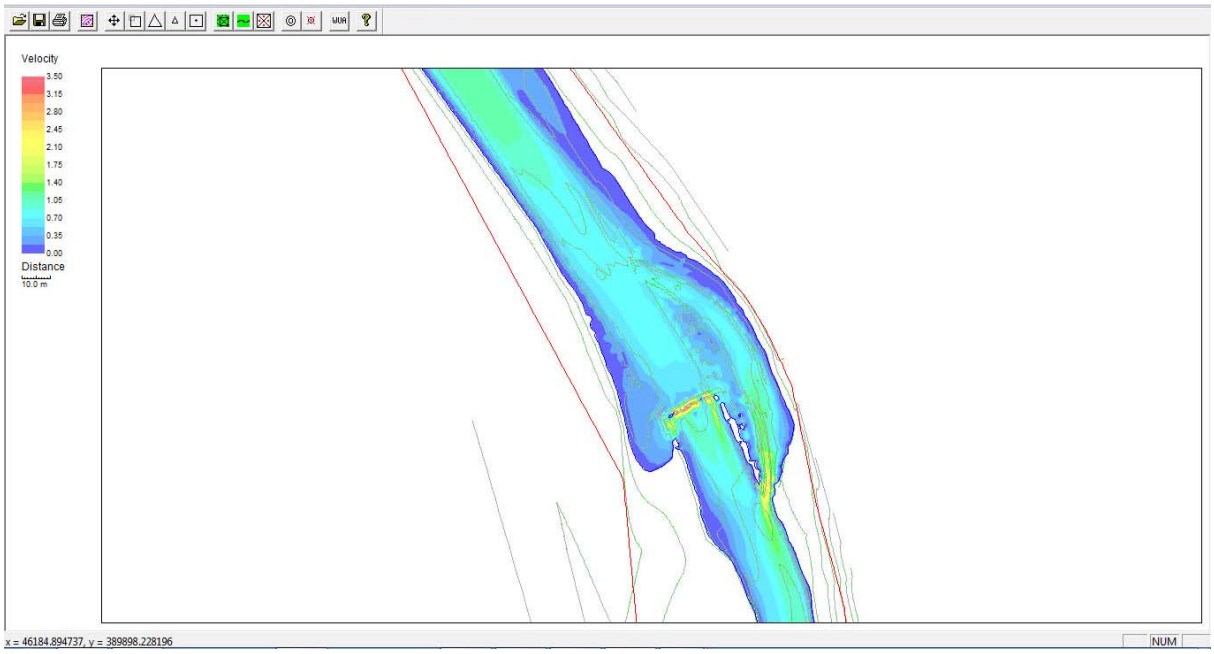

Figure 85 Ice cover on sidearm and jam in the main channel, scenario 20m³/S, River2D

In case of an ice jam the island is completely flooded from discharges higher than 20[m³/s]. The highest velocities found in that case are occurring at the section where the sidearm enters the main channel.

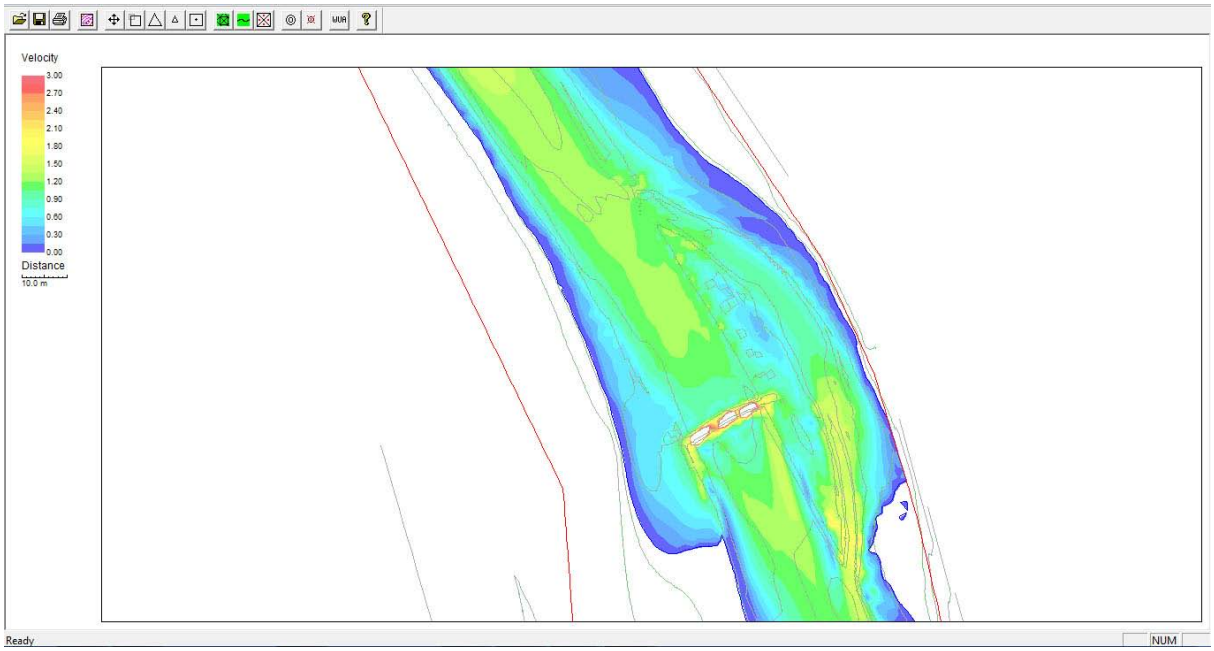

Figure 86 Ice cover on sidearm and jam in the main channel, scenario 40m³/s, River2D

In case of an annual flood event (Q=40[m³/s]) the whole area is inundated. The velocities are highest along the river bed. The influence of the jammed section decreases as the water flows over the surrounding areas. If the jam stays in place the water overtops the jam and the velocities increases to a value higher than 3[m/s] while flowing over the jam. At the spawning areas in the sidearm the velocities reach a maximum value of 1[m/s] in the midsection of the sidearm to 1.8[m/s] at the narrowing section towards the former out flowing area into the main channel (Figure 86).

3.3. Comparison of the simulation results

In the following chapter the results of the modelling approaches will be compared. First of all the differences between the different scenarios (free flowing, ice covered, ice cover and jam) will be compared for the two programs. This will be done by looking at the general flow behaviour and the main spawning sides observed in the field observations in River2D and for the longitudinal sections in HEC-RAS. Further on the differences between the results of the two programs will be compared. Hereby the cross sections at the spawning sides from HEC-RAS will be used and compared with the same area in River2D.

3.3.1. Results deriving from HEC-RAS

The following chapter will describe the changes in flow velocity between the three scenarios and the discharges modelled in HEC-RAS. Hereby the graphs and results for the sidearm section will be compared. First of all the general trend will be pointed out and later on the comparison will be done for the discharges mainly occurring during the winter season (1[m³/s], 3[m³/s], 5[m³/s] and 10[m³/s]) as well as for the high flood event with 40[m³/s].

Looking at the general overview graphs in chapter 3.1 (Figure 41, Figure 48, Figure 57) it can be seen that for the open water flow scenario the highest peaks are found in the inlet section of the sidearm. This is for low flow condition and outreaches the highest velocities even for the high flood events in all three scenarios. The highest peak is found at the open flow scenario with a velocity of 2.71[m/s] which is the highest velocity reached at all in the HEC-RAS part. This can be seen in Table 5. The first column shows the distance from the joining section (0m) to the dividing section upstream (116.79m).

Comparing the depth averaged velocities from Profile 1 it can be said that over all the velocity decreases due to the ice cover. As the riverbed does change in shape and topography the influence to the velocity given by the ice varies. The largest change in velocity is found at the inlet step (111.03m) where the velocity drops by about 2.1 [m/s] in the ice cover scenario. After this section the decrease varies due to the flow depth. At the most upstream cross section it can be observed that the velocity as well for the ice cover scenario as for the jam scenario increases whereas the velocity for the low flow conditions change slightly at the jam scenario compared to the open flow. For Profile 1 it can be seen that between the open flow scenario and the ice cover scenario the velocity decreases. Due to the shape of the riverbed the change in velocity is not constant through out the river section.

With increasing discharge the flow behaviour changes. The velocity in the sidearm slightly increases when the scenarios of open flow and ice cover are compared. At 3 [m³/s] a significant change in velocities between the first two scenarios and the ice jam can be observed.

While the increase in velocity for the midsection varies between 0.04 [m/s] and 0.13[m/s] the changes for the downstream part are in the range of 0.18[m/s] to 1.58[m/s] (Table 5).

Table 5 Depth averaged velocity in the sidearm; comparisons of Profiles 1 (1[m³/s]) and 3 (3[m³/s])

Channel Distance [m]	Profile 1- open water [m/s]	Profile 1- ice cover [m/s]	Profile 1- jam [m/s]	Profile 3- open water [m/s]	Profile 3- ice cover [m/s]	Profile 3- jam [m/s]
116.79	0.03	0.66	2.31	0.1	0.09	0.29
111.03	2.71	0.63	0.76	2.44	2.46	0.37
105.16	0.43	0.15	0.43	0.65	0.63	0.8
98.47	0.48	0.53	0.44	0.46	0.46	0.57
92.32	0.13	0.03	0.13	0.24	0.23	0.39
87.59	0.25	0.11	0.24	0.33	0.33	0.46
82.61	0.38	0.18	0.37	0.44	0.44	0.51
77.68	0.35	0.21	0.34	0.41	0.41	0.45
72.95	0.19	0.05	0.19	0.3	0.3	0.43
68.75	0.33	0.15	0.32	0.41	0.42	0.52
64.52	0.47	0.18	0.46	0.57	0.59	0.64
60.71	0.56	0.52	0.55	0.63	0.66	0.78
53.43	0.61	0.14	0.89	0.81	0.96	1.14
45.34	0.32	0.06	0.44	0.6	0.68	1.16
38.24	0.26	0.04	0.33	0.54	0.6	1.16
30.69	0.28	0.04	0.37	0.59	0.67	1.43
20.45	0.24	0.04	0.3	0.53	0.6	2.18
13.38	0.03	0.01	0.04	0.08	0.08	0.27
0	0.04	0.01	0.05	0.08	0.09	0.29

For Profile 3 it can be seen that the velocity rapidly increases at the outlet section of the channelized part at the jam scenario. This happens while the influence of the inlet decreases. This behaviour can also be seen in Profiles 4 and 5. The rapid increase in velocity at the inlet step seen in the open flow scenario is not given for the other two scenarios. The velocities are slightly higher for the midsection of the side arm as well in the ice cover scenario as in the jammed river scenario.

While at a discharge of 5[m³/s] the velocity increases along the channelized section from one scenario to the other, at 10[m³/s] the velocities between the ice covered scenario and the jammed scenario mainly decrease for this part of the sidearm.

Table 6 Depth averaged velocity in the sidearm; comparison of Profiles 4 (5[m³/s]) and 5 (10[m³/s])

Channel Distance [m]	Profile 4- open water [m/s]	Profile 4- ice cover [m/s]	Profile 4- jam [m/s]	Profile 5- open water [m/s]	Profile 5- ice cover [m/s]	Profile 5- jam [m/s]
116.79	0.17	0.23	0.34	0.29	0.34	0.41
111.03	2.14	1.07	0.4	0.38	0.41	0.46
105.16	0.72	0.78	0.27	0.78	0.28	0.3
98.47	0.49	0.55	0.59	0.55	0.61	0.31
92.32	0.3	0.36	0.44	0.39	0.45	0.3
87.59	0.38	0.44	0.5	0.45	0.51	0.31
82.61	0.45	0.5	0.53	0.5	0.55	0.61
77.68	0.4	0.44	0.46	0.43	0.48	0.53
72.95	0.35	0.41	0.46	0.42	0.47	0.53
68.75	0.45	0.51	0.53	0.49	0.55	0.59
64.52	0.6	0.67	0.62	0.6	0.65	0.3
60.71	0.68	0.8	0.71	0.7	0.75	0.75
53.43	0.89	1.15	0.96	0.96	1.06	0.96
45.34	0.77	1.08	1.13	1.03	1.27	1.13
38.24	0.72	1.05	1.17	1.03	1.34	1.23
30.69	0.81	1.27	1.53	1.23	2.15	2.58
20.45	0.74	1.31	2.4	0.3	0.39	0.55
13.38	0.11	0.18	0.32	0.15	0.23	0.35
0	0.11	0.18	0.33	0.15	0.23	0.35

Table 7 Depth averaged velocity in the sidearm; comparison of Profile 11 (40[m³/s])

Channel Distance [m]	Profile 11-open water [m/s]	Profile 11-ice cover [m/s]	Profile 11-jam [m/s]
116.79	0.69	0.92	1.08
111.03	0.66	0.93	1.09
105.16	0.42	0.6	0.7
98.47	0.42	0.6	0.69
92.32	0.42	0.6	0.69
87.59	0.43	0.61	0.71
82.61	0.43	0.61	0.71
77.68	0.42	0.6	0.7
72.95	0.42	0.6	0.7
68.75	0.41	0.59	0.69
64.52	0.4	0.57	0.67
60.71	0.39	0.55	0.64
53.43	0.37	0.5	0.59
45.34	0.38	0.48	0.57
38.24	0.35	0.43	0.51
30.69	0.48	0.65	0.78
20.45	0.42	0.6	0.71
13.38	0.27	0.41	0.49
0	0.28	0.43	0.51

At the simulated flood discharge it can be observed that the velocities in the sidearm increase in both winter scenarios compared to the open water flow. The flow behaviour remains the same. After the first two stations the velocity drops by about 0.3[m/s] and slowly decreases. Right before the sidearm enters the main channel again the velocity goes up by 0.13[m/s] at the free flowing water scenario, 0.22[m/s] for the ice cover and 0.27[m/s] for the jammed river.

Comparing all scenarios it can be said that the flow characteristic changes with increasing discharge. While at low flow conditions the highest velocities are found at the inlet step, where the ice cover scenario show the smallest peak, the influence of the step decreases with higher discharges and the peak is found further downstream at the narrow part of the outlet section. The exception to that is the jammed river scenario where most of the discharge is forced to flow through the sidearm. Here the peak in the downstream section is already found at Profile 3.

The data in the tables above is shown in the graphs below for each discharge. In every graph the three scenarios are shown for the specific profile (discharge). This was done to get a better understanding of the differences in velocity distribution along the sidearm section.

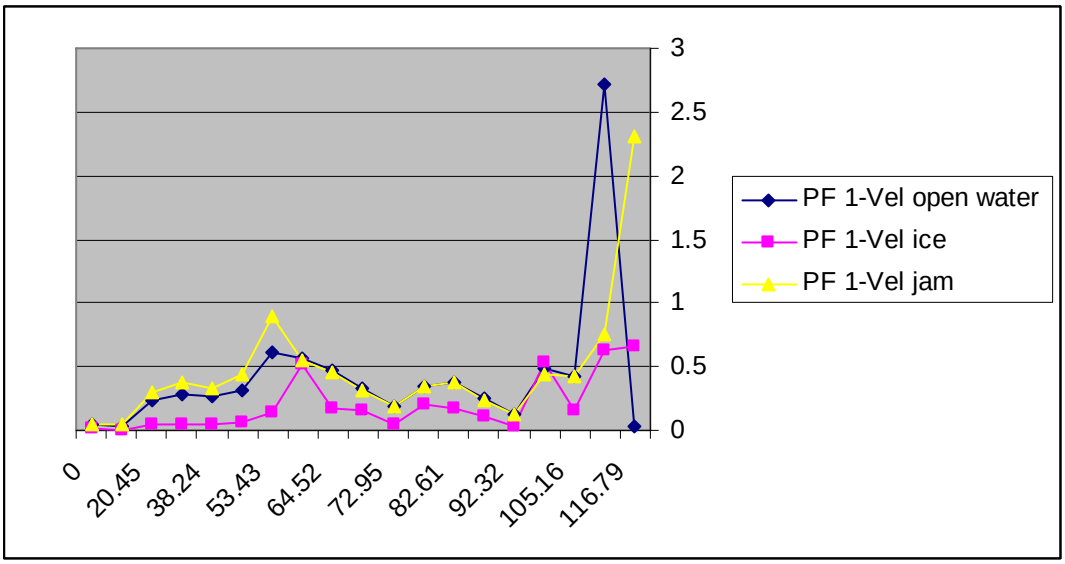

Figure 87 Comparison of HEC-RAS results; Profile 1 (1[m³/s])

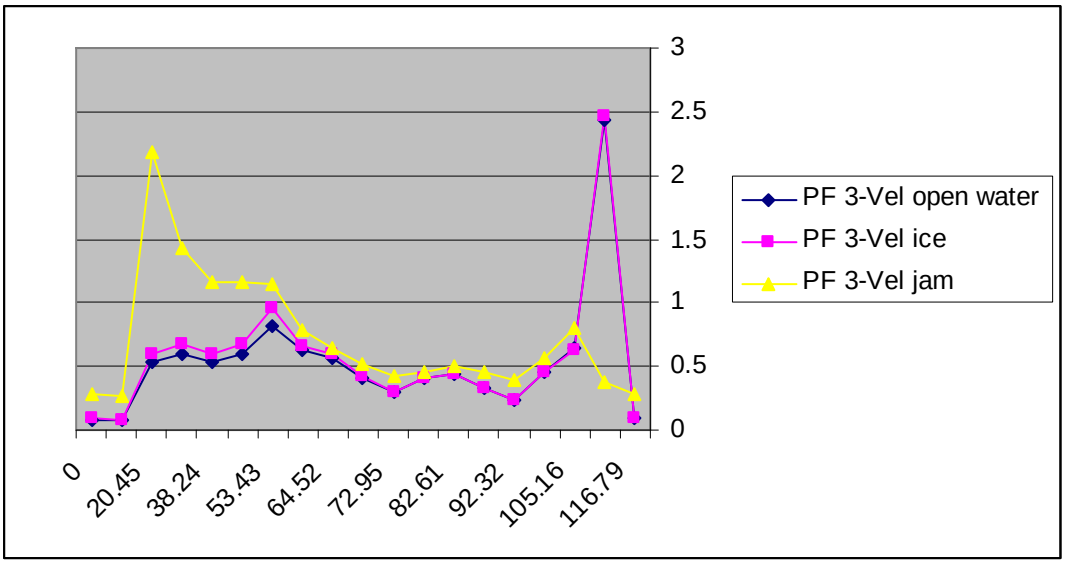

Figure 88 Comparison of HEC-RAS results; Profile 3 (3[m³/s])

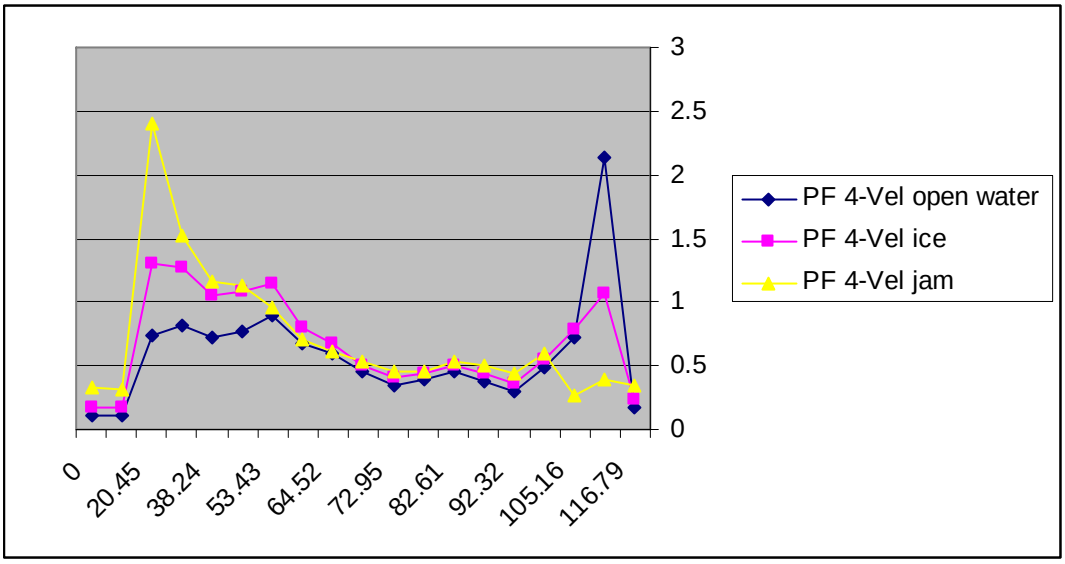

Figure 89 Comparison of HEC-RAS results; Profile 4 (5[m³/s])

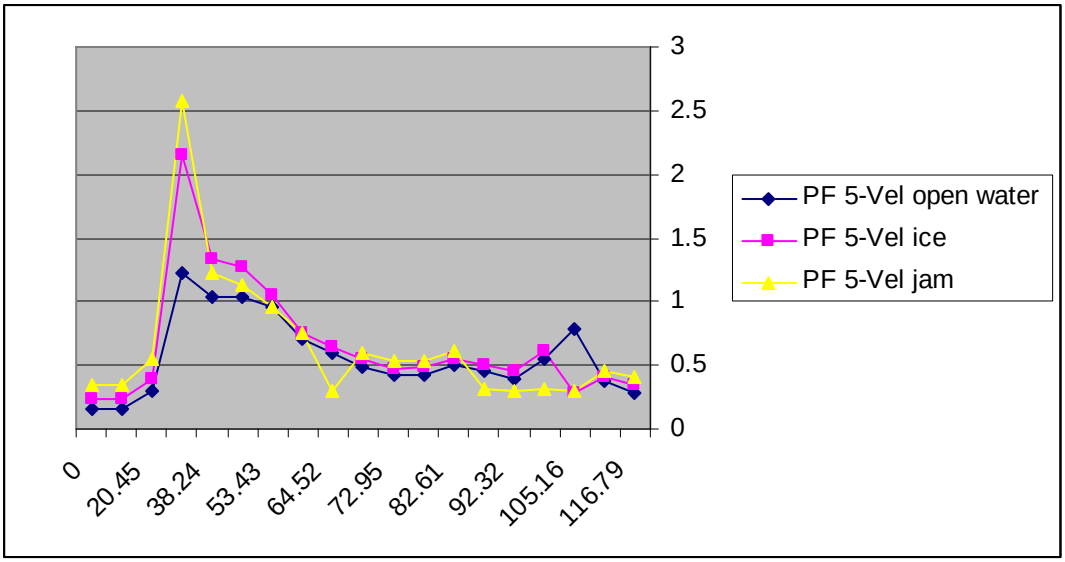

Figure 90 Comparison of HEC-RAS results; Profile 5 (10[m³/s])

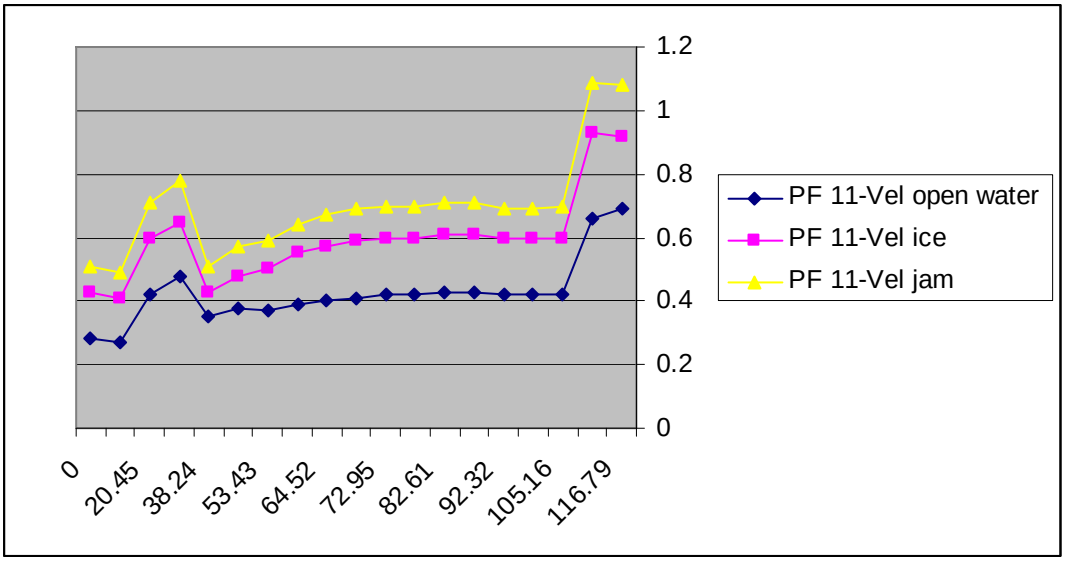

Figure 91 Comparison of HEC-RAS results; Profile 11 (40[m³/s])

3.3.2. Results deriving from River2D

In the following chapter the differences for the results produced in River2D will be compared. Therefore three sections of the simulation area will be used. The first on is the inlet step to the sidearm, the second area is found at the midsection of the sidearm where two spawning sides were observed during the on-site observations and the last part will be the outlet to the main channel. The location of the areas within the simulated river section can be seen in Figure 29.

The discharges compared are the same as used in chapter 3.3.1 as these are the frequent discharges occurring during spawning and hedging periods. For each discharge the areas to compare are put next to each other with the related colour legends for the velocities. If the range of colours varies between the pictures, the legend according to the picture is put next to it.

Starting with the low flow conditions of 1 [m³/s] Figure 92 shows the upstream part of the sidearm. At the dividing section it can be seen that the velocity is highest in the open flow scenario. Here the water exceeds the set range of velocities and velocities higher than 0.75[m/s] are found. It also can be seen that the lowest velocity profile is found at the ice cover scenario where as the flow velocity increases at the jammed scenario. The most right picture shows that the discharge is redirected towards the sidearm and compared to the two other scenarios the velocity in the main channel downstream of the divide is the lowest of all three scenarios.

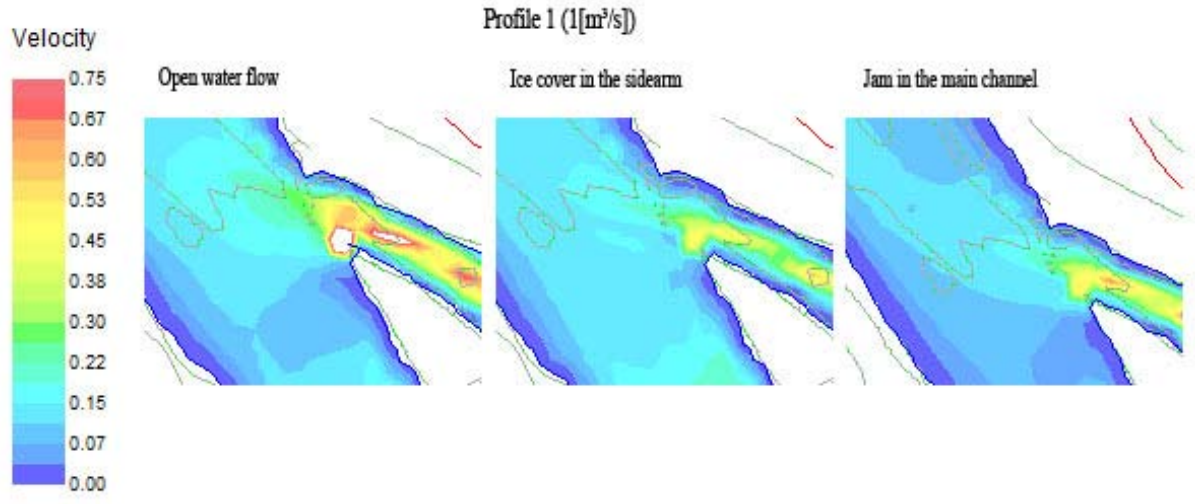

Figure 92 Comparison of River2D results; Profile 1 (1[m³/s]); inlet section

Looking further downstream at the area with the spawning hotspot the situation is about the same. The highest velocities are still found at the open flow scenario while the influence given by the ice cover decreases the velocity at the side arm. At the main spawning site the

velocity range remains about the same for all three scenarios between 0.1[m/s] and 0.2[m/s]. Leaving out the section where the water enters the channelized part the highest velocity for the midsections are found in the open flow scenario. Comparing all three the ice cover scenario has the lowest velocity profile with a maximum velocity of about 0.3[m/s].

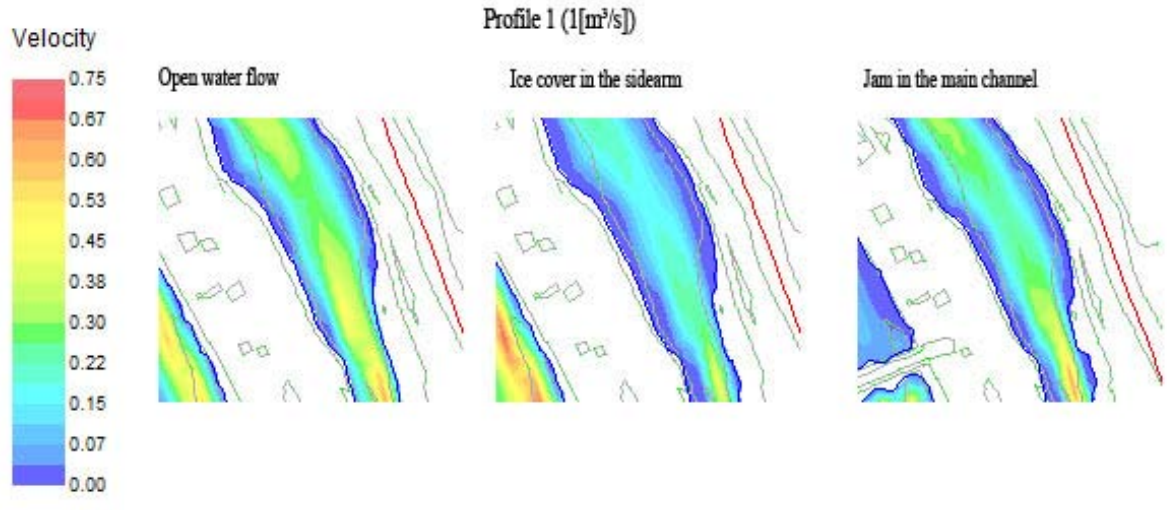

Figure 93 Comparison of River2D results; Profile 1 (1[m³/s]); mid section

At the joining section a similar result as in the pictures above is shown. It can be seen that different to the free flowing and the jammed scenario the velocity at the ice cover scenario is low in the sidearm whereas it is higher in the main channel compared to the other two. The velocity distribution is most homogeneous throughout the open water flow scenario whereas it varies in the scenarios influenced by ice.

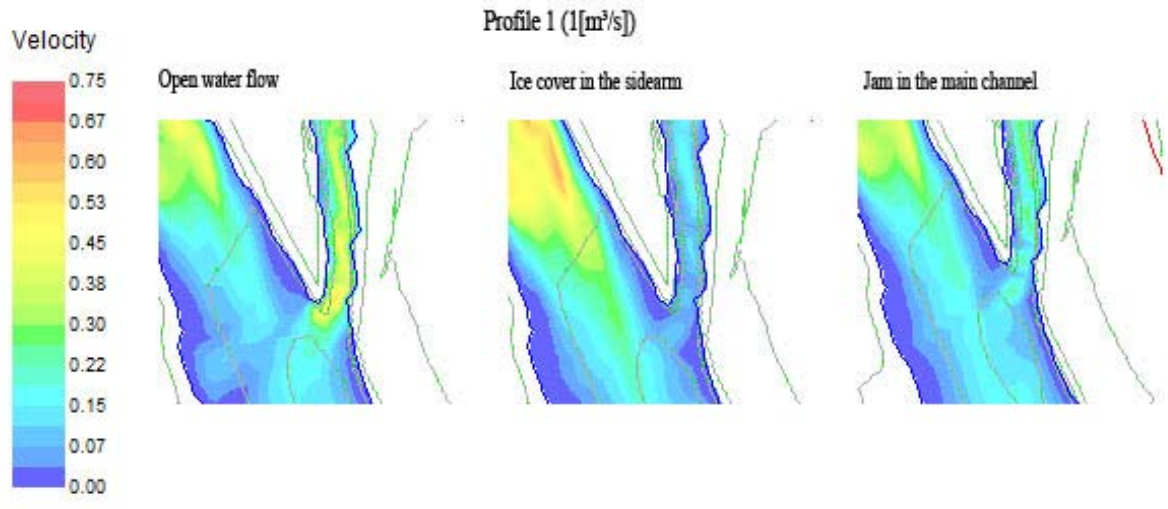

Figure 94 Comparison of River2D results; Profile 1 (1[m³/s]); outlet section

With increasing discharge some changes on the hydraulic situation can be figured out. While a difference of about 0.4[m/s] between the open flow and the ice cover scenario is shown the most significant changes can be seen at the jammed scenario. Here the flow area is extended due to the increasing discharge running through the sidearm. Larger areas with low flow velocities are seen and the highest velocities are found in the midsection of the flow channel.

Further downstream the characteristic changes. In the midsection of the channel the velocities of the open low and the jammed scenarios are almost the same whereas the ice cover scenario still shows the lowest velocity. The main difference seen here is the extended flow area in the jammed scenario which derives from the fact that different to the other scenarios, almost all of the discharge flows though the sidearm. At the beginning of the channelized part the velocity increases in all three scenarios where the highest increase is found in the jammed scenario. It can be seen that in average the velocity increases by 0.3[m/s].

At the outlet the situation changes again. As there is only little possibility for the river to widen the highest velocities occur at the jammed scenario where the two reaches join again.

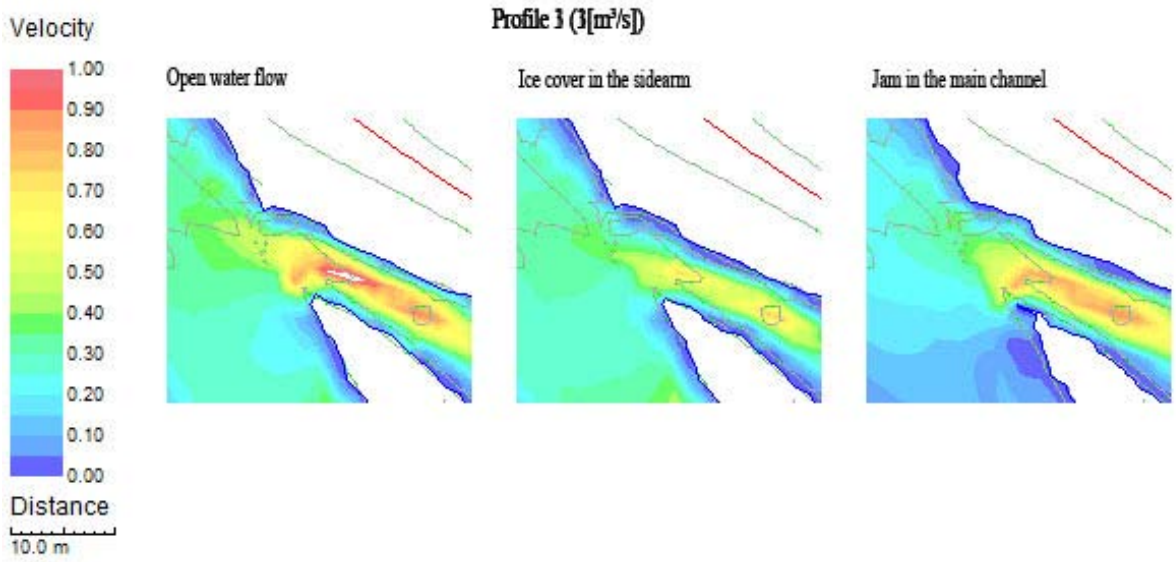

Figure 95 Comparison of River2D results; Profile 3 (3[m³/s]); inlet section

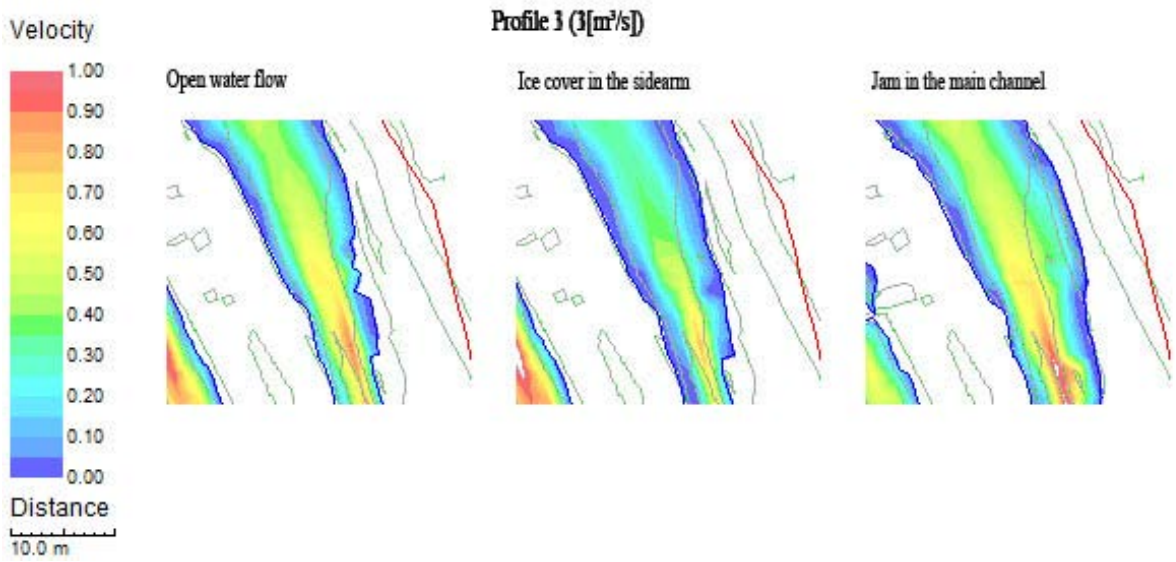

Figure 96 Comparison of River2D results; Profile 3 (3[m³/s]); mid section

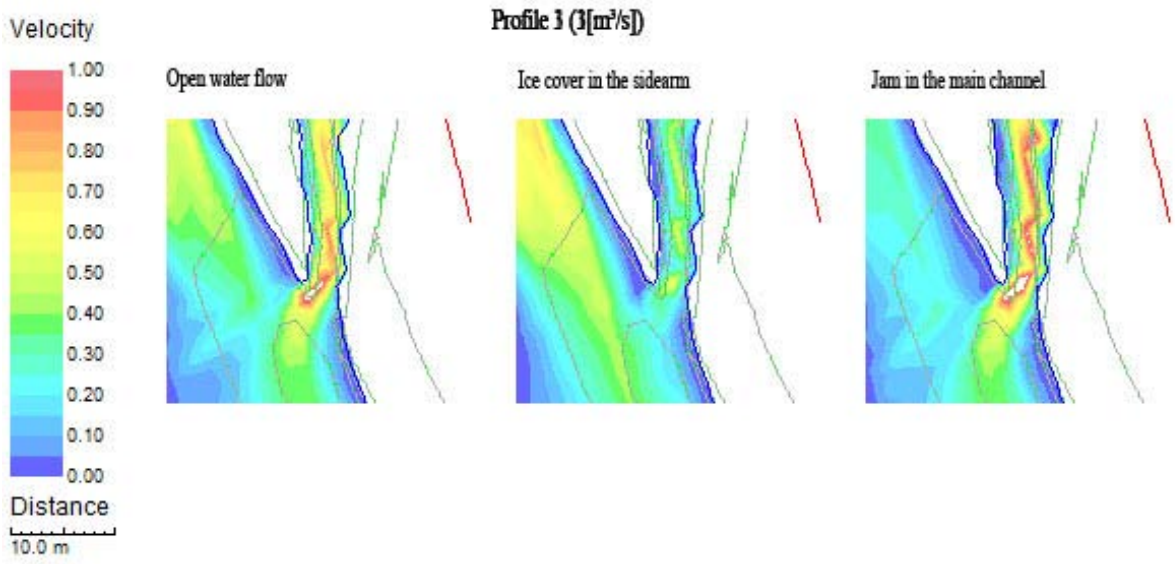

Figure 97 Comparison of River2D results; Profile 3 (3[m³/s]); outlet section

At Profile 4 (Q = 5[m³/s]) it can be seen that the influence given by the change in the situation increases. While at the open flow scenario the water follows the riverbed, it starts to overtop the island at the second scenario. For the jammed scenario it can be seen that the surrounding areas of the divide are flooded as well as parts of the island. In comparison the overall highest velocities occur at the jammed scenario where the river overtops the island at the inlet. (Figure 98) But looking at the riverbed the velocities in the open flow scenario are slightly higher with a peak of 1.1[m/s].

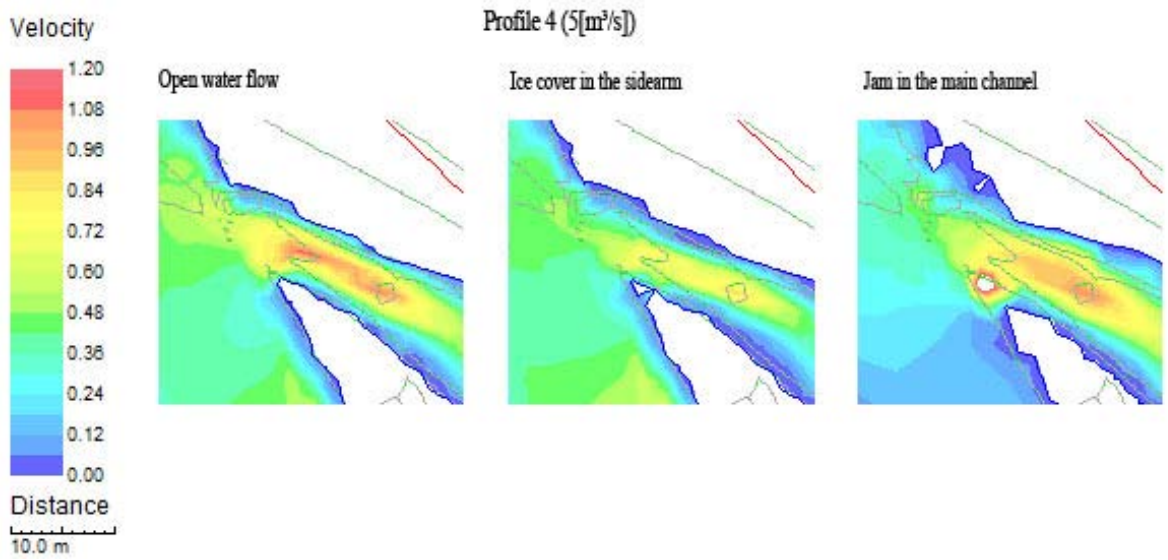

Figure 98 Comparison of River2D results; Profile 4 (5[m³/s]); inlet section

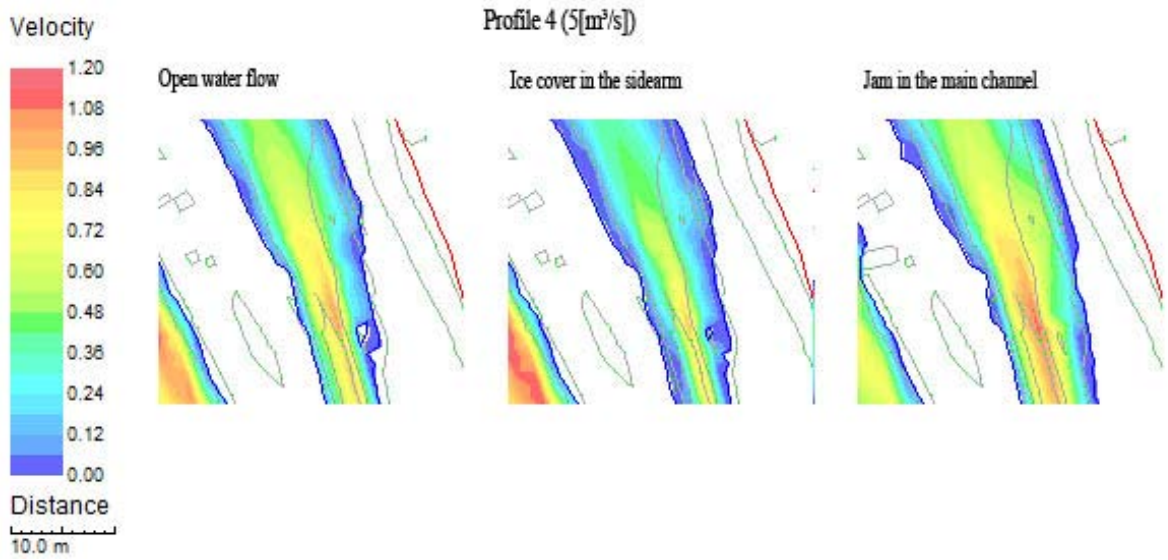

Figure 99 Comparison of River2D results; Profile 4 (5[m³/s]); mid section

At the spawning areas a similar behaviour can be observed. The smallest depth is found at the first scenario while the velocities at the ice cover scenario are lowest. The velocities are, as seen before, almost the same for the jam and the free flowing scenario (Figure 99).

The characteristics observed in Profile 3 for the outlet section continues. While the flow exceeds the riverbed upstream here the limits given by the topography lead to the effect that the velocities exceed the range set with 1.2[m/s]. While this happens only at the joint in the first scenario, it is the case throughout the channelized part for the third case.

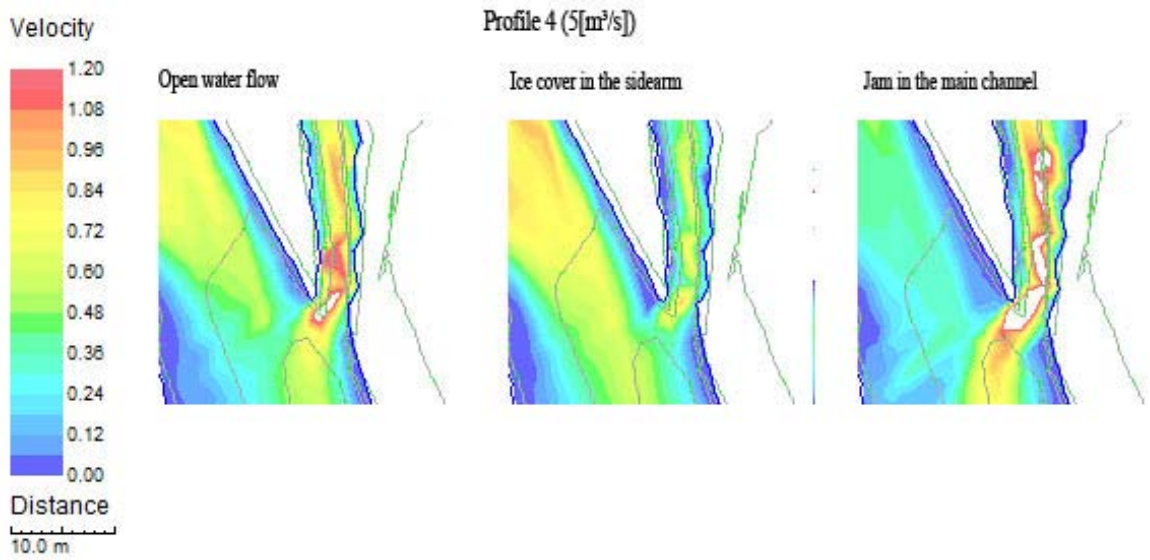

Figure 100 Comparison of River2D results; Profile 4 (5[m³/s]); outlet section

At the discharge of 10[m³/s] the river exceeds the channel capacity in all three scenarios. But the extension of the overtopping varies. While for scenario one, only small parts of the surrounding areas and the island are flooded, in scenario two larger parts of the upstream area are flooded. In scenario three the whole upstream part of the island is inundated and the river has flooded the first step in landscape beside the riverbank. The velocities along the riverbed in the sidearm are almost the same for all three scenarios.

Regarding the velocities it can be said that the velocity along the riverbed are almost the same. The increase caused by the inlet step can be observed in all three scenarios but the over all influence compared to smaller discharges decreases. The velocity downstream of the step is about 1.15[m/s] independent from the scenario. The main difference found is in the extension of the velocity field as seen in Figure 101. Looking along the compared sections the same characteristic and the same differences can be observed throughout the areas.

The exception to this is again the outlet area (Figure 103). Here the velocity in the jammed scenario is higher than in the other two. While the velocities in the two first scenarios are between 1.35 [m/s] and 1.65 [m/s] in the jammed scenario the velocity goes up to higher than 2 [m/s].

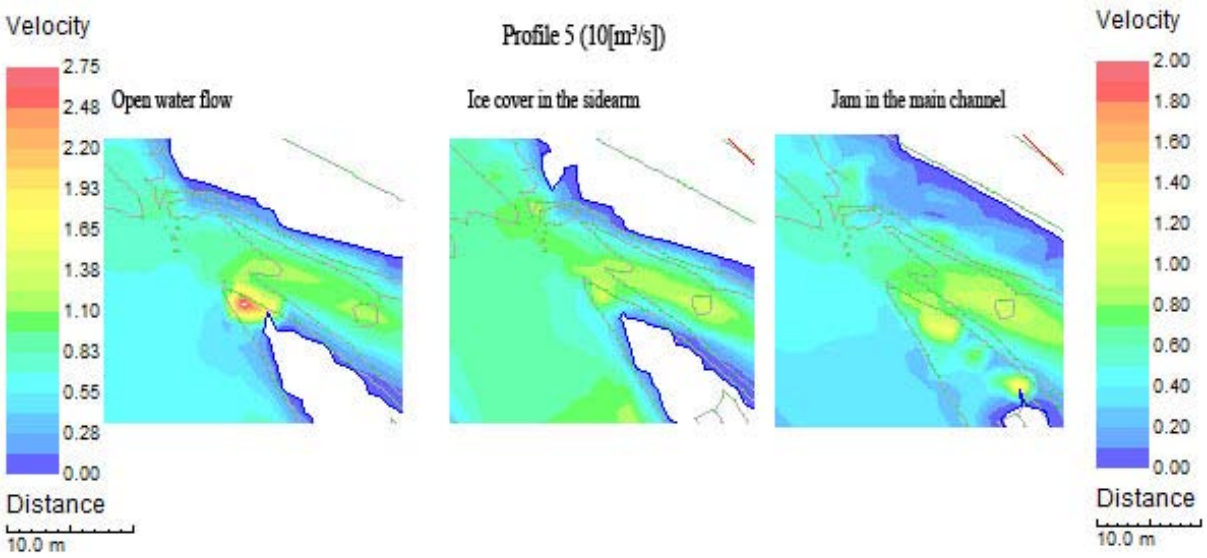

Figure 101 Comparison of River2D results; Profile 5 (10[m³/s]); inlet section (legend on left side of the picture valid for open flow and ice cover)

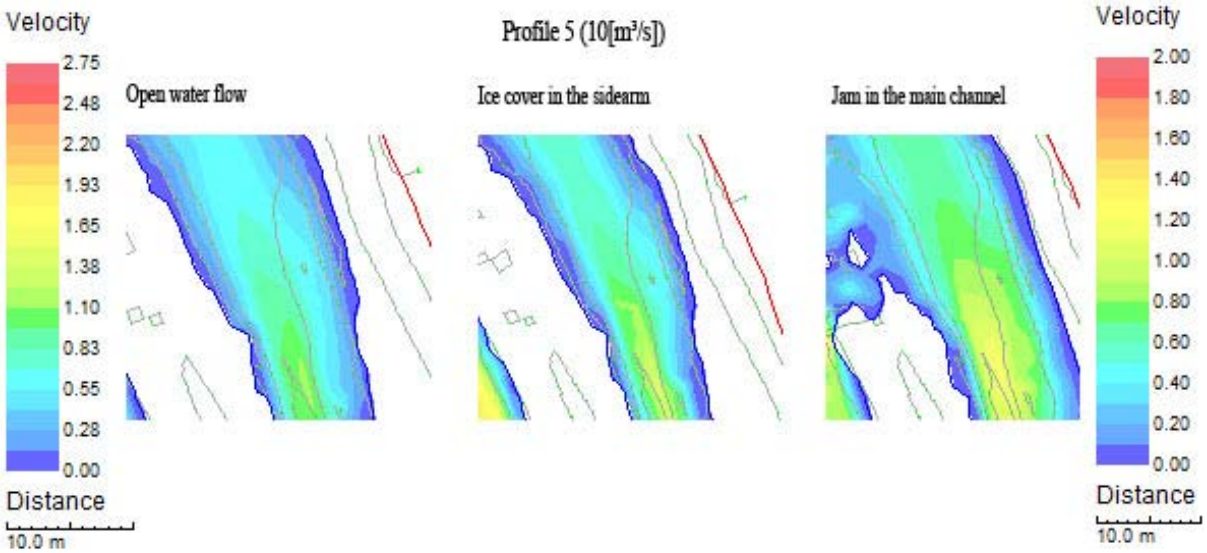

Figure 102 Comparison of River2D results; Profile 5 (10[m³/s]); mid section (legend on left side of the picture valid for open flow and ice cover)

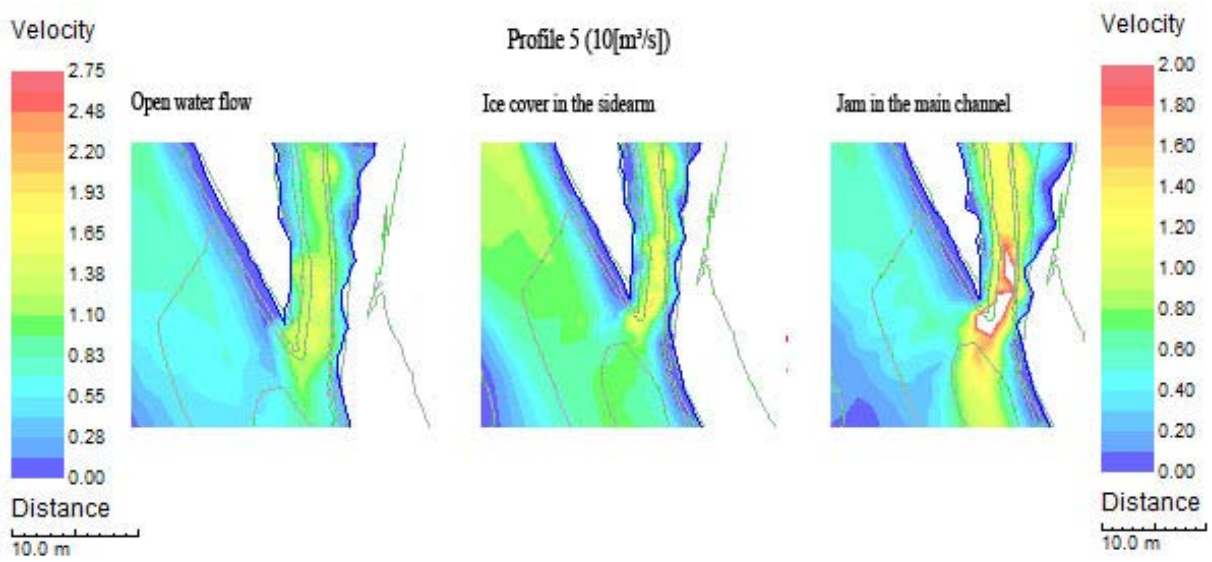

Figure 103 Comparison of River2D results; Profile 5 (10[m³/s]); outlet section (legend on left side of the picture valid for open flow and ice cover)

For Profile 11 (Q = 40[m³/s]) it can be seen that in all three cases the whole area is flooded. Even though the whole area is now covered with water the extensions of the flowing areas are different. The influence of the jam is still given and therefore the whole section of the river upstream is still influenced. The velocity distribution for the free flowing water and the ice cover scenario is almost the same. Here the highest velocities are found along the riverbed (main channel and sidearm) as well as at the shallow upstream part of the island. In the jammed scenario the highest velocity is found in the main channel while the sidearm has low flower velocities than the main channel.

If the velocities are compared it can be seen that besides the different flow behaviour due to the channel the velocities in all three scenarios are about the same along the side channel. (Figure 104)

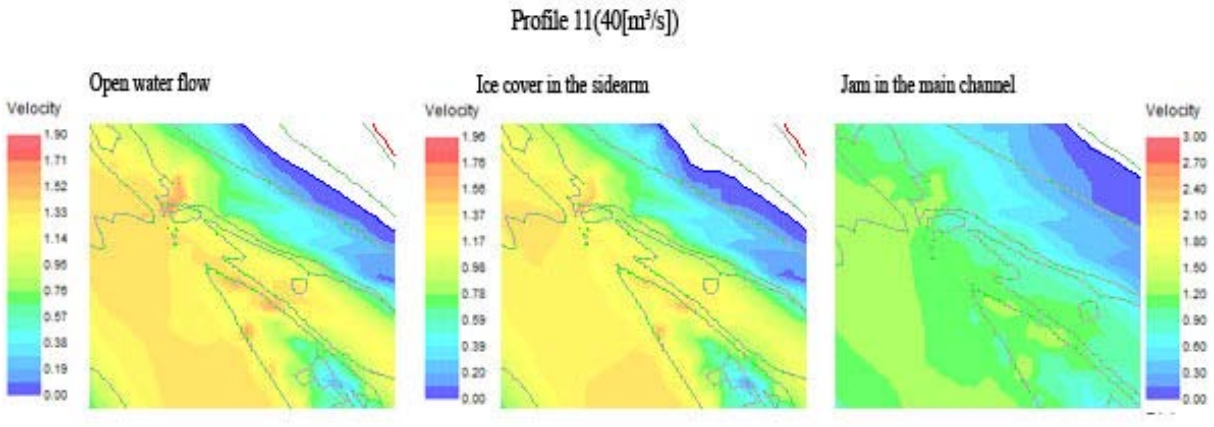

Figure 104 Comparison of River2D results; Profile 11 (40[m³/s]); inlet section

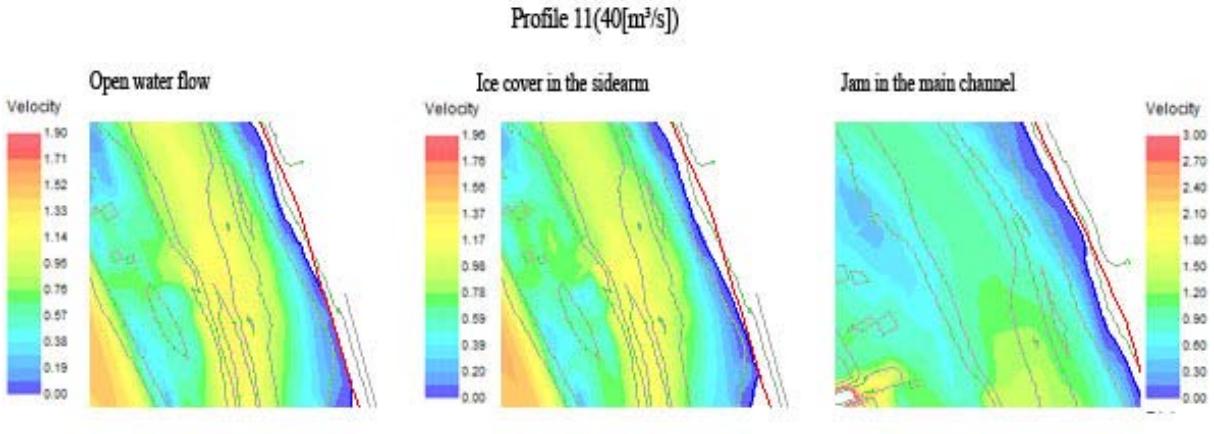

Figure 105 Comparison of River2D results; Profile 11 (40[m³/s]); mid section

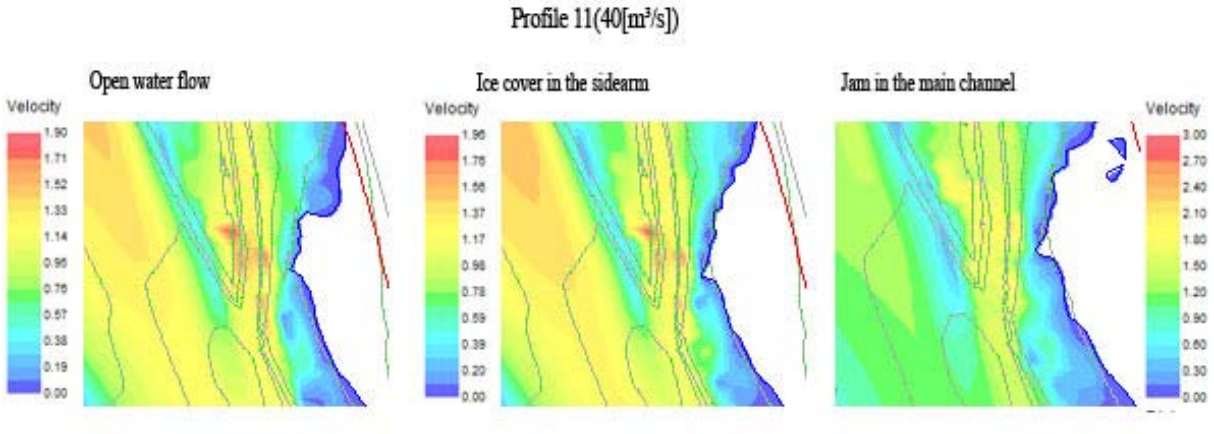

Figure 106 Comparison of River2D results; Profile 11 (40[m³/s]); outlet section

Further downstream the range of velocity in the riverbed is still the same for the free flowing and the ice cover scenario (about 1.3[m/s] up to 1.8[m/s]) whereas the velocities in the jammed scenario increase again to a peak of 2.2[m/s]. The velocity increases downstream of the jam as the water flows into the sidearm over the lowest point in the midsection of the island. It should be mentioned here that the velocities for the river banks and the surrounding areas might differ from the results in HEC-RAS as the roughness was set on an average value for the riverbed. The comparison between the results of the two programs will be shown in the next chapter.

3.3.3. Comparing HEC-RAS results with River2D results

In this chapter the results of HEC-RAS and River2D are compared with each other. This will be done regarding to the velocities in the sidearm. As the form of the output of both programs

is different, the velocity distributions across the sections closest to the two main spawning sites (Figure 29) in the sidearm from HEC-RAS are compared with the related section in River2D. The comparison in this chapter is done for the discharges of 3[m³/s] and 5[m³/s] and two cross sections. The water from the main channel is not displayed in the HEC-RAS results because it is not relevant for the analysis. The positions of the cross sections chosen are shown in Figure 107. Further on it has to be mentioned that the HEC-RAS results are displayed looking in flow direction.

After analyzing both simulations it can be said that the results of both simulations vary only in small parts. The general flow behaviour can be said to be the same. In both sets of simulation the influence of the inlet step decreases with increasing discharge. The ice cover slows down the flow in the sidearm and leads to higher water levels while the velocity in the main channel increases. With the jammed section in the main channel the main part of the discharge flows through the sidearm and the water level rises again. As the ice cover floats in top of the water it rises with the water level. Due to the limitations given by the ice cover the velocity in the jammed scenario increases throughout the sidearm. The largest changes in velocity are shown in the downstream part of the sidearm as the possibility to exceed the riverbed is limited by the topographic characteristics. While the resulting velocities within the riverbed are more or less the same the results for the surrounding areas vary due to the differences in roughness and the differences in the modelling approaches of the programs. Therefore the results for the extension in flow area at the high flood scenario can be compared in general but have to be looked at with care.

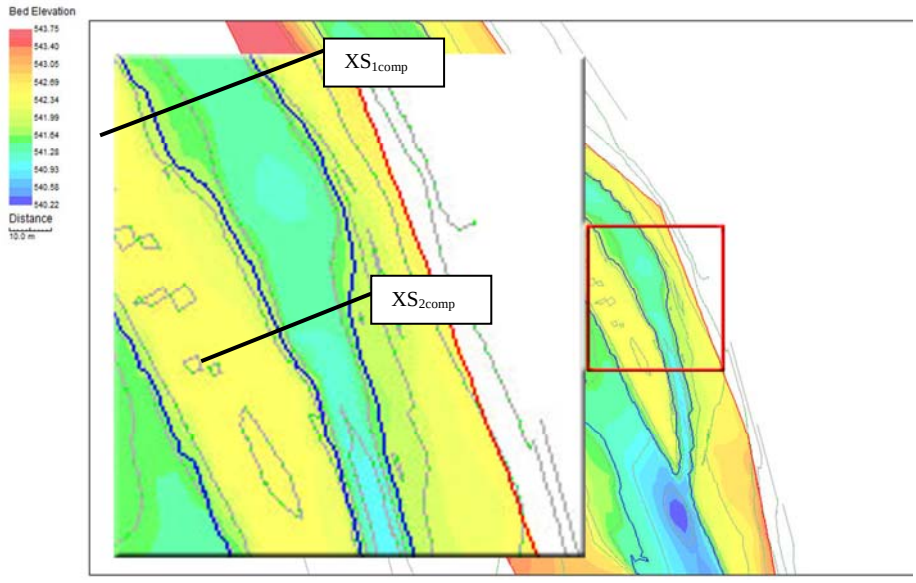

Figure 107 Positions of the reference cross sections

The first part of this chapter compares the results from the discharge scenario of profile 3 (3[m³/s]). As pointed out earlier this is the average discharge for early winter month. Therefore it is the most common after the spawning season. When compared both results show that in general the velocities at the main spawning spot (XS_{1comp}) are lower than at XS_{2comp}. Both simulation attempts show that the water level increase compared to the open flow scenario. While the water at XS_{1comp} has a velocity range between 0.2[m/s] and 0.4[m/s] which does not change much between the three scenarios the velocity at XS_{2comp} increases most at the jammed scenario. The highest velocity found there is about 0.8[m/s] (Figure 108 and Figure 109).

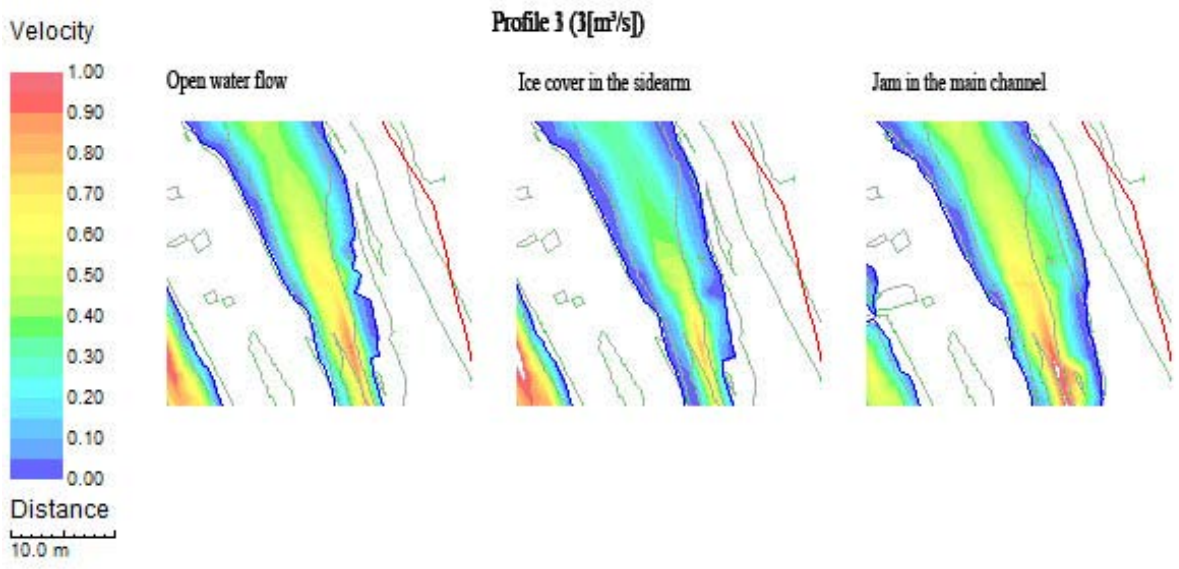

Figure 108 Results Profile 3 River2D for the comparison

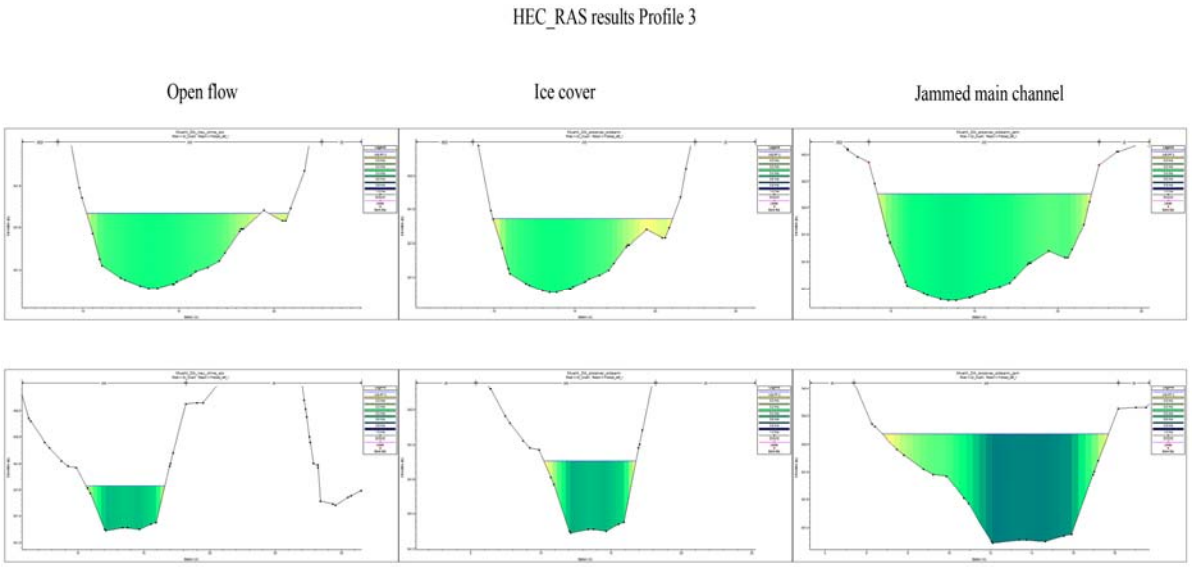

Figure 109 Results Profile 3 HEC-RAS for the comparison; XS_{1comp} on top, XS_{2comp} bottom line

While for Profile 3 both simulations show the same results, the results for the 5[m³/s] profile differ. At XS_{1comp} the velocities still in same range and show the same characteristics for the three scenarios. The water table and the extension of the flow area are about the same as well. For XS_{2comp} the general trend can be said to be the same. There is an increase in water level between the scenarios. The velocities increase as well. A slight difference can be found at the ice cover scenario and the jam scenario in the velocity distribution. In River2D the velocity decreases at the ice cover scenario (compared to the open flow) and increases at the jam scenario again. In HEC-RAS the velocity increases in the ice cover scenario and then slightly decreases (compared with the ice cover) at the jam scenario. Here the highest velocities are found in the ice cover scenario which is not the case in River2D. This is a local effect but the general trend along the sidearm is about the same and the average velocities correlate within the range of tolerance. The difference found can be explained with the difference in resolution of the data points or with the difference in the roughness values. Also the ways to calculate the velocities in the programs differ. As mentioned before in HEC-RAS the velocity is calculated column by column and there is no interference taken into account whereas this is the case in River2D.

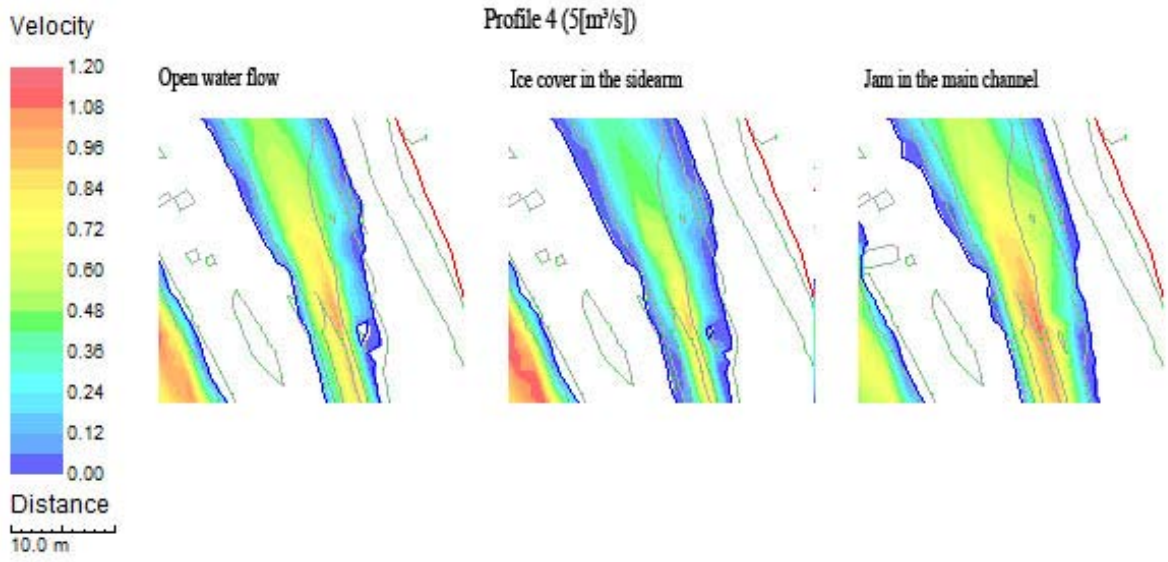

Figure 110 Results Profile 4 River2D for the comparison

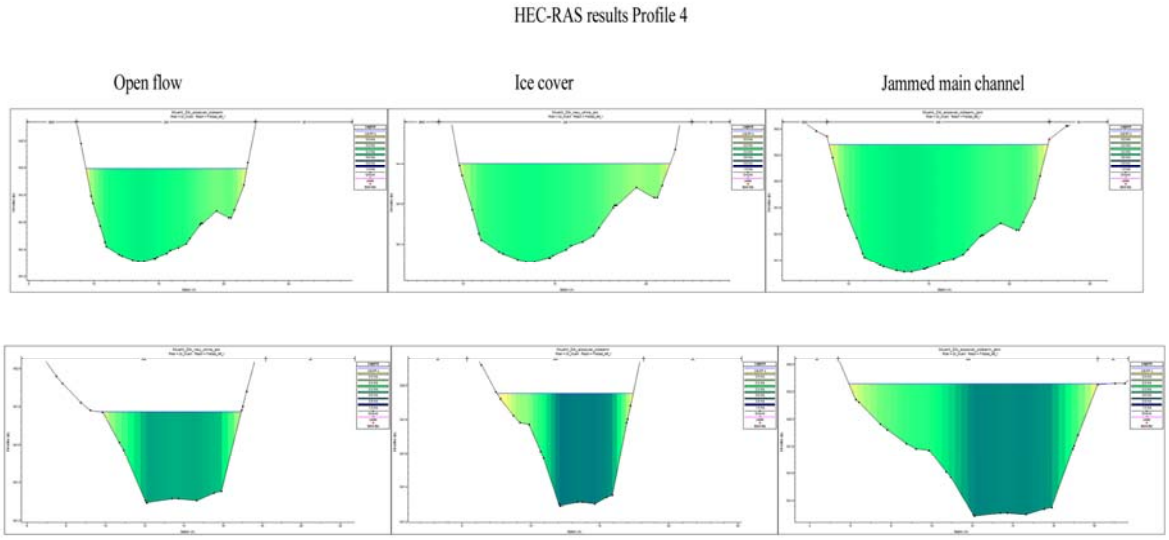

Figure 111 Results Profile 4 HEC-RAS for the comparison; XS_{1comp} on top, XS_{2comp} bottom line

Even though there are differences occurring between the two programs the results are nearly the same for the flow depth and the velocity distribution. The differences in velocities compared are within the range of $\pm 0.1[m/s]$ throughout the models.

3.4. Temperature data

This chapter shows the results of the analysis of the data measured by the temperature sensors.

Starting with the temperature series from 2009 the graph in Figure 112 shows, that the temperature from the beginning of the year until the end of February was about 0°C (0.08°C). On site observation showed that in fact the river was frozen in this period. The difference to 0°C is a systematic error of the sensor and therefore can be neglected. During March the temperature remains on a constant level. This is due to the influence given by the melting snow. Later on the temperature increases until mid May when it drops from 17.6°C after strong rainfalls and a high flood event to 9.1°C. The water warms up again during the summer month and cools down from the end September. The river was frozen again for some days in December 2009.

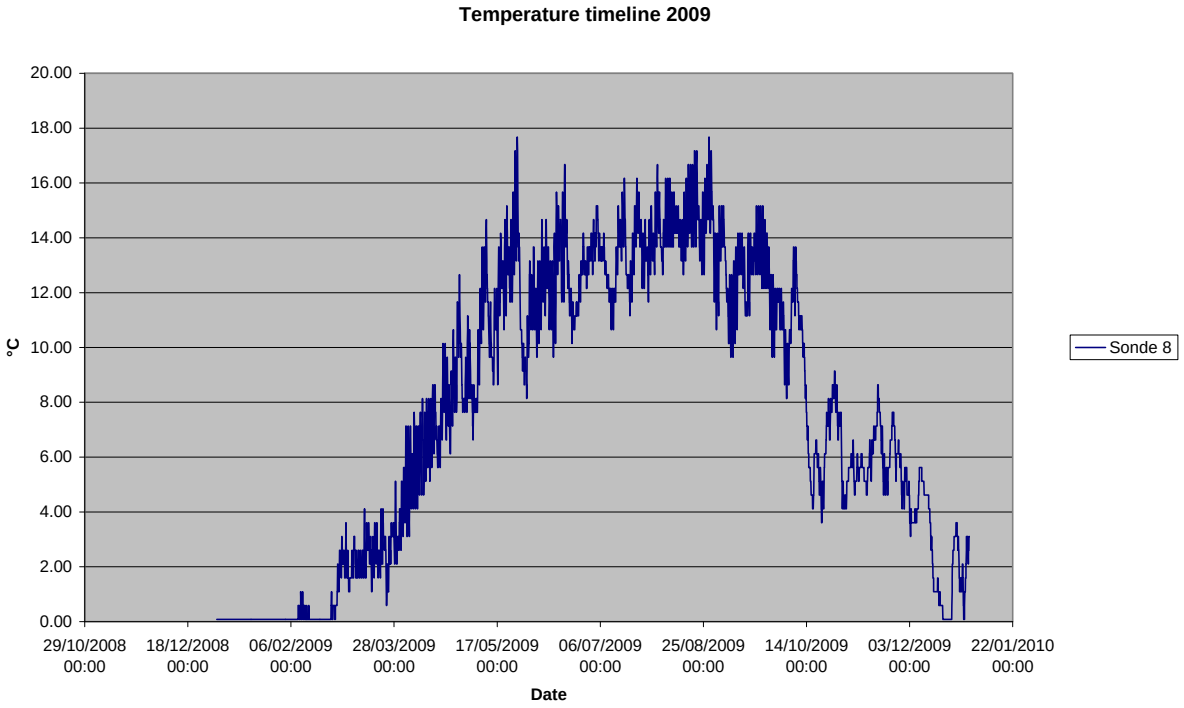

Figure 112 Temperature timeline recorded for the open water flow 2009

Going on with the temperature timeline of 2010 it can be seen that the river was frozen at the beginning of the year until mid March. The peak seen in mid April can be neglected. It derives from a data log while the sensor was taken out of the water for maintenance. No fast changes in temperature can be observed during the year until the end of November where the temperature drops. In Figure 113 a period of temperatures below 0°C can be observed. As there is no longer period of cold before, this can be explained by the supercooling effect described in chapter 1.5, which might have lead to the formation of slush ice during this period. But as the period was short, the formation of a closed ice cover is rather unlikely.

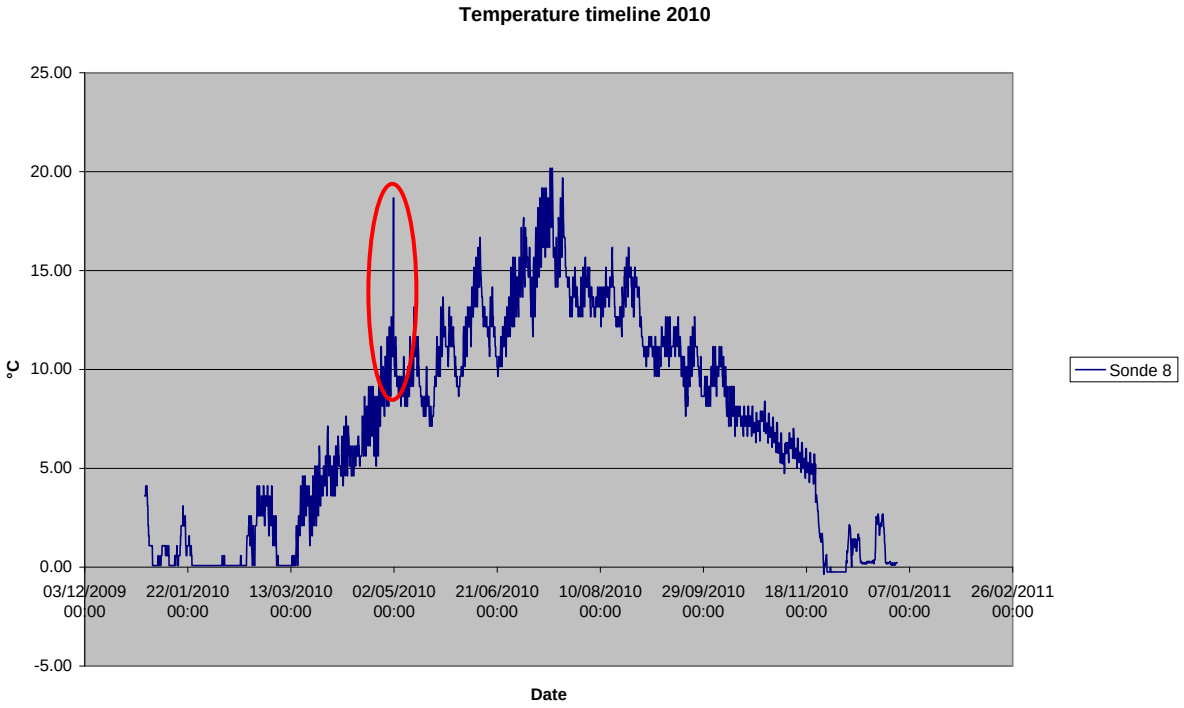

Figure 113 Temperature timeline recorded for the open water flow 2010

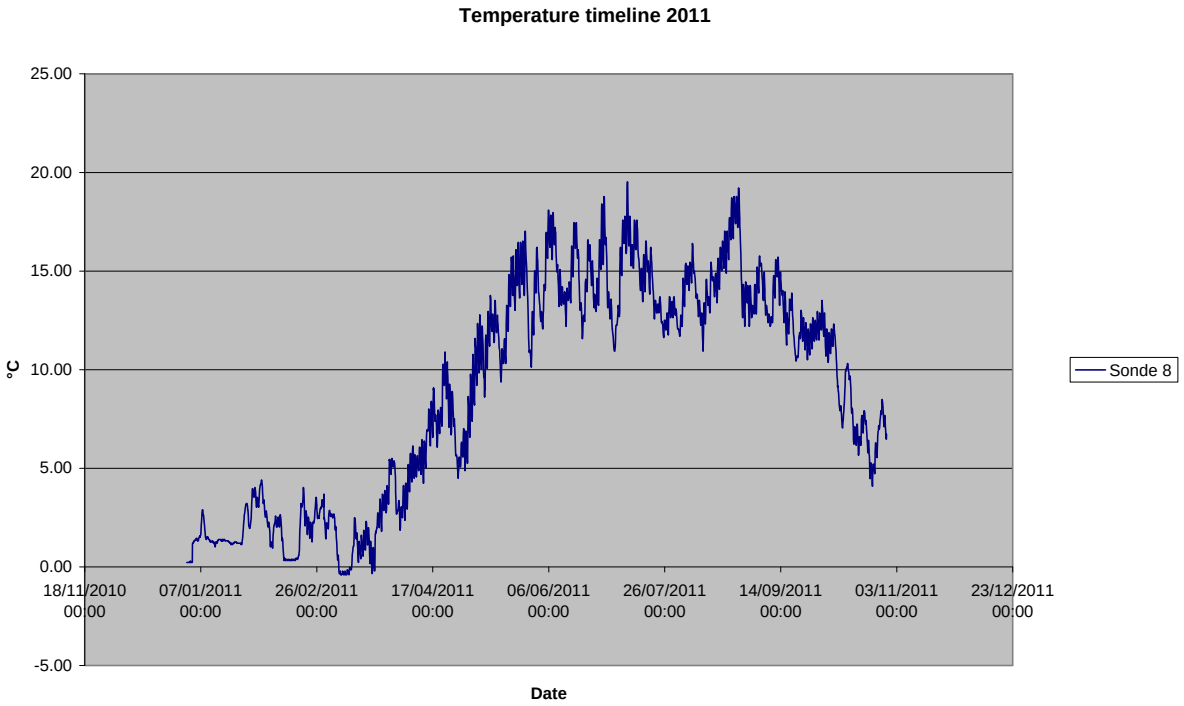

Figure 114 Temperature timeline recorded for the open water flow 2011

In 2011 the temperature during the winter month is higher than in the years before. Except for a short period in the beginning of March 2011 temperatures below 0°C the temperature curve of this year shows that the river has not been frozen at all. It also shows that the year had unstable weather conditions during the summer months. This can be seen with the ups and

downs from June to September. The temperature curve ends on October 29th due to an internal error in the data logging system. This error was fixed on January 4th 2012. For the time in between there is no temperature data available.

The first thing that can be seen looking at the timeline of 2012 is that the temperature never got close to the freezing point. This allows saying that the river did not freeze at all over the winter seasons within 2012 which has been proofed by field observations.

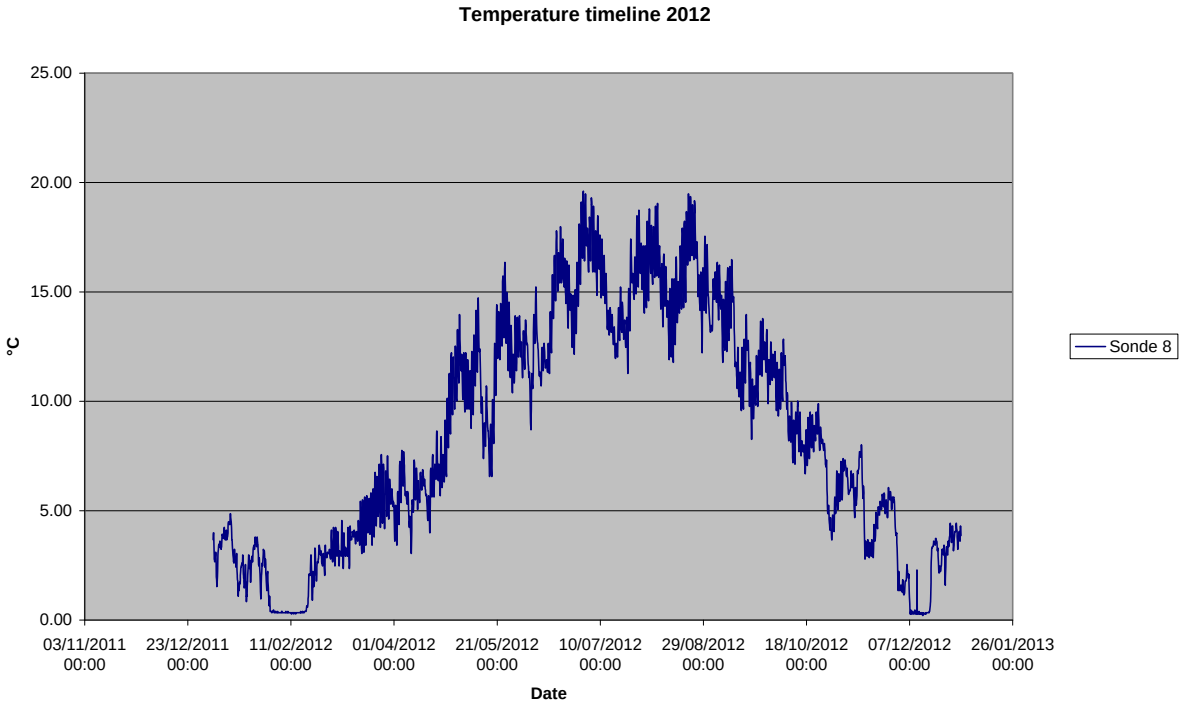

Figure 115 Temperature timeline recorded for the open water flow 2012

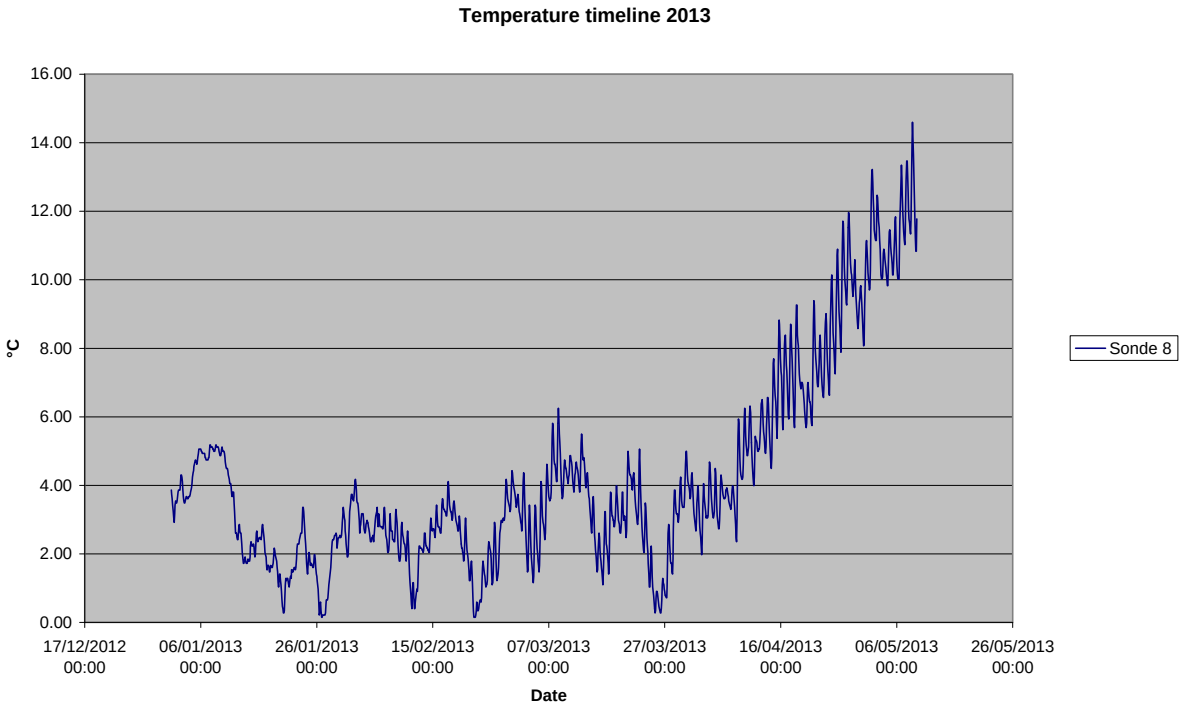

Figure 116 Temperature timeline recorded for the open water flow 2013

The temperature curve of 2013 ends with Mai 2013 as the dataset given by the institute ends here. The graph shows relative high temperature for the beginning of January of about 5°C. Further on it can be seen that the temperature most of the time is in a range between 2°C and 4°C. This means that there was hardly any kind of ice formation during the winter of 2012/13. In Figure 116 the variation between day and night time can be seen more clearly as in the figures above as the timeline is for a shorter period.

Looking at the temperature graph derived from the interstitial sensor it can be seen that the temperature variation during the day does not occur. The timeline shows that there was no period during the monitoring when then temperature reached the freezing point. Therefore it can be said that the area around the sensor was not frozen (“anchor ice”) during winter season 2012/13.

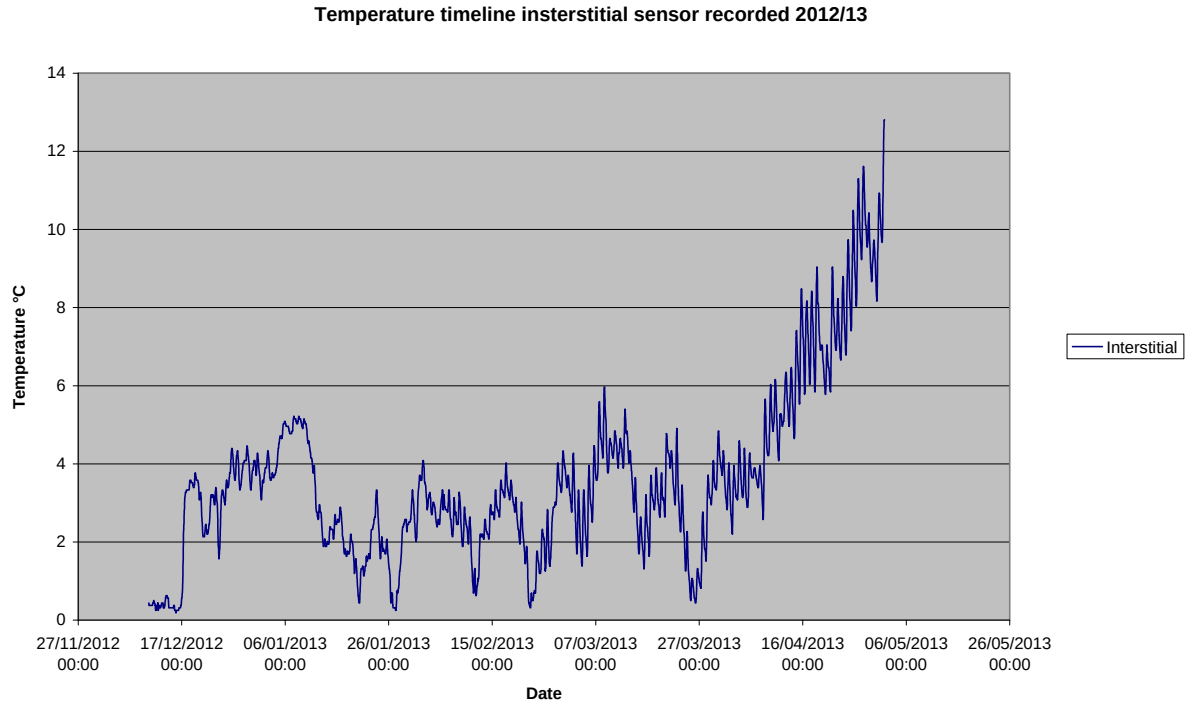

Figure 117 Temperature timeline recorded in the interstitial winter season 2012/13

3.4.1. Comparison of the temperature between open water and interstitial

In this chapter the difference in temperature between the open water and the interstitial area will be analysed. As mentioned before, this is done to see if the differences in temperature lead to a significant change in the hedging times. This is important for the forecast of the hedging of the juvenile fish and for monitoring programs.

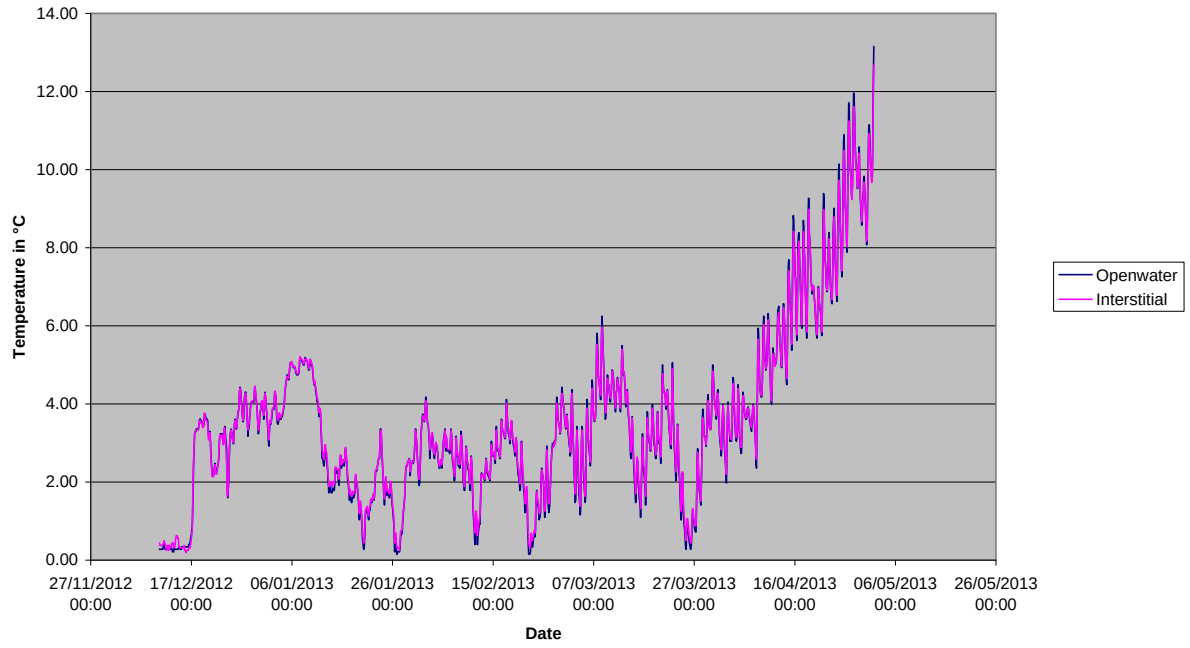

Figure 118 Temperature timeline; overlay of interstitial and open water; winter season 2012/13

The comparison was done for the whole recording period of the interstitial sensor (December 10th 2012 – May 1st 2013). The results of the analysis show that at the depth, where the interstitial sensor was buried, the temperature is still influenced from the surface water. The base temperature is the same as in the open water. Changes in temperature during the day can be seen but to a smaller extend as the water is not influenced by incoming radiation from the sun or outgoing radiation during clear nights as seen in Figure 118. The highest temperature difference found in the data was 0.47°C. As the difference occurs during the changes in day and night the average temperature over the whole day remains almost the same for both sensors. This means that the temperature in the interstitial is on a more constant level than in the open water.

As shown in Figure 119 the day-degrees between the interstitial and the open water differ in a small range for the time monitored at Große Mühl River. On the y-axis the sum of the day-degrees is displayed. The x-axis describes the dates starting with the monitoring period of the interstitial area. The difference in the sum of day-degrees increases with the warming up of the water. Regarding the mentioned range of day-degrees for the hedging time in chapter 1.4.1 (378 – 480 day-degrees) the difference between the hedging time between the open water day-degrees sum and the interstitial day-degrees sum is one day. Therefore it can be said that a forecast in hedging times done with a sensor placed in the open water should be sufficient.

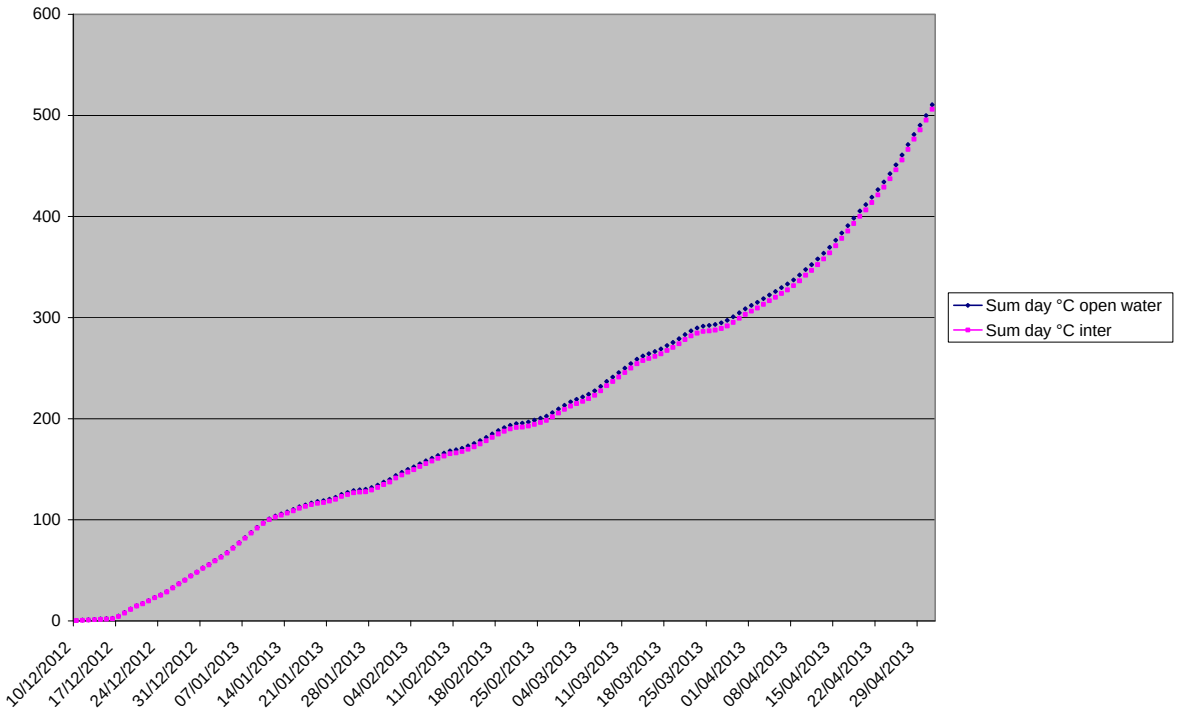

Figure 119 Sum of day-degrees; overlay open water – interstitial area

3.5. Stability analysis of the bed material

After analyzing the flow behaviour and the differences in temperature this chapter shows the results of another parameter in Brown trout spawning. In the following the grain size distribution of the riverbed will be described. As mentioned in the methodology part of this thesis different probes of the riverbed were excavated and sieved afterwards. This was done for the surface layer and for the subsurface layer. The results of the sieving are shown in a log-distribution plot. As seen in Figure 120 the probes show that the highest percentage of materials smaller than 1mm is found in the subsurface layers. The highest concentration of fine materials is found in the probe SSL_3 with a percentage of 13.58% finer than a diameter of 1mm. The results also show that there is no material found smaller than 0.5mm.

For all three samples of the surface layer (SL) deliver suitable material for spawning with a low percentage of fine materials and of material not larger than 80mm in diameter.

Based on this analysis of the bed material the next chapters show the results of the calculation for the critical shear stress and the critical velocity. This was done to see if the natural renewing process and stability is given at the research site to washout fine materials. The focus in the analysis is set on the sidearm.

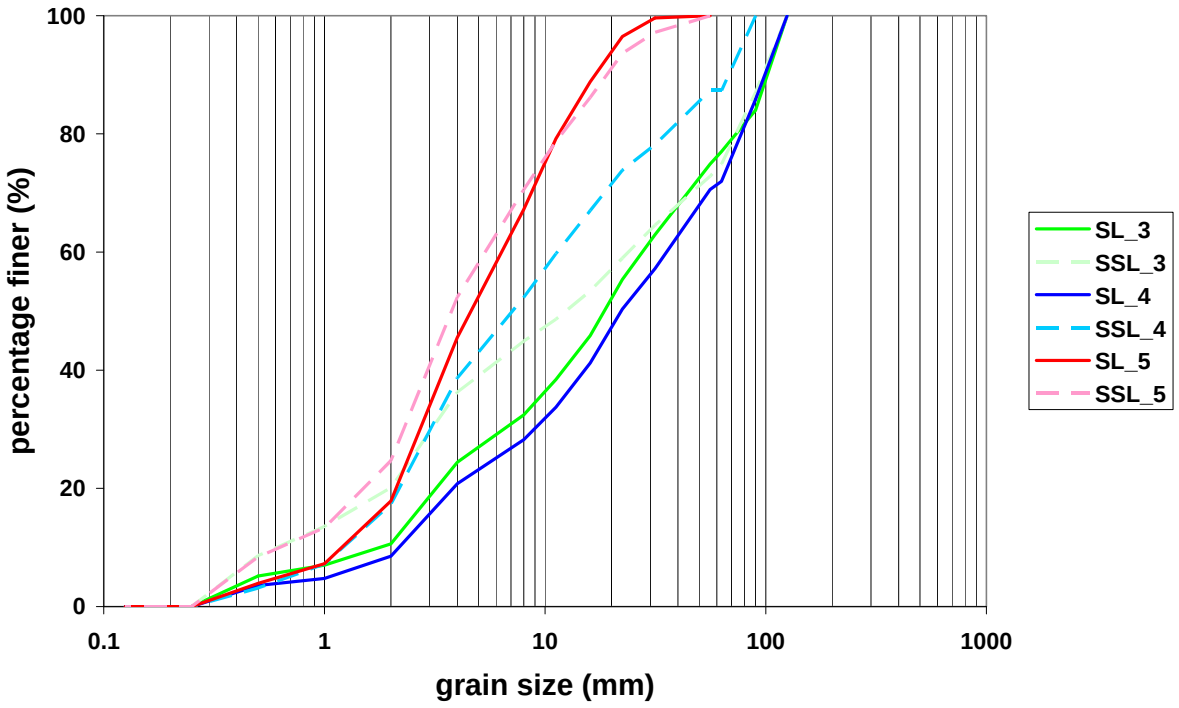

Figure 120 Log-distribution plot; results for the sieving of the bed material

3.5.1. Critical shear stress after Meyer-Peter&Müller

As already mentioned the critical shear stress is the stress applied to the bed material. If the shear stress is higher than the critical value the material starts to move. The diameters used for the calculation of the critical shear stress after Meyer-Peter&Müller are described in chapter 2.6. After calculating the critical shear stress for the bed material the results are compared with the results of the occurring shear stress derived by the HEC-RAS models. The following table (Table 8) shows the values used for the calculation as well as the resulting critical shear stress.

Densities	[kg/m³]	
Gravel	2650	
Water	1000	
Acceleration due to gravity [kg*m/s²]		
g	9.81	
	Diameter [mm]	Critical shear stress [N/m²]
$D_{min\ theor}$	8	6.09
$D_{50\ min}$ SL	4.61	3.51
D_{50} SL	15.08	11.47
$D_{50\ max}$ SL	22.11	16.82
$D_{50\ min}$ SSL	3.77	2.87
D_{50} SSL	7.76	5.90
$D_{50\ max}$ SSL	12.40	9.43
$D_{max\ theor}$	64	48.69

Table 8 Results for the critical shear stress for the bed material observed

As shown in the table above the critical shear stress for washing out the fine materials of the riverbed ($D_{50\ min}$) starts at 2.87 [N/m²]. But as this value is valid for $D_{50\ min}$ for the sub surface layer, this value is only important if the surface layer is eroded. For the surface layer the erosion starts at a shear stress of 3.51[N/m²]. If this shear stress is applied the fine materials start to move and therefore it has a positive impact on the spawning grounds. To fulfil a complete renewing of the material relevant for the spawning a shear stress of 48.69[N/m²] has to be applied to the bed material.

In the plots below (Figure 121, Figure 122 and Figure 123) the shear stress occurring in the sidearm is displayed. The shear stress occurring at the inlet has been cut off as it is not relevant for the spawning sites. It can be seen that at the section with the spawning areas (40m – 90m on the x-axis) the highest averaged stress applied to the riverbed in the side channel is found at about 30[N/m²]. This correlates with a discharge of 25[m³/s] or higher. It increases downstream to a maximum of 50[N/m²] whereas upstream the shear stress hardly exceeds 10[N/m²]. In this case complete exchange of bed material hardly occurs at the sidearm for the free flowing scenario. The shear stress applied for low flow conditions is sufficient to transport the finer material.

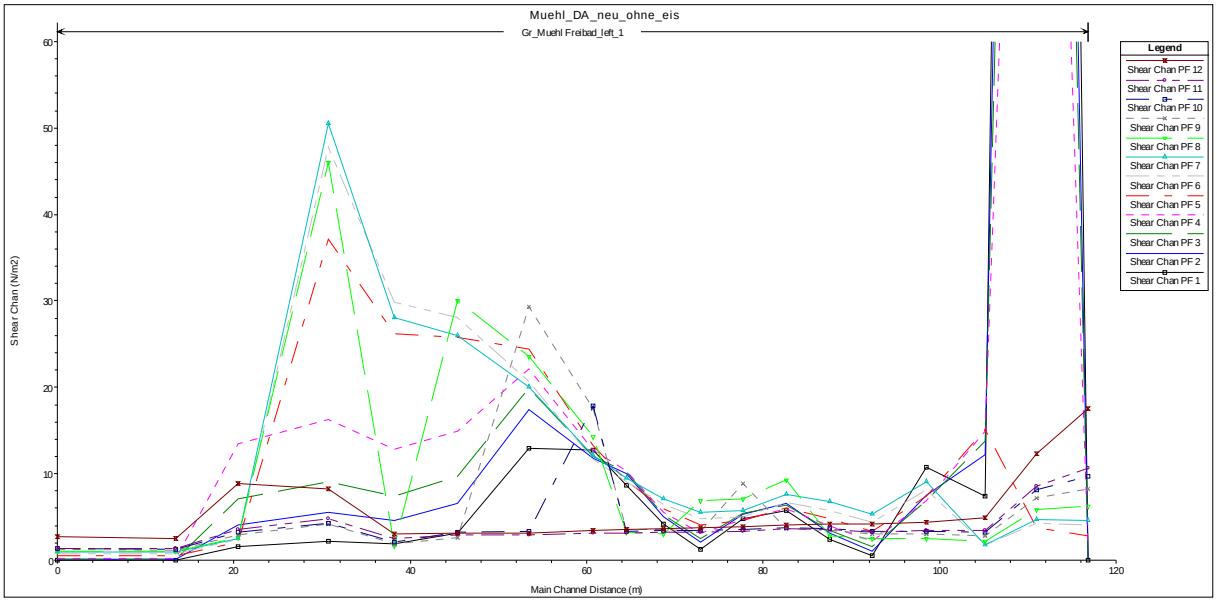

Figure 121 Shear stress occurring in the sidearm for the open flow scenario

If ice cover is formed at the sidearm the shear increases within the section of the spawning areas. In the section of 40m to 65m the shear stress reaches a high of 35.7[N/m²] at Profile 11. From Profile 3 (3[m³/s]) on the discharge produces a shear stress high enough to transport material of 8mm or smaller. Also the value of $D_{50\ max}$ for the surface layer (16.82[N/m²]) is reached within this section. So the material is transported. (Compare Figure 122)

If the discharge is redirected by an ice jam the shear stress in the sidearm increases further. Looking at Figure 123 it can be seen that from 40m to 60m the shear stress for most profiles (PF2-PF7) reaches the 11.47[N/m²] which are needed to start movement of the average D_{50} of the surface layer. The highest peak in this area is actually found at Profile 9 with a value of 77.6[N/m²]. This means that a scenario where the main channel is jammed and the discharge

of 15[m³/s] applied on the sidearm is enough to completely erodes and renew the riverbed at the spawning section.

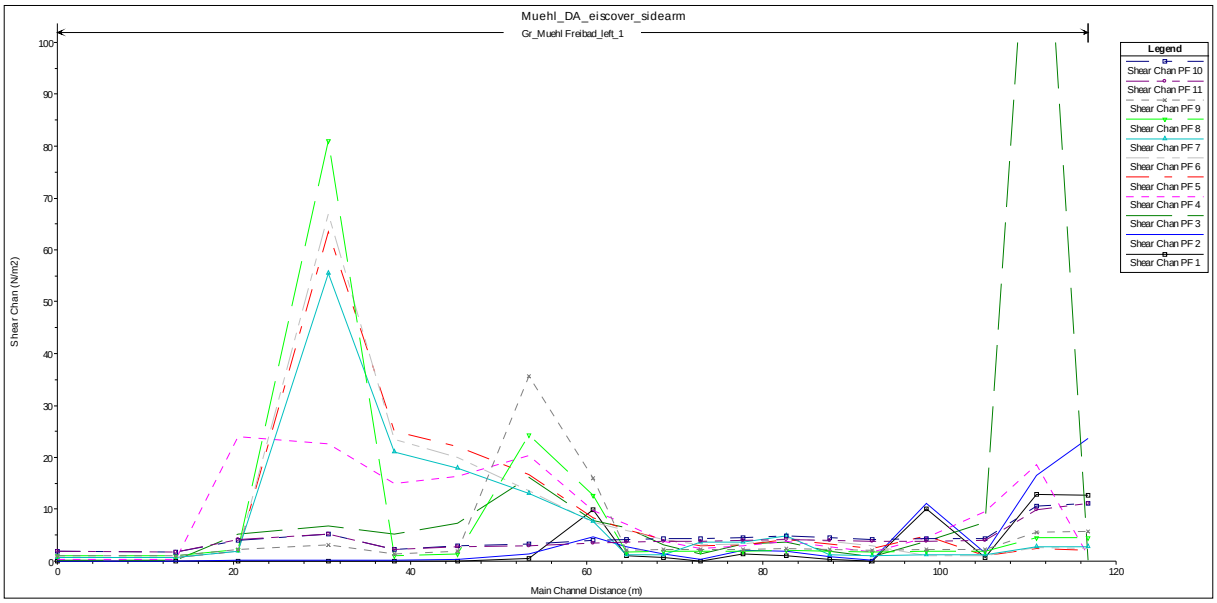

Figure 122 Shear stress occurring in the sidearm for the ice cover scenario

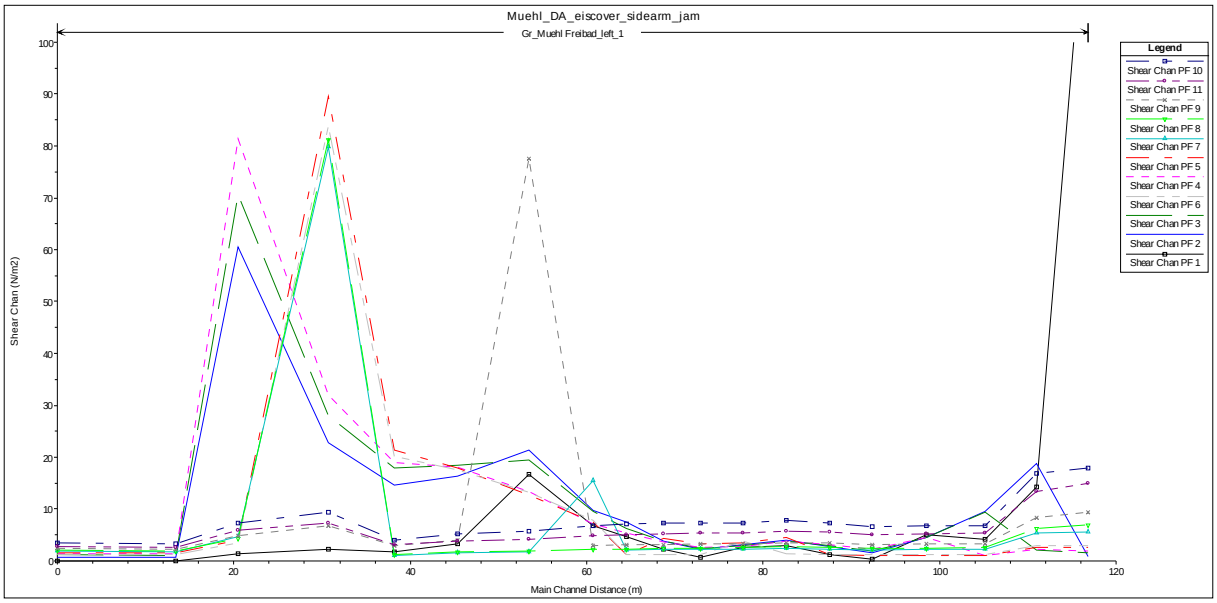

Figure 123 Shear stress occurring in the sidearm for the ice jam scenario

3.5.2. Critical velocities after Hjulström curves

As mentioned before River2D does not produce an output in form of shear stress applied to the riverbed like in HEC-RAS. Therefore the critical velocities have been analysed and compared with the Hjulström curves for 4 different grain sizes. The grain sizes analyzed are already mentioned in chapter 2.6. In Figure 124 the analyzed grain sizes are marked in the Hjulström diagram and the resulting velocities are as follows:

Table 9 Resulting critical velocities from Hjulström curves

	Grain size [mm]	Critial velocity [m/s]	Colours in diagram
Dmin theo	8	1.05	Green
D50 SSL	7.78	1.01	Red
D50 SL	15.08	1.5	Yellow
Dmay theo	64	3	Blue

This means that velocities higher than 1.05[m/s] start to erode material up to 8mm in diameter from redds. At a velocity of 3[m/s] the whole redd will be eroded. In case of the redds observed the average diameter was 15mm. For this material a velocity of 1.5[m/s] is needed to start movement.

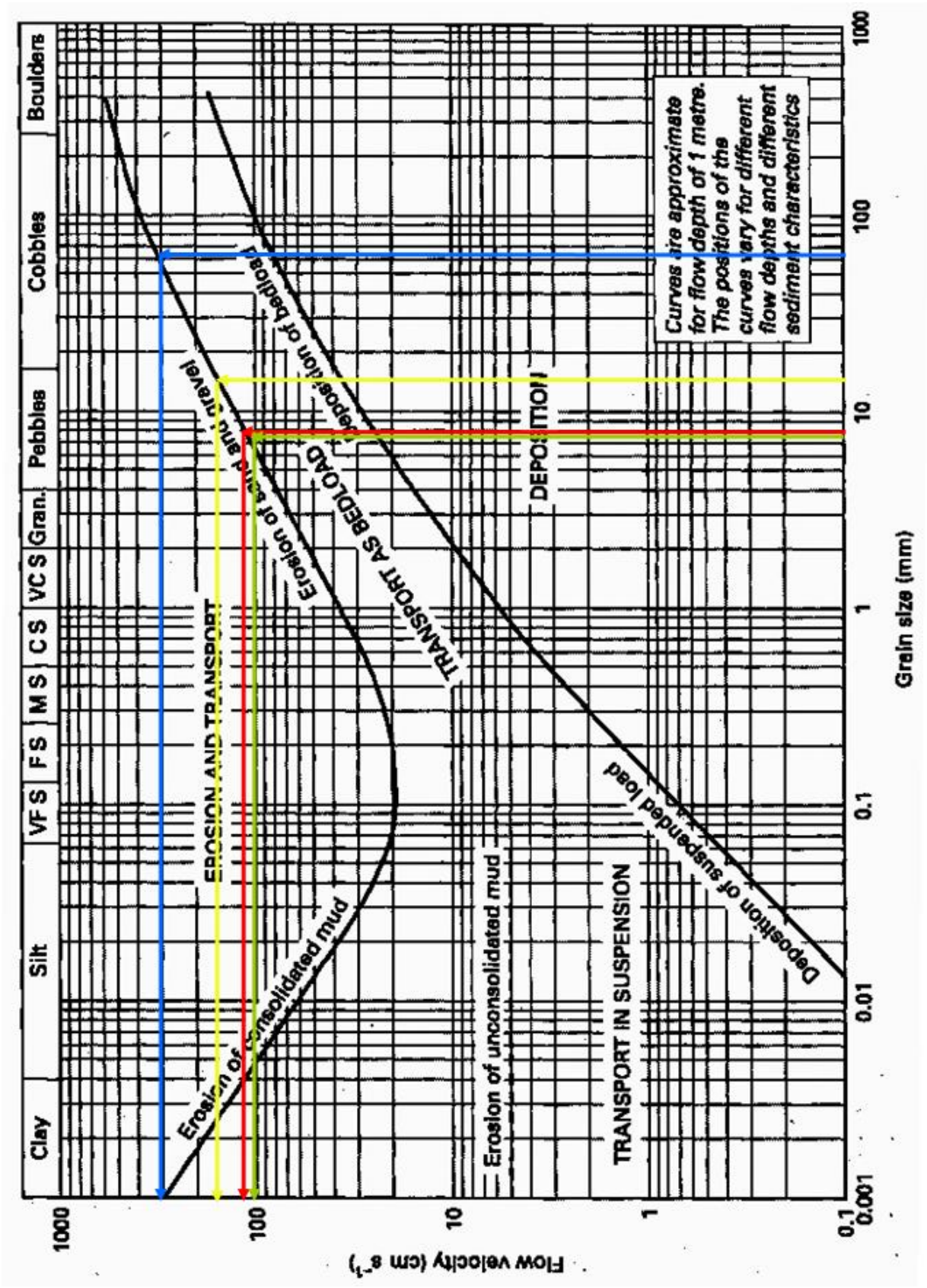

Figure 124 resulting critical velocities after Hjulström curves

3.5.3. Comparison of the critical discharges

After calculating the critical shear stress and deriving the critical velocities from the Hjulström curves the results will be compared in this chapter. Therefore the results from chapters 3.5.1 and 3.5.2 are used to figure out, which discharges start may erode redds observed in the sidearm and which discharge is needed to fulfil a complete renewal of the bed material in the spawning area. The discharges pointed out in this chapter are the input discharges to the models and not the specific ones in the sidearm.

As seen in chapter 3.5.1 the erosion of redds and the material appropriate for spawning starts at a shear stress of 6.09[N/m²]. The material with D_{50} from the surface layer is eroded from 16.82[N/m²]. Looking at Figure 121 it can be figured out that those shear stresses are reached in the free flowing scenario at a discharge of 3[m³/s] at the spawning area. The results derived from HEC-RAS are averaged locally the shear stress can be higher. At the inlet section the shear stress locally exceeds the critical shear stress for the $D_{max\ theor}$. This means that material eroded there can be transported downstream and settle in the spawning areas. The maximum shear stress in the area with redds is reached at a discharge of 25[m³/s]. The maximum critical shear stress is not reached at the spawning areas but at the inlet section and the beginning of the channelized part downstream of redds. While the higher shear stress is found at discharges between 1[m³/s] and 5[m³/s] for the inlet section into the sidearm, it is reached between 15[m³/s] and 25[m³/s] in the downstream part.

For the ice covered scenario the critical shear stress for the D_{50} is reached at a discharge of 5[m³/s]. The maximum shear stress found at the whole reach is at the inlet section at a discharge of 3[m³/s]. The maximum critical shear stress is not reached in the area with the spawning sites but is reached downstream and reaches a high of 81.12[N/m²] at profile 8.

For the jammed scenario the critical shear stress of 16[N/m²] is already reached at an input discharge of 1[m³/s]. It can be said that the shear stress in the sidearm is generally higher for the jammed scenario than for the other two. If the main channel is jammed the shear stress outreaches the maximum shear stress at 30[m³/s] at the spawning region.

If looking at the critical velocities the velocities needed to transport the bed material smaller than D_{50SL} at the spawning areas (Table 9) in HEC-RAS are reached at:

- Profile 5 (10[m³/s]) for the open flow scenario. (Figure 41)
- Profile 4 (5[m³/s]) for the ice cover scenario (Figure 50)
- Profile 2 (2[m³/s]) for the jammed scenario (Figure 58)

A similar result is shown in the River2D modelling results. Here the critical velocities at (or close to) the spawning sites in the sidearm are reached at:

- Between 10 [m³/s] and 15[m³/s] at the open flow scenario (Figure 65 and Figure 66)
- Between 5 [m³/s] and 10 [m³/s] at the ice cover scenario (Figure 73 and Figure 74)
- About 3 [m³/s] for the jammed scenario

In both simulations the threshold value of 3[m/s] are not reached close to the spawning areas in the side channel (compare chapter 3.2).

4. Discussion

In this chapter the results of this thesis are discussed. Further on they will be put into perspective with the criteria described in the theoretical part. The main focus on this thesis was to point out the changes in physical characteristics for spawning areas in alpine rivers during the winter season with focus on their influence at spawning sites.

The analysis of the hydrograph showed a typical behaviour for mountainous rivers. The changes in discharge happen in a short time. The water level rises fast due to precipitation and only little retention effect after the peak of a high flood event can be observed. Therefore the area investigated can be seen as mountainous river even though the section of the river has small slope at this section.

Three different scenarios were simulated with different discharges. The discharges chosen correlate with the run off characteristics of Große Mühl River. The discharges are at a finer scale for low flow conditions (from 1[m³/s] to 5[m³/s]) and in steps of an increase of 5[m³/s] for higher discharges. This worked out as sufficient for the changes in general flow behaviour. The analysis of the low flow conditions were used to see if the criteria for lowland river spawning sites can be used for mountainous rivers as well and for the changes during the winter month. The higher discharges were mainly used to see which changes occur during high flood events and for the analysis of the critical shear stress.

As mentioned before in River2D one roughness value was chosen for the whole modelling area. The roughness value was calibrated for the river bed only. Therefore the results for the high flood events in River2D and all resulting velocities for the areas where the water overtops the riverbanks have to be looked at with care. The choice of using one roughness value was taken as the focus was set on the low flow conditions. It figured out to be sufficient to get a general overview of the flow characteristics and flow directions at high flood events.

The general changes in flow characteristics are the same for both programs. As pointed out in the comparison part of the modelling results, local differences in flow velocities are possible. Those differences can be explained with the differences in the background of the programs. HEC-RAS was basically developed for the simulation of flood events and the extension of flood plains. Therefore a 1-dimensional approach is sufficient. This means that the flow velocities in HEC-RAS are only calculated in one direction whereas River2D is a 2 dimensional program developed for habitat modelling. Furthermore the grade of details is much higher in River2D. While HEC-RAS is based on cross sections with a routing from one section to the next in River2D the physical properties are calculated for each point in the grid.

The resolution of the mesh put over the simulation area defines the grade of details and can locally be changed in River2D.

The main characteristics figured out in the results part of this thesis are that a closed ice cover in general slows down the velocity underneath for low flow conditions. This can be explained with the additional roughness added to the cross sections due to the ice.

The roughness influence of the ice decreases with increasing discharge. This can be explained with the fact that the ice cover lifts with the increasing water level as long as it is not fixed by the riverbanks or frozen to branches or rocks. For higher discharges the velocity increases due to the limitation in extension given by the ice.

As mentioned before the influence given by hanging dams cannot be analyzed as the randomly form. Further on the limitations given by time and extend of this thesis didn't allow further investigation in this specific form of ice cover.

Slush ice had been observed in the research area. According to Brown et al. (2011) slush ice has no influence to the flow behaviour as long as it floats in the water. As soon as it gets caught it consolidates and can form dams or other obstacles (anchor ice) which change the flow behaviour. Options given by the simulation programs and the data available did not allow analysis of the formation of slush ice and its influence. But according to the literature used for this thesis anchor ice, that is mobilized again, lifts bed material and transports it downstream.

The discharge flowing through the side channel slightly decreases as long as the main channel remains ice free. This is at least the case for low flow conditions. The simulation results show that the water level increases in the ice cover scenario compared to the open flow. So it could have an influence to the cover material of redds. But as mentioned before limitations given did not allow a detailed analysis of the influence given.

Different to the scenario, where the ice cover is added, at the jammed scenario the results show that a significant change in flow behaviour occurs. Due to the blockage of the main channel most of the discharge runs through the sidearm. In this case water level and flow velocity increase compared to the base scenario. This increase of velocity and discharge can lead to a "wash out" of the redds. The results show that the shear stress occurring in the jammed scenario can reach a level where the material suitable for spawning sites is washed away. If the scenario occurs before the juveniles hedged, the eggs might be transported downstream or destroyed.

When put into relation with the criteria for spawning habitats mentioned in the introduction of this thesis it has to be looked at the open flow scenario. According to Armstrong et al. (2003)

Brown Trout prefer areas with flow velocities between 0.2 [m/s] and 0.55 [m/s] in rivers with a mean annual discharge lower than 10[m³/s]. Those velocities are given in the sidearm during low flow conditions in late autumn.

Further on the examples taken from the bed material show that the sidearm area has a low concentration of fine materials. The results of the sieving show, that the criteria of a content of particles smaller than 0.125mm should not be higher than 1.5% given by (Louhi, et al., 2008)) as well as the conditions pointed out by Armstrong et al. (2003) (material smaller than 1mm <15%) are fulfilled. In general it can be said that the bed material in the sidearm matches the criteria given by the literature. As written in the introduction part the studies used in this thesis for spawning habitats and habitats for Brown Trout were done for low land rivers. The results of the sieving and the flow velocity measuring show that those criteria are also valid for rivers with alpine characteristics like Große Mühl River.

Observations showed that the low velocities occurring during summer in the sidearm lead to sedimentation of sand and fine material. As the analysis of the critical shear stress and velocities showed that a natural renewing process occurs only at higher discharges or when the main channel is jammed. The low concentration of the fine material in the examples taken can be explained with the human interference during summer. As the section analyzed is used as a river bath during summer people are moving the bed material and the fine sediments are lift up and washed away. Therefore it can be said that the usage as a river bath keeps the area suitable for spawning and the artificial influence can bee seen as good.

In the theoretical part it was described that Brown Trout start to spawn when the temperature of the water decreases to a value below 13°C. The monitored temperatures show that this is the case mostly at the end of September or beginning of October. This matches with the observations made at Große Mühl River.

The analysis of the temperature data showed that the river froze several times in the last years. Times of constant temperature of 0°C are an indicator when the river was covered with ice. During the time period that was comparable between the open flow and the interstitial the data showed a water temperature where no ice occurs in the water.

Furthermore the comparison of the data sets given showed that a difference between the open flow sensor and the sensor positioned in the interstitial is given. This difference in temperature can make the difference if the eggs freeze or not. But a clear answer to this point cannot bee given as the data set available for this thesis did not include a period where the river section was covered with ice.

It can be seen that the temperature in the interstitial is less volatile than in the open flow. This can be because of the decreased influence given by radiation. Another reason for that can be groundwater springs as Brown et al. (2011) point out. If this is the case in the interstitial area where the sensor was placed cannot be said for sure but it is rather unlikely as the temperature would show less volatility and influence by the surface water.

5. Conclusion and Outlook

The following chapter will sum up the thesis and point out problems that occurred during the research period. Further on an outlook will be given. Suggestions will be given for further projects dealing with this topic.

Brown Trout is one of the leading species in alpine rivers. Research has been done on the habitats of adult fish and juveniles but there is little knowledge about the habitats the fish use for spawning. As Brown Trout is a autumn/winter spawning fish redds are prone to the influence given by ice formation on the river. This thesis is an attempt to figure out how ice formation and the processes around its change the physical properties at spawning sites. Two different simulation tools were used to analyze the changes in flow behaviour and velocities. Three scenarios that can occur during the developing period of the eggs were chosen which are significant for the winter in alpine rivers. The first scenario is the open flow scenario. This indicates the spawning time in late autumn and early winter. The river has low flow conditions and the temperature in the water decreases. During the winter season the river might freeze. To see how this changes the flow the sidearm was covered with ice in the modelling part of this thesis. Close to the time of hedging in early spring ice covers along the river break up and the floating ice shelves can cause jams in the main channel. The sidearm is still covered with ice. This is the scenario was the third approach. All three scenarios were computed with a variation of discharges to see if there are changes in velocities and flow behaviour. The variation in discharge chosen reached from low flow conditions (1[m^3/s]) to a high flood event with a discharge of 40[m^3/s]. For the calibration of the model on-site observations were done. The results of the two modelling approaches were compared. Both programs showed similar results with the changes in velocities and for the flow behaviour in high flood events. Local differences in flow velocities have been observed between the two programs which can be explained in the differences in the numerical background. The results of the simulations were further used to define the critical discharges, where the material smaller than 8mm in diameter is eroded and transported from the spawning sites. Another point was the critical discharge where the shear stress applied to the riverbed is high enough

to lead to a complete renewal of the bed material. It had been shown that the discharges between 5[m³/s] and 10[m³/s] in the main channel as input into the system is sufficient to wash away the fine materials and the D_{50} figured out in the analysis of the bed material. The HEC-RAS simulations showed that only when the sidearm is covered with ice or the main channel is jammed the shear stress is high enough to reach the critical shear stress needed for a complete turnover of the bed material. Further the temperature change in the water and the interstitial were monitored beforehand of the thesis. It has been shown that there is a difference occurring. To see if there is a difference occurring and how large it is, more monitoring has to be done. The time period for the comparison was rather short and the river did not freeze during the winter season observed. It was analysed if the differences in temperature lead to a difference in hedging times. As mentioned before there is a difference occurring. For the incubation times the daily averaged temperature is used and summed up. When the sum of day degrees reaches a value of about 380 to 480 day degrees the difference figured out to be about 1 day. Due to the fact that the average temperature is used the difference between the resulting times is small. The analysis of the temperature timelines showed that the difference in the daily highs and lows is higher at the open flow sensor. If influence is given by groundwater has to be questioned as the influence given by the surface water is strong.

Over all it can be said that ice formation has an impact on spawning habitats of Brown Trout. Especially when it comes to flow velocity and flow behaviour changes between the autumn, winter and spring scenarios can be seen. The other parameters observed for this thesis show that there is an influence occurring but it can't be said for sure. More monitoring especially in the case of the temperature has to be done. The comparable time period for the temperatures covered one incubation season but the river did not freeze so it can't be said if there is a influence given when a complete ice cover occurs. As mentioned earlier also the appearance of groundwater springs have an influence on the spawning sites. The fact that only two sensors were used for the temperature monitoring at only one spawning site leads to the conclusion that no general statement can be made for the temperature parameter. After the hedging more spawning sites which are used frequently by the fish should be monitored to be able to give a more detailed answer to the question if there is a temperature difference given or not. The fact that the river did not freeze during the whole monitoring period is another fact that has to be taken into account. This is also a point where a longer period of monitoring will be useful but couldn't be worked out during this thesis due to limitations in time.

As this thesis is one of the first approach to model winter conditions at spawning site of Brown Trout in alpine rivers it delivers basic knowledge of this topic. To receive more detailed answers to every single parameter used for the analysis further research on every single parameter and therefore more monitoring has to be done. This thesis shows one way to approach the problematic given by ice formation and the change of season during the incubation time. It is very important to gain further knowledge of this topic as a lack of suitable spawning sites can either lead to an over spawning effect or stress for the fish. It also has to be pointed out that lack of spawning areas lead to a bottle neck effect in the reproduction process and the population in the river. If the population is not “healthy” and at a level where it can be seen as “able to reproduce by itself” the status of ecologically good quality for the river required by the EWFD (European Water Framework Directive) is not given anymore. As it is mandatory to keep this status at least for the leading species in alpine rivers there should be enough possibilities given for spawning. This requires a good knowledge of the conditions needed for a breeding success. As other publications already pointed out, e.g. (Riedl & Peter, 2013) and others, there is a broad basis of knowledge for habitats of Brown Trout living in lowland rivers or lakes but only little for the alpine areas. The problem is that it is hard to collect the required data in alpine rivers due to accessibility of the sites. As mentioned before another limitation is given by the slope in the rivers for the modelling and the DEMs available. In the case of this thesis the data for the DEM was available from former modelling done at the river. But even if DEMs for mountainous regions are available the question is if the programs are able to compute the model derived from the data. The models used have limitations in the inclination of the slope. If the slope is too steep the results might not be accurate for an analysis of the area.

6. Figures

7. Tables

8. References

Alp, A. (2010). Eggs Incubation, Early Development and growth in Frys of Brown Trout (Salmo trutta macrostigma) and Black Sea Trout (Salmo trutta labrax). Turkish journal of fisheries and aquatic sciences, 10(3), 387 - 394.

Armstrong, J. D., Kemp, P. S., Kennedy, G. J. A., Ladle, M., & Milner, N. J. (2003). Habitat requirements of Atlantic salmon and brown trout in rivers and streams. Fisheries Research, 62(2), 143-170. doi: http://dx.doi.org/10.1016/S0165-7836(02)00160-1

Bisaillon, J.-F., & Bergeron, N. E. (2009). Modeling anchor ice presence–absence in gravel bed rivers. Cold Regions Science and Technology, 55(2), 195-201. doi: http://dx.doi.org/10.1016/j.coldregions.2008.08.007

Brown, R. S., Hubert, W. A., & Daly, S. F. (2011). A Primer on Winter, Ice, and Fish: What Fisheries Biologists Should Know about Winter Ice Processes and Stream-Dwelling Fish. Fisheries, 36(1), 8-26. doi: 10.1577/03632415.2011.10389052

Brunner, G. W. (2010a). HEC-RAS - River System User's Manual (Vol. Version 4.1, pp. 766). Davis, California: US Army Corps of Engineering; Institute for Water Resources.

Brunner, G. W. (2010b). HEC-RAS, River Analysis System - Hydraulic Reference Manual. Davis, California: US Army Corps of Engineering.

Fink, M., Moog, O., & Wimmer, R. (2000). Fließgewässer Naturräume Österreichs. Vienna: Umwelt Bundesamt.

Hauer, C., Unfer, G., Tritthart, M., & Habersack, H. (2011). Effects of stream channel morphology, transport processes and effective discharge on salmonid spawning habitats. Earth Surface Processes and Landforms, 36(5), 672-685. doi: 10.1002/esp.2087

Huet, M. (1959). Profiles and Biology of Western European Streams as Related to Fish Management. Transactions of the American Fisheries Society (1900), 88(3), 155 - 163. doi: 10.1577/1548-8659(1959)88[155:PABOWE]2.0.CO;2

Klemetsen, A., Amundsen, P. A., Dempson, J. B., Jonsson, B., Jonsson, N., O'Connell, M. F., & Mortensen, E. (2003). Atlantic salmon Salmo salar L., brown trout Salmo trutta L. and Arctic charr Salvelinus alpinus (L.): a review of aspects of their life histories. Ecology of Freshwater Fish, 12(1), 1-59. doi: 10.1034/j.1600-0633.2003.00010.x

Lahnsteiner, F. (2012). Thermotolerance of brown trout, Salmo trutta, gametes and embryos to increased water temperatures. Journal of Applied Ichthyology, 28(5), 745-751. doi: 10.1111/j.1439-0426.2012.01934.x

Lindenschmidt, K.-E., Sydor, M., & Carson, R. W. (2012). Modelling ice cover formation of a lake–river system with exceptionally high flows (Lake St. Martin and Dauphin River, Manitoba). Cold Regions Science and Technology, 82(0), 36-48. doi: http://dx.doi.org/10.1016/j.coldregions.2012.05.006

Louhi, P., Mäki-Petäys, A., & Erkinaro, J. (2008). Spawning habitat of Atlantic salmon and brown trout: general criteria and intragravel factors. River Research and Applications, 24(3), 330-339. doi: 10.1002/rra.1072

Patt, H., & Gonsowski, P. (2011). Feststofftransport, Gewässerbettdynamik und Fließgewässertypologie Wasserbau - Grundlagen, Gestaltung von wasserbaulichen Bauwerken und Anlagen (Vol. X, pp. 57 - 88). Berlin: Springer-Verlag.

Riedl, C., & Peter, A. (2013). Timing of brown trout spawning in Alpine rivers with special consideration of egg burial depth. Ecology of Freshwater Fish, 22(3), 384-397. doi: 10.1111/eff.12033

Schuh, A. (2011). Eishochwasser an Oder und Elbe aus historischen und meteorologischen Gesichtspunkten und im Hinblick auf mögliche Gefährdungen. PhD Dissertation, Brandenburgische Technische Universität, Cottbus.

Shen, H. T. (2010). Mathematical modeling of river ice processes. Cold Regions Science and Technology, 62(1), 3-13. doi: http://dx.doi.org/10.1016/j.coldregions.2010.02.007

Spindler, T. (1997). FISCHFAUNA IN ÖSTERREICH; Ökologie – Gefährdung – Bioindikation - Fischerei – Gesetzgebung. Wien.

Steffler, P. (2002). R2D_Bed - Bed Topography File Editor - User's Manual: University of Alberta.

Steffler, P., & Blackburn, J. (2002a). River2D - Two-Dimensional Depth Averaged Model of River Hydrodynamics and Fish Habitat - Introduction to Depth Averaged Modeling and User's Manual: University of Alberta.

Steffler, P., & Blackburn, J. (2002b). River2D - Two-Dimensional Depth Averaged Model of River Hydrodynamics and Fish Habitat - Introduction to Depth Averaged Modeling and User's Manual (pp. 21 - 22): University of Alberta.

Timalsina, N. P., Charmasson, J., & Alfredsen, K. T. (2013). Simulation of the ice regime in a Norwegian regulated river. Cold Regions Science and Technology, 94(0), 61-73. doi: http://dx.doi.org/10.1016/j.coldregions.2013.06.010

Turcotte, B., Morse, B., Bergeron, N. E., & Roy, A. G. (2011). Sediment transport in ice-affected rivers. Journal of Hydrology, 409(1–2), 561-577. doi: http://dx.doi.org/10.1016/j.jhydrol.2011.08.009

Unfer, G., Hauer, C., & Lautsch, E. (2011). The influence of hydrology on the recruitment of brown trout in an Alpine river, the Ybbs River, Austria. Ecology of Freshwater Fish, 20(3), 438-448. doi: 10.1111/j.1600-0633.2010.00456.x

Wang, J., Chen, P.-p., & Sui, J.-y. (2011). Progress in studies on ice accumulation in river bends. Journal of Hydrodynamics, Ser. B, 23(6), 737-744. doi: http://dx.doi.org/10.1016/S1001-6058(10)60171-0